Reaction Kinetics under Anomalous Diffusion

D i s s e r t a t i o n

zur Erlangung des akademischen Grades

d o c t o r r e r u m n a t u r a l i u m

(Dr. rer. nat.)

im Fach Physik

eingereicht an der

Mathematisch-Naturwissenschaftlichen Fakultät I

Humboldt-Universität zu Berlin

von

Dipl.-Phys. Daniela Frömberg
12.08.1981, Berlin

Präsident der Humboldt-Universität zu Berlin:
Prof. Dr. J.-H. Olbertz

Dekan der Mathematisch-Naturwissenschaftlichen Fakultät I:
Prof. Dr. A. Herrmann

Gutachter:

1. Prof. Dr. I. M. Sokoklov
2. Prof. Dr. L. Schimansky–Geier
3. Prof. Dr. R. Metzler

Tag der mündlichen Prüfung: 23. 06. 2011

Zusammenfassung

Die vorliegende Arbeit befaßt sich mit der Verallgemeinerung von Reaktions–Diffusions–Systemen auf Subdiffusion. Die subdiffusive Dynamik auf mesoskopischer Skala wurde mittels Continuous–Time Random Walks mit breiten Wartezeitverteilungen $\psi(t) \propto t^{-1-\alpha}$ modelliert. Bezüglich der Reaktion wurde angenommen, dass sie auf mikroskopischer Skala stattfindet und lokal dem klassischen Massenwirkungsgesetz unterliegt. Dieses Modell entspricht der Situation in einem porösen Medium, wo Teilchen in Poren und Hohlräumen für längere Zeit gefangen sein können, jedoch während der Wartezeiten miteinander reagieren. Nach einer Diskussion der Subdiffusionsgleichung und Möglichkeiten ihrer Lösung, insbesondere unter dem Aspekt der Einführung von Quellen neuer Teilchen, wird das Augenmerk auf die Reaktions–Subdiffusionsgleichungen gerichtet. Dabei handelt es sich um Integro–Differentialgleichungen, die unter den vorliegenden Annahmen eine Abhängigkeit des Transportterms von der Reaktion aufweisen. Der langreichweitige Integralkern der reinen Subdiffusionsgleichung ist hierbei durch einen zusätzlichen Faktor modifiziert, der der Erzeugung und Vernichtung von Teilchen durch Reaktion Rechnung trägt. Im Falle linearer Reaktionskinetik ist dieser Faktor bestimmt durch die Ratenkoeffizienten der Reaktion. Bei nichlinearer Reaktionskinetik besteht eine zusätzliche Abhängigkeit des Kerns von den Konzentrationen der Reaktionspartner zu allen vorausgegangenen Zeiten.

Im Falle der Zerfallsreaktion $\mathrm{A} \to 0$ konnte ein allgemeiner Ausdruck für die Lösungen beliebiger Dirichlet–Randwertprobleme hergeleitet werden. Diese Lösungen ließen sich auf Lösungen desselben Randwertproblems für die reine Subdiffusionsgleichung ohne Zerfallsreaktion zurückführen. Die daraus resultierenden stationären Profile unterscheiden sich qualitativ nicht von denen, die man unter normaler Diffusion mit Teilchenzerfall erhält. Die Annahme, dass die Reaktion dem Massenwirkungsgesetz unterliegt, ist eine entscheidende Voraussetzung für die Existenz stationärer Profile unter Subdiffusion.

Als Beispiel für eine nichtlineare Reaktion wurde die irreversible autokatalytische Reaktion $\mathrm{A} + \mathrm{B} \to 2\mathrm{A}$ unter Subdiffusion untersucht. Die Gesamtteilchenkonzentration wurde als konstant, $A(x,t) + B(x,t) = \text{const}$, sowie die Reaktion als Teilchenumbenennung angenommen. Damit konnte ein Analogon zur klassischen Fisher–Kolmogorov–Petrovskii–Piscounov (FKPP) Gleichung aufgestellt und die resultierenden propagierenden Fronten der A–Teilchen untersucht werden. Numerische Simulationen legten die Existenz zweier verschiedener Regimes nahe, die sowohl mit Hilfe eines Crossover–Argumentes als auch durch analytische Berechnungen zum asymptotischen Frontverhalten untersucht wurden. Das erste Regime kann im Rahmen der kontinuierlichen subdiffusiven FKPP–Gleichung beschrieben werden und ist charakterisiert durch eine Front, deren Breite und Geschwindigkeit sich entsprechend $t^{\frac{\alpha-1}{2}}$ verringert. Aufgrund der Verringerung der Frontbreite stellt sich im Laufe der Zeit die Situation ein, in der die Front atomar scharf definiert ist. Ein zweites Regime setzt ein, das fluktuationsdominiert ist und nicht im Geltungbereich der kontinuierlichen Gleichungen liegt. In diesem Fall beobachtet man eine stärkere Abnahme der Frontgeschwindgkeit gemäß $t^{\alpha-1}$. Weitere Simulationen des fluktuationsdominierten Regimes offenbarten zusätzliche subdiffusionsbedingte Effekte.

Ein anderes Szenario, bei dem eine Spezies A in ein mit immobilen B–Partikeln besetztes subdiffusives Medium hineindiffundiert und gemäß dem Schema $\mathrm{A} + \mathrm{B} \to (\mathit{inert})$ reagiert, wurde ebenfalls betrachtet. Unter bestimmten Voraussetzungen kann diese Anordnung für die Konzentration der Spezies A näherungsweise als ein Randwertproblem mit einem beweglichen Rand, ein sog. Stefan–Problem, formuliert werden. Wichtigstes Resultat war dabei, daß die Position des beweglichen Randes sich wie $R(t) \propto t^{\alpha/2}$ verhält. Die analytisch gewonnenen Ergebnisse wurden durch numerische Simulationen untermauert.

Abstract

The present work studies the generalization of reaction–diffusion schemes to subdiffusion. The subdiffusive dynamics was modelled by means of continuous–time random walks on a mesoscopic scale with a heavy–tailed waiting time pdf $\psi(t) \propto t^{-1-\alpha}$ lacking the first moment. The reaction itself was assumed to take place on a microscopic scale, obeying the classical mass action law. This situation is assumed to apply in a porous medium where the particles are trapped within the catchments, pores and stagnant regions of the flow, but are still able to react during their waiting times. After discussing the subdiffusion equation and different methods of their solution, especially under the aspect of particles being introduced into the system in the course of time, the reaction–subdiffusion equations are addressed. These equations are of integro–differential form and under the assumptions made, the reaction explicitly affects the transport term. The long ranged memory of the subdiffusion kernel is modified by an additional factor accounting for the conversion and survival probabilities due to reaction during the waiting times. In the case of linear reaction kinetics, this factor is governed by the rate coefficients. For nonlinear reaction kinetics the transport kernel depends additionally on the concentrations of the respective reaction partners at all previous times.

The simplest linear reaction, the degradation $\mathrm{A} \to 0$ was considered and a general expression for the solution to arbitrary Dirichlet Boundary Value Problems was derived. This solution can be expressed in terms of the solution to the corresponding Dirichlet Problem under mere subdiffusion, i.e. without degradation. The resultant stationary profiles do not differ qualitatively from the stationary profiles in normal reaction diffusion. For stationary solutions to exist in reaction–subdiffusion, the assumption of reactions according to classical rate kinetics is essential.

As an example for a nonlinear reaction–subdiffusion system, the irreversible autocatalytic reaction $\mathrm{A} + \mathrm{B} \to 2\mathrm{A}$ under subdiffusion is considered. Under the assumptions of constant overall particle concentration $A(x,t) + B(x,t) = \text{const}$ and re–labelling of the converted particles, a subdiffusive analogue of the classical Fisher–Kolmogorov–Petrovskii–Piscounov (FKPP) equation was derived and the resultant fronts of A–particles propagating into the B–domain were studied. Two different regimes were detected in numerical simulations. These regimes were discussed using both crossover arguments and analytic calculations. The first regime can be described within the framework of the continuous reaction–subdiffusion equations and is characterized by the front velocity and width going as $t^{\frac{\alpha-1}{2}}$ at larger times. As the front width decays, the front gets atomically sharp at very large times and a transition to a second regime, the fluctuation dominated one, is expected. The fluctuation dominated regime is not within the scope of the continuous description. In that case, the velocity of the front decays faster in time than in the continuous regime, $v_{fluct} \propto t^{\alpha-1}$. Further simulations pertaining the reaction on contact scenario, i.e. the fluctuation dominated regime, revealed additional fluctuation effects that are genuinely due to subdiffusion.

Another nonlinear reaction–subdiffusion system where reactants A penetrate a medium initially filled with immobile reactants B and react according to the scheme $\mathrm{A} + \mathrm{B} \to (\mathit{inert})$ was considered. Under certain presumptions, this problem can be described in terms of a moving boundary problem, a so–called Stefan–problem, for the concentration of a single species. The main result was that the propagation of the moving boundary between the A– and B–domain goes as $R(t) \propto t^{\alpha/2}$. The theoretical predictions concerning the moving boundary were corroborated by numerical simulations.

Contents

1 Introduction: Random Walks and Reactions

Diffusive transport can either be described as a stochastic process accounting for the erratic motion (Brownian motion) of a particle, or in terms of a differential equation for the probability density. It was Einstein (1905) who established the relationship between these two concepts and has shown that the Brownian motion of a macroscopic particle in a suspension arises from basic postulates of kinetic theory of heat [1]. For low concentrations, the motions of the particles can be regarded as mutually independent. Moreover, if correlations decay within a certain interval of time, the corresponding subsequent displacements of a moving particle are independent as well, which accounts for the Markovian nature of the motion [2]. These assumptions allow for a stochastic formulation as a random walk process. The respective continuum description is given by the diffusion equation or Fick's second law. The corresponding probability densities to find the particle at a point x at a certain time are Gaussian, and the mean squared displacement of the diffusing particle is linear in time, $\left\langle x^2 \right\rangle = 2Dt$ with D being the diffusion constant.

Complex systems are made up of subunits that feature a large diversity and/or strong interactions among them, giving rise to long range correlations that in some cases may even be scale free in the sense that no typical time or space scale exists [3]. Therefore, transport processes occurring in complex systems usually deviate from Gaussian characteristics. In particular, the linear time dependence of the mean squared displacement is violated, $\left\langle x^2 \right\rangle \propto t^\alpha$, $\alpha \neq 1$ [4]. Situations where the mean squared displacement grows faster than in normal diffusion, $1 < \alpha < 2$, are referred to as superdiffusion. The mean squared displacement growing sublinearly with time, $0 < \alpha < 1$, corresponds to subdiffusion.

The present work considers only the latter. Subdiffusive behavior may either be due to spatial disorder as in diffusion within restricted geometries like fractals, or to energetic disorder [5, 6, 7]. Subdiffusive dynamics was reported for phenomena as different as the motion of RNA–molecules or other macromolecules within cytoplasm [8, 9, 10] whose anomaly is due to macromolecular crowding, diffusion of beads in a polymer network [11], charge carrier transport in amorphous semiconductors [12], the spread of tracer plumes in geological formations [13, 14], or financial time series [15].

The focus is here on a special case of energetic disorder, namely on trapping processes that can be successfully modelled by continuous–time random walks (CTRW) with heavy–tailed power law waiting time probability densities lacking their mean, $\psi(t) \propto t^{-1-\alpha}$, $0 < \alpha < 1$. In contrast to diffusion on constrained geometries, the continuum limit of the heavy–tailed CTRW is given by time–fractional diffusion equations, i. e. integro–differential equations with slowly decaying kernels which account for long ranging memory effects [16]. Processes described by heavy–tailed CTRWs are nonergodic [17]: the ensemble average of the mean squared displacement exhibits the power–law characteristics mentioned above, whereas the moving time average of the

mean squared displacement remains a linear function of time, however with strongly fluctuating prefactors [18, 19]. The longer the time interval of observation, the more likely it becomes to find long waiting times of the order of the observation time, which induces ageing of the system.

Many phenomena in systems out of equilibrium can be described in terms of reactions [20]. Apart from the obvious example of chemical reactions between molecules, applications can be found in various fields such as physics or ecology. An example for a monomolecular reaction is the isomerization $A \rightleftharpoons B$ or, as an irreversible special case, the reaction $A \to 0$ describing e.g. particle decay. Reaction models including a zero at the product side also account for reactions where the product is some inert species that is not of importance to the overall kinetics.
The bimolecular reaction scheme $C \to A + B$ may account for ionization in electrolytes or plasma [20]. The recombination of charge carriers in semiconductors (electrons and holes) can be described by the annihilation scheme $A + B \to 0$. One may as well think of the one–species–annihilation $A + A \to 0$ e.g. for chemical reactions on surfaces where the desorption of the product occurs rapidly, or the one–species–coalescence $A + A \to A$ [7]. The simplest autocatalytic reaction is given by $A + B \to 2A$, which has been used to model a system of competing varieties of a species and the perpetuation of an advantageous gene, or as well the dynamics of infectious diseases [21, 22]. The predator–prey– and competing–species relationships in ecology can be described in terms of more complicated systems of reactions [23] that exhibit a rich dynamics. In the case of a homogeneous mixture of reactants, the temporal change of the respective concentrations is given by the classical rate equations.

Nonequilibrium systems that feature spatially spreading and mutually interacting particles or individuals can often be successfully modelled by means of reaction–diffusion equations, if all concentrations are at least locally homogeneous and fluctuations are hence negligible [24]. Such systems comprise e.g. the spatial spread of populations, or animal coat patterns [22]. The respective reaction–subdiffusion equations are obtained by adding the kinetic rate term to the transport term on the right hand side of the diffusion equation.
Reactions between different (initially separated) species often give rise to reaction fronts, constituting a characteristic feature of the system under study. Especially the reaction $A + B \to 2A$ describing the propagation of a stable into an unstable state has been studied extensively [25, 26, 27].

An important question that arises is to what extent the dynamical behavior of systems featuring reactions in combination with subdiffusion differs from the normal diffusive one. It has turned out that simply adding a reaction rate term in the time–fractional diffusion equation, analogously to the proceeding in normal reaction–diffusion, is not feasible [28]. A promising approach to derive the reaction–subdiffusion equations is to analyze the situation from the viewpoint of the CTRW.

The derivation of the reaction–subdiffusion equations as well as their (approximate) solution and the investigation of the resultant dynamics requires some non–standard mathematical means that are not commonly known. A rather large part of this work is therefore dedicated to a detailed introduction to the basic mathematical tools and concepts that will come to application later on. In chaper two, integral transforms will be addressed as well as the Riemann–Liouville fractional differintegration and the important Mittag–Leffler and H–functions, which play an important role in the solution of time–fractional equations.

The third chapter presents the generating functions approach, the stable laws and their application to sums of random variables and random walks. The fourth chapter generalizes the random walk to the continuous–time random walk, demonstrating the different methods available to derive the governing equations for the resultant probability densities. Alongside with the derivation of the time–fractional diffusion equation (subdiffusion equation) as the continuum limit of the heavy–tailed continuous–time random walk, the subordination principle is introduced.

Before selected problems in reaction–subdiffusion can be attacked, some preparatory considerations on partial time–fractional differential equations have to be made. Especially the different types of initial conditions and the time–fractional operator need to be discussed very carefully, in order to guarantee that the mathematical objects we deal with properly describe physical entities. These subjects are treated in chapter five. First, time–fractional differential equations are briefly introduced, giving an own derivation of the solution to a particular initial value problem that includes the time–fractional relaxation equation as a special case.
Then, a compilation of the methods of solution for the subdiffusion equation is provided. In particular, the inclusion of source terms, boundary conditions, or, later on, reactions, involves introduction of particles into the system. Consequently, the memory of these particles does not range back to the time of preparation of the system. It will be made plausible that the time–fractional diffusion equation with a memory ranging back to the preparation of the system also applies to densities or concentrations of "mixed ages" as they emerge from sources, which is not obvious at first glance. Hence, the lower terminal of the Riemann–Liouville time–fractional derivative can be interpreted as the time of preparation of the system also in cases where a proportion of the particles is introduced later in the course of time. With these results at hand, boundary value problems can be attacked equivalently by using different methods relying either on symmetry or on source introduction at the boundary, or even by using both in combination. Especially Dirichlet boundary value problems will be solved. Moreover, the subordination principle will be applied to time–fractional diffusion with sources.

Chapter six first gives an overview of the state–of–the–art in reaction–subdiffusion. Then, the reaction–subdiffusion equations are derived on the basis of CTRW.
Basically, two scenarios are conceivable. The first pertains to the situation where the reaction takes place with a given probability whenever a jump event occurs. In this model, reactions are not allowed to take place during the waiting periods between the particle jumps, the reaction on small scales is subdiffusion controlled. Consequently, the anomalous dynamics carries over to the reaction term, and the reaction–subdiffusion equations describing that situation exhibit reaction– and transport terms that are acted upon by a time–fractional derivative. Just as in the classical picture of normal diffusion, the reaction– and transport effects are separable in that case and simply need to be combined additively in order to account for the total evolution of the densities of species. This type of fractional reaction–subdiffusion equations were studied by many authors [29, 30, 31, 32], and can in principle be solved by the same means as the corresponding normal reaction–diffusion equations. [1]
The present work focuses on a situation that is somewhat more complicated. The CTRWs take place on a mesoscopic scale, and the reactions are assumed to obey the mass action law on a

[1] This does of course not mean that an analytical solution is always available. Even in normal reaction–diffusion an analytical solution is only possible in the minority of cases [33].

microscopic scale, i.e. the reactions take place during the waiting time periods. This case accounts for the situation e.g. in a porous medium where the particles are trapped within cavities and pores, but the trapped particles are still able to react. The resultant reaction–subdiffusion equations are not fractional equations anymore [28, 34, 35]. The reaction explicitly affects the transport term, the long ranged memory kernel is modified by an additional factor. This factor is governed by the rate coefficients in the case of linear reaction kinetics, and depends additionally on the concentrations of the respective reaction partners at all previous times if the reaction kinetics is nonlinear. For species that vanish at reaction, this additional factor corresponds to a cutoff of the long ranged memory, which ensures that only those particles jump that did not vanish during the waiting time. We will see later that in general the nonlinear reaction–subdiffusion equations cannot be put up in a closed form since the additional factor appearing in the memory kernel is not always amenable to an explicit analytic representation. However, in some simple, irreversible cases a formulation of nonlinear reaction–subdiffusion equations is possible , though. The resultant effects of the interplay of transport with memory and reactions is not well understood yet. Unfortunately, methods of solution and even proofs of existence are still lacking for such partial integro–differential equations with an intrinsically nonlinear memory. Therefore one has to settle with analyzing either only the stationary solutions, where they exist as e.g. in section 6.6, or special cases of such nonlinear reaction–subdiffusion problems where the qualitative dynamical behavior of the system is not governed by the concentration dependencies in the kernel, so that e. g. linearizations are justified. Such approximations often lead in turn to time–fractional equations.
Before going into the details of nonlinear reaction–subdiffusion, an alternative general derivation of linear reaction–subdiffusion equations will be given. In addition, the solution to the general Dirichlet boundary value problem for degrading particles under subdiffusion is presented. It turns out that this solution can be expressed in terms of the solution to the same boundary value problem for subdiffusion without degradation discussed in chapter five.
Chapter seven considers the simplest nonlinear reaction that accounts for front solutions, $A + B \rightarrow 2A$, under subdiffusion. The respective reaction–subdiffusion equations are derived, and the characteristics of the resultant front of A–particles propagating into the domain of B–particles, the most important of which is the front velocity, are investigated by analytic and numerical means. The analytic methods used here are adopted from those used in the corresponding normal reaction–diffusion analogue. It has to be stressed that these methods rely on assumptions for which proofs are still lacking, e.g. that the emerging fronts are pulled ones and that the memory does not qualitatively change the stability or relaxation behavior. Although we are far from a rigorous mathematical analysis, strong evidence is found for the front width and velocity decaying with time as $t^{\frac{\alpha-1}{2}}$. These findings may provide a good starting point for mathematicians to go deeper into the subject of propagating fronts under subdiffusion. Some first efforts in this direction were made by Nec et al. [36]. Moreover, a second interesting regime is found where the continuous reaction–subdiffusion picture breaks down. This fluctuation dominated regime corresponds to the final large time asymptotics, and exhibits atomically sharp fronts whose velocity decays even faster than in the continuous regime.

Another nonlinear reaction–subdiffusion system that is strongly motivated by recent experiments [37] will be examined in chapter eight. These experiments pertain the anomalously slow diffusion of a quencher A into a polyelectrolyte multilayer containing a fluorescent marker B.

From a supply at a fixed boundary, reactants A penetrate the medium initially filled with immobile reactants B and react according to the scheme $A + B \rightarrow (inert)$. Under certain circumstances, this problem can be described in terms of a moving boundary problem for the concentration of species A, the so–called Stefan–problem [38, 39]. The asymptotic A–profiles and the temporal behavior of the position of the moving boundary are the object of investigation.
The last chapter gives a conclusion of the gained knowledge.

The appendices contain supplements and details of calculations that would have interrupted the flow of reading. They will be referred to at the respective passages of the text. Each of the appendices belongs to one chapter of the work and may comprise several consecutive sections that are not specifically numbered. Appendix A corresponds to chapter two, B to chapter three, C to five, D to seven and appendix E to chapter eight.
A glossary is supplied at the end of this exposition.

2 Mathematical Foundations

In the following, the basic mathematical tools that will be used in the course of this exposition will be presented. First, the issue of integral transforms will be addressed, in particular the Mellin–, the Fourier– and the Laplace transform. Then, a brief definition and a compilation of the most important rules of fractional calculus will be given. In the continuum description of subdiffusion processes the Mittag–Leffler functions and the more general class of Fox's H–functions are ubiquitous. Since these function classes are not commonly known, the respective definitions, main properties and relations will presented in the last part of this section.

2.1 Integral Transforms

An integral transform of a function $f(x)$ with transform parameter y is defined as

$$\mathcal{I}\{f(x),y\} = \int_{x_1}^{x_2} K(x,y) f(x)\, dx \,.$$

Depending on the kernel K there is a large variety of integral transforms, such as Bessel transforms, Hankel transforms etc. [40, 41]. In the following, three basic integral transforms are briefly presented that will be of tremendous use in this work. Especially the Fourier– and Laplace transforms find a broad range of application, e.g. in probability theory or in the solution of partial differential equations.

2.1.1 Mellin Transform

The Mellin-transform of a function $f(t)$, $t \in \mathbb{R}$ with $t \geq 0$ with parameter $s \in \mathbb{C}$ is defined as:

$$\mathcal{M}\{f(t),s\} = \bar{f}(s) = \int_0^\infty t^{s-1} f(t)\, dt \,. \tag{2.1}$$

The inversion formula for the Mellin-transform is

$$\mathcal{M}^{-1}\left\{\bar{f}(s),t\right\} = \frac{1}{2\pi \mathrm{i}} \int_{c-\mathrm{i}\infty}^{c+\mathrm{i}\infty} t^{-s} f(s)\, ds \,. \tag{2.2}$$

A shift theorem of the Mellin transform follows from the definition (2.1) [40, 42],

$$\mathcal{M}\{t^\nu f(t),s\} = \bar{f}(s+\nu) \,. \tag{2.3}$$

Taking powers of the variable results in scaling of the argument of the transformed expression,

$$\mathcal{M}\{f(\lambda t^{\nu}), s\} = \nu^{-1}\lambda^{-\frac{s}{\nu}}\bar{f}\left(\frac{s}{\nu}\right), \tag{2.4}$$

$$\mathcal{M}\{f(\lambda t^{-\nu}), s\} = \nu^{-1}\lambda^{\frac{s}{\nu}}\bar{f}\left(-\frac{s}{\nu}\right), \tag{2.5}$$

where $\lambda > 0,\ \nu > 0$ [40].

2.1.2 Fourier Transform

The Fourier-transform of a function $f(x)$, $x \in \mathbb{R}$ with parameter $k \in \mathbb{R}$ is

$$\mathcal{F}\{f(x), k\} = \hat{f}(k) = \int_{-\infty}^{\infty} e^{\mathrm{i}kx} f(x)\, dx\,. \tag{2.6}$$

The respective inverse transform is given by

$$\mathcal{F}^{-1}\left\{\hat{f}(k), x\right\} = \frac{1}{2\pi}\int_{-\infty}^{\infty} e^{-\mathrm{i}kx}\hat{f}(k)\, dk\,, \tag{2.7}$$

Differentiation

Differentiation in original domain corresponds to multiplication with the Fourier parameter in Fourier domain, hence

$$\mathcal{F}\left\{\frac{\partial^n}{\partial x^n} f(x), k\right\} = (\mathrm{i}k)^n \hat{f}(k) \tag{2.8}$$

for n–fold derivatives.

Convolution theorem

The Fourier-transform of a convolution is, up to a factor, equal to the product of the Fourier transforms of the convolution factors,

$$\mathcal{F}\{f_1(x) * f_2(x), k\} = 2\pi\hat{f}_1(k)\hat{f}_2(k)\,. \tag{2.9}$$

2.1.3 Laplace Transform

The Laplace transform relates a given original function $f(t)$, $t \in \mathbb{R}$ and $t \geq 0$, to an image function where $u \in \mathbb{C}$:

$$\mathcal{L}\{f(t),u\} = \tilde{f}(u) = \int_0^\infty e^{-ut} f(t)dt \ . \tag{2.10}$$

The domains of t and u will be referred to as original domain and Laplace-domain, respectively. For the sake of convergence, it has to be assumed that the original function is piecewise steady and infinitely differentiable and tends to infinity not faster than $e^{\beta t}$ with $\beta > 0$ [43]. The inverse Laplace transform is given by

$$\mathcal{L}^{-1}\left\{\tilde{f}(u),t\right\} = \frac{1}{2\pi \mathrm{i}} \int_{c-\mathrm{i}\infty}^{c+\mathrm{i}\infty} e^{ut} \tilde{f}(u)du = f(t) \ . \tag{2.11}$$

This integral is often referred to as Bromwich–Integral and yields the inverse Laplace transform $f(t)$ for $t > 0$. The contour of integration (Bromwich contour) is a parallel line with respect to the imaginary axis where the constant c has to be chosen such that all singularities are located at the left of this parallel.
The relation between the original function and the respective image function will be denoted by the symbols "$\fallingdotseq$" and "$\risingdotseq$". Hence, $f(t) \fallingdotseq \tilde{f}(u)$ and $\tilde{f}(u) \risingdotseq f(t)$.
In the following, some important properties of the Laplace transform are listed [40, 44]. These properties provide the basis for the broad applicability of the Laplace transform, especially in the solution of initial value problems for differential– and some types of integro–differential equations.

Shift theorem

An exponential factor in original domain corresponds to a shift in the Laplace variable u,

$$\mathcal{L}\left\{e^{-at} f(t),u\right\} = \tilde{f}(u+a) \ . \tag{2.12}$$

Integration and Differentiation

Differentiation in original domain corresponds to multiplication with the Laplace variable u, integration in original domain results in division by u,

$$\mathcal{L}\left\{\frac{\partial^n}{\partial t^n} f(t),u\right\} = u^n \tilde{f}(u) - \sum_{l=0}^{n-1} u^l \left[\frac{\partial^{(n-1-l)} f(t)}{\partial t^{(n-1-l)}}\right]_{t\to 0} \tag{2.13}$$

$$\mathcal{L}\left\{\int_0^t f(t')dt', u\right\} = \frac{1}{u}\tilde{f}(u) \ . \tag{2.14}$$

Convolution theorem

The Laplace transform of a convolution is, equal to the product of the Laplace transforms of the convolution factors,

$$\mathcal{L}\{f_1(t) * f_2(t), u\} = \tilde{f_1}(u) \cdot \tilde{f_2}(u) \ . \tag{2.15}$$

Abelian and Tauberian theorem

The inversion of the Laplace transform can turn out to be involved, if not impossible. However, in many applications it suffices to know the asymptotic behavior of a function or its Laplace transform so that explicitly carrying out the transform or inversion is not necessary. The connection between the asymptotic behavior of a function and its Laplace transform is given by the related Abelian and Tauberian theorems [44]. The Abelian theorem states that if the asymptotic behavior of $f(t)$, $t \to \infty$ is given by

$$f(t) \sim t^{\alpha} \ , \tag{2.16}$$

the asymptotic behavior $u \to 0$ of the Laplace transform is

$$\tilde{f}(u) \sim \frac{\Gamma(1+\alpha)}{u^{1+\alpha}} \ . \tag{2.17}$$

Conversely, if $\tilde{f}(u)$ has the asymptotic form

$$\tilde{f}(u) \sim \frac{\Gamma(1+\alpha)}{u^{\alpha+1}} \ , \tag{2.18}$$

and if $f(t)$ is bounded, we have

$$\int_0^t f(t')dt' \sim \frac{t^{\alpha+1}}{\alpha+1} \ . \tag{2.19}$$

2.2 The Riemann–Liouville Fractional Integral and Derivative

Historically, the idea of the generalization of the notion of differentiation to noninteger orders of differentiation came up with the beginnings of differential calculus itself. The first record of such an idea is in the correspondence of Leibniz (1695), where some remarks were made concerning the possibility of order $1/2$ derivatives. The modern formulations basically go back to works of Liouville in the years 1832-1837, and to works of Riemann from 1847 on [45]. Since then, the theory of fractional integro-differentiation has been developed further by Holmgren, Grünwald,

Letnikov, Hardy, Riesz, Weyl, Erdélyi, and others. There is a large variety of definitions of fractional derivatives, accounting for e.g. the domain or periodicity of the functions they are applied to. We restrict ourselves to the definition that is related to the description of time-fractional diffusion processes, namely the Riemann–Liouville fractional derivative. Moreover, we shall use only the left Riemann–Liouville derivative, i.e. the one with a fixed lower terminal indicating the time of preparation of the system. This choice accounts for the causality of physical processes, since only a left fractional derivative constitutes an operation on the past states of the system under consideration. A survey of other definitions of fractional derivatives and integrals is given e.g. in [46, 45].

2.2.1 Definition

The Cauchy-formula for the n-fold iterated integration of a function $f(t)$, $n \in \mathbb{N}$, reads [42]

$$f^{(-n)}(t) = \frac{1}{\Gamma(n)} \int_{t_0}^{t} \frac{1}{(t-t')^{1-n}} f(t')dt' \ , \tag{2.20}$$

which can be generalized by introducing the α-fold Riemann–Liouville–integral,

$${}_{t_0}\mathrm{D}_t^{-\alpha} f(t) = \frac{1}{\Gamma(\alpha)} \int_{t_0}^{t} \frac{1}{(t-t')^{1-\alpha}} f(t')dt' \ , \tag{2.21}$$

where $\alpha \in \mathbb{R}$ and $\alpha > 0$. The Riemann-Liouville fractional integration ${}_{t_0}\mathrm{D}_t^{-\alpha} f(t)$ hence corresponds to a (Laplace type) convolution with $f(t) * t^{\alpha-1}/\Gamma(\alpha)$.

Applying n-fold differentiation, $n \in \mathbb{N}$ and $n - \alpha > 0$, yields the $(n-\alpha)$-fold fractional derivative of $f(t)$:

$${}_{t_0}\mathrm{D}_t^{n-\alpha} f(t) = \frac{1}{\Gamma(\alpha)} \frac{d^n}{dt^n} \int_{t_0}^{t} \frac{1}{(t-t')^{1-\alpha}} f(t')dt' \ , \tag{2.22}$$

where $0 < \alpha < 1$. With $t_0 = 0$ and the substitution $n - \alpha = \nu$, we have

$${}_{t_0}\mathrm{D}_t^{\nu} f(t) = \frac{1}{\Gamma(n-\nu)} \frac{d^n}{dt^n} \int_{t_0}^{t} \frac{1}{(t-t')^{1-n+\nu}} f(t')dt' \ . \tag{2.23}$$

The operator ${}_{t_0}\mathrm{D}_t^{\nu}$ is referred to as the Riemann-Liouville operator.

2.2.2 Properties and Relations

Laplace Transform

The Laplace transform of a fractional Riemann–Liouville integral results in

$$\mathcal{L}\{{}_0\mathrm{D}_t^{-\alpha} f(t)\} = u^{-\alpha}\tilde{f}(u)\ , \tag{2.24}$$

and the Laplace transform of a Riemann-Liouville fractional derivative yields

$$\mathcal{L}\{{}_0\mathrm{D}_t^{\nu} f(t)\} = u^{\nu}\tilde{f}(u) - \sum_{l=0}^{n-1} u^l \left[{}_0\mathrm{D}_t^{\nu-1-l} f(t)\right]_{t=0}\ , \tag{2.25}$$

with $n-1 < \nu < n$.

Linearity

Fractional differ–integration is a linear operation,

$${}_{t_0}\mathrm{D}_t^{\nu}(\lambda_1 f_1(t) + \lambda_2 f_2(t)) = \lambda_1 {}_{t_0}\mathrm{D}_t^{\nu} f_1(t) + \lambda_2 {}_{t_0}\mathrm{D}_t^{\nu} f_2(t)\ . \tag{2.26}$$

Composition Rules

In general, the Riemann–Liouville operators do not commute. The composition rules are as follows [42]: For $m-1 \le \mu < m$ and $n-1 \le \nu < n$ we have

$${}_{t_0}\mathrm{D}_t^{\mu}({}_{t_0}\mathrm{D}_t^{\nu} f(t)) = {}_{t_0}\mathrm{D}_t^{\nu+\mu} f(t) - \sum_{l=1}^{m} \left[{}_{t_0}\mathrm{D}_t^{\nu-l} f(t)\right]_{t=t_0} \frac{(t-t_0)^{-\mu-l}}{\Gamma(1-\mu-l)}\ . \tag{2.27}$$

By interchanging μ and ν it becomes clear that the relation

$${}_{t_0}\mathrm{D}_t^{\mu}({}_{t_0}\mathrm{D}_t^{\nu} f(t)) = {}_{t_0}\mathrm{D}_t^{\nu+\mu} f(t) \tag{2.28}$$

only applies if

$$\left[{}_{t_0}\mathrm{D}_t^{\nu-l} f(t)\right]_{t=t_0} = 0, \qquad (l = 1,2,\ldots,n) \tag{2.29}$$

$$\left[{}_{t_0}\mathrm{D}_t^{\mu-l} f(t)\right]_{t=t_0} = 0, \qquad (l = 1,2,\ldots,m)\ . \tag{2.30}$$

In case of $f(t)$ having a sufficient number of continuous derivatives, these conditions are equivalent to

$$f^{(l)}(t_0) = 0, \qquad (l = 0,2,\ldots,n-1) \tag{2.31}$$

$$f^{(l)}(t_0) = 0, \qquad (l = 0,2,\ldots,m-1)\ . \tag{2.32}$$

The composition rules also imply that fractional differentiation and fractional integration are reciprocal operations.

Leibniz– and Chain Rule

The Leibniz-rule for fractional differentiation reads [42, 45]

$$\begin{aligned} {}_{t_0}\mathrm{D}_t^{\nu}\left[f_1(t)f_2(t)\right] &= \sum_{l=0}^{\infty}\binom{\nu}{l} f_1^{(l)}(t)\,{}_{t_0}\mathrm{D}_t^{\nu-l} f_2(t) \\ \text{with } \binom{\nu}{l} &= \frac{\Gamma(\nu+1)}{\Gamma(l+1)\Gamma(\nu-l+1)} \end{aligned} \tag{2.33}$$

or

$$\begin{aligned} {}_{t_0}\mathrm{D}_t^{\nu}\left[f_1(t)f_2(t)\right] &= \sum_{l=-\infty}^{\infty}\binom{\nu}{l+\mu}\left[{}_{t_0}\mathrm{D}_t^{\nu-\mu-l} f_1(t)\right]\left[{}_{t_0}\mathrm{D}_t^{\mu+l} f_2(t)\right] \\ \text{with } \binom{\nu}{l+\mu} &= \frac{\Gamma(\nu+1)}{\Gamma(l+\mu+1)\Gamma(\nu-l-\mu+1)} \end{aligned} \tag{2.34}$$

with $\nu,\mu \in \mathbb{R}$, μ non–integer.
The overview of fractional calculus is completed by the chain rule,

$${}_{t_0}\mathrm{D}_t^{\nu}\left[f(g(t))\right] = \sum_{l=0}^{\infty}\binom{\nu}{l}\left({}_{t_0}\mathrm{D}_t^{\nu-l}1\right)\left({}_{t_0}\mathrm{D}_t^{l}\left[f(g(t))\right]\right), \tag{2.35}$$

which produces an infinite sum of integer order differentiations.

2.3 Special Functions

This section introduces some special functions that will prove very useful in the description of systems involving subdiffusive transport. The Mittag–Leffler function is a generalization of the exponential function and plays a role e.g. in anomalous relaxation patterns. The Fox H-functions arise e.g. in probability theory as probability densities.

2.3.1 The Mittag–Leffler Functions of One and Two Parameters

Definition

The Mittag–Leffler Function of two parameters α and β is defined as follows [42, 47]:

$$\mathrm{E}_{\alpha,\beta}(z) = \sum_{n=0}^{\infty} \frac{z^n}{\Gamma(\alpha n + \beta)} \tag{2.36}$$

with $\alpha > 0, \beta > 0$. As a special case, $\beta = 1$ yields the Mittag–Leffler Function of one parameter. The Mittag–Leffler Function of two parameters is often referred to as the generalized Mittag–Leffler Function.

Laplace–Transform

For the generalized Mittag–Leffler Function, the following relation holds [41]:

$$\mathcal{L}\left\{t^{\beta-1}\mathrm{E}_{\alpha,\beta}(\lambda t^{\alpha})\right\} = \frac{u^{\alpha-\beta}}{u^{\alpha}-\lambda}\,, \tag{2.37}$$

$\left|\frac{\lambda}{u^{\alpha}}\right| < 1$. Consequently, the Laplace Transform of the Mittag–Leffler Function of one parameter is:

$$\mathcal{L}\{\mathrm{E}_{\alpha}(\lambda t^{\alpha})\} = \frac{u^{\alpha-1}}{u^{\alpha}-\lambda}\,. \tag{2.38}$$

Examples

$$\begin{aligned}
\mathrm{E}_1(\lambda t) &= \exp[\lambda t] \\
\mathrm{E}_2(\lambda t) &= \cosh\left[\sqrt{\lambda t}\right] \\
\mathrm{E}_{1/2}(\lambda t^{1/2}) &= \frac{2}{\sqrt{\pi}} \exp\left[-\lambda^2 t\right] \mathrm{erfc}\left[-\lambda t^{\frac{1}{2}}\right]
\end{aligned}$$

Asymptotics

The Mittag–Leffler function interpolates between the stretched exponential behavior for small arguments,

$$\mathrm{E}_{\alpha}\left(-\left(\frac{t}{\tau}\right)^{\alpha}\right) \sim \exp\left[-\frac{t^{\alpha}}{\tau^{\alpha}\Gamma(1+\alpha)}\right], \tag{2.39}$$

and the power law pattern for large arguments,

$$\mathrm{E}_{\alpha}\left(-\left(\frac{t}{\tau}\right)^{\alpha}\right) \sim \frac{1}{\Gamma(1-\alpha)}\left(\frac{t}{\tau}\right)^{-\alpha}\,, \tag{2.40}$$

see Fig. 2.1.

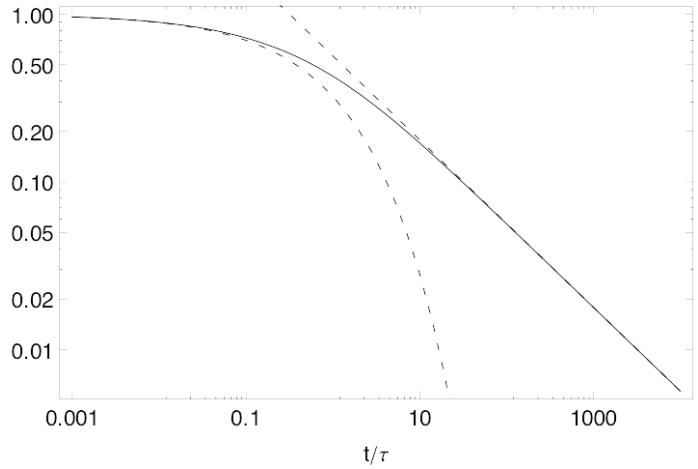

Figure 2.1: The Mittag–Leffler function $E_{1/2}$ (solid line); the stretched exponential and power law asymptotics for small and large arguments, respectively (dashed lines).

Fractional–order integration and differentiation

A general relationship for the fractional–order differentiation of the generalized Mittag–Leffler Function is [42]:

$$ {}_0D_t^{\nu}\left(t^{\beta-1}E_{\alpha,\beta}(\lambda t^{\alpha})\right) \quad = \quad t^{\beta-\nu-1}E_{\alpha,\beta-\nu}(\lambda t^{\alpha}) \; . \tag{2.41} $$

The fractional–order integration of the generalized Mittag–Leffler Function is [42]

$$ {}_0D_t^{-\nu}\left(t^{\beta-1}E_{\alpha,\beta}(\lambda t^{\alpha})\right) \quad = \quad t^{\beta+\nu-1}E_{\alpha,\beta+\nu}(\lambda t^{\alpha}) \; , \tag{2.42} $$

which can be proven by means of the term–by–term integration of the Series (2.36). In particular, for $\beta = 1$, $\nu = \alpha$, we find

$$ {}_0D_t^{-\alpha}E_{\alpha}(\lambda t^{\alpha}) \quad = \quad t^{\alpha}E_{\alpha,1+\alpha}(\lambda t^{\alpha}) \; . \tag{2.43} $$

2.3.2 The Fox's *H*-Functions

Although integrals of Mellin-Barnes-type have already been investigated from around 1900 on, e.g. by Pincherle (1888), Mellin (1910) and Barnes (1908), and others, it was Charles Fox (1961) [48] who defined the H-function in terms of a general integral of Mellin-Barnes type in his works on symmetrical Fourier kernels. The importance of the Fox-H-functions is based on the fact that they comprise nearly all special functions appearing in applied statistics and mathematics [49, 50]. Some examples are Maitland's generalized hypergeometric function, the Mittag-Leffler function, Mac-Robert's E-function, Meijer's G-function or Wright's generalized Bessel function.

Definition

We use the notation

$$H_{p,q}^{m,n}(x) = H_{p,q}^{m,n}(x)\left[x \left| \begin{array}{l}(a_p, A_p)\\(b_q, B_q)\end{array}\right.\right] \tag{2.44}$$

$$= H_{p,q}^{m,n}(x)\left[x \left| \begin{array}{l}(a_1, A_1), (a_2, A_2), \ldots (a_p, A_p)\\(b_1, B_1), (b_2, B_2) \ldots (b_q, B_q)\end{array}\right.\right]. \tag{2.45}$$

The H-Function is defined via the Mellin-Barnes type integral [49, 50]

$$\begin{aligned} H_{p,q}^{m,n}(x) &= \frac{1}{2\pi \mathrm{i}} \int_L \Xi(s) x^s ds \quad \text{with} \\ \Xi(s) &= \frac{\prod_{l=1}^{m} \Gamma(b_l - B_l s) \prod_{l=1}^{n} \Gamma(1 - a_l + A_l s)}{\prod_{l=n+1}^{q} \Gamma(1 - b_l + B_l s) \prod_{l=m+1}^{p} \Gamma(a_l - A_l s)} \end{aligned} \tag{2.46}$$

where the m, n, p, q are non-negative integers throughout this section; $0 \le n \le p$, $1 \le m \le q$. The A_l $(l = 1, \ldots, p)$, B_l $(l = 1, \ldots, q)$ are positive real numbers. The a_l $(l = 1, \ldots, p)$ and b_l $(l = 1, \ldots, q)$ are complex and satisfy the relation $A_{l_1}(b_{l_2} + n_1) \neq B_{l_2}(a_{l_1} - n_2 - 1)$ for all $n_1, n_2 = 0, 1, 2, \ldots$, $l_1 = 1, \ldots, n$, $l_2 = 1, \ldots, m$. The contour L separates the poles of $\Gamma(b_l - B_l s)$ from those of $\Gamma(1 - a_l + A_l s)$. The H-function is analytic in x and exists if either $x \neq 0$ and $c_\mu = \sum_{l=1}^{q} B_l - \sum_{l=1}^{p} A_l > 0$, or $0 < x < \left(\prod_{l=1}^{p} A_l^{A_l} \prod_{l=1}^{q} B_l^{-B_l}\right)^{-1}$ and $c_\mu = \sum_{l=1}^{q} B_l - \sum_{l=1}^{p} A_l = 0$. In the following some useful properties of the H-function are listed [50].

Properties and Relations

- The H-function is symmetric in the parameter pairs $(a_1, A_1) \ldots (a_n, A_n)$, $(a_{n+1}, A_{n+1}) \ldots (a_p, A_p)$, in $(b_1, B_1 \ldots (b_m, B_m)$ and in $(b_{m+1}, B_{m+1}) \ldots (b_q, B_q)$.
- If one of the (a_l, A_l) with $l = 1, \ldots, n$ is equal to one of the (b_l, B_l) with $l = n + 1, \ldots q$, the order of the H-function reduces. The same applies for one of the (b_l, B_l),

$l = 1,\dots m$ and one of the (a_l, A_l) with $l = m+1,\dots p$ equal. As a consequence, p, q, and n or m decrease by unity so that we obtain the reduction formula

$$H^{m,n}_{p,q}(x)\left[x\left|\begin{array}{l}(a_1,A_1),(a_2,A_2),\dots(a_p,A_p)\\(b_1,B_1),(b_2,B_2)\dots(b_{q-1},B_{q-1}),(a_1,A_1)\end{array}\right.\right] \tag{2.47}$$

$$= H^{m,n-1}_{p-1,q-1}(x)\left[x\left|\begin{array}{l}(a_2,A_2),\dots(a_p,A_p)\\(b_1,B_1),\dots(b_{q-1},B_{q-1})\end{array}\right.\right] \tag{2.48}$$

as long as $n \geq 1$ and $q > m$.

- An H-function of argument x can be transformed to an H-function with argument $1/x$,

$$H^{m,n}_{p,q}(x)\left[x\left|\begin{array}{l}(a_p,A_p)\\(b_q,B_q)\end{array}\right.\right] = H^{n,m}_{q,p}(x)\left[\frac{1}{x}\left|\begin{array}{l}(1-b_q,B_q)\\(1-a_p,A_p)\end{array}\right.\right]. \tag{2.49}$$

  The constant $c_\mu = \sum_{l=1}^{q} B_l - \sum_{l=1}^{p} A_l$ changes sign in this transformation.

- For $\rho > 0$,

$$\frac{1}{\rho}H^{m,n}_{p,q}(x)\left[x\left|\begin{array}{l}(a_p,A_p)\\(b_q,B_q)\end{array}\right.\right] = H^{m,n}_{p,q}(x)\left[x^\rho\left|\begin{array}{l}(a_p,\rho A_p)\\(b_q,\rho B_q)\end{array}\right.\right]. \tag{2.50}$$

- For the multiplication of an H-function with a power we have

$$x^\varsigma H^{m,n}_{p,q}(x)\left[x\left|\begin{array}{l}(a_p,A_p)\\(b_q,B_q)\end{array}\right.\right] = H^{m,n}_{p,q}(x)\left[x\left|\begin{array}{l}(a_p+\varsigma A_p,A_p)\\(b_q+\varsigma B_q,B_q)\end{array}\right.\right]. \tag{2.51}$$

Laplace transform of the *H*-function

The Laplace transform of an H-function of argument t with transform parameter u is given by [49]

$$\mathcal{L}\left\{H_{p,q}^{m,n}(t),u\right\} = \frac{1}{u}\begin{cases} H_{q,p+1}^{n+1,m}\left[u\,\middle|\,\begin{matrix}(1-b_q,B_q)\\(1,1),(1-a_p,A_p)\end{matrix}\right] & \text{for } 0\le c_\mu\le 1 \\ H_{p+1,q}^{m,n+1}\left[\frac{1}{u}\,\middle|\,\begin{matrix}(0,1),(a_p,A_p)\\(b_q,B_q)\end{matrix}\right] & \text{for } c_\mu\ge 1\,. \end{cases} \tag{2.52}$$

The corresponding inverse transform results in

$$\mathcal{L}^{-1}\left\{H_{p,q}^{m,n}(u),t\right\} = \frac{1}{t}\begin{cases} H_{q,p+1}^{n,m}\left[t\,\middle|\,\begin{matrix}(1-b_q,B_q)\\(1-a_p,A_p),(1,1)\end{matrix}\right] & \text{for } 0\le c_\mu\le 1 \\ H_{p+1,q}^{m,n}\left[\frac{1}{t}\,\middle|\,\begin{matrix}(a_p,A_p),(0,1)\\(b_q,B_q)\end{matrix}\right] & \text{for } c_\mu\ge 1\,. \end{cases} \tag{2.53}$$

Fractional Differentiation

The application of the fractional Riemann-Liouville operator on an H-function results in

$${}_0\mathrm{D}_x^\nu\left(x^\gamma H_{p,q}^{m,n}\left[\lambda x^\mu\,\middle|\,\begin{matrix}(a_p,A_p)\\(b_q,B_q)\end{matrix}\right]\right) = x^{\gamma-\nu}H_{p+1,q+1}^{m,n+1}\left[(\lambda x)^\mu\,\middle|\,\begin{matrix}(-\gamma,\mu),(a_p,A_p)\\(b_q,B_q),(\nu-\gamma,\mu)\end{matrix}\right], \tag{2.54}$$

where $\nu\in\mathbb{R}$, and $\gamma,\mu>0$ are restricted to $\gamma+\mu\min(b_l/B_l)>-1$ for the $1\le l\le m$.

Special Cases/ Examples

For functions involving exponentials, the following H-function representation often proves useful:

$$x^a e^{-x} = H_{0,1}^{1,0}\left[x\middle|(a,1)\right]\,. \tag{2.55}$$

The Mittag- Leffler functions can be expressed as follows [41]

$$\mathrm{E}_{\alpha,\beta}(x) = H_{1,2}^{1,1}\left[-x\,\middle|\,\begin{matrix}(0,1)\\(0,1),(1-\beta,\alpha)\end{matrix}\right] \tag{2.56}$$

for real $\alpha \geq 0$ and $\beta \in \mathbb{C}$.

When $A_1 = \ldots = A_p = 1 = B_1 = \ldots = B_q$, the H-function reduces to a Meijer G-function [41],

$$H_{p,q}^{m,n}\left[z \left| \begin{array}{c} (a_p, 1) \\ (b_q, 1) \end{array} \right.\right] = G_{p,q}^{m,n}\left[z \left| \begin{array}{c} a_p \\ b_q \end{array} \right.\right]. \tag{2.57}$$

For rational A_l and B_l it is always possible to express the H-function in terms of a Meijer G-function: transform the Mellin-variable s in (2.46) by division with the common denominator of all the A_l and B_l. The new coefficients A'_l, B'_l of the new Mellin-variable s' are then positive integers. The resultant Gamma functions can be expanded by means of the multiplication formula, see Appendix A, so that in the end the coefficients of s' are all one. In contrast to the more general H-function, the G-function is implemented in MATHEMATICA [51]. Hence, this procedure may be of practical use especially in cases where the common denominator of the A_l and B_l is small.

3 Sums of Independent Random Variables: Random Walks

3.1 Moment Generating Functions

Let P be the distribution of a random variable X that can take all values of the real line. The corresponding distribution function $P(x)$ is a never decreasing function which is zero at $-\infty$ and one at ∞. For continuous distributions we have

$$P(x) = Prob\{X \leq x\} = \int_{-\infty}^{x} p(x')\,dx' \;, \tag{3.1}$$

where $p(x)$ is the respective probability density function (pdf).
The characteristic function of a distribution $P(x)$, $x \in (-\infty, \infty)$ is defined as the expectation [52, 53]

$$\left\langle e^{\mathrm{i}kx} \right\rangle \;=\; \int_{-\infty}^{\infty} \exp[\mathrm{i}kx]\,dP(x) \;. \tag{3.2}$$

The characteristic function of a distribution is hence the Fourier-transform of the respective probability density $p(x)$, and will be denoted by $\hat{p}(k)$. Thus,

$$\hat{p}(k) \;=\; \int_{-\infty}^{\infty} p(x)\exp[\mathrm{i}kx]\,dx \tag{3.3}$$

when x is continuous and

$$\hat{p}(k) \;=\; \sum_{x=-\infty}^{\infty} p(x)\exp[\mathrm{i}kx] \tag{3.4}$$

for discrete random variables x, for which the $p(x)$ are probabilities rather than densities. Note that the corresponding inversion formulas differ only by the limits of integration,

$$p(x) = \frac{1}{2\pi}\int_{-\infty}^{\infty}\hat{p}(k)\exp[-\mathrm{i}kx]\,dk \quad \text{for continuous, and} \tag{3.5}$$

$$p(x) = \frac{1}{2\pi}\int_{-\pi}^{\pi}\hat{p}(k)\exp[-\mathrm{i}kx]\,dk \quad \text{for discrete random variables.} \tag{3.6}$$

For non-negative independent continuous variables such as time t, it is more convenient to consider the expectation of the kernel of the Laplace transform in order to derive the characteristic function. For an arbitrary pdf $p(t)$, $t \geq 0$,

$$\begin{aligned}\left\langle e^{-ut}\right\rangle &= \int_0^{\infty}\exp[-ut]\,dP(t) = \\ \tilde{p}(u) &= \int_0^{\infty}p(t)\exp[-ut]\,dt\,.\end{aligned} \tag{3.7}$$

As will be seen later, the characteristic functions are of tremendous use since they allow for exact representations of many functions that characterize the solutions of problems in probability theory. Especially in problems involving sums of random variables, e.g. in Random walks, very complicated representations of the resultant pdfs in terms of convolution integrals are converted to products of the characteristic functions of each of the component variables.
If the characteristic function of a pdf is known, it is possible to extract the moments in a straightforward manner. Therefore the characteristic functions are sometimes referred to as the moment–generating functions. Let us define the nth moment M_n of a pdf $p(x)$ of the variable $-\infty < x < \infty$ and of a one-sided pdf $p(t)$ with $0 \leq t < \infty$, respectively,

$$\langle x^n\rangle = \int_{-\infty}^{\infty}x^n p(x)\,dx \tag{3.8}$$

$$\langle t^n\rangle = \int_0^{\infty}t^n p(t)\,dt\,. \tag{3.9}$$

Expanding the Fourier– and Laplace transforms of $p(x)$ and $p(t)$, respectively, we have

$$\hat{p}(k) = \int_{-\infty}^{\infty}\sum_{n=0}^{\infty}\frac{(\mathrm{i}kx)^n}{n!}p(x)\,dx = \sum_{n=0}^{\infty}\frac{\mathrm{i}^n k^n}{n!}\langle x^n\rangle \tag{3.10}$$

$$\tilde{p}(u) = \int_0^{\infty}\sum_{n=0}^{\infty}\frac{(-ut)^n}{n!}p(t)\,dt = \sum_{n=0}^{\infty}\frac{(-u)^n}{n!}\langle t^n\rangle\,, \tag{3.11}$$

provided that $\langle x^n\rangle$, $\langle t^n\rangle$ are finite, so that the moments arise from the respective derivatives of the moment generating functions where the argument is put to zero, i.e.

$$M_{n,x} = \frac{1}{\mathrm{i}^n} \frac{\partial^n}{\partial k^n} \hat{p}(k)|_{k=0} \tag{3.12}$$

for two-sided distributions and

$$M_{n,t} = (-1)^n \frac{\partial^n}{\partial u^n} \tilde{p}(u)|_{u=0} \tag{3.13}$$

for one-sided distributions. All pdfs are normalized, i.e. the zeroth moment is always one, $M_0 = 1$. The set of integer moments is frequently used in order to characterize a distribution. However, the integer moments of a distribution are not necessarily finite. For such distributions one can define moments of arbitrary order $\langle x^\nu \rangle$ for ν real [54].

In the following section we will encounter distribution functions where the generating function is not analytic, i.e. cannot be described by a polynomial. An example for such cases is the Cauchy–distribution [55],

$$p(x) = \frac{b}{\pi(b^2 + x^2)} \tag{3.14}$$

with the characteristic function

$$\hat{p}(k) = \exp\left[-b|k|\right] , \tag{3.15}$$

which possesses no integer moment except for the zeroth, but all moments of order $\nu < 1$. The Smirnov distribution is an example for a one–sided distribution with the pdf [55]

$$p(t) = \frac{1}{2\sqrt{\pi}} x^{-3/2} \exp\left[-\frac{1}{2x}\right] \tag{3.16}$$

$$\tilde{p}(u) = \exp\left[-\sqrt{\frac{u}{2}}\right] . \tag{3.17}$$

Note that the fractional moments of the one–sided distributions can be obtained by taking the Riemann–Liouville fractional derivative of the generating function in $u = 0$, so that in analogy to (3.13)

$$\langle t^\nu \rangle = (-1)^n \, {}_0\mathrm{D}_u^\nu \tilde{p}(u)\Big|_{u=0} , \tag{3.18}$$

with $n - 1 < \nu < n$ [54].

3.2 Stable Distributions

In this section we adhere to some basic definitions and properties of stable densities. Mathematically more rigorous and extensive expositions can be found in [56, 57, 52, 53, 55]. The distribution P is a stable one if for any $c_1, c_2 > 0$ and γ_1, γ_2 there exist constants $c > 0$ and γ for which [53]

$$P(c_1 x + \gamma_1) * P(c_2 x + \gamma_2) = P(cx + \gamma) \; . \tag{3.19}$$

This means that stable distributions are closed under convolution, so that a sum of random variables x obeying stable distributions of the common family belongs to the same family of distributions. Distributions P_1, P_2 belong to the same family if there exist constants $c > 0, \gamma$ for which $P_1(cx + \gamma) = P_2(x)$ [57]. It suffices to consider $\gamma_1, \gamma_2 = 0$, so that in terms of characteristic functions the relation (3.19) is equivalent to

$$\hat{p}(k/c_1)\hat{p}(k/c_2) = \hat{p}(k/c)e^{-\mathrm{i}k\gamma} \; . \tag{3.20}$$

Moreover, if in addition $\gamma = 0$, the distribution is called strictly stable.

The distribution of a sum of random variables is given by the convolution of the distributions of the random variables. Due to the convolution theorems of Fourier- and Laplace transform, this results in the multiplication of the respective moment generating functions. In the following we make use of this advantageous feature.
For a distribution P to be stable it is necessary and sufficient that P be infinitely divisible [53]. A distribution P is said to be infinitely divisible if there exists a distribution P_n for which

$$P = P_n^{*n} \tag{3.21}$$

for each n, the exponent $*n$ denoting the n–fold convolution, so that the random variable can be expressed as a sum S_n of n iid random variables $x_{i,n}$. Together with the definition of stable distributions (3.19), the relation

$$S_n = \sum_{l=1}^{n} x_l \quad \stackrel{d}{=} \quad c_n x + \gamma_n \tag{3.22}$$

holds. The equality sign with superscript d denotes "equal in distribution".

Going to Fourier domain we find for the respective pdf $p(x)$

$$\hat{p}^n(k) = \hat{p}(c_n k)e^{\mathrm{i}k\gamma_n} \tag{3.23}$$

which can be resolved exactly and results in the characteristic function representation for stable

laws,

$$\log \hat{p}^{c,\gamma}_{\alpha,\beta}(k) = \mathrm{i}\gamma k - c|k|^{\alpha}\left[1 - \mathrm{i}\beta\frac{k}{|k|}\omega(k,\alpha)\right] \tag{3.24}$$

$$\tag{3.25}$$

with

$$\omega(k,\alpha) = \tan\left[\frac{\pi}{2}\alpha\right] \quad \text{for } \alpha \neq 1\ , \tag{3.26}$$

$$\omega(k,\alpha) = \frac{2}{\pi}\log|k| \quad \text{for } \alpha = 1\ . \tag{3.27}$$

Note that the norming constant in (3.22) can only be $c_n = n^{1/\alpha}$. The first expression (3.26) can always be reduced to the strictly stable laws by a constant shift of the random variable [1] [56]. The second one (3.27) represents a non-trivial generalization to distributions that cannot be reduced to strictly stable laws and hence are called "stable in the broad sense" [57].
The parameters γ and c are simply scale factors that effect a shift or a dilation, respectively, and hence irrelevant for the qualitative designation of the stable distribution under study. In particular, one can always write

$$p^{c,\gamma}_{\alpha,\beta}(x) = c^{-1/\alpha}p^{1,0}_{\alpha,\beta}\left(c^{-1/\alpha}(x-\gamma)\right) \tag{3.28}$$

so that only two important parameters remain, of which α is the characteristic exponent or Lévy-index, and β accounts for the skewness of the distribution. Thus, the Lévy stable laws are denoted by $L_{\alpha,\beta}$, where $0 < \alpha \leq 2$, $-1 < \beta < 1$. α characterizes the large x behavior of the distribution:

$$L_{\alpha,\beta} \simeq |x|^{-1-\alpha} \tag{3.29}$$

for $\alpha < 2$. For symmetric distributions, $\beta = 0$, whereas for the one-sided distributions we have $0 < \alpha < 1$ and β takes the values 1 if the pdf is concentrated on the positive and -1 if the pdf is concentrated on the negative half axis. Obviously we have

$$p_{\alpha,\beta}(-x) = p_{\alpha,-\beta}(x)\ . \tag{3.30}$$

The density of a stable law is given by the inverse Fourier transform of the expression (3.24). We note that in the case of one-sided distributions, $\beta = \pm 1$, it is often more practical to use the Laplace representation instead of applying the (one-sided) Fourier transform [58]. The respective pdfs of the one-sided Lévy-stable distributions $L_{\alpha,1}$ are the inverse Laplace transforms of

[1] For another representation of stable laws that often provides better manageability, cf. Appendix B.

$$\tilde{p}_{\alpha,1}(u) = \exp\left[-c^* u^\alpha\right] , \tag{3.31}$$

if u is the Laplace variable and $c^* = c/\cos\left(\frac{\pi\alpha}{2}\right)$, cp. (7) in Appendix B.

Stable distributions with characteristic exponent α possess absolute moments $\langle |x|^n \rangle$ of order $n < \alpha$. For $n > \alpha$ these moments are infinite. In particular, $L_{\alpha,\beta}$ possesses no variance if $\alpha < 2$.

Examples

The class of Lévy stable laws comprises some well known distribution functions. As $\omega(k,\alpha)$ in (3.24) vanishes for $\alpha = 2$, we obtain the Normal law

$$p_{2,0}(x) = \frac{1}{\sqrt{4\pi}} \exp\left[-\frac{x^2}{4}\right] . \tag{3.32}$$

Another example of a symmetric stable law is the Cauchy distribution

$$p_{1,0}(x) = \frac{1}{\pi(1+x^2)} . \tag{3.33}$$

A stable density encountered in astronomy which describes the distribution of the gravitational force in a stellar system of randomly distributed points with randomly varying masses, is the Holtsmark distribution where $\alpha = 3/2, \beta = 0$ [59, 52].
An example for a one sided stable distribution is the Smirnov-distribution

$$p_{1/2,1}(t) = \frac{1}{2\sqrt{\pi}} t^{-3/2} \exp\left[-\frac{1}{2t}\right] . \tag{3.34}$$

This density emerges as the limiting law of return times to the origin for a symmetrical one dimensional random walk.
However, for most Lévy–stable distributions a proper representation requires the use of generalized special functions. More precisely, the Lévy–stable laws are expressible in terms of Fox's H–functions, cf. 2.3.2. At this point, only two examples that will be of use later on shall be given. For a more general analytic expression of stable laws, cf. Appendix B. The Fox's H–function representation of the density of a symmetrical stable law $L_{\alpha,0}$, $1 < \alpha \leq 2$, is given by

$$p_{\alpha,0}(x) = \frac{1}{\alpha} H^{1,1}_{2,2}\left[x \,\middle|\, \begin{matrix} (1-1/\alpha, 1/\alpha) & (1/2,1/2) \\ (0,1) & (1/2,1/2) \end{matrix}\right] . \tag{3.35}$$

For $\alpha = 2$ this expression reduces to the Gaussian normal law.
The densities of one sided stable laws $L_{\alpha,1}$ with $0 < \alpha < 1$ corresponding to (3.31), have the analytical representation

$$p_{\alpha,1}(t^{-1}) = \frac{1}{\alpha} t^2 H^{1,0}_{1,1}\left[t \,\middle|\, \begin{matrix} (-1,1) \\ (-1/\alpha, 1/\alpha) \end{matrix}\right] . \tag{3.36}$$

3.3 Generalized Central Limit Theorem

As many physical quantities emerge from a large number of random events, it is important to examine the distributions of normed sums of independent random variables. Of particular interest are the possible asymptotic distributions of these sums of random variables and the preconditions for them to arise.
The classical central limit theorem (CLT) establishes conditions under which the asymptotic distribution of the normed sum of independent random variables is subject to a normal law. More specifically, the necessary and sufficient condition for the sum of independently identically distributed (iid) random variables to be asymptotically normally distributed is that the pdf of the random variable must not decay too slowly [58], which means in particular

$$\lim_{X\to\infty}\left(X^2\frac{\int_{|x|>X}p(x)dx}{\int_{|x|>X}x^2p(x)dx}\right)=0\,. \tag{3.37}$$

This is even true for $p(x)\propto x^{-3}$, x large, although its variance is infinite (i.e. diverges logarithmically), and it is always true if $p(x)$ decays faster than that, i.e. if mean and variance of the underlying distribution exist. This is the reason for the range of the Lévy parameter $0<\alpha\leq 2$. For all $\alpha\geq 2$ the first and second moment exist and the respective pdf can only belong to the basin of attraction of the Normal law. If the third (centered) moment exists, the convergence to the Gaussian limit is even uniform, and the theorem of Berry-Esséen holds. For the (cumulative) distribution function P_n of the normed sum of n variables with zero mean there exists a positive constant C_{BE} such that

$$|P_n(x)-P_{Gauss}(x)|\leq\frac{C_{BE}\left\langle|x|^3\right\rangle}{\left\langle x^2\right\rangle^{3/2}\sqrt{n}} \tag{3.38}$$

for all x and n. $\left\langle|x|^3\right\rangle$ is the third moment, $\left\langle x^2\right\rangle$ the second moment. The upper bound does not depend on the individual distribution, and $C_{BE}\approxeq\frac{33}{4}$ [52].

However, condition (3.37) does not apply for all statistical distributions. In the following we will see that the classical CLT can be generalized to other distributions that lack mean or variance. The limiting distributions of normed sums of iid random variables can only be stable distributions, which accounts for their importance in practice [2].
Let us now consider the normed sum (3.39) of iid random variables that are not necessarily subject to a stable distribution, but to a general distribution $P(x)=\int_{-\infty}^{x}p(x')dx'$. Then, the distribution P is said to belong to the domain of attraction of a stable distribution P_{st} if there exist norming constants a_n and b_n so that the distribution of the normed sum

[2] In fact, if such limiting distribution exists, this statement is even true for any stationarily dependent random variables [53]. However, in the present exposition the consideration of sums of independent variables will suffice and hence we restrict ourselves to this special case.

$$\frac{\left(\sum_{l=1}^{n} x_l\right) - b_n}{a_n} \,, \tag{3.39}$$

tends to a stable distribution P_{st} as $n \to \infty$. By virtue of (3.22) we find that for every n the normed sum of the iid random variables x_l obeying a stable law P_{st},

$$\frac{\left(\sum_{l=1}^{n} x_l\right) - \gamma_n}{c_n} \,, \tag{3.40}$$

has the same distribution function P. Hence, in accordance with the definition of stable laws, every stable law belongs to its own domain of attraction. For a distribution to lie in the domain of attraction of the stable law $L_{\alpha,\beta}$, it is necessary and sufficient that $P(x)$ satisfies the following relations for any r

$$\begin{aligned} \lim_{X\to\infty} \frac{P(-X)}{1-P(X)} &= \frac{1-\beta}{1+\beta} \,, \\ \lim_{X\to\infty} \frac{1-P(X)+P(-X)}{1-P(rX)+P(-rX)} &= r^{\alpha} \,. \end{aligned}$$

This means, loosely speaking, that the distributions that behave as $L_{\alpha,\beta}$ at infinity belong to its domain of attraction [58, 60]. A very useful statement that can be made on pdfs with algebraic tails, $\alpha \neq 1, 2$ is that the normalization constant is $a_n = n^{1/\alpha}$, and

$$\begin{aligned} p(x) &\simeq c_- |x|^{-1-\alpha} \text{ for } x \to -\infty \\ p(x) &\simeq c_+ x^{-1-\alpha} \text{ for } x \to \infty \end{aligned} \tag{3.41}$$

belongs to the domain of attraction of $L_{\alpha,\beta}$ with $\beta = (c_+ - c_-)/(c_+ + c_-)$. The normalization constants of $p(x)$ and the limiting Lévy pdf $p_{\alpha,\beta}(x)$ in (3.39) and (3.24), (3.26), are related as follows:

$$\begin{aligned} &\text{for } 0 < \alpha < 1 \quad : \quad \frac{b_n}{a_n} = 0 \,; \qquad c = \frac{\pi(c_+ + c_-)}{2\alpha \sin(\pi\alpha/2)\Gamma(\alpha)} \\ &\text{for } 1 < \alpha < 2 \quad : \quad b_n = n\langle x \rangle \,; \; c = \frac{\pi(c_+ + c_-)}{2\alpha^2 \sin(\pi\alpha/2)\Gamma(\alpha-1)} \,. \end{aligned} \tag{3.42}$$

3.4 The Random Walk

This chapter gives a short introduction to the generating function approach to the discrete time Random Walk (RW). For the sake of simplicity, only the one dimensional situation is considered here. Generalization to more dimensions is straightforward, see e.g. [54].
In a discrete time Random Walk, the walker performs steps with certain displacements. Let these single step displacements x_l of the lth step be random variables that are independent identically distributed according to a jump length pdf $\varphi(x)$ with $\varphi(x)dx$ specifying the probability that the jump performed is of a length within the interval $(x, x+dx)$.
A basic quantity of the RW is the position of the walker after n steps, given a certain initial position which is here $x_0 = 0$ without loss of generality. The overall displacement x after n steps will be the sum of these iid displacements x_l,

$$x = x_1 + x_2 + \ldots + x_n \,, \tag{3.43}$$

which is a random variable itself. Using the fact that the RW is Markovian, we can relate the pdfs of the overall displacement $p_n(x|x_0)$ for the successive jumps by a recursion relation

$$p_{n+1}(x|x_0) = \int_{-\infty}^{\infty} p_n(x'|x_0)\varphi(x-x')\,dx' \tag{3.44}$$

if we allow for transitions in continuous space or

$$p_{n+1}(x|x_0) = \sum_{x'=-\infty}^{\infty} p_n(x'|x_0)\varphi(x-x') \tag{3.45}$$

if the RW takes place on a discrete lattice. In this case the p_n have to be interpreted as probabilities and not as densities. In the following, the pdf of finding a particle at x after n steps is derived using the generating function approach.

3.4.1 Random Walk Generating Function

The moment generating function of the jump length pdf $\varphi(x)$ is given by the Fourier transform

$$\hat{\varphi}(k) = \left\langle e^{\mathrm{i}kx} \right\rangle = \int_{-\infty}^{\infty} \varphi(x) \exp\left[\mathrm{i}kx\right] dx \tag{3.46}$$

when x is continuous and

$$\hat{\varphi}(k) \quad = \quad \sum_{x=-\infty}^{\infty} \varphi(x) \exp[\mathrm{i}kx] \tag{3.47}$$

for lattice RW. The generating function of the step length distribution $\hat{\varphi}(k)$ is often referred to as the structure function. In particular, probability conservation (i.e. particle conservation) determines $\int_{-\infty}^{\infty} \varphi(x)\,dx = 1$ or $\sum_{x=-\infty}^{\infty} \varphi(x) = 1$, i.e. $\hat{\varphi}(k=0) = 1$.
Note that the corresponding inversion formulas differ only by the limits of integration,

$$\varphi(x) \quad = \quad \frac{1}{2\pi} \int_{-\infty}^{\infty} \hat{\varphi}(k) \exp[-\mathrm{i}kx]\,dk \quad \text{for continuous step lengths, and} \tag{3.48}$$

$$\varphi(x) \quad = \quad \frac{1}{2\pi} \int_{-\pi}^{\pi} \hat{\varphi}(k) \exp[-\mathrm{i}kx]\,dk \quad \text{for lattice walks.} \tag{3.49}$$

Furthermore, the description of RWs in discrete time requires the discrete counterpart of the Laplace transform with equidistant jump times, so that the generating function of the RW is given by the $\mathcal{Z}$-transform [61, 52], with z being the transform parameter conjugate to the amount of steps n,

$$\mathcal{Z}\{p_{RW}(x,n)\} = \bar{p}_{RW}(x,z) \quad = \quad \sum_{n=0}^{\infty} z^n p_{RW}(x,n)\,. \tag{3.50}$$

The connection between Laplace- and $\mathcal{Z}$-Transform is established as follows:
Although the time intervals between the successive jumps are actually not a random variable in the RW, they can be interpreted as drawn from a δ-peaked waiting time distribution function $\psi(t)$. When τ is the time interval between successive jumps, we have $\psi(t) = \delta(t-\tau)$ so that we have a sampled function,

$$p_{RW}(x,t) \quad = \quad p(x,t) \sum_{n=0}^{\infty} \delta(t-n\tau) = \sum_{n=0}^{\infty} p(x,n\tau)\delta(t-n\tau)\,. \tag{3.51}$$

Applying the Laplace transform and with the substitutions $t = n\tau$, $p(x,n\tau) = p_{RW}(x,n)$ and $e^{u\tau} = z$ we arrive at (3.50). Note that the utilization of the waiting time pdf $\psi(t) = \delta(t-\tau)$ defined on a continuous domain is here only a formal procedure helping us to derive a discrete, sampled function from a continuous one and allowing for using the Laplace transform. In the discrete RW with time variable n, the time intervals between the jump events do not belong to the time axis, i.e. the domain of definition of jumping times, so that n is immediately followed by $(n+1)$. Only in this notion the Markovian character of the process is maintained.

We now calculate the Random Walk generating function (3.50), i.e. the probability $p_n(x|x_0)$

for the particle to be at x after n steps. Therefore, rewrite (3.44, 3.45) in $\mathcal{Z}$-domain:

$$p_0(x) + \bar{p}_{RW}(x,z) = z \sum_{x'} \varphi(x-x')\bar{p}_{RW}(x',z) \quad \text{or} \tag{3.52}$$

$$p_0(x) + \bar{p}_{RW}(x,z) = z \int_{-\infty}^{\infty} \varphi(x-x')\bar{p}_{RW}(x',z)\,dx' \ , \tag{3.53}$$

where $p_0(x) = \delta(x)$ or $p_0(x) = \delta_{x,x_0=0}$, respectively, is the initial condition. In Fourier domain, by using the convolution theorem, we finally find the Random Walk generating function

$$\hat{\bar{p}}_{RW}(k,z) \quad = \quad \frac{1}{1-z\hat{\varphi}(k)} = \sum_{n=0}^{\infty} [z\hat{\varphi}(k)]^n \ . \tag{3.54}$$

By comparison with (3.50), or more precisely, its Fourier transform, it is immediately clear that

$$\hat{p}_{RW}(k,n) = [\hat{\varphi}(k)]^n \ , \tag{3.55}$$

i.e. the nth power of the structure function is the Fourier transform of the probability to be at x after n steps.
Let us illustrate the above result by three examples.

3.4.2 Examples

Gaussian step length pdf

For a Gaussian step length pdf the characteristic function is a Gaussian:

$$\varphi(x) \quad = \quad \frac{1}{\sigma\sqrt{2\pi}} \exp\left[-\frac{x^2}{2\sigma^2}\right]; \tag{3.56}$$

$$\hat{\varphi}(k) \quad = \quad \exp\left[-\frac{\sigma^2 k^2}{2}\right] . \tag{3.57}$$

Using (3.55) we finally find the probability for a particle to be at x after n steps:

$$p_{RW}(x,n) = \frac{1}{\sigma\sqrt{2\pi n}} \exp\left[-\frac{x^2}{2n\sigma^2}\right] , \tag{3.58}$$

the result we expected from the fact that the Gaussian distribution is a stable distribution and hence the variance σ_Σ of a sum of n iid random variables is the sum of all variances, $\sigma_\Sigma^2 = \sigma_1^2 + \ldots + \sigma_l^2 = n\sigma^2$.

Lattice walk with nearest-neighbor transition

Consider a RW on a discrete lattice in one dimension with a probability r to take a step to the right and a probability $1-r$ to take a step to the left. The spatial variable can take values $x = 0, \pm 1, \pm 2, \ldots$. Here we have the step length pdf and the corresponding characteristic function, cp. e.g. [62],

$$\varphi(x) = (1-r)\delta(x+1) + r\delta(x-1) \,, \tag{3.59}$$

$$\hat{\varphi}(k) = re^{\mathrm{i}k} + (1-r)e^{-\mathrm{i}k} \,, \tag{3.60}$$

so that with (3.55) the pdf of being at x after n steps is given by

$$p_{RW}(x,n) = \frac{1}{2\pi}\int_{-\pi}^{\pi} e^{-\mathrm{i}kx}\left[pe^{\mathrm{i}k} + (1-p)e^{-\mathrm{i}k}\right]^n dk \,. \tag{3.61}$$

Note that $(2\pi)^{-1}\int_{-\pi}^{\pi} e^{-\mathrm{i}kx+\mathrm{i}mx}\,dk = \delta_{k,m}$ which filters out the respective coefficients which accounts for the fact that, starting at 0, a particle can only occupy lattice sites with even (odd) numbers after an even (odd) amount of steps n. In the symmetric case $r = 1/2$ we find

$$p_{RW}(x,n) = 2^{-n}\frac{n!}{\left(\frac{n+x}{2}\right)!\left(\frac{n-x}{2}\right)!} \,. \tag{3.62}$$

In the large n limit we find by using Stirling's approximation [3]

$$p_{RW}(x,n) = \frac{1}{\sqrt{2\pi n}}\exp\left[-\frac{x^2}{2n}\right] \,, \tag{3.63}$$

which is the discrete in space version of the Gaussian pdf (3.58). If the lattice spacing is a, the discrete lattice point x can be replaced by a continuous variable $ax = x'$, so that $p_{RW}(x,n)dx = p_{RW}(x',n)dx'$ with $dx = 1$,

$$p_{RW}(x',n) = \frac{1}{a\sqrt{2\pi n}}\exp\left[-\frac{x'^2}{2na^2}\right] \,. \tag{3.64}$$

The squared lattice spacing a^2 formally takes the role of the variance σ^2 of the respective continuous step length pdf at large l, cp. Eq. (3.58).

As a consequence of the CLT, Brownian motion emerges as the continuum limit of all RW with step length pdfs possessing the second moment. The next example illustrates a situation where the Gaussian continuum limit does not apply.

[3] Stirling's formula: $n! \simeq \sqrt{2\pi n}n^n e^{-n}$

Cauchy distributed step lengths

Consider the step length pdf

$$\varphi(t) = \frac{b}{\pi(b^2 + x^2)} , \tag{3.65}$$

$$\hat{\varphi}(k) = \exp\left[-b|k|\right] . \tag{3.66}$$

The Cauchy distribution is stable, so that we end up with the probability for a particle to be at x after n steps being again a Cauchy distribution:

$$p_{RW}(x,n) = \frac{nb}{\pi(n^2b^2 + x^2)} . \tag{3.67}$$

Due to the generalized CLT, cp. section 3.3, the resultant distributions of sums of random variables share universal properties for asymptotically large l and, going to a continuum, for large t so that Abelian and Tauberian theorems can be used and an explicit Laplace inversion becomes obsolete.

4 Continuous Time Random Walks

The continuous–time random walk (CTRW) model is based on the idea that, in contrast to the simple Random Walk, not only the step length is a random variable, but also the waiting times between the successive steps. Hence, both variables are drawn from a probability density function (pdf) $\Psi(x,t)$ for the particle to perform a step of length x after an elapsed waiting time t. In general, CTRWs feature a non–Markovian behavior. Besides the probability of occupancy of the sites at time t, the arrival times at each site are needed in addition in order to determine the state of the system. On the other hand, the steps of the walkers themselves do not depend on the previous ones. Therefore such processes are often referred to as semi–Markovian [63].

4.1 Limitations of the Random Walk Model

From the physical point of view, the Random Walks constitute a microscopic model for transport, reflecting the randomness of the motion. However, since the elementary steps occurring at equidistant points in time are independent of each other, the standard Random Walk is not suited to describe non–Markovian behavior. Such a non-Markovian aspect in stochastic motion can be incorporated via the choice of a specific waiting time distribution function.

Random Walks with the waiting time being a stochastic variable were first considered in the pioneering work of Montroll and Weiss [61], who considered CTRWs on lattices with the jump lengths being independent of the waiting times. This formalism first came to practical application in the description of charge carrier transport in amorphous semiconductors. Scher and Montroll [12] set up a time-of-flight experiment for a packet of holes in an amorphous semiconductor that was subjected to an external electric field. The transient current was measured and the hole packet was shown to undergo a significant broadening so that Gaussian statistics could no longer be applied. The hole transport had to be characterized by a broad distribution of event times that reaches into the range of observation times. The choice of an algebraic waiting time pdf $\psi(t) \propto t^{-1-\alpha}$ with $0 < \alpha < 1$ allowed for a complete mathematical description of the observed transient current with α being the only relevant parameter.
Such power law waiting time pdfs may emerge from multiple trapping of the charge carriers into localized states as follows [64]:
Disorder in the lattice induces the smearing out of the band edges of the energy density so that a tail of localized states looms into the energy gap. This tail can roughly be described by an exponential, $p_{loc}(E) \approx \frac{1}{E_0} e^{-E/E_0}$. Escape of the carriers to the conduction band requires thermal activation, so that the typical escape times for a fixed energy E can be estimated by the Arrhenius law $\tau = \tau_0 e^{E/k_B T}$ where T is the temperature and k_B is the Boltzmann constant. Taking into account the energy distribution of the localized states, we rewrite $p_{loc}(\tau) = p_{loc}(E)\frac{\partial E}{\partial \tau} = \frac{k_B T}{E_0}\left(\frac{\tau}{\tau_0}\right)^{-1-k_B T/E_0}$. Using this expression as a weighting factor for the sum of the probabilities to

be released from one of the levels, we arrive at an overall waiting time distribution to escape a trap, $\psi(t) = \int_0^\infty p_{loc}(\tau)\frac{1}{\tau}e^{-t/\tau}\,d\tau \propto t^{-1-\alpha}$ with $\alpha = k_B T/E_0$. Recall that E_0 is the measure of the width of the density-of-states tail inside the energy gap. Hence decreasing α indicates increasing disorder.

A more general model where the waiting-time and jump-length pdfs are coupled was first considered by Scher and Lax [65] and can be used for modelling other transport mechanisms such as hopping conduction. The main difference to multiple trapping lies in the fact that the release rates are no longer an independent single-site quantity, but depend on the respective site separations and site energy fluctuations. Klafter and Silbey [66] have shown for hopping on a random lattice where the migration in each individual configuration is Markovian and hence governed by a master equation, that averaging over all possible configurations results in an exact equation for CTRW on a translationally invariant lattice.

The application of CTRW that is in the focus of this work is in modelling diffusion in porous media such as gels, or sediments and other geological formations. Experiments in laboratory as well as in field have demonstrated a time- or length scale dependence of dispersivity [67, 68, 69, 70]. These findings rule out approaches based on advection-dispersion equations which assume a Fickian diffusive behavior on the macroscopic level. On the contrary, transport has to be considered to be anomalous in these cases. In order to quantify and characterize this anomalous transport, the CTRW formalism is well suited, and in fact there was a striking consistency with CTRW predictions e.g. for the long tailed shapes of breakthrough curves of tracer plumes in porous media [71, 68]. Moreover, experiments justify the use of an algebraic waiting time pdf $\psi(t) \propto t^{-1-\alpha}$ instead of an explicitly coupled space-time jump pdf [14]. The parameter α is expected to be a constant if the medium is statistically self-similar, which is the case in some geological formations at least within a certain range of length scales. Pore scale network simulations have also proven to be consistent with the CTRW approach. The typical exponent is predominantly determined by the distribution of average velocities between the throats within the porous medium [72, 73]. This variation in the flow speeds is a direct consequence of the heterogeneity of the pore space. The assumption of space independent $\psi(t)$ is equivalent to a trap model where the distribution of release rates is site independent. Besides the above explanation there have been speculations about other trapping mechanisms that may play a role in porous media, for example trapping in slow flow regions near the pore surface (boundary layers) [74].

In general, the identification of the microscopic mechanisms that account for the respective waiting time pdfs in the CTRW is rather ambiguous. In the following we settle for using the waiting time pdfs as the primary input, since the CTRWs with independent waiting time and jump length pdfs represent the important level of description in modelling transport in porous media. It is clear that the CTRW approaches can only be valid for a large amount of steps taken so that the walker samples a wide variety of environments corresponding to the entire waiting time distribution $\psi(t)$, which characterizes the disordered medium.

Let us now turn to the derivation of the governing equations of the CTRW. For simplicity, we restrict ourselves to the one-dimensional situation. We infer the jump length pdf $\varphi(x)$ and the waiting time pdf $\psi(t)$ by

$$\varphi(x) = \int_0^\infty \Psi(x,t)\,dt \quad \text{and}$$
$$\psi(t) = \int_{-\infty}^\infty \Psi(x,t)\,dx\,.$$

For a CTRW on a discrete lattice, the waiting time pdf is given by

$$\psi(t) = \sum_{x'} \Psi(x',t). \tag{4.1}$$

Throughout the present work, the CTRW model with decoupling step length and waiting time pdfs will be used, so that $\Psi(x,t) = \varphi(x)\psi(t)$.

4.2 From Random Walks to Continuous Time Random Walks

For CTRWs with the jump length pdf being independent of the waiting time pdf, all dependencies on the number n of jumps performed should be the same as in Random Walks. Therefore we recall the $\mathcal{Z}$-transform of the probability density of the particle to be at x after n steps for a Random Walk in one dimension (cp. section 3.4.1)

$$\bar{p}_{RW}(x,z) = \sum_{n=0}^{\infty} z^n p_{RW}(x,n)\,, \tag{4.2}$$

which represents the generating function of the simple discrete time Random Walk.
Now we include a second stochastic process, so that the increments in time are no longer equal, but take continuous values drawn from the waiting time pdf $\psi(t)$. The pdf of being at x at time t is then

$$p(x,t) = \sum_{n=0}^{\infty} p_n(t) p_{RW}(x,n)\,, \tag{4.3}$$

where $p_{RW}(x,n)$ is the pdf of being at x after n steps and $p_n(t)$ is the pdf to make n steps within time t,

$$p_n(t) = \int_0^t \psi_n(t') \int_{t-t'}^\infty \psi(t'')\,dt''\,dt'\,, \tag{4.4}$$

with $\int_{t-t'}^{\infty} \psi(t'')dt'' = \Phi(t-t')$ being the probability of taking no step after $t-t'$ and $\psi_n(t)$ being the pdf of performing the nth step exactly at time t given by an n-fold convolution satisfying the recursion relation

$$\begin{aligned} \psi_n(t) &= \int_0^t \psi_{n-1}(t')\psi(t-t')\,dt', \quad n>1 \\ & \psi_1(t) = \psi(t)\,; \quad \psi_0(t) = \delta(t)\,. \end{aligned} \tag{4.5}$$

Using the convolution theorems of the Laplace transform, Eq.(4.3) yields

$$\begin{aligned} \tilde{p}(x,u) &= \sum_{n=0}^{\infty} \tilde{\Phi}(u)\tilde{\psi}^n(u)p_{RW}(x,n), \\ &= \frac{1-\tilde{\psi}(u)}{u}\sum_{n=0}^{\infty}\tilde{\psi}^n(u)p_{RW}(x,n) \end{aligned} \tag{4.6}$$

an expression that resembles formally of the discrete Random Walk generating function, so that in Laplace domain the generating function of the CTRW $\tilde{p}(x,u)$ can be expressed in terms of the generating function of the discrete RW $\bar{p}_{RW}(x,z)$:

$$\tilde{p}(x,u) = \frac{1-\tilde{\psi}(u)}{u}\bar{p}_{RW}\left(x, z=\tilde{\psi}(u)\right)\,. \tag{4.7}$$

As we will see later, the continuum limit of this mapping from generating functions of discrete Random Walks to those of CTRWs corresponds to an integral transformation in time domain from an operational time n reflecting the number of events to the physical time t, see section 4.7. This transformation, or rather its representation in Laplace domain (4.7), can be exploited in order to compute all quantities of the CTRW derived from its generating function, just by knowing the generating function of the corresponding discrete RW, Eq. (3.54). Consequently, in Fourier-Laplace domain the probability to find the particle at x at time t is given by

$$\hat{\tilde{p}}(k,u) = \frac{1-\tilde{\psi}(u)}{u}\frac{1}{1-\tilde{\psi}(u)\hat{\varphi}(k)}\,, \tag{4.8}$$

an equation first derived by Montroll and Weiss [61] and therefore sometimes referred to as the Montroll–Weiss equation.

Note that there is as well the possibility to let the particle sit at x_0 at $t_0 = 0$ without starting a waiting time period at the initial time. In that case the Montroll–Weiss equation is not valid since the first waiting time must be considered separately, see e.g. [75, 76]. Hence, if we allow

for arbitrarily chosen initial times that may lie within a waiting time period, the first waiting time is determined by the forward recurrence time t_{fwd} from the beginning of observation t_0 to the next step. Consequently, $\tilde{p}_n(u)$ has to be replaced by $\tilde{p}^*_n(u) = \frac{\tilde{p}_{fwd}(t_0,u)\tilde{\psi}(u)^{n-1}(1-\tilde{\psi}(u))}{u}$ for $n \geq 1$, and $\tilde{p}^*_0(u) = \frac{1-\tilde{p}_{fwd}(t_0,u)}{u}$ (persistence pdf). The forward recurrence time pdf $p_{fwd}(t_0, t-t_0)$ is explicitly depending on the lower bound t_0 of the interval and u is here the Laplace variable conjugate to the interval length, for details cf. [77]. This dependence on t_0 vanishes for exponential waiting time pdfs, yielding Poisson distribution for $p_n(t)$. However, this ageing phenomenon plays a role if the waiting time pdf has a broad tail.
Anyway, we are not going to pursue this matter further. The physical problems treated in this work are supposed to provide a proper initial condition, so that the processes under study can be modelled in terms of the conditional probabilities arising from CTRWs where the beginning of the first waiting time period is fixed, rather than by ongoing renewal processes.

4.3 Some Characteristics of the CTRW Solutions

Different cases of the CTRW model emerge from the specific choice of the waiting-time and step-length pdfs. Depending on whether these distributions are wide or not, different classes of dynamical behaviors are observed. The solutions of CTRW problems are characterized by some basic functions for which exact representations can be produced by means of Fourier–and Laplace transforms. Two examples of such functions will be given in the following.

4.3.1 Mean Number of Steps Taken in an Interval of Time

Suppose the beginning of the interval t_0 is chosen such that it coincides with the beginning of a waiting time period, so that $t_0 = 0$ without loss of generality. Recall that the probability $\psi_n(t)$ to perform the nth step at time t yields in Laplace domain $\tilde{\psi}^n(u)$, and the probability to pause at least for a time t is

$$\begin{aligned} \Phi(t) &= 1 - \int_0^t \psi(t')\,dt' = \int_t^\infty \psi(t')\,dt' \\ &\doteq \frac{1-\tilde{\psi}(u)}{u}\,, \end{aligned} \tag{4.9}$$

so that the pdf $p_n(t)$ of having performed n steps up to t can be written down explicitly in Laplace domain,

$$\tilde{p}_n(u) = \frac{\tilde{\psi}(u)^n(1-\tilde{\psi}(u))}{u}\,. \tag{4.10}$$

In order to obtain the mean number of steps $\langle n(t)\rangle$ performed in the time interval $(0,t)$, this expression has to be multiplied by n and summed over all possible n, $\sum_{n=0}^{\infty}(n\tilde{p}_n(u))$. Making use

of the identity $\sum_{n=0}^{\infty} n z^{n-1} = (1-z)^{-2}$ we have for the mean number of steps in Laplace domain

$$\mathcal{L}\{\langle n(t)\rangle, u\} = \frac{\tilde{\psi}(u)}{u\left(1-\tilde{\psi}(u)\right)} . \tag{4.11}$$

Markovian case
For exponential waiting time pdfs $\psi(t) = \frac{1}{\tau}\exp\left[-\frac{t}{\tau}\right]$ we find for $p_n(t)$:

$$p_n(t) = \frac{(1/\tau)^n}{n!}\exp\left[-\frac{t}{\tau}\right] ,$$

the Poisson-distribution with $\langle n(t)\rangle = t/\tau$.

Non-Markovian case
For waiting time pdfs behaving as $\psi \propto \tau^{\alpha} t^{-1-\alpha}$ at long times we have $\tilde{\psi}(u) \simeq 1-(u\tau)^{\alpha}$, see Appendix B. Hence,

$$\begin{aligned} \mathcal{L}\{\langle n(t)\rangle, u\} &\simeq \frac{1}{\tau^{\alpha} u^{1+\alpha}}; \\ \langle n(t)\rangle &\simeq \frac{t^{\alpha}}{\tau^{\alpha}\Gamma(1+\alpha)} \end{aligned} \tag{4.12}$$

for large t.

4.3.2 Mean Squared Displacement

For both step length and waiting time pdf being narrow, we find the familiar normal diffusive behavior of Brownian motion, $\left\langle x^2\right\rangle \propto t$. As an example, consider an exponential waiting time pdf, $\psi(t) = \frac{1}{\tau}\exp\left[-\frac{t}{\tau}\right]$, with the Laplace transform $\tilde{\psi}(u) = \frac{1}{1+u\tau}$. The step-length pdf is assumed to be Gaussian, $\varphi(x) = \frac{1}{\sqrt{2\pi\sigma^2}}\exp\left[-\frac{x^2}{2\sigma^2}\right]$, hence the Fourier transform obtains the form $\hat{\varphi}(k) = \exp\left[-\frac{\sigma^2 k^2}{2}\right]$. Using the generating function of the CTRW (4.8), the mean squared displacement results in

$$\begin{aligned} \mathcal{L}\left\{\left\langle x^2(t)\right\rangle, u\right\} &= \frac{\partial^2 \hat{\tilde{p}}(k,u)}{\partial k^2}|_{k=0} = \frac{\sigma^2}{\tau} u^{-2} \\ \left\langle x^2(t)\right\rangle &= \frac{\sigma^2}{\tau} t . \end{aligned} \tag{4.13}$$

The CTRW governed by a wide waiting time pdf lacking the first moment and a step-length pdf with finite second moment results in subdiffusive behavior a signature of which is the mean

squared displacement growing sublinearly in time, $\left\langle x^2 \right\rangle \propto t^\alpha$ with $0 < \alpha < 1$. To see this, consider again the Gaussian step length pdf, and a waiting time pdf with the Laplace transform $\frac{1}{1-\tau^\alpha \Gamma(1-\alpha) u^\alpha}$ corresponding asymptotically to a power law in time domain $\varphi(t) \propto t^{1-\alpha}$. The second moment in Laplace domain can be inverted by using Tauberian Theorems,

$$\begin{aligned} \mathcal{L}\left\{\left\langle x^2(t)\right\rangle, u\right\} &= \frac{\partial^2 \hat{\tilde{p}}(k,u)}{\partial k^2}|_{k=0} = \frac{\sigma^2}{\Gamma(1-\alpha)\tau^\alpha} u^{-1-\alpha} \\ \left\langle x^2(t)\right\rangle &= \frac{\sigma^2}{\Gamma(1-\alpha)\tau^\alpha} \frac{t^\alpha}{\Gamma(1+\alpha)} \,. \end{aligned} \tag{4.14}$$

If the first moment of the waiting time pdf exists, but the step-length pdf is wide with lacking second moment, superdiffusive behavior is observed. Such step length pdf can be exemplified by a Lévy pdf so that $\hat{\varphi}(k) = \exp\left[-\frac{\sigma^\gamma |k|^\gamma}{2}\right]$. Here, the mean squared displacement is not defined and hence not suitable as a measure of dispersal. Therefore several authors introduced a pseudo mean squared displacement by using rescaling of the fractional moment $\left\langle |x|^\delta \right\rangle \propto t^{\frac{\delta}{\gamma}}$ with $0 < \delta < \gamma \leq 2$. Applying this new measure, the dispersal was found to grow faster than in normal diffusion, $\left[x^2\right] \propto t^{\frac{2}{\gamma}}$ with $1 < \gamma \leq 2$; $\gamma = 2$ accounts for the Gaussian limiting case. Both pdfs being wide leads to a competition between the long waiting times and long jumps so that a measure defining a (pseudo) mean squared displacement goes as $t^{\frac{2\alpha}{\gamma}}$ [78, 79, 58, 4]. Dispersal processes involving step length distributions with lacking second moment are referred to as Lévy-flights.

4.4 The CTRW Equation

This section addresses a derivation of the governing equation for the probability to find the particle performing a CTRW at x at a time t and does not make use of the generating function explicitly. The method presented here was used e.g. by Scher and Lax [65] and is somewhat more general since it allows for the description of situations where it is not possible to infer the CTRW solutions from the simple RW analogue in a straightforward manner. In particular, this approach provides a tool which will enable us to attack CTRW problems including chemical reactions or source terms later on. For now we adhere to the mere CTRW without reaction in order to familiarize with the approach.

In the following we derive the equation that determines the pdf $p(x,t|x_0,0)$ that a walker is situated at x at time t via the probability density $\eta(x,t|x_0,0)$ that the walker arrived at position x at time t, on condition that the same walker just started a jump at position x_0 at an earlier time $t_0 = 0$. For this purpose, we first consider the conditional n-step probability density $\eta_n(x,t|x_0,0)$ that, starting from x_0 at $t_0 = 0$, a walker arrives at x at time t after exactly n steps, which yields the recursion relation

$$\eta_{n+1}(x,t|x_0,0) = \sum_{x'} \int_0^t \Psi(x-x',t-t')\eta_n(x',t'|x_0,0)\,dt' \,, \tag{4.15}$$

with the summation index x' containing x. With this in mind, we are able to establish the conditional probability density $\eta(x,t|x_0,0)$ to arrive at x at time t irrespective of the amount of steps it takes the particle to do so, provided that the walk was initiated at x_0 at $t_0 = 0$:

$$\eta(x,t|x_0,0) = \sum_{n=0}^{\infty} \eta_n(x,t|x_0,0) \,. \tag{4.16}$$

We separate the initial condition for convenience, since it is known from the start. The initial condition is given by the conditional probability to be at x at time t if the particle did not perform any step,

$$\eta_0(x,t|x_0,0) = \delta_{x,x_0}\delta(t) \,, \tag{4.17}$$

which normalizes as it should, $\sum_{x'} \int_0^\infty \eta_0(x',t'|x_0,0)dt' = 1$. Hence, (4.16) becomes:

$$\eta(x,t|x_0,0) = \delta_{x,x_0}\delta(t) + \sum_{n=1}^{\infty} \eta_n(x,t|x_0,0). \tag{4.18}$$

Performing the summation over n, we arrive at

$$\eta(x,t|x_0,0) = \delta_{x,x_0}\delta(t) + \sum_{x'} \int_0^t \Psi(x',t')\eta(x-x',t-t'|x_0,0)\,dt' \,. \tag{4.19}$$

The probability density $p(x,t|x_0,0)$ that a walker is at position x at time t is the probability $\eta(x,t'|x_0,0)$ that the particle, which started at x_0 at time $t_0 = 0$, arrived at x at a time t' and has not moved since. With

$$\Phi(t) = 1 - \int_0^t \psi(t')\,dt' \tag{4.20}$$

being the probability not to take a step in a time interval $[0,t]$ we find

$$p(x,t|x_0,0) = \int_0^t \eta(x,t-t'|x_0,0)\Phi(t')\,dt' \,. \tag{4.21}$$

This together with (4.19) describes the pdf $p(x,t|x_0,0)$ of a CTRW process. Performing the

Laplace transformation, we have for Eqs. (4.19) and (4.21)

$$\tilde{\eta}(x,u|x_0,0) = \delta_{x,x_0} + \sum_{x'} \tilde{\Psi}(x',u)\tilde{\eta}(x-x',u|x_0,0) \tag{4.22}$$

and

$$\tilde{p}(x,u|x_0,0) = \tilde{\eta}(x,u|x_0,0)\tilde{\Phi}(u)\ . \tag{4.23}$$

Inserting (4.22) into (4.23),

$$\begin{aligned}\tilde{p}(x,u|x_0,0) &= \left[\delta_{x,x_0} + \sum_{x'} \tilde{\Psi}(x',u)\tilde{\eta}(x-x',u|x_0,0)\right]\tilde{\Phi}(u) \\ &= \delta_{x,x_0}\tilde{\Phi}(u) + \sum_{x'} \tilde{\Psi}(x',u)\tilde{p}(x-x',u|x_0,0)\ ,\end{aligned} \tag{4.24}$$

and going back to time domain,

$$p(x,t|x_0,0) = \delta_{x,x_0}\Phi(t) + \sum_{x'}\int_0^t p(x',t'|x_0,0)\Psi(x-x',t-t')\,dt'\ , \tag{4.25}$$

finally results in the sought equation for the pdf $p(x,t|x_0,0)$ of a particle being at x at time t after having started at x_0 at $t_0 = 0$, cp. [65, 80, 81, 4, 16]. The corresponding version that allows for continuous step length distributions reads

$$p(x,t|x_0,0) = \delta_{x,x_0}\Phi(t) + \int_0^t \int_{-\infty}^{\infty} p(x',t'|x_0,0)\Psi(x-x',t-t')\,dx'\,dt'\ . \tag{4.26}$$

4.5 The Generalized Master Equation

The equation (4.25) is formally equivalent to an expression referred to as the Generalized Master Equation (GME) of the CTRW for $p(x,t|x_0,0)$ [80, 81]. To see this, perform the Fourier–Laplace transform:

$$\hat{\tilde{p}}(k,u|x_0,0) = \tilde{\Phi}(u) + \hat{\tilde{p}}(k,u|x_0,0)\hat{\tilde{\Psi}}(k,u)\,, \tag{4.27}$$

so that with $\tilde{\Phi}(u) = \frac{1-\tilde{\psi}(u)}{u}$ we get

$$\hat{\tilde{p}}(k,u|x_0,0) = \frac{1-\tilde{\psi}(u)}{u(1-\hat{\tilde{\Psi}}(k,u))}\,, \tag{4.28}$$

an equation first derived by Scher and Lax in 1973 [65]. In the case of decoupling $\hat{\tilde{\Psi}}(k,u) = \hat{\varphi}(k)\tilde{\psi}(u)$, this formulation corresponds to the Montroll-Weiss equation.
After some algebra we obtain

$$\begin{aligned} u\hat{\tilde{p}}(k,u|x_0,0) - 1 &= \frac{\hat{\tilde{\Psi}}(k,u) - \tilde{\psi}(u)}{1-\hat{\tilde{\Psi}}(k,u)} \\ &= \frac{u\left[\hat{\tilde{\Psi}}(k,u) - \tilde{\psi}(u)\right]}{1-\tilde{\psi}(u)}\hat{\tilde{p}}(k,u|x_0,0) \end{aligned} \tag{4.29}$$

which yields in original domain

$$\frac{\partial p(x,t|x_0,0)}{\partial t} = \sum_{x'}\int_0^t K(x-x',t-t')p(x',t'|x_0,0)\,dt'\,, \tag{4.30}$$

with the initial condition $p(x_0,0|x_0,0) = \delta_{x_0,x}$, an integro–differential equation with the kernel K being defined in Fourier–Laplace domain:

$$\hat{\tilde{K}}(k,u) = \frac{u\left[\hat{\tilde{\Psi}}(k,u) - \tilde{\psi}(u)\right]}{1-\tilde{\psi}(u)}\,. \tag{4.31}$$

Eq. (4.30) is called the generalized master equation since its right hand side represents the gain and loss rates of the density $p(x,t|x_0,0)$ at site x. This becomes more obvious by decomposing the kernel K, assuming that all lattice points are equivalent, i.e. $\Psi(x,t) = \varphi(x)\psi(t)$ is separable. Introducing a mere temporal part of the kernel $\tilde{M}(u) = \frac{u\tilde{\psi}(u)}{1-\tilde{\psi}(u)}$, inserting into (4.29) and inverting the Fourier- and Laplace transform, the GME (4.30) becomes

$$\frac{\partial p(x,t|x_0,0)}{\partial t} = \int_0^t M(t-t')\left[-p(x,t'|x_0,0)+\sum_{x'}\varphi(x-x')p(x',t'|x_0,0)\right]dt' , \tag{4.32}$$

where the relation $\sum_{x'}\varphi(x'-x)=1$ was used for the overall loss at x. In contrast to classical master equations a time dependent kernel appears which leads to a non-Markovian character of the equation. The transition rates are determined not by the current densities at other sites, but by the histories of the densities at the other sites.

Markovian Limit

Bedeaux et al. [82] have shown that the solution of the CTRW with a waiting time pdf possessing the first moment τ converges to the simple Random Walk solution for large enough times

$$t > \sup\left[\frac{<t^m>}{m!}\right]^{\frac{1}{m}} \tag{4.33}$$

if all moments $<t^m>$ of the waiting time pdf $\psi(t)$ are finite. Moreover, if the waiting time pdf is an exponential,

$$\psi(t) = \frac{1}{\tau}\exp\left[-\frac{t}{\tau}\right] \tag{4.34}$$

for which the probability of making n steps until t is given by the familiar Poisson distribution

$$p_n(t) = \frac{1}{n!}\left(\frac{t}{\tau}\right)^n \exp\left[-\frac{t}{\tau}\right] , \tag{4.35}$$

the CTRW is equivalent to the simple Random Walk for all times, that is from the beginning on. In this case, the CTRW is Markovian and possesses an exact representation in terms of a Master Equation. Moreover, it can be shown that there is no other waiting time pdf than the Poissonian for which the CTRW is Markovian [75]. The limit of a Markovian Master Equation requires the kernel M of the GME (4.32) to be a delta-function $c_t\cdot\delta(t)$, hence in Laplace domain:

$$\begin{aligned}\tilde{M}(u) &= \frac{u\tilde{\psi}(u)}{1-\tilde{\psi}(u)} = c_t \\ \tilde{\psi}(u) &= \frac{c_t}{c_t+u} ,\end{aligned} \tag{4.36}$$

which is exactly the Laplace Transform of the exponential (4.34) where the constant c_t can be identified as the inverse mean waiting time or mean jump rate $\frac{1}{\tau}$.

4.6 The Continuum Limit: Time–Fractional Diffusion

When the number of performed steps is very large, the passage from the (continuous time) random walk picture to a (fractional) diffusion equation provides a good approximation. A continuous description of the evolution of the pdf $p(x,t)$, or of the concentration profile $C(x,t)$, respectively, is often desirable, since it permits to solve problems that are not amenable to treatment by the generating functions approach such as e.g. the implementation of different types of boundaries or sources. The transition from a discrete random walk to a process which allows spatial and temporal increments to take arbitrarily small continuous values is attained by letting the jump rates go to infinity while, at the same time, the spacing of the underlying lattice tends to zero. These large jump rates correspond to a transition to small Fourier- and Laplace variables, $(k,u) \to (0,0)$. In order to obtain a continuum description of the CTRW at a large number of performed steps, i.e. at large times, we adopt this approach. It is clear that these limiting processes cannot be carried out independently of each other, since in general the increments of the physical variables x and t are connected by a partial (fractional) differential equation for $p(x,t)$ or $C(x,t)$, the information of which is all contained in Eq. (4.28). We will see that in the particular case of Brownian motion, the result is a partial differential equation of first order in time and second order in space [54], the diffusion equation.
The starting point of the following considerations is the Montroll-Weiss equation (4.28). Our investigations focus on the dynamics arising from step length pdfs with existing second moment and power law waiting time pdfs which lack the first moment, i.e. subdiffusive dispersal. In what follows, the normal diffusive case and the subdiffusive case are discussed in more detail.

Brownian motion

To exemplify the CTRW with finite mean waiting time and jump length variance, we choose again the exponential waiting time pdf $\psi(t) = \tau^{-1}\exp[-t/\tau]$ having a mean $\langle t\rangle = \tau$, and the Gaussian step length pdf, $\varphi(x) = \frac{1}{\sqrt{2\pi\sigma^2}}\exp\left[-\frac{x^2}{2\sigma^2}\right]$. The Laplace– and Fourier transforms are $\tilde{\psi}(u) = \frac{1}{1+u\tau}$ and $\hat{\varphi}(k) = \exp\left[-\frac{\sigma^2k^2}{2}\right]$, respectively. Going to the $(k,u) \to (0,0)$ limit of the Fourier- and Laplace transforms of the step-length and waiting time pdfs yields

$$\begin{aligned} \hat{\varphi}(k) &\sim 1 - \frac{\sigma^2}{2}k^2 + O(k^4)\,, \\ \tilde{\psi}(u) &\sim 1 - \tau u + O(u^2)\,. \end{aligned} \tag{4.37}$$

Inserting these pdfs into Eq. (4.8), one readily infers the Fourier-Laplace transform of the propagator

$$\hat{\tilde{p}}(k,u) = \frac{1}{u+Dk^2}\,, \tag{4.38}$$

where D is the diffusion constant. We see from (4.37) that the transition to the diffusion limit or long-time limit $(k,u) \to (0,0)$ corresponds to $(\sigma^2,\tau) \to (0,0)$ so that $D = \sigma^2/(2\tau) = const.$ defines the diffusion constant. The notion of long times is defined relative to the internal time scale, $t \gg \tau$.
The mean squared displacement of a diffusing particle is a linear function of time,

$$\left\langle x^2(t)\right\rangle = 2Dt\,. \tag{4.39}$$

Note that this signature of Brownian motion found to be exact for exponential waiting time pdfs and Gaussian step length pdfs for all times, cp. (4.13), is reproduced in the continuum limit of large times if only the respective waiting time and jump length pdfs are described by the asymptotic forms (4.37).
Back in (x,t)-domain, the Gaussian propagator

$$p(x,t) = \frac{1}{\sqrt{4\pi Dt}}\exp\left[-\frac{x^2}{4Dt}\right] \tag{4.40}$$

is identified. Multiplication of (4.38) with the denominator at its right hand side and making use of the respective differentiation theorems for Fourier and Laplace transformations leads to the diffusion equation or Fick's second law:

$$\frac{\partial p(x,t)}{\partial t} = D\Delta p(x,t)\,. \tag{4.41}$$

with $p(x,0) = \delta(x)$ as initial condition. As already noted in section 4.2, the exponential waiting time pdf is special in that it represents the only pdf for which the resulting CTRW is Markovian. Nonetheless, in the continuum limit the special shapes of the waiting time and step length pdfs are not of importance, since for large times (or rather a large amount of steps performed) subleading terms in their Laplace–and Fourier transforms (4.37) may be neglected. If the waiting times possess the first moment and if the variance of the step length pdf exists, any CTRW propagator will approach the Markovian one and is described by the diffusion equation (4.41) in the continuum limit.
Fig. 4.1 shows the Gaussian propagator at different times, anticipating the notation $G(x,t)$ used later for the propagator or Green function of Eq.(4.41) in order to distinguish it from other pdfs.

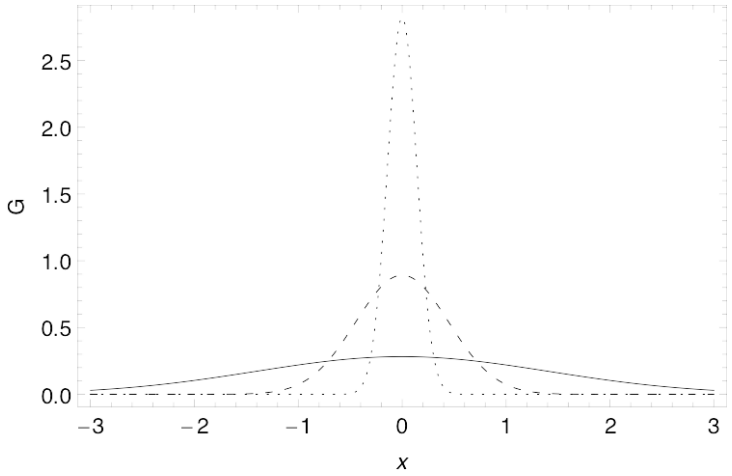

Figure 4.1: Gaussian propagtor at times $t = 0.01,\ 0.1,\ 1$ (dotted, dashed and full line, respectively); $D = 1$.

Subdiffusion

We choose again the Gaussian jump-length pdf as above, but a power-law waiting-time pdf $\psi(t) \propto t^{-1-\alpha}$ with $0 < \alpha < 1$, so that the waiting time pdf lacks the first moment. The small (k,u) expansion yields

$$\begin{aligned} \hat{\varphi}(k) &\sim 1 - \frac{\sigma^2}{2}k^2 + O(k^4)\,, \\ \tilde{\psi}(u) &\sim 1 - \Gamma(1-\alpha)(\tau u)^\alpha\,, \end{aligned} \tag{4.42}$$

equivalent to $(\sigma^2, \tau^\alpha) \to (0,0)$, i.e. the limiting process has to fulfil a constraint defining a generalized diffusion constant $K_\alpha = \sigma^2/(2\Gamma(1-\alpha)\tau^\alpha) = const.$
The corresponding propagator is hence in Fourier-Laplace domain

$$\hat{\tilde{p}}(k,u) = \frac{1}{u + K_\alpha u^{1-\alpha} k^2}\,, \tag{4.43}$$

which results in the sublinear time dependence of the mean squared displacement already found in (4.14),

$$\left\langle x^2(t) \right\rangle = \frac{2K_\alpha}{\Gamma(1+\alpha)} t^\alpha\,. \tag{4.44}$$

This sublinear growth of the mean squared displacement constitutes the characteristic feature of subdiffusion. Moreover, we find that the subdiffusion propagator can be identified as an H-function:

$$\begin{aligned}
\tilde{p}(x,u) &= \frac{1}{\sqrt{4K_\alpha u^{2-\alpha}}}\exp\left[-\sqrt{\frac{u^\alpha}{K_\alpha}}|x|\right] \\
&= \frac{|x|^{\frac{2}{\alpha}-1}}{2K_\alpha^{\frac{1}{\alpha}}}H_{0,1}^{1,0}\left[\left(u\frac{|x|^{\frac{2}{\alpha}}}{\sqrt{K_\alpha^{\frac{1}{\alpha}}}}\right)^{\frac{\alpha}{2}}\middle|\left(1-\frac{2}{\alpha},1\right)\right] \\
&\doteq \frac{|x|^{\frac{2}{\alpha}}}{K_\alpha^{\frac{1}{\alpha}}t}\frac{1}{\alpha|x|}H_{1,1}^{1,0}\left[\frac{|x|^{\frac{2}{\alpha}}}{K_\alpha^{\frac{1}{\alpha}}t}\middle|\begin{matrix}(0,1)\\(1-2/\alpha,2/\alpha)\end{matrix}\right] \\
p(x,t) &= \frac{1}{\sqrt{4K_\alpha t^\alpha}}H_{1,1}^{1,0}\left[\frac{|x|}{\sqrt{K_\alpha t^\alpha}}\middle|\begin{matrix}(1-\alpha/2,\alpha/2)\\(0,1)\end{matrix}\right]. \qquad (4.45)
\end{aligned}$$

This representation allows for the derivation of the asymptotic behavior for large arguments $\frac{|x|}{\sqrt{K_\alpha t^\alpha}}$, which corresponds to a stretched Gaussian [50],

$$p(x,t) \sim \frac{1}{\sqrt{4\pi K_\alpha t^\alpha}}\sqrt{\frac{1}{2-\alpha}}\left(\frac{2}{\alpha}\right)^{\frac{1-\alpha}{2-\alpha}}\left(\frac{|x|}{\sqrt{K_\alpha t^\alpha}}\right)^{-\frac{1-\alpha}{2-\alpha}}\exp\left[-\frac{2-\alpha}{2}\left(\frac{\alpha}{2}\right)^{\frac{\alpha}{2-\alpha}}\left(\frac{|x|}{\sqrt{K_\alpha t^\alpha}}\right)^{\frac{1}{1-\alpha/2}}\right].$$

Multiplication of (4.43) with the denominator at its right side yields, after Fourier–Laplace inversion, the representation of the corresponding propagator in terms of a partial integro-differential equation,

$$\frac{\partial p(x,t)}{\partial t} = K_{\alpha 0}\mathrm{D}_t^{1-\alpha}\Delta p(x,t)\,, \qquad (4.46)$$

with the Riemann-Liouville fractional operator ${}_0\mathrm{D}_t^{1-\alpha}f(t) = \Gamma(\alpha)^{-1}\partial/\partial t\int_0^t(t-t')^{-1+\alpha}f(t')\,dt'$. Here the differentiation rule for fractional derivatives was used, cf. 2.2.
Note that the subdiffusion equation (4.46) converts formally to the normal diffusion equation (4.41) when α is put to 1 and K_α to D. Nevertheless, the limit $\alpha \to 1$ does not yield the Markovian limiting case since the mean of a power law waiting time pdf $\psi \propto t^{-2}$ still diverges logarithmically [58]. This divergence is also mirrored in the divergent $\Gamma(1-\alpha)$ factor in (4.42). Hence, for a rigorous discussion of normal diffusion it is necessary to explicitly use (4.37) instead of treating it as a limiting case of subdiffusion.

Fig. 4.2 shows the subdiffusion propagator (4.45) or Green function $G(x,t) \coloneqq p(x,t)$ of the time–fractional diffusion equation (4.46) for $\alpha = 0.5$ at different times. In contrast to the Gaussian propagator, the shape of the sudiffusion propagator features a persisting cusp at $x = 0$.

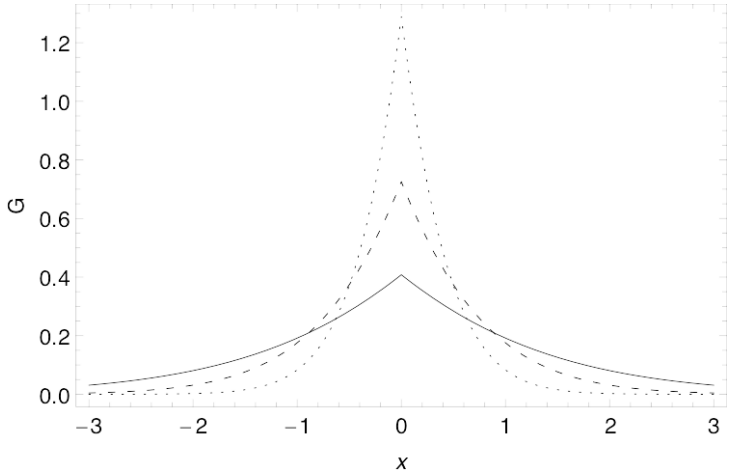

Figure 4.2: Subdiffusion propagator at times 0.01, 0.1, 1 (dotted, dashed, solid line); $\alpha = 0.5$, $K_\alpha = 1$.

For the sake of completeness it should be mentioned that a diverging step length variance generates another type of dynamical behavior called Lévy flights. In the limit the characteristic function of the step length pdf and the resultant propagator for finite mean waiting time are then

$$\begin{aligned} \hat{\varphi}(k) &\sim 1 - \frac{\sigma^\gamma}{2}|k|^\gamma \\ \hat{\tilde{p}}(k,u) &\sim \frac{1}{u + K^\gamma |k|^\gamma} \end{aligned} \tag{4.47}$$

with $K^\gamma = \sigma^\gamma/(2\tau)$ and $0 < \gamma < 2$. Step length pdfs with diverging variance lead to space-fractional transport equations [83, 4].
Laplace inversion of the propagator yields $\hat{p}(k,t) = \exp[-tK^\gamma|k|^\gamma]$, the Fourier representation of a symmetrical Lévy law. Although the mean squared displacement does not exist for Lévy flights, it is possible to define a width of the propagator which grows faster than linear with time. Hence, this type of transport is often referred to as superdiffusion. As the present work focuses on long rests and the emerging subdiffusive dynamical behavior, the issue of long jumps will not be pursued further.

4.7 Subordination

Equation (4.3) uses the pdf $p_n(t)$ of the walker to make n steps within t in order to derive the probability $p(x,t)$ of the subdiffusive CTRW to be at x at time t from the simple Random Walk.

It is possible to set up the corresponding continuous analogue of this relation leading to an integral transform which will prove especially useful in solving some types of time-fractional differential equations. This transform corresponds to a random time change by means of an increasing Lévy process and is called subordination [84, 52, 2].
First, recall that the continuum limit $n \gg 1$ of the Random Walk is given by the Gaussian propagator of Brownian motion

$$p_{BM}(x,n) = \frac{1}{\sqrt{2\pi\sigma^2 n}} \exp\left[-\frac{x^2}{2\sigma^2 n}\right] . \tag{4.48}$$

Rewrite (4.10) as

$$\tilde{p}_n(u) = \frac{1-\tilde{\psi}(u)}{u} \exp\left[n \log \tilde{\psi}(u)\right] , \tag{4.49}$$

and assume a heavy-tailed waiting time pdf, so that with no loss of generality $\tilde{\psi}(u) \simeq 1 - u^\alpha$ in the long-time ($u \to 0$) limit. The pdf to make n steps within t is then in Laplace domain

$$\tilde{p}_n(u) = u^{\alpha-1} \exp\left[n \log(1-u^\alpha)\right] \simeq u^{\alpha-1} \exp\left[-nu^\alpha\right] , \tag{4.50}$$

which involves the generating function of a one-sided stable law,

$$\exp\left[-nu^\alpha\right] \fallingdotseq \frac{1}{n^{1/\alpha}} p_{\alpha,1}\left(\frac{t}{n^{1/\alpha}}\right) . \tag{4.51}$$

Rewriting (4.50) as $-\int_0^t \frac{d}{dn}\frac{1}{n^{1/\alpha}} p_{\alpha,1}\left(\frac{t'}{n^{1/\alpha}}\right) dt'$ finally results in

$$p_n(t) \simeq \frac{1}{\alpha}\frac{t}{n^{1+1/\alpha}} p_{\alpha,1}\left(\frac{t}{n^{1/\alpha}}\right) \tag{4.52}$$

for the pdf to make n steps within t. The pdf to be at x at a time t is therefore in continuous coordinates

$$\begin{aligned} p(x,t) &= \int_0^\infty T(t,t') p_{BM}(x,t')\, dt' := \mathcal{T}_\alpha\{p_{BM}(x,t'),t\} \quad \text{with} \\ T(t,t') &= \frac{1}{\alpha}\frac{t}{t'^{1+1/\alpha}} p_{\alpha,1}\left(\frac{t}{t'^{1/\alpha}}\right) \end{aligned} \tag{4.53}$$

where t' indicates the operational time, i.e. the continuous counterpart to the amount of steps n, and t denotes the physical time. The resultant $p(x,t)$ are subordinated to Brownian motion. In equation (4.53) the Gaussian propagator depending on the number of steps is weighted according to the rates at which the steps take place [55, 52, 85, 86]. The integral transform $\mathcal{T}_\alpha$ maps the Gaussian propagator onto the CTRW propagator with subdiffusion parameter $0 < \alpha < 1$. Observe

that this transform takes on a very convenient form when applied in Laplace domain:

$$\begin{aligned}\tilde{p}(x,u) &= \int_0^\infty u^{\alpha-1}\exp\left[-t'u^\alpha\right]p_{BM}(x,t')\,dt' \\ &= u^{\alpha-1}\tilde{p}_{BM}(x,u^\alpha)\,. \end{aligned} \tag{4.54}$$

The inverse of the subordination in Laplace domain is given by

$$\tilde{p}_{BM}(x,u) = u^{1/\alpha-1}\tilde{p}(x,u^{1/\alpha})\,. \tag{4.55}$$

4.8 From Probabilities to Particle Concentrations

The above sections deal with the evolution of the pdf to find a particle at a site x at time t that began its walk at a prescribed x_0 at the initial time $t_0 = 0$. Later on in this work we will refer rather to particle concentrations or number densities than to probabilities, and we will be interested in the particle concentration profiles. Therefore it is shown here that the CTRW equation applies for such quantities as well since they are proportional to probabilities. Let for now all particles be concentrated at x_0 initially. By normalizing the particle density $C(x,t|x_0,t_0)$, the equation (4.25) can be expressed as

$$\frac{C(x,t|x_0,0)}{C(x_0,0|x_0,0)} = \delta_{x,x_0}\Phi(t) + \sum_{x'}\int_0^t \frac{C(x',t'|x_0,0)}{C(x_0,0|x_0,0)}\Psi(x-x',t-t')\,dt'\,, \tag{4.56}$$

so that after multiplication with the initial concentration the CTRW equation for the number density of particles yields

$$\begin{aligned}C(x,t|x_0,0) &= \delta_{x,x_0}C(x_0,0|x_0,0)\Phi(t) \\ &\quad + \sum_{x'}\int_0^t C(x',t'|x_0,0)\Psi(x-x',t-t')\,dt'\,. \end{aligned} \tag{4.57}$$

or, in terms of a GME,

$$\frac{\partial C(x,t|x_0,0)}{\partial t} = \int_0^t M(t-t')\left[-C(x,t'|x_0,0)\sum_{x'}\varphi(x-x')C(x',t'|x_0,0)\right]dt'\,. \tag{4.58}$$

Regarding particle densities, a reasonable question to be posed is the one for the evolution of

the spatial profiles with respect to the initial arrangement of particles in space. If we allow for extended initial conditions, the equation for the overall number density $C(x,t|t_0=0)$ of particles at x becomes

$$\begin{aligned} C(x,t|0) &= \sum_{x_0} C(x,t|x_0,0) \\ &= \sum_{x_0} \delta_{x,x_0} C(x_0,0|x_0,0)\Phi(t) + \sum_{x_0}\sum_{x'} \int_0^t C(x',t'|x_0,0)\Psi(x-x',t-t')\,dt' \\ &= C(x,0|0)\Phi(t) + \sum_{x'} \int_0^t C(x',t'|0)\Psi(x-x',t-t')\,dt' \ . \end{aligned} \tag{4.59}$$

A further generalization where the overall concentration is no longer constant in time due to incorporation of sources or sinks will be addressed in the next section.

4.9 An Alternative Derivation of the GME

The previous section has shown that the large time behavior of the decoupled CTRW is determined by the behavior of the step length- and waiting time pdfs at large absolute arguments. In the continuum limit, CTRW with jump variance a^2 can therefore be modelled effectively by a CTRW between the nearest neighbors of a lattice with lattice constant a. In the remainder of this work the particles are restricted to perform unbiased jumps only. With these basic assumptions, the GME can be derived explicitly by considering the flux balance at each lattice site. The method was developed in [87] and used in [88] in order to derive a time–fractional diffusion equation with time–fractional derivative of variable order, accounting for an inhomogeneous medium. The merit of this approach lies in its straightforwardness especially with respect to implementation of chemical reactions. These extensions will be addressed in chapter 6.
For now, we sketch the method by deriving the GME of the mere CTRW and its respective continuum limit, the time–fractional diffusion equation.
Allowing only for nearest neighbor transitions, the sum over x' in Eq. (4.30) can be written down explicitly with a minimal number of summands, the rate terms being represented by probability fluxes or, in the notion of section 4.8, fluxes of particles. Mass balance requires

$$j_i^+(t) = w_{i-1,i} j_{i-1}^-(t) + w_{i+1,i} j_{i+1}^-(t), \tag{4.60}$$

where i is the number index of the current lattice site, $j_i^-(t)$ is the loss flux and $j_i^+(t)$ is the gain flux at site i. In the case of unbiased walks, the transition probabilities to site i from $i-1$ and $i+1$ are $w_{i-1,i} = w_{i+1,i} = \frac{1}{2}$. This situation is sketched in Fig. 4.3.

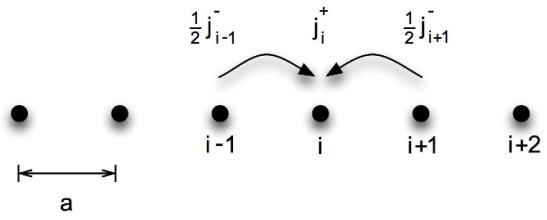

Figure 4.3: Flux balance for CTRW on a lattice with lattice constant a. In situations without external fields, conservation of probability requires that the gain at a site is composed of $1/2$ the losses of both neighboring sites.

The change in occupation number at site i is then

$$\begin{aligned} \frac{\partial C_i(t)}{\partial t} &= j_i^+(t) - j_i^-(t) \\ &= \frac{1}{2} j_{i-1}^-(t) + \frac{1}{2} j_{i+1}^-(t) - j_i^-(t) \,. \end{aligned} \tag{4.61}$$

With the waiting time density $\psi(t)$, the equation for the loss flux reads

$$\begin{aligned} j_i^-(t) &= \psi(t) C_i(0) + \int_0^t \psi(t-t') j_i^+(t')\, dt' \\ &= \psi(t) C_i(0) + \int_0^t \psi(t-t') \left[\frac{\partial C_i(t)}{\partial t} + j_i^-(t') \right] dt' \,, \end{aligned} \tag{4.62}$$

i.e. the loss flux of particles at site i at time t is made up of particles that were at that site from the very beginning, and of those particles which came there at a time t' and waited until t for the next jump. Changing to Laplace domain, we find

$$\tilde{j}_i^-(u) = \tilde{M}(u) \tilde{C}_i(u) \tag{4.63}$$

with the kernel

$$\tilde{M}(u) = \frac{u \tilde{\psi}(u)}{1 - \tilde{\psi}(u)} \,, \tag{4.64}$$

which is the memory kernel of the GME of the CTRW (4.32). In time domain, the loss flux can be expressed as

$$j_i^-(t) = \int_0^t M(t-t')C_i(t')\,dt' \ , \tag{4.65}$$

so that with (4.61) we have

$$\frac{\partial C_i(t)}{\partial t} = \int_0^t M(t-t')\left[\frac{1}{2}C_{i-1}(t') + \frac{1}{2}C_{i+1}(t') - C_i(t')\right]dt' \ . \tag{4.66}$$

Transition to a continuous space coordinate $x = ai$ results in

$$\frac{\partial C(x,t)}{\partial t} = \frac{a^2}{2}\int_0^t M(t-t')\Delta C(x,t')\,dt' \ . \tag{4.67}$$

Let us first reproduce Fick's second law or the normal diffusion equation by inserting the exponential waiting time pdf $\frac{1}{\tau}\exp\left[-\frac{t}{\tau}\right]$. The memory kernel becomes a Dirac delta function,

$$\begin{aligned}\tilde{M}(u) &= \frac{1}{\tau} \\ &\doteq \frac{1}{\tau}\delta(t) \ ,\end{aligned} \tag{4.68}$$

indicating Markovian behavior. Insertion into (4.67) and $\frac{a^2}{2\tau} = D$ yields the diffusion equation

$$\frac{\partial C(x,t)}{\partial t} = D\Delta C(x,t') \ . \tag{4.69}$$

For power law waiting time pdfs, $\psi(t) \propto \tau^\alpha t^{-1-\alpha}$ with $\tilde{\psi}(u) \simeq 1 - \tau^\alpha\Gamma(1-\alpha)u^\alpha$, $0 < \alpha < 1$ in leading order, the memory kernel reads

$$\tilde{M}(u) \sim \frac{1}{\tau^\alpha\Gamma(1-\alpha)}u^{1-\alpha} \ ,$$

which is proportional to the Riemann-Liouville fractional derivative, so that with $K_\alpha = \frac{a^2}{2\tau^\alpha\Gamma(1-\alpha)}$

$$\begin{aligned}\frac{\partial C(x,t)}{\partial t} &= K_\alpha \frac{1}{\Gamma(\alpha)} \frac{d}{dt} \int_0^t \frac{1}{(t-t')^{1-\alpha}} \Delta C(x,t')\, dt' \\ &= K_{\alpha 0} \mathrm{D}_t^{1-\alpha} \Delta C(x,t)\ . \end{aligned} \tag{4.70}$$

Implementation of a Source Term

The inhomogeneous subdiffusion equation can be derived following the CTRW scheme put forward by Montroll and Weiss by supplementing the Ansatz for the GME (4.26) with an added source term, and then use an appropriate step length pdf, as done in [31]. However, for our purposes it is not necessary to carry along all the details of the step length pdf throughout the calculation, and we use the method and notation as above. We have

$$\frac{\partial C_i(t)}{\partial t} = \frac{1}{2} j^-_{i-1}(t) + \frac{1}{2} j^-_{i+1}(t) - j^-_i(t) + f_i(t)\ . \tag{4.71}$$

The balance equation for the fluxes is then

$$\begin{aligned} j^-_i(t) &= \psi(t) C_{0,i} + \int_0^t \psi(t-t') \left[j^+_i(t') + f_i(t') \right] dt' \\ &= \int_0^t \psi(t-t') \left[\frac{\partial C_i(t)}{\partial t} + j^-_i(t') \right] dt'\ , \end{aligned} \tag{4.72}$$

i.e. the loss flux yields the same expression as in the source-free case,

$$\begin{aligned} j^-_i &= \int_0^t M(t-t') C_i(t')\, dt' \\ \tilde{M}(u) &= \frac{u\tilde{\psi}(u)}{1-\tilde{\psi}(u)} \end{aligned}$$

which, inserted into (4.71) and converted to continuous coordinates, yields the inhomogeneous time-fractional diffusion equation,

$$\frac{\partial C(x,t)}{\partial t} = K_{\alpha 0} \mathrm{D}_t^{1-\alpha} \Delta C(x,t) + f(x,t)\ . \tag{4.73}$$

Note that the addition of the source term $f(x,t)$ is until now a rather formal procedure that lacks

physical interpretation. In particular, it is not yet clear whether the memory ranging back to $t = 0$ in the above equation and acting upon partial concentrations that were introduced at later times, imposes certain requirements on the age profile of the newly introduced particles. The inhomogeneous subdiffusion equation and especially the physical meaning of such a source term will be discussed in detail later on, cf. section 5.2.4.

5 Fractional Differential Equations

In the last sections the CTRW approach was used in order to derive the time–fractional diffusion equation which represents an appropriate continuum description of subdiffusive transport. In the following, methods will be discussed that enable us to solve such equations. First of all, the issue of the Initial Value Problem (IVP) in time–fractional ordinary differential equations is addressed. Thereby we closely adhere to the general analysis in [45] and give some examples slightly generalizing the time–fractional relaxation equation considered e.g. in [89]. The physical meaning of different initial conditions will be discussed.
Then, we pass to partial time–fractional differential equations, in particular the time–fractional diffusion equation. Different methods that are in use to solve boundary value problems of partial time–fractional diffusion equations are introduced, such as the method of images or the Laplace method. Both methods will be shown to lead to equivalent results, which, due to the non–Markovian character of time–fractional diffusion, is not immediately clear. These findings allow to use both methods in conjunction, for which some examples will be given. Moreover, source terms will be considered under the aspect of subordination.

5.1 Initial Value Problem for Time–Fractional Ordinary Differential Equations

In this section we consider equations establishing a relationship between an unknown function $y(t)$ and fractional derivatives thereof, i.e. equations of the general form

$$F(t, y(t), {}_{t_1}\mathrm{D}_t^{\nu_1}\omega_1(t)y(t), \ldots, {}_{t_n}\mathrm{D}_t^{\nu_n}\omega_n(t)y(t)) \quad = \quad g(t)\,. \tag{5.1}$$

These equations can be subdivided into linear, homogeneous and inhomogeneous ordinary differential equations of fractional order. The fractional analogue of the IVP or Cauchy Problem consists in solving (5.1) under prescribed initial conditions at t_0,

$$\begin{aligned} {}_b\mathrm{D}_t^{\beta_1} y(t)\Big|_{t=t_0} &= b_1 \\ &\vdots \\ {}_b\mathrm{D}_t^{\beta_n} y(t)\Big|_{t=t_0} &= b_n\,. \end{aligned} \tag{5.2}$$

Let us now take a closer look at a special case of (5.1),

$$ {}_0\mathrm{D}_t^{\nu} y(t) \quad = \quad f(y,t), \qquad n-1 < \nu < n,\ n = 1,2,\ldots \tag{5.3} $$

with the initial conditions

$$ {}_0\mathrm{D}_t^{\nu-i} y(t)\Big|_{t=0} \quad = \quad b_i, \qquad i = 1,2,\ldots,n\ . \tag{5.4} $$

The solution of the above problem (5.3) and (5.4) exists and is unique, provided that $f(y,t)$ is a well-behaved function, i.e. a real valued, finite, continuous function in a certain domain that satisfies the Lipschitz condition with respect to y [45, 42]. Let us first assume $n = 1$ and integrate (5.3),

$$ {}_0\mathrm{D}_t^{-\nu}\, {}_0\mathrm{D}_t^{\nu} y(t) \quad = \quad {}_0\mathrm{D}_t^{-\nu} f(y,t)\ , \tag{5.5} $$

so that with (5.4) we have

$$ y(t) \quad = \quad b_1 \frac{t^{\nu-1}}{\Gamma(\nu)} + \int_0^t \frac{(t-t')^{\nu-1}}{\Gamma(\nu)} f(y,t')\, dt'\ , \tag{5.6} $$

an integral equation equivalent to (5.3) and (5.4). To check, we obtain

$$ \begin{aligned} {}_0\mathrm{D}_t^{\nu} y(t) \quad &= \quad \frac{b_1}{\Gamma(\nu)}\, {}_0\mathrm{D}_t^{\nu} t^{\nu-1} + {}_0\mathrm{D}_t^{\nu}\, {}_0\mathrm{D}_t^{-\nu} f(y,t) \\ &= \quad f(y,t)\ , \end{aligned} \tag{5.7} $$

and for the initial condition

$$ \begin{aligned} {}_0\mathrm{D}_t^{\nu-1} y(t) \quad &= \quad \frac{b_1}{\Gamma(\nu)}\, {}_0\mathrm{D}_t^{\nu-1} t^{\nu-1} + {}_0\mathrm{D}_t^{-1} f(y,t) \\ &= \quad b_1 + \int_0^t f(y(t'),t')\, dt'\ , \end{aligned} $$

where the transition to the limit $t \to 0$ has to be performed. This yields the required expressions

for the respective differential equation of fractional order and initial condition. For $n > 1$, we have

$$y(t) = \sum_{i=1}^{n} b_i \frac{t^{\nu-i}}{\Gamma(\nu-i+1)} + \int_0^t \frac{(t-t')^{\nu-1}}{\Gamma(\nu)} f(y,t')\,dt' \,, \tag{5.8}$$

accordingly.

Example

Let now $f(y,t) = \lambda y(t)$ so that the above Cauchy-problem obtains the form

$$\begin{aligned} {}_0\mathrm{D}_t^{\nu} y(t) &= \lambda y(t), \qquad n-1 < \nu < n,\ n = 1,2,\ldots \\ {}_0\mathrm{D}_t^{\nu-i} y(t)\big|_{t=0} &= b_i, \qquad i = 1,2,\ldots,n \end{aligned} \tag{5.9}$$

so that

$$y(t) = \sum_{i=1}^{n} b_i \frac{t^{\nu-i}}{\Gamma(\nu-i+1)} + \lambda \int_0^t \frac{(t-t')^{\nu-1}}{\Gamma(\nu)} y(t')\,dt' \,. \tag{5.10}$$

This implicit expression can be attacked by the method of successive approximations, where

$$\begin{aligned} y_0(t) &= \sum_{i=1}^{n} b_i \frac{t^{\nu-i}}{\Gamma(\nu-i+1)} \\ y_l(t) &= y_0(t) + \lambda \int_0^t \frac{(t-t')^{\nu-1}}{\Gamma(\nu)} y_{l-1}(t')\,dt' \qquad l = 1,2,\ldots \end{aligned} \tag{5.11}$$

We find

$$\begin{aligned} y_1(t) &= y_0(t) + \lambda \sum_{i=1}^{n} b_i \frac{t^{2\nu-i}}{\Gamma(2\nu-i+1)} \\ y_2(t) &= y_1(t) + \lambda^2 \sum_{i=1}^{n} b_i \frac{t^{3\nu-i}}{\Gamma(\nu-i+1)} \\ &\vdots \\ y_l(t) &= \sum_{i=1}^{n} b_i \sum_{j=1}^{l+1} \lambda^{j-1} \frac{t^{j\nu-i}}{\Gamma(j\nu-i+1)} \,, \qquad l = 1,2,\ldots \end{aligned} \tag{5.12}$$

and finally, after passing to the limit $l \to \infty$,

$$\begin{aligned} y(t) &= \sum_{i=1}^{n} b_i \sum_{j=1}^{\infty} \lambda^{j-1} \frac{t^{j\nu-i}}{\Gamma(j\nu-i+1)} \\ &= \sum_{i=1}^{n} b_i t^{\nu-i} \mathrm{E}_{\nu,1+\nu-i}(\lambda t^{\nu}) \,, \end{aligned} \tag{5.13}$$

where $\mathrm{E}_{\alpha,\beta}$ is the generalized Mittag-Leffler function.
We now consider the initial value problem for the corresponding inhomogeneous fractional differential equation,

$$\begin{aligned} {}_0\mathrm{D}_t^{\nu} y(t) - \lambda y(t) &= h(t), \qquad n-1 < \nu < n,\ n = 1,2,\ldots \\ {}_0\mathrm{D}_t^{\nu-i} y(t)\big|_{t=0} &= b_i, \qquad i = 1,2,\ldots,n \end{aligned} \tag{5.14}$$

The corresponding integral equation is then

$$y(t) = y_0(t) + \frac{1}{\Gamma(\nu)} \int_0^t (t-t')^{\nu-1} \left[h(t') + \lambda y(t') \right] dt' \,, \tag{5.15}$$

so that in the end

$$\begin{aligned} y_l(t) &= \sum_{i=1}^{n} b_i \sum_{j=1}^{l+1} \lambda^{j-1} \frac{t^{j\nu-i}}{\Gamma(j\nu-i+1)} \\ &\quad + \sum_{j=1}^{l} \frac{\lambda^{j-1}}{\Gamma(j\nu)} \int_0^t (t-t')^{j\nu-1} h(t')\, dt' \,. \end{aligned} \tag{5.16}$$

Passing to $l \to \infty$,

$$\begin{aligned} y(t) &= \sum_{i=1}^{n} b_i t^{\nu-i} \mathrm{E}_{\nu,1+\nu-i}(\lambda t^{\nu}) \\ &\quad + \int_0^t (t-t')^{\nu-1} \mathrm{E}_{\nu,\nu}\left(\lambda (t-t')^{\nu}\right) h(t')\, dt' \,. \end{aligned} \tag{5.17}$$

Identifying t with the time and for negative λ, the above fractional ordinary differential equa-

tion (5.9) bears a formal resemblance to the relaxation equation often encountered in physical contexts. In complex systems such as polymers or glassy systems, the relaxation function is nonexponential. Due to the fact that the large number of elementary subunits responsible for the relaxation are highly coupled, the resultant decay takes place more slowly, according to either a stretched exponential or an asymptotic power law. The latter behavior can be described by fractional relaxation. Indeed, fractional relaxation equations were obtained by replacing the first-order time derivatives $\frac{\partial}{\partial t}$ by derivatives of fractional order $\frac{\partial^\nu}{\partial t^\nu}$, and have partly been discussed and compared to other fractional generalizations of relaxation by several authors, [90, 91, 92].

However, initial value problems of the type (5.3, 5.4) are not well posed, since the initial conditions given by a fractional derivative of the sought function $y(t)$ at $t = 0$ diverge, and there is no physical interpretation for such divergence. This problem could be circumvented e.g. by putting the initial conditions to zero in a rather arbitrary manner [42].
A more natural initial condition to be posed for a physical quantity $y(t)$ is to determine the physical quantity at the initial time, $y(t = 0) = y_0$, or, more general, to prescribe as well the initial value of integer order derivatives of such quantity. Such an initial value problem was posed and solved e.g. by [89] for a different fractional relaxation equation, for $0 < \nu < 1$. In the following we slightly generalize their equations to equations involving arbitrary $\nu > 0$, but allowing for a proper initial condition. Apart from the physical soundness of initial conditions there is yet no physical motivation for such equations. Nevertheless, we consider this more general form in order to conform with the previous analysis. Hence,

$$\begin{aligned} \frac{\partial^n y(t)}{\partial t^n} &= \lambda\, {}_0\mathrm{D}_t^{n-\nu} y(t), \qquad n-1 < \nu < n,\ n = 1,2,\dots \\ \left.\frac{\partial^{n-i} y(t)}{\partial t^{n-i}}\right|_{t=t_0} &= b_i, \qquad i = 1,2,\dots,n \end{aligned} \tag{5.18}$$

Depending on ν, we have $y(t = 0)$ and its integer derivatives at $t = 0$ given as the initial conditions. An analogy to (5.9) can be made clear by transforming (5.18) using the substitution ${}_0\mathrm{D}_t^{n-\nu} y(t) = y^*(t)$, which yields exactly the problem (5.9) for $y^*(t)$. With (5.13) and the properties of fractional derivatives of the Mittag-Leffler function, see section 2.3.1, we find the solution

$$\begin{aligned} y(t) &= {}_0\mathrm{D}_t^{\nu-n} y^*(t) = {}_0\mathrm{D}^{\nu-n} \sum_{i=1}^{n} b_i t^{\nu-i} \mathrm{E}_{\nu,1+\nu-i}(\lambda t^\nu) \\ &= \sum_{i=1}^{n} b_i t^{n-i} \mathrm{E}_{\nu,1+n-i}(\lambda t^\nu)\,, \end{aligned} \tag{5.19}$$

and in particular for $n = 1$ and $0 < \nu < 1$, we obtain

$$y(t) = \mathrm{E}_{\nu,1}(\lambda t^\nu)\,. \tag{5.20}$$

Obviously, the solution to the IVP of the fractional relaxation equation (5.18) differs from the solutions of (5.3, 5.4), especially in its asymptotics $t \to \infty$. This type of fractional relaxation equation will prove useful in the solution of partial fractional differential equations with mutually independent variables, where it describes the mode decay.
For the inhomogeneous counterpart to (5.18),

$$\begin{aligned} \frac{\partial^n y(t)}{\partial t^n} - \lambda_0 \mathrm{D}_t^{n-\nu} y(t) &= h(t), \qquad n-1 < \nu < n,\ n = 1,2,\ldots \\ \left.\frac{\partial^{n-i} y(t)}{\partial t^{n-i}}\right|_{t=0} &= b_i, \qquad i = 1,2,\ldots,n \end{aligned} \tag{5.21}$$

we find the solution

$$y(t) = \sum_{i=1}^{n} b_i t^{n-i} \mathrm{E}_{\nu,1+n-i}(\lambda t^\nu) + \int_0^t (t-t')^{n-1} \mathrm{E}_{\nu,n}\left(\lambda (t-t')^\nu\right) h(t')\, dt' \,. \tag{5.22}$$

These results can be obtained via the above method of successive approximation as well, see appendix C.

5.2 Partial Linear Fractional Differential Equations

We consider here in particular the time-fractional diffusion equation for subdiffusing particles,

$$\frac{\partial C(x,t)}{\partial t} = K_\alpha {}_0\mathrm{D}_t^{1-\alpha} \Delta C(x,t) \tag{5.23}$$

with $0 < \alpha < 1$ and $C(x,t)$ the particle concentration.

5.2.1 Separation of Variables

We may attempt to find a solution to problems of that kind by assuming that the involved variables are independent of each other, i.e. can be separated [93, 33, 38]:

$$C(x,t) = X(x)T(t) \tag{5.24}$$

so that

$$X(x)\frac{\partial T(t)}{\partial t} = {}_0\mathrm{D}_t^{1-\alpha} T(t) K_\alpha \Delta X(x) \,. \tag{5.25}$$

By some algebraic manipulation we extract two ordinary differential equations, one of second order and one of fractional order. We have

$$\begin{aligned} c_{1,x}\frac{\partial T(t)}{\partial t} &= {}_0\mathrm{D}_t^{1-\alpha} T(t) K_\alpha c_{2,x} \\ X(x) c_{1,t} &= c_{2,t} K_\alpha \Delta X(x)\,, \end{aligned} \tag{5.26}$$

so that with $-\lambda^2 = \frac{c_{2,x}}{c_{1,x}} = \frac{c_{1,t}}{K_\alpha c_{2,t}}$:

$$\Delta X(x) = -\lambda^2 X(x), \tag{5.27}$$

$$\frac{\partial T(t)}{\partial t} = -\lambda^2 K_\alpha {}_0\mathrm{D}_t^{1-\alpha} T(t)\,. \tag{5.28}$$

The solution of these equations requires specification of initial- and boundary conditions. In a physical context, the initial condition is usually given as the particle concentration at the initial time $t_0 = 0$,

$$C(x,t)|_{t=t_0} = C_0(x)\,, \tag{5.29}$$

i.e.

$$T(t)|_{t=t_0} = \text{const.} \tag{5.30}$$

Without loss of generality we put the above constant equal to one, so that

$$X(x) = c_1 \sin\lambda x + c_2 \cos\lambda x, \tag{5.31}$$

$$T(t) = \mathrm{E}_{\alpha,1}(-\lambda^2 K_\alpha t^\alpha)\,, \tag{5.32}$$

which finally leads us to a solution of the form

$$C(x,t) = [c_1 \sin\lambda x + c_2 \cos\lambda x]\,\mathrm{E}_{\alpha,1}(-\lambda^2 K_\alpha t^\alpha)\,, \tag{5.33}$$

and due to the linearity of our equation more generally:

$$C(x,t) = \sum_{l=1}^{\infty} [c_{1,l}\sin(\lambda_l x) + c_{2,l}\cos(\lambda_l x)]\,\mathrm{E}_{\alpha,1}(-\lambda_l^2 K_\alpha t^\alpha)\,, \tag{5.34}$$

where the constants of integration have to be chosen appropriately, according to the given initial- and boundary conditions. This representation of a solution to the time-fractional diffusion equation is especially convenient for subdiffusion on bounded domains and large t. The modes decay according to the Mittag-Leffler pattern, which emerges from the temporal part of the fractional diffusion equation (5.28) having the form of the fractional relaxation equation considered in the previous section, Eq. (5.18).

Example

The following example anticipates the solution to a special initial-boundary value problem in order to illustrate the above method of separation of variables. A deeper and more comprising presentation on the issue of boundary value problems of time-fractional PDEs is given in 5.3.
We consider subdiffusion on a bounded domain $[0, L]$ with an initially homogeneous particle concentration $C(x, t = 0) = C_0$ within the domain and absorbing boundaries, i.e. $C(0,t) = C(L,t) = 0$. Then,

$$c_{2,l} = 0\,, \qquad \lambda_l = \frac{l\pi}{L}\,, \tag{5.35}$$

and the initial condition can be expressed as the Fourier-Series

$$C_0 = \sum_{l=1}^{\infty} c_{1,l}\sin\left(\frac{l\pi}{L}x\right)\,, \tag{5.36}$$

where we find for the coefficients by making use of the orthogonality relationships of the sine functions [38],

$$\begin{aligned}\int_0^L C_0\sin\left(\frac{n\pi}{L}x\right)dx &= \int_0^L \sin\left(\frac{n\pi}{L}x\right)\left[\sum_{l=1}^{\infty} c_{1,l}\sin\left(\frac{l\pi}{L}x\right)\right]dx \\ &= \frac{L}{2}c_{1,l} \\ \frac{4C_0}{\pi l} &= c_{1,l}\,, \qquad i = 1,3,5\ldots \end{aligned} \tag{5.37}$$

Substituting $l = 2n + 1$, we finally obtain the solution

$$C(x,t) = \frac{4C_0}{\pi}\sum_{n=0}^{\infty}\frac{1}{2n+1}\sin\left(\frac{(2n+1)\pi}{L}x\right)\mathrm{E}_{\alpha,1}\left(-\frac{(2n+1)^2\pi^2}{L^2}K_\alpha t^\alpha\right). \tag{5.38}$$

Fig. 5.1 shows the solutions (5.38) for normal diffusion and for subdiffusion with parameter $\alpha = 1/2$ at different times. The normal case is given by formally setting $\alpha = 1$ and substituting K_α by D.

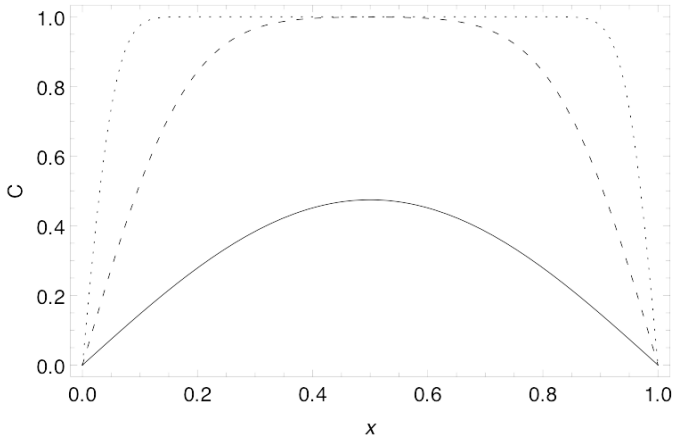

(a)

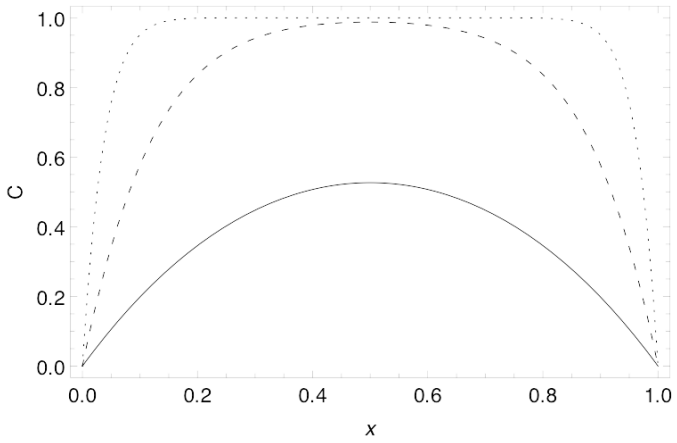

(b)

Figure 5.1: Concentration profiles for zero boundary values and homogeneous initial concentration $C_0 = 1$, $t = 10^{-6}$ (dotted), 10^{-4} (dashed),10^{-2} (solid line) (a) under normal diffusion, $D = 1$, (b) under anomalous diffusion with $\alpha = 0.5$ and $K_\alpha = 1$.

The initial concentration is $C_0 = 1$, the absorbing boundaries are located at $x = 0$ and $x = L = 1$.

At the short times depicted the resultant concentration profiles in the anomalous case do not qualitatively differ from the normal one, except for a slightly slower decay and a slightly larger slope in the vicinity of the boundary. For larger times, a very slow decay of the profile is expected in the anomalous case, due to the large time power law asymptotics of the Mittag–Leffler function (2.40).

5.2.2 Laplace's Method

Historically, the setup of alternative methods to those touched in the previous sections aimed at converting equations involving complicated operations such as differentiation to more simple to solve algebraic equations. In the late 19th century in the pioneer work of O. Heaviside an operational method was developed, which found widespread application in electric circuit theory. Lacking mathematical foundation, this calculus led to correct, but as well to doubtful results [94].
The Laplace transform put this operational method on a firm theoretical basis. Mikusinsky [95] later extended the field of applicability of the operational method to distributions, sometimes called generalized functions, comprising e.g. the Dirac delta function. Both being based upon convolution, the operational method and Laplace transform method are closely connected with each other [96]. In the context of fractional differential equations, the operational calculus has been developed e.g. in [97]. Despite the preferability of the Mikusinsky operational method regarding the treatment of distributions, we adhere to the presentation of the Laplace transform method.
The basic idea of the Laplace transform method is to subject the problem posed in original domain of variable t to the Laplace transform, so that the same problem in Laplace domain with variable u is represented in a much simpler form. In particular, differential operators in original domain and as well some special integral operators, i.e. those of convolutional form, are transformed to algebraic factors depending on u, and the problem can easily be solved in Laplace domain. This advantageous feature of transferring operators in original domain to algebraic expressions in Laplace domain is maintained as well for Riemann–Liouville fractional integrals and derivatives, which are composed of convolution integrals and derivatives [1]. Hence, the Laplace transform method can be directly adopted to time-fractional equations. The actual remaining difficulty consists in performing the inverse Laplace transform on the solutions found in this way. A sketch of the method's idea is given in Fig. 5.2.
The Laplace transform method is especially useful for the solution of initial value problems of linear (fractional) differential equations or initial-boundary value problems of linear (time–fractional) PDEs with constant (in time) coefficients, the first being represented by algebraic expressions, the latter being reduced to ordinary differential equations in Laplace domain.

[1] The term "algebraic" is used here in the wider sense, i.e. as a contrast to the notion of "integro–differential"

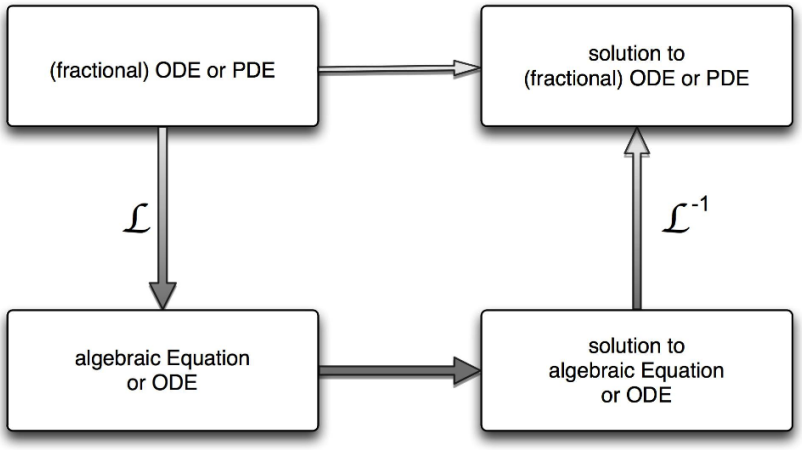

Figure 5.2: Laplace Transform Method. Time–fractional ODEs or PDEs are solved via a detour to Laplace domain (lower boxes).

Recall the Laplace Transform of the Riemann-Liouville fractional derivative of order ν, $\nu > 0$:

$$ {}_0\mathrm{D}_t^{\mu} f(t) \quad \doteqdot \quad u^{\mu}\tilde{f}(u) - \sum_{i=1}^{n} u^{i-1}\left[{}_0\mathrm{D}_t^{\nu-i} f(t)\right]_{t=0} , \qquad n-1 < \nu < n \, . $$

We note here that this formula is valid for integer derivatives as well, $\nu \in \mathbb{N}$. Since the Laplace representation of derivatives (whether fractional or not) requires initial conditions, transforming (time–fractional) differential equations and the respective initial conditions to Laplace domain yields an algebraic expression with the initial conditions included.
For the sake of comparability with other methods, we illustrate the Laplace transform method by application to a few problems already discussed.

Application to Time–fractional Ordinary Differential Equations

Let us again consider the initial value problem

$$ \begin{aligned} {}_0\mathrm{D}_t^{\nu} y(t) - \lambda y(t) &= h(t), \qquad n-1 < \nu < n,\ n = 1,2,\ldots \\ {}_0\mathrm{D}_t^{\nu-i} y(t)\big|_{t=0} &= b_i, \qquad i = 1,2,\ldots,n \end{aligned} \tag{5.39} $$

and pass to Laplace domain

$$\begin{aligned} u^\nu \tilde{y}(u) - \sum_{i=1}^{n} b_i u^{i-1} - \lambda \tilde{y}(u) &= \tilde{h}(u)\,, \qquad n-1 < \nu < n,\ \ n = 1,2,\ldots \\ i &= 1,2,\ldots,n \end{aligned} \tag{5.40}$$

so that after some algebra and with (2.37)

$$\tilde{y}(u) = \sum_{i=1}^{n} b_i \frac{u^{i-1}}{u^\nu - \lambda} + \frac{\tilde{h}(u)}{u^\nu - \lambda} \tag{5.41}$$

$$\begin{aligned} &\doteq \sum_{i=1}^{n} b_i t^{\nu-i} E_{\nu,\nu-i+1}(\lambda t^\nu) + \int_0^t (t-t')^{\nu-1} E_{\nu,\nu}(\lambda (t-t')^\nu) h(t')\, dt' \\ &= y(t)\,. \end{aligned} \tag{5.42}$$

For the initial value problem

$$\begin{aligned} \frac{\partial^n y(t)}{\partial t^n} - \lambda\, {}_0\mathrm{D}_t^{n-\nu} y(t) &= h(t)\,, \qquad n-1 < \nu < n,\ \ n = 1,2,\ldots \\ \left.\frac{\partial^{n-i} y(t)}{\partial t^{n-i}}\right|_{t=0} &= b_i\,, \qquad i = 1,2,\ldots,n \end{aligned}$$

we find in Laplace domain

$$\begin{aligned} u^n \tilde{y}(u) - \sum_{i=1}^{n} u^{i-1} b_i &= \left[\lambda u^{n-\nu} \tilde{y}(u) + {}_0\mathrm{D}_t^{(n-\nu)-1} y(t)|_{t=0}\right] + \tilde{h}(u) \\ &= \lambda u^{n-\nu} \tilde{y}(u) + \tilde{h}(u)\,. \end{aligned} \tag{5.43}$$

Here we made use of the fact that the sought function $y(t)$ is given at $t = 0$ and is well-behaved. Hence the fractional integral ${}_0\mathrm{D}_t^{(n-\nu)-1} y(t)|_{t=0}$ appearing in the Laplace transform of the fractional derivative (note again that $n-1 < \nu < n$) must vanish. The solution is then:

$$\begin{aligned}\tilde{y}(u) &= \sum_{i=1}^{n} b_i \frac{u^{i-1}}{u^n - \lambda u^{n-\nu}} + \frac{\tilde{h}(u)}{u^n - \lambda u^{n-\nu}} \\ &\doteq \sum_{i=1}^{n} b_i t^{n-i} E_{\nu,1+n-i}(\lambda t^\nu) + \int_0^t (t-t')^{n-1} E_{\nu,n}(\lambda (t-t')^\nu) h(t')\, dt' \\ &= y(t)\,,\end{aligned} \tag{5.44}$$

which reproduces the solution (5.22) obtained previously.

5.2.3 Initial Value Problem of the Time–fractional Diffusion Equation

Let us now apply the Laplace transform method to a partial fractional differential equation. Consider the IVP of the time–fractional diffusion equation

$$\begin{aligned}\frac{\partial C(x,t)}{\partial t} &= K_\alpha {}_0\mathrm{D}_t^{1-\alpha} \Delta C(x,t)\,, \\ \lim_{x\to\pm\infty} C(x,t) &= 0\,, \qquad [C(x,t)]_{t=0} = C_0(x)\end{aligned} \tag{5.45}$$

with $0 < \alpha < 1$, $t > 0$. The Laplace transform with respect to t results in

$$u\tilde{C}(x,u) - C_0(x) = K_\alpha u^{1-\alpha} \Delta \tilde{C}(x,u)\,, \tag{5.46}$$

an inhomogeneous ordinary differential equation for $\tilde{C}(x,u)$ in x. Solving the respective homogeneous equation yields the propagator in Laplace domain,

$$\tilde{C}_{hom}(x,u) = \frac{1}{\sqrt{K_\alpha u^{2-\alpha}}} \exp\left[-\sqrt{\frac{u^\alpha}{K_\alpha}}|x|\right] \tag{5.47}$$

$$= \tilde{G}(x,u)\,, \tag{5.48}$$

so that the full solution is the spatial convolution of (5.47) with the initial condition. The sought solution back in original domain is hence:

$$\begin{aligned}C(x,t) &= \int_{-\infty}^{\infty} G(x-x',t) C_0(x')\, dx' \\ G(x,t) &= \frac{1}{\sqrt{4K_\alpha t^\alpha}} H_{1,1}^{1,0}\left[\frac{|x|}{\sqrt{K_\alpha t^\alpha}}\,\middle|\, \begin{matrix}(1-\alpha/2, \alpha/2)\\ (0,1)\end{matrix}\right].\end{aligned} \tag{5.49}$$

The propagator $G(x,t)$ corresponds to the response of the system to a Dirac-delta-peak-like initial condition and is also referred to as the Green function of the fractional PDE (5.45).

5.2.4 Time–fractional Diffusion Equation with Source Term

In what follows, we consider the subdiffusion equation (4.46) with an added source term $f(x,t)$,

$$\frac{\partial C(x,t)}{\partial t} = K_{\alpha 0} \mathrm{D}_t^{1-\alpha} \Delta C(x,t) + f(x,t) \tag{5.50}$$

where $f(x,t)$ is a real-valued function. [2]

Physical Interpretation

From the physical point of view, a source term entails a certain proportion of particles that enter the system at a time $t' > 0$. This raises the question of the meaning of the Riemann-Liouville operator especially when it is applied to concentrations of particles that were introduced into the system at a later point of time than denoted by its lower integration limit. It is not clear whether Eq. (5.50) imposes additional, probably unphysical assumptions on the age profile of the newly introduced particles. We check the physical soundness of the notation (5.50) by introducing partial concentrations $C_{t'}(x,t)$ of particles introduced at time $t' > 0$. The newly introduced particles should begin their first waiting time at the time of introduction t', hence each of these partial concentrations must obey the IVP of subdiffusion:

$$\begin{aligned} \frac{\partial C_{t'}(x,t)}{\partial t} &= K_{\alpha t'} \mathrm{D}_t^{1-\alpha} \Delta C_{t'}(x,t) \\ [C_{t'}(x,t)]_{t=t'} &= f(x,t') \end{aligned} \tag{5.51}$$

which has the solution:

$$C_{t'}(x,t) = \int_{-\infty}^{\infty} G_{t'}(x-x',t) f(x,t')\, dx' \,. \tag{5.52}$$

The respective partial Green functions $G_{t'}(x,t)$ are defined only for $t \geq t'$, i.e. the partial Green functions are equal to the Green functions of the Subdiffusion equation shifted in time, $G_{t'}(x,t) = G(x,t-t')$. On the other hand, using the fact that $C_{t'}(x,t) = 0$ for $t < t'$, (5.51) can be rewritten as

[2] Sources with non-positive sign are sometimes referred to as drains in the literature, but since our notion of a source does not impose any restriction concerning sign, we only use the term source here.

$$\frac{\partial C_{t'}(x,t)}{\partial t} = K_\alpha \left[{}_0\mathrm{D}_{t'}^{1-\alpha} \Delta C_{t'}(x,t) + {}_{t'}\mathrm{D}_t^{1-\alpha} \Delta C_{t'}(x,t) \right] \tag{5.53}$$

$$= K_\alpha {}_0\mathrm{D}_t^{1-\alpha} \Delta C_{t'}(x,t) \, . \tag{5.54}$$

In this special constellation, the operators ${}_0\mathrm{D}_t^{1-\alpha}$ and ${}_{t'}\mathrm{D}_t^{1-\alpha}$ are equivalent, so that the integration of the partial concentrations over their initial times and the Riemann-Liouville Operator acting upon them can be interchanged. The overall particle concentration is obtained by integrating all partial concentrations over their initial times:

$$\begin{aligned} C(x,t) &= \int_0^t C_{t'}(x,t)\, dt' \\ &= \int_0^t \int_{-\infty}^{\infty} G_{t'}(x-x',t) f(x,t')\, dx'\, dt' \\ &= \int_0^t \int_{-\infty}^{\infty} G(x-x',t-t') f(x',t')\, dx'\, dt' \, . \end{aligned} \tag{5.55}$$

We have seen that the operator ${}_{t'}\mathrm{D}_t^{1-\alpha}$ acting upon partial concentrations that were introduced into the system at $t = t' > 0$ can be replaced by ${}_0\mathrm{D}_t^{1-\alpha}$ without difficulty. Hence, the lower terminal of the Riemann–Liouville Operator has to be interpreted as the time of preparation of the physical system. The inhomogeneous subdiffusion equation (5.50) describes correctly also the partial concentrations of particles that enter the system at a later time than the preparation time. These partial concentrations obey the fractional diffusion equation with initial time (and lower terminal of the Riemann–Liouville Operator) t'. From this we may also conclude that the inhomogeneity $f(x,t)$ in Eq. (5.50) can be interpreted as source term in the physical sense and conforms with the picture of newly entering particles having "age zero" at the time of their introduction into the system.
As a result, the inhomogeneous fractional PDE can be treated as a superposition of solutions to the homogeneous IVPs with initial times t' and initial profiles of partial concentrations $f(x,t')$. Later on, these findings will help us to put up reaction–subdiffusion equations where new particles are created in the course of time due to a reaction. The validity of the superposition principle in time fractional PDEs, especially in cases with the overall particle number changing in time, provides as well a powerful tool in solving Boundary Value Problems.
But before we turn to the discussion of boundary value problems, we briefly sketch an alternative method to treat inhomogeneous time–fractional linear PDEs.

Subordination of the Inhomogeneous Time-fractional Diffusion Equation

In the following we solve the time–fractional diffusion equation with source term by exploiting the fact that anomalous time-fractional diffusion is subordinated to normal Brownian diffusion. The propagators of both are related with each other via an integral transformation $\mathcal{T}_\alpha$ given by Eq. (4.53).

In order to formulate an inhomogeneous normal diffusion equation that a given inhomogeneous time fractional diffusion problem is subordinated to, the rate of newly introduced particles has to be adapted to the operational time of the system, which requires a transformation of the source term. The concentration of C-particles in Brownian diffusion results from the convolution (denoted $*$) with respect to x and t of the respective Green function G_{BM} and the source f_{BM},

$$C_{BM}(x,t) = G_{BM}(x,t) * f_{BM}(x,t) \; . \tag{5.56}$$

Eq. (4.53) establishes the relation between the Green functions of normal and time fractional diffusion, so that for the latter the particle concentration is

$$\begin{aligned} C_{SD}(x,t) &= G_{SD}(x,t) * f_{SD}(x,t) \\ &= \mathcal{T}_\alpha\{G_{BM}(x,t)\} * f_{SD}(x,t) \; . \end{aligned} \tag{5.57}$$

The aim is now to find a source term $f_{BM}(x,t)$ such that the sought concentration C_{SD} resulting from the given source f_{SD} is subordinated to the (normal) concentration C_{BM} with that auxiliary source f_{BM}. This means that if we subordinate our underlying jump process to the Brownian one, we have to modify our source term in the following manner, provided this transform of the source term exists, [3]

$$f_{BM}(x,t) = \mathcal{T}_\alpha^{-1}\left\{{}_0\mathrm{D}_t^{\alpha-1} f_{SD}(x,t)\right\} \; , \tag{5.58}$$

for which we solve the normal diffusion equation. Applying the transform $\mathcal{T}_\alpha\{C_{BM}(x,t)\}$ to the solution of the normal analogue (5.56) with (5.58) yields the solution to the original subdiffusion problem. Let us briefly prove this statement: Since the subordination transform is displayed most conveniently in Laplace domain, cp. (4.54), we use this picture and write

$$\tilde{C}_{SD}(x,u) = \int_{-\infty}^{\infty} \tilde{G}_{SD}(x-x',u)\tilde{f}_{SD}(x',u)\,dx' =$$

[3] This transform does not exist if the source term is a non–smooth function of time. If we take for example a piecewise smooth source as the sum of several smooth terms shifted by t_s , the transform entails factors of $\exp\left[-t_s u^{1/\alpha}\right]$, $0 < \alpha < 1$ in Laplace domain, which has no counterpart in original domain.

$$
\begin{aligned}
&= \int_{-\infty}^{\infty} \frac{\tilde{G}_{BM}(x-x',u^\alpha)}{u^{1-\alpha}} \tilde{f}_{SD}(x',(u^\alpha)^{\frac{1}{\alpha}})\, dx' \\
&= \mathcal{T}_\alpha \left\{ \int_{-\infty}^{\infty} \tilde{G}_{BM}(x-x',u) \tilde{f}_{SD}(x',u^{\frac{1}{\alpha}})\, dx' \right\} \\
&:= \mathcal{T}_\alpha \tilde{C}_{BM}(x,u) \\
\tilde{C}_{BM}(x,u) &= \int_{-\infty}^{\infty} \tilde{G}_{BM}(x-x',u) \mathcal{T}_\alpha^{-1} \left\{ u^{\alpha-1} \tilde{f}_{SD}(x',u) \right\} dx' \,, \qquad (5.59)
\end{aligned}
$$

where $\mathcal{T}_\alpha^{-1}\left\{u^{\alpha-1}\tilde{f}_{SD}(x,u)\right\} = \tilde{f}_{BM}(x,u)$ is the modified source term. Hence, the inversely subordinated solution of the inhomogeneous subdiffusion equation corresponds indeed to the solution of a normal diffusion equation with the modified source term.

As an example, let us assume a point source at $x = 0$, prescribed by $\tilde{f}_{SD}(u) = C_0 \sqrt{\frac{K_\alpha}{u^\alpha}}$ in Laplace domain. Such a point source maintains a constant value of the concentration at $x = 0$. The modified source term and the new normal diffusion equation is then:

$$
\begin{aligned}
\tilde{f}_{BM}(u) &= C_0 \sqrt{\frac{K_\alpha}{u}}, \\
\tilde{C}_{BM}(u) = \tilde{G}_{BM}(x,u)\tilde{f}_{BM}(u) &= \frac{C_0}{u} \exp\left[-\sqrt{\frac{u}{K_\alpha}}|x| \right] . \qquad (5.60)
\end{aligned}
$$

The corresponding inversely subordinated constant boundary value $C_{BM}(x = 0, u)$ of the normal diffusive equation is also constant, as it should. Applying the back-transform, i.e. subordination, yields

$$
\begin{aligned}
\tilde{C}_{SD}(u) &= \frac{C_0}{u^\alpha} \exp\left[-\sqrt{\frac{u^\alpha}{K_\alpha}}|x| \right] u^{\alpha-1} \\
&= \frac{C_0}{u} \exp\left[-\sqrt{\frac{u^\alpha}{K_\alpha}}|x| \right] . \qquad (5.61)
\end{aligned}
$$

5.3 Boundary Value Problems under Subdiffusion

In the following we will employ the method of Laplace in the context of boundary value problems (BVP). This approach is commonly used in normal diffusion, and is the method of choice in the case of time varying boundary conditions. The method basically consists in the solution of the free diffusion equation in Laplace domain and a subsequent fitting of the Laplace transformed boundary condition. Analogously to the procedure used in normal diffusion, the fitting

of boundaries in Laplace domain was applied to time–fractional PDEs, see e.g. Ref. [98].
We have already shown that the introduction of a source term into time–fractional PDEs corresponds to the introduction of particles into the system, each of whose first waiting time period begins at the time of introduction. Therefore a physical interpretation of the Laplace method can be given by considering a source at the boundary that compensates for the gains and losses such that the prescribed boundary condition is maintained.
Later on, the method of images will be discussed and supplemented by some examples, before we turn to using combinations of both Laplace's method and the method of images in order to solve initial–BVPs of the subdiffusion equation.

5.3.1 Laplace's Method in Boundary Value Problems

Semi–infinite Domain

For simplicity, consider only one boundary at x_b. We label the particles according to the time t' they were introduced into the system, so that e.g. $C(x,t|t')dt'$ is the partial concentration at x at time t of particles that were introduced between t' and $t'+dt'$. Each partial concentration will behave according to the Green function G of subdiffusion. The boundary value will be maintained by a point source at the boundary that compensates for losses, so that we can write

$$C(x,t|t')dt' \quad = \quad G(x-x_b,t-t')f(t')dt' \tag{5.62}$$

where $f(t')dt'$ is the amount of particles inserted between t' and $t'+dt'$. The spatial integration is already carried out, so that the location of the source is included in G shifted by x_b. The initial particle concentration be zero in the interior of the system. The overall concentration is the integral of (5.62) with respect to t' from 0 to t, which is a temporal convolution, and yields in Laplace domain:

$$\tilde{C}(x,u) = \tilde{f}(u)\tilde{G}(x-x_b,u)\ . \tag{5.63}$$

Recall the subdiffusion propagator in Laplace domain:

$$\tilde{G}(x,u) \quad = \quad \frac{1}{\sqrt{K_\alpha u^{2-\alpha}}}\exp\left[-\sqrt{\frac{u^\alpha}{K_\alpha}}\,|x|\right]\ ,$$

so that we find the required source term by Eq. (5.63) at the boundary x_b

$$\tilde{f}(u) = \tilde{C}(x_b,u)\,\sqrt{K_\alpha}u^{1-\alpha/2}\ . \tag{5.64}$$

Hence, the full solution yields

$$\tilde{C}(x,u) = \tilde{C}(x_b,u)\exp\left[-\sqrt{\frac{u^\alpha}{K_\alpha}}|x-x_b|\right] \tag{5.65}$$

and is equivalent to the one obtained by directly fitting the boundary in Laplace domain.
A very common type of BVP is the one with constant values at the boundaries, the so-called Dirichlet BVP. This type of boundary condition may be pertinent to the situation where the traps within the medium have a finite capacity. If the particle concentration in a reservoir in contact with that medium is large enough, the concentration will take a finite value at the boundary layer of the medium.
In the case of $C(x_b,t) = C_0$ or $\tilde{C}(x_b,u) = \frac{C_0}{u}$, we have

$$\tilde{C}(x,u) = \frac{C_0}{u}\exp\left[-\sqrt{\frac{u^\alpha}{K_\alpha}}|x-x_b|\right], \tag{5.66}$$

which can be expressed in terms of an H-function in original domain, cf. Appendix C,

$$C(x,t) = C_0 H^{1,0}_{1,1}\left[\frac{|x-x_b|}{\sqrt{K_\alpha t^\alpha}}\middle|\begin{matrix}(1,\alpha/2)\\(0,1)\end{matrix}\right]. \tag{5.67}$$

The solution to the Dirichlet BVP on the half line under normal diffusion is obtained by putting formally $\alpha = 1$ and $K_\alpha = D$ in (5.67), so that this expression becomes $C(x,t) = C_0\mathrm{erfc}\left[\frac{x}{\sqrt{4Dt}}\right]$.

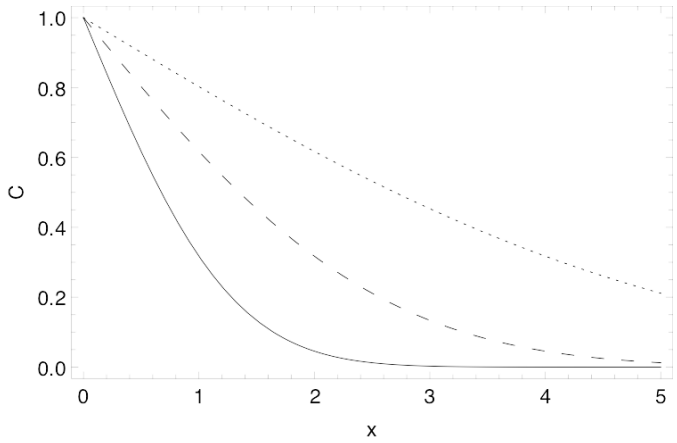

Figure 5.3: Concentration profiles in the normal case of the Dirichlet problem on the semi–infinite domain for $t = 0.5$ (solid), 2 (dashed), 8 (dotted line). The boundary value at $x = 0$ is kept at $C_0 = 1$. The diffusion constant is $D = 1$.

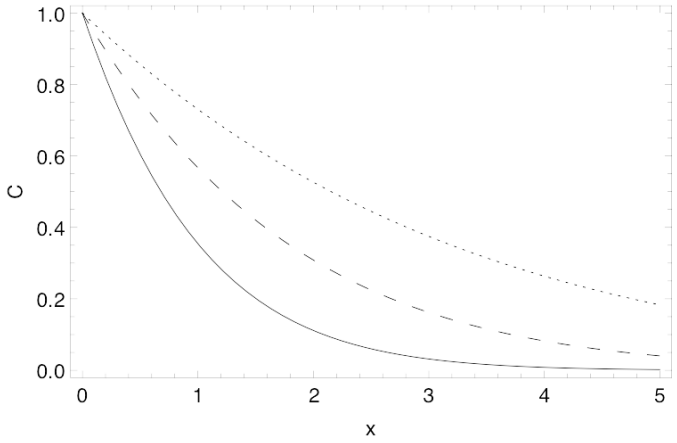

Figure 5.4: Concentration profiles under subdiffusion of the Dirichlet problem on the semi–infinite domain for $t = 0.5$ (solid), 5 (dashed), 50 (dotted line); $\alpha = 0.5$. The boundary value at $x = 0$ is again $C_0 = 1$, and the generalized diffusion constant is $K_\alpha = 1$.

In some cases it is more convenient to expand the exponential function in (5.66) in its Taylor series and Laplace invert the resultant expression term by term instead of using the H–function representation of the solution. Fig. 5.4 shows the concentration profiles at different times obtained from such series representation for $\alpha = 0.5$. The profiles at different times under normal diffusion were obtained by plotting the error–function and are depicted in Fig. 5.3. The temporal change of the profiles in the anomalous case takes place much more slowly than in the normal diffusive case. Note that the profiles depicted in the anomalous case correspond to times covering a range of an order of magnitude more than the times for which the normal profiles are shown.

Boundary conditions can also be imposed upon the concentration flux. From continuity we find the flux to be defined as $J(x,t) = -K_{\alpha 0}\mathrm{D}_t^{1-\alpha}\frac{\partial}{\partial x}C(x,t)$. Therefore the flux basically obeys the same equation as the particle concentration, and the solution of such problems is straightforward. We now pass on to give some more examples for the application of the Laplace method to BVPs.

Bounded Domain

We now consider subdiffusion on a bounded domain $x \in [0, L]$, namely a Dirichlet BVP where both boundaries have non-zero constant values $C(0,t) = C_0$, $C(L,t) = C_L$. The solution takes the form of a linear combination of convolutions of functions of the type (5.63), The construction of sources at the boundaries yields the Ansatz in Laplace domain:

$$\tilde{C}(x,u) = C_0\tilde{f}_0(u)\tilde{G}(x,u) + C_L\tilde{f}_L(u)\tilde{G}(x-L,u)\ . \tag{5.68}$$

Fitting the boundaries results in

$$\tilde{C}(x,u) = \\ \frac{1}{u}\left[C_0\left(1-\frac{C_L}{C_0}\frac{\exp\left[-\sqrt{\frac{u^\alpha}{K_\alpha}}L\right]-\frac{C_0}{C_L}\exp\left[-\sqrt{\frac{u^\alpha}{K_\alpha}}2L\right]}{1-\exp\left[-\sqrt{\frac{u^\alpha}{K_\alpha}}2L\right]}\right)\exp\left[-\sqrt{\frac{u^\alpha}{K_\alpha}}x\right]\right. \\ \left.+C_L\left(\frac{1-\frac{C_0}{C_L}\exp\left[-\sqrt{\frac{u^\alpha}{K_\alpha}}L\right]}{1-\exp\left[-\sqrt{\frac{u^\alpha}{K_\alpha}}2L\right]}\right)\exp\left[-\sqrt{\frac{u^\alpha}{K_\alpha}}(L-x)\right]\right] . \tag{5.69}$$

The stationary solution is obtained by sending the Laplace variable to zero,

$$\begin{aligned}\tilde{C}(x,u\to 0) &= \frac{1}{u}\left[\frac{C_L-C_0}{L}x+C_0\right] \\ C(x,t\to\infty) &= \frac{C_L-C_0}{L}x+C_0 \ .\end{aligned}$$

The stationary particle profile is clearly linear in x, just as in normal diffusion. In leading order, the system approaches the stationary state as

$$\frac{C_L x(-5L+3x)+C_0(6L^2-Lx+3x^2)}{12K_\alpha}u^{\alpha-1} \ , \tag{5.70}$$

corresponding to

$$\frac{C_L x(-5L+3x)+C_0(6L^2-Lx+3x^2)}{12K_\alpha\Gamma[1-\alpha]}t^{-\alpha}$$

in time domain. The relaxation behavior differs from normal diffusion and is very slow, in compliance with the asymptotic inverse power law behavior of the Mittag-Leffler mode decay in time-fractional diffusion.

5.3.2 The Method of Images

The method of images plays an important role in the theory of electricity, but has also proven useful in its application to the Dirichlet BVP in diffusion, especially when the boundaries kept at constant concentration are planes. The volume under consideration is being continued analytically in all directions, and images are taken in the bounding planes. This procedure results in a distribution of sources/ sinks that maintains the given boundary condition. The method works as well for zero-flux boundary conditions. If there are no sources within the bounded volume under consideration, the method of images converts the BVP to a homogeneous IVP on an unbounded domain. In the case of existing sources in the original volume, the BVP becomes an inhomogeneous IVP.
This method was partially discussed in [93] for subdiffusion, though avoiding the problem of incorporation of sources. In the examples treated there, all particles entered the system at the same initial time and none was created later. In some cases particles were vanishing in the course of time.
This raises the question of the general applicability of the method of images in the case of subdiffusion. As we have seen above, the prescription of boundary values in one dimension corresponds to the introduction of point sources (or drains) at the boundaries. Since memory plays an important role in subdiffusion, it is not immediately clear whether e.g. the situation with sources at the boundaries and no sources within the bounded volume is equivalent to a homogeneous IVP under subdiffusion, where all particles are introduced at the initial time, so that in the different situations the involved particles have a different age profile. These different age profiles do not affect the resultant evolution of the overall particle profiles.
The preparatory work in the section on IVPs has pointed out that in time fractional diffusion equations involving the Riemann-Liouville fractional derivative, the superposition principle is valid for all partial concentrations as long as their history does not begin before the lower integration limit indicated in the time fractional derivative, i.e. the time of preparation of the system. This ensures that the situation of subdiffusion involving sources is properly described by the inhomogeneous time fractional diffusion equation (5.50). Thus, the subdiffusion equation with the Riemann-Liouville fractional derivative acting upon partial concentrations introduced later than indicated by its lower terminal provides a consistent mathematical description of the situation. On the stochastic level this property is obvious and can be explained by the independence of the consecutive waiting time periods of the particle jumps. Particles that perform a jump at the same time t are not distinguishable by their time of introduction to the system anymore.
It should therefore make no difference whether a boundary value is maintained by a source or by symmetry. This enables us to determine the boundary values by appropriately constructed symmetries and boil the problem down to an IVP under subdiffusion. Hence, the method of images does not only apply to the solution of boundary value problems of the normal diffusion equation, but can be adopted to problems in time-fractional diffusion as well, even if particles are introduced into the considered domain during observation time. This fact also provides a basis for combining the methods of Laplace and of images in order to solve the time–fractional diffusion equation.

Semi–infinite Domain: Dirichlet BVP

Let us illustrate the aforementioned conclusions by the following simple example using the method of images. In order to solve the Dirichlet BVP with $C(x=0,t)=C_0$ in the domain $[0,\infty]$ which is assumed to be empty initially, we consider the time-fractional diffusion Eq. (5.45) on the domain $x \in [-\infty,\infty]$ under the initial condition

$$C(x,0) \quad = \quad 2C_0\theta(-x),$$

where $\theta(x)$ is the Heaviside step function. Since the transport is spatially symmetric, we will have a constant concentration C_0 at $x=0$. The amount of particles travelling to the right a distance x is in average the same as the number of particles going to the left (distance $-x$).
We divide the extended initial distribution into infinitesimal intervals $x', x'+dx'$, so that in the limit an integral over $2C_0\delta(x+x')$ emerges. The solution to the original problem can be obtained by superimposing the elementary solutions corresponding to the δ initial conditions. The initial condition is sketched in Fig. 5.5.

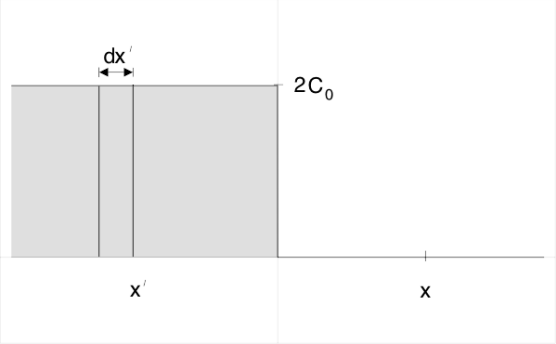

Figure 5.5: Sketch of the initial concentration profile maintaining the boundary condition $C(0,t)=C_0$.

At x, the concentration C will be:

$$\begin{aligned} C(x,t) &= 2C_0 \int_{-\infty}^{-x} G(x',t)\,dx' \\ &= 2C_0 \left[\int_{-\infty}^{0} G(x',t)\,dx' - \int_{-x}^{0} G(x',t)\,dx' \right] \\ &= C_0 - 2C_0 \int_{0}^{x} G(x',t)\,dx' \ . \end{aligned} \tag{5.71}$$

In Laplace domain, the solution is

$$\begin{aligned}\tilde{C}(x,u) &= C_0\left[\frac{1}{u} - 2\int_0^x \tilde{G}(x',u)\,dx'\right] \\ &= \frac{C_0}{u}\left[1+\exp\left[-\sqrt{\frac{u^\alpha}{K_\alpha}}|x|\right]-1\right]. \end{aligned} \tag{5.72}$$

Note that this result obtained from spatial superposition of Green functions is exactly the same as the one obtained by using the Laplace method corresponding to a temporal superposition of Green functions, cp. Eq. (5.66).
Inserting the Green function of normal diffusion $G(x,t) = \frac{1}{\sqrt{4\pi Dt}}\exp\left[-\frac{x^2}{4Dt}\right]$ yields the well-known complementary error function

$$C(x,t) = C_0\left[1-\mathrm{erf}\left[\frac{x}{\sqrt{4Dt}}\right]\right] = C_0\mathrm{erfc}\left[\frac{x}{\sqrt{4Dt}}\right]. \tag{5.73}$$

Semi–infinite Domain: Absorbing and Reflecting Boundary
The method of images is especially convenient in the case of totally absorbing or totally reflecting boundaries, i.e. for zero flux or zero concentration at a boundary. We first recall the solution of the mere initial value problem of the subdiffusion equation with an absorbing boundary as given e.g. in [93]. The solution of the subdiffusive initial value problem with initial concentration $C(x,0) = \delta(x)$ and an absorbing or reflecting boundary $C(L,t) = 0$ reads:

$$C(x,t) = G(x,t) \pm G(x-2L,t) \tag{5.74}$$

where $G(x,t)$ is the Green function of the free problem given by (4.45), and the "−" and "+" account for absorption and reflection at the boundary, respectively. Laplace transforming (5.74) yields:

$$\tilde{C}(x,u) = \frac{1}{\sqrt{K_\alpha}u^{1-\alpha/2}}\left[\exp\left[-\sqrt{\frac{u^\alpha}{K_\alpha}}|x|\right]-\exp\left[-\sqrt{\frac{u^\alpha}{K_\alpha}}|x-2L|\right].\right] \tag{5.75}$$

For an absorbing boundary at $L = 1$, the profiles for subdiffusion (and their odd continuation to $x > L$), $\alpha = 0.5$, are shown in Fig. 5.6, and the profiles under normal diffusion in Fig. 5.7. In the case of sudiffusion, the profiles were obtained by a series expansion and term–by–term inversion of (5.75). The normal diffusive case corresponds again to the formal substitution $\alpha = 1$, $K_\alpha \to D$. Note that the shown profiles for subdiffusion cover more orders of magnitude of the times than the normal diffusive ones.

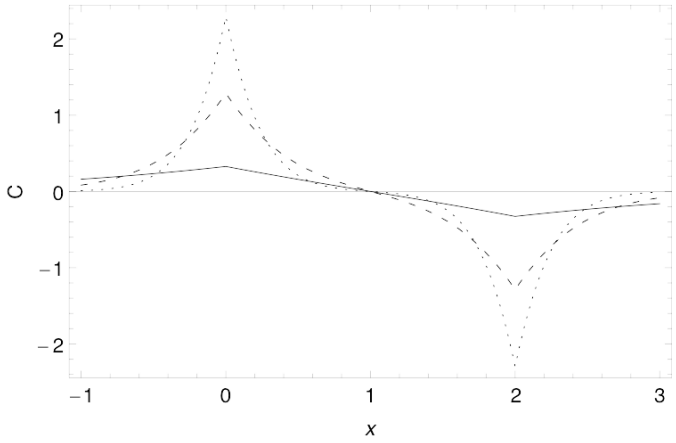

Figure 5.6: Construction of the concentration profiles in the anomalous case $\alpha = 0.5$ for an absorbing boundary at $L = 1$ for $t = 0.001$ (dotted), 0.01 (dashed), 1 (solid line); $K_\alpha = 1$, initial condition $C(x,0) = \delta(x)$.

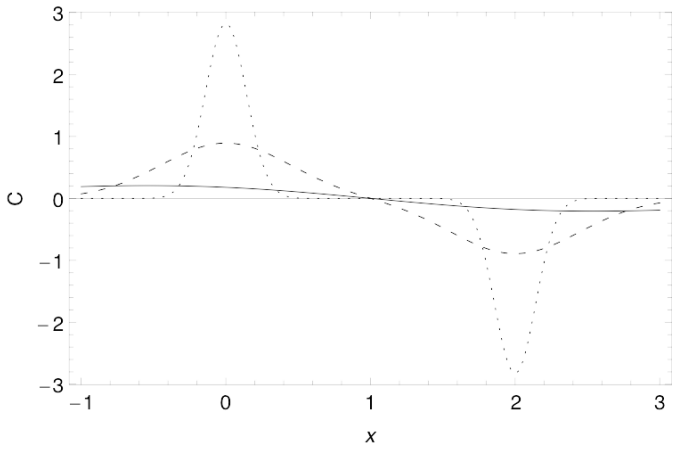

Figure 5.7: Construction of the concentration profiles in the normal case for an absorbing boundary at $L = 1$, for $t = 0.01$ (dotted), 0.1 (dashed), 1 (solid line); $D = 1$.

The method of images can also be applied to bounded domains. Problems of this type were investigated for subdiffusion in Ref. [93] in the case of IVPs with all the boundaries being either totally reflecting or absorbing. First, a short compilation of the main results will be given. Then, the focus will be on the more general situations comprising other boundary conditions which correspond to introduction of particles after the time of preparation of the system and require additional application of the method of Laplace.

Bounded Domain: Absorbing and Reflecting Boundary

Assume absorbing boundaries at $\pm L$, i.e. $C(-L,t) = C(L,t) = 0$. We successively reflect the free Green function (4.45) about $\pm L$ along the x–axis, which ensures that $C(x = \pm L) = 0$. Following [93], we first incorporate the absorbing boundary $C(L,t) = 0$. The exact solution is constructed as:

$$C(x,t) = \sum_{n=-\infty}^{\infty} G(x+4nL,t) - G(-x+4nL+2L,t) \, . \tag{5.76}$$

The Poisson summation formula (see Appendix C), $2\pi\delta(x-x') = \int_{-\infty}^{\infty} \exp[\mathrm{i}kx - x']\,dk$ and hence $\sum_{n=-\infty}^{\infty} \exp[\mathrm{i}kn] = \exp[\mathrm{i}k/2] \sum_{n=-\infty}^{\infty} (-1)^n \delta(k/(2\pi)+n)$ allows to rewrite (5.76) in Laplace–domain:

$$\tilde{C}(x,u) = \frac{1}{4L} \sum_{n=-\infty}^{\infty} e^{\mathrm{i}\pi nx/(2L)} \left[\tilde{G}\left(k = \frac{\pi n}{2L}, u\right) - (-1)^n \tilde{G}\left(k = -\frac{\pi n}{2L}, u\right) \right] . \tag{5.77}$$

Recalling that the Fourier-Laplace Transform of the Green function is

$$\hat{\tilde{G}}(k,u) = \frac{u^{\alpha-1}}{u^\alpha + K_\alpha k^2} \, , \tag{5.78}$$

and with the condition $C(x = \pm L, t) = 0$, Eq. (5.77) becomes

$$\tilde{C}(x,u) = \frac{u^{\alpha-1}}{L} \sum_{n=0}^{\infty} e^{\pi\mathrm{i}(2n+1)x/(2L)} \frac{1}{u^\alpha + K_\alpha (2n+1)^2 \pi^2 / 4L^2} \, . \tag{5.79}$$

Back in time domain we have

$$C(x,t) = \frac{1}{L} \sum_{n=0}^{\infty} e^{\pi\mathrm{i}(2n+1)x/(2L)} E_\alpha \left[-K_\alpha \frac{(2n+1)^2 \pi^2}{4L^2} t^\alpha \right] . \tag{5.80}$$

Fig. 5.8 and 5.9 show the solutions (5.80) for normal diffusion and for subdiffusion, $\alpha = 0.5$, at different times. The absorbing walls are located at $L = \pm 1$, the initial condition is $C(x,0) = \delta(x)$. Note again that the depicted profiles under subdiffusion cover more orders of magnitude in time than the normal diffusive ones, which emphasizes the slow relaxation in the anomalous case.

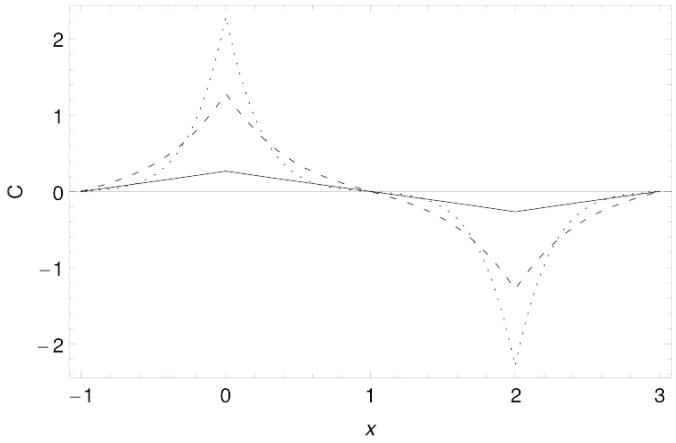

Figure 5.8: $C(x,t)$ for two absorbing boundaries at $x=-1$ and $x=1$ and initial condition $C(x,0)=\delta(x)$. $\alpha=0.5$ at $t=0.001$ (dotted), 0.01 (dashed), 1 (solid line); $K_\alpha=1$.

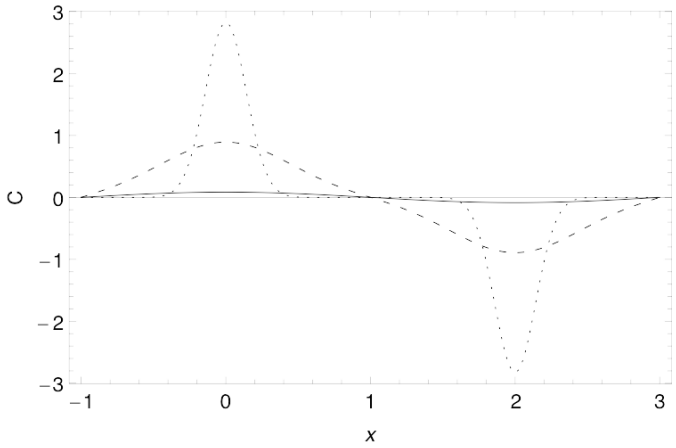

Figure 5.9: $C(x,t)$ under normal diffusion for two absorbing boundaries at $x=-1$ and $x=1$ and initial condition $C(x,0)=\delta(x)$. $t=0.01$ (dotted), 0.1 (dashed), 1 (solid line); $D=1$.

Likewise, the solution can be found for reflecting boundaries $\frac{\partial}{\partial x}C(x,t)\big|_{x=\pm L}=0$. The ansatz is changed to

$$C(x,t) \;=\; \sum_{n=-\infty}^{\infty} G(x+4nL,t)+G(-x+4nL+2L,t)\;, \tag{5.81}$$

so that the solution in Laplace domain takes on the form

$$\tilde{C}(x,u) = \frac{1}{4L}\sum_{n=-\infty}^{\infty} e^{\mathrm{i}\pi nx/(2L)}\left[\tilde{G}(k=\frac{\pi n}{2L},u)+(-1)^n\tilde{G}(k=-\frac{\pi n}{2L},u)\right] \tag{5.82}$$

and finally in time domain

$$C(x,t) = \frac{1}{L}\left[\sum_{n=1}^{\infty} e^{\pi \mathrm{i}nx/L}E_\alpha\left[-K_\alpha\frac{n^2\pi^2}{L^2}t^\alpha\right]\right]. \tag{5.83}$$

Bounded Domain: Dirichlet BVP

Now let the boundary conditions be given by $C(0,t)=C_0$ and $C(L,t)=0$. The above results from the method of images for absorbing boundary conditions (5.80) will serve as a basis for the solution, providing that $C(L,t)=0$. The next step consists in applying the Laplace method and fitting the other boundary, $C(0,t)=C_0$. Let us now take the solution to the absorbing boundary problem (5.80) as an auxiliary function and denote it by $C^*(x,t)$. In the same spirit as in section 5.3.1, we introduce sources at the boundaries $x_{BD}=2nL$ to compensate for the losses. With $\sum_{n=0}^{\infty}\frac{1}{1+(2n+1)^2c}=\frac{\pi}{4\sqrt{c}}\tanh[\frac{\pi}{2\sqrt{c}}]$ we find for the temporal behavior of $\tilde{C}^*(x_{BD},u)$ in Laplace domain:

$$\begin{aligned}\tilde{C}^*(x_{BD},u) &= \pm\frac{u^{\alpha-1}}{L}\sum_{n=0}^{\infty}\frac{1}{u^\alpha+K_\alpha(2n+1)^2\pi^2/4L^2}\\ &= \pm\frac{u^{\frac{\alpha}{2}-1}}{2\sqrt{K_\alpha}}\tanh\left[\frac{Lu^{\frac{\alpha}{2}}}{\sqrt{K_\alpha}}\right],\end{aligned} \tag{5.84}$$

where the "+" applies for the $x_{BD}=4Ln$ and the "−" for $x_{BD}=2L(2n+1)$. Consequently, the solution to the full Dirichlet BVP with $C(0,t)=C_0$, $C(L,t)=0$ is obtained by multiplying the respective source term to (5.82):

$$\begin{aligned}\tilde{C}(x,u) = {} & C_0\frac{2\sqrt{K_\alpha}}{u^{\frac{\alpha}{2}}}\coth\left[\frac{Lu^{\frac{\alpha}{2}}}{\sqrt{K_\alpha}}\right]\times\\ & \frac{u^{\alpha-1}}{L}\sum_{n=0}^{\infty}e^{\pi\mathrm{i}(2n+1)x/(2L)}\frac{1}{u^\alpha+K_\alpha(2n+1)^2\pi^2/4L^2}.\end{aligned} \tag{5.85}$$

For t large, the source term can be approximated by $\frac{2K_\alpha}{L}u^{-\alpha}$, so that we find the long time behavior

$$C(x,t) \simeq 8C_0 \sum_{n=0}^{\infty} \frac{e^{\pi \mathrm{i}(2n+1)x/(2L)}}{\pi^2(2n+1)^2}\left[1 - E_\alpha\left[-K_\alpha \frac{\pi^2(2n+1)^2}{4L^2}t^\alpha\right]\right], \tag{5.86}$$

which involves again the Mittag–Leffler–function. Hence the decay of the modes goes as $t^{-\alpha}$ at large times. For details of the calculation see Appendix C.
The above BVP can be solved alternatively by constructing the solution from (5.74), which ensures that $C(L,t) = 0$, and fitting the remaining boundary at $x = 0$ in Laplace domain. This method avoids the problem of overshoot which often occurs in the approximation of the profile by means of truncating the Fourier series representation. In general, a full Laplace inversion of the solution is possible in terms of H–functions. However, series expansions at small u are often more practicable, especially in investigating the the long-time behavior of the concentration profile.
We construct again an odd continuation of our function to the interval of double length:

$$C(x,t) = G(x,t) - G(2L-x,t)$$

where $G(x,t)$ is the Green function of the free problem, so that the solution of the BVP can be found by fitting the boundary:

$$\tilde{C}(x,u) = \frac{C_0}{u}\frac{\exp\left[-\sqrt{\frac{u^\alpha}{K_\alpha}}x\right] - \exp\left[-\sqrt{\frac{u^\alpha}{K_\alpha}}(2L-x)\right]}{1-\exp\left[-\sqrt{\frac{u^\alpha}{K_\alpha}}2L\right]}. \tag{5.87}$$

Expanding this expression around $u = 0$ and keeping only the leading orders we find the stationary solution

$$\begin{aligned} \tilde{C}(x,u\to 0) &= \frac{C_0}{u}\frac{L-x}{L} \\ C(x,t\to\infty) &= C_0\left(1-\frac{x}{L}\right) \end{aligned}$$

and the lowest order u-correction:

$$\frac{2C_0}{3K_\alpha}\left[Lx - L^2\right]u^{\alpha-1}, \tag{5.88}$$

which in time domain behaves as

$$\frac{2C_0}{3K_\alpha \Gamma[1-\alpha]}\left[Lx - L^2\right]t^{-\alpha}$$

and hence conforms with the long time relaxation behavior obtained in Eq. (5.86).

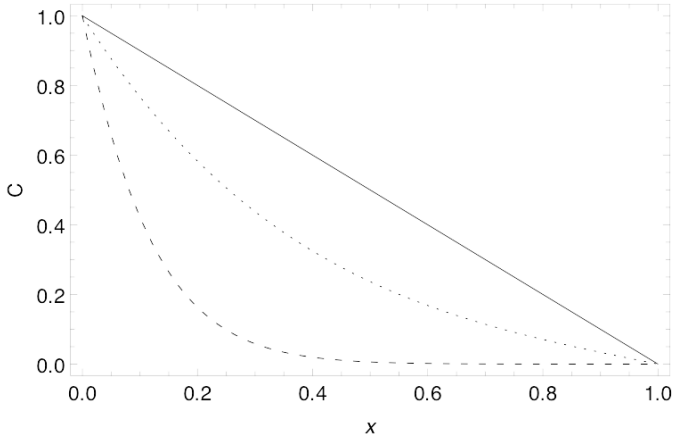

Figure 5.10: $C(x,t)$ for $\alpha = 0.5$ at $t = 0.0001$ (dashed), 0.01 (dotted), 1 (solid line). $L = 1$, $K_\alpha = 1$. The boundary values are $C(0,t) = 1$ and $C(1,t) = 0$.

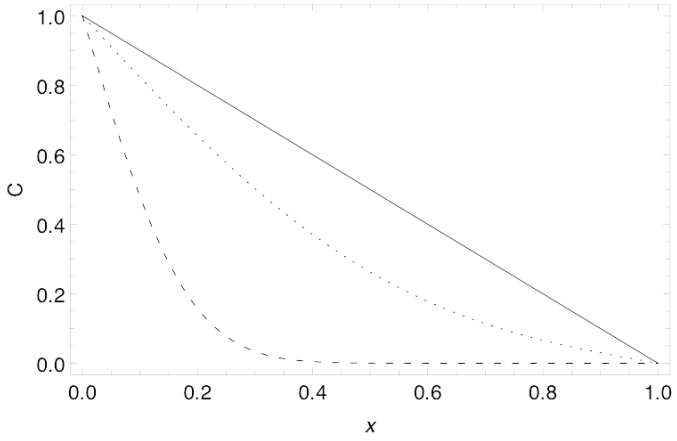

Figure 5.11: $C(x,t)$ under normal diffusion at $t = 0.01$ ((dashed), 0.1 (dotted), and the stationary profile $t = \infty$ (solid line); $D = 1$. The boundary values are $C(0,t) = 1$ and $C(1,t) = 0$.

Figs. 5.10 and 5.11 show the particle profiles for subdiffusion and normal diffusion at different times, respectively, for boundary values $C(0,t) = 1$ and $C(1,t) = 0$. The profiles were obtained by a small u series expansion of the solution (5.87) and subsequent inversion. Note again the different range of times for which the profiles are shown in the anomalous and normal case.

6 Chemical Reactions under Subdiffusion

There are basically two different concepts of reaction–subdiffusion. The first accounts for the situation where, from the CTRW point of view, the reaction of a particle coincides with a jump event. The particle reacts with a certain probability at the instant a jump occurs, provided the respective reaction partners are present. Such reaction–subdiffusion equations exhibit decoupled reaction– and transport terms, both being acted upon by a time–fractional derivative. In order to obtain solutions to this type of equations, it is often promising to extend the methods known from the normal reaction–diffusion analogue, e.g. by making use of scaling or subordination, or quasi-static approaches, where applicable. This type of reaction subdiffusion will only briefly be touched upon.

The second concept is pertinent to the situation where reactions take place during the waiting time periods and obey locally the classical reaction rate kinetics and is the main focus of our considerations. This type of equations is characterized by a transport term that is influenced by reaction. More precisely, the classical rate kinetics modifies the subdiffusion kernel by an additional factor, depending in general on the particle concentrations at previous times. Before this issue is treated in detail, a brief introduction to classical reaction rate equations and an overview of different types of reaction–subdiffusion will be given. Then, we will give a derivation of reaction–subdiffusion equations under arbitrary classical linear rate kinetics by means of the CTRW approach. These equations can be presented in a closed form since the memory cutoff in the transport term is governed only by the reaction rate coefficient. The solution to a simple linear reaction–subdiffusion equation under Dirichlet boundary conditions will turn out to be representable in terms of a solution to the subdiffusion equation without reaction. Finally, nonlinear reaction–subdiffusion will be discussed.

6.1 Classical Rate Description of Chemical Reactions

Chemical reactions are often described in terms of reaction rates. Assume a reaction of N components C_l,

$$\sum_{l=1}^{N} n_l \mathrm{C}_l \underset{\kappa_-}{\overset{\kappa_+}{\rightleftharpoons}} \sum_{l=1}^{N} m_l \mathrm{C}_l \tag{6.1}$$

where κ_+ and κ_- denote the rate coefficients of the reaction in both directions, and $n_l, m_l \in \mathbb{N}$ are stoichiometry factors. The rate for a reaction to take place is given by:

$$\kappa_+ \prod_{l=1}^{N} C_l^{n_l} \qquad \text{and} \qquad \kappa_- \prod_{l=1}^{N} C_l^{m_l}, \tag{6.2}$$

i.e. the mean reaction rates are assumed to be proportional to the product of the concentrations C_l of the reaction partners. In practice, the sum of the stoichiometry factors does not exceed 2 since reactions of three particles are extremely rare [24]. Let us denote these rate terms by $R_l(x,t) = R_l(C_1(x,t),...,C_N(x,t))$ in the following. Throughout this exposition the reaction rates of the above type will be referred to as classical reaction rates.
The rate coefficient κ comprises contributions κ_r stemming from the probability to react on encounter, and κ_d which is related to the probability of particle collisions, so that

$$\kappa^{-1} = \kappa_d^{-1} + \kappa_r^{-1} \ . \tag{6.3}$$

Hence, a constant rate coefficient κ requires constant probabilities for the particles to collide and to react on encounter. The first of these probabilities is transport dependent. Smoluchowski [99] has shown that in a mean field description of particle coagulation in the case of normal diffusion in three dimensions, the transport dependent contribution to the rate coefficient must be constant. His approach was based on showing that the diffusive flux J onto the surface of a totally absorbing sphere with radius r_S reaches stationarity. With the initial homogeneous concentration C_0 and diffusion constant D, this stationary flux at large times is given by

$$J_{stat} = 4\pi D r_S C_0 \tag{6.4}$$

whose inverse determines the coagulation time and from which we conclude the contribution to the rate coefficient stemming from diffusion,

$$\kappa_d = 4\pi D r_S \ . \tag{6.5}$$

However, in most of the cases, when reactions are slow, the contribution κ_r is the dominant one [100]. Note that for slow coagulation, Smoluchowski refined the above approach by introducing a partially reflecting boundary at r_S. The result differs from the above one only by constants, proportionalities with reaction radius and diffusion constant remain the same. For a constant probability to react on encounter, it is necessary that the Maxwell velocity distribution holds throughout the reaction volume and at all times. To this end, the temperature must be constant and the particles have to perform frequent elastic collisions without reacting. The inner degrees of freedom of the particles are required to be in thermal equilibrium as well. Moreover, the particle concentrations have to be at least locally homogeneous [24].
With constant rate coefficients, the rate equation for the temporal change of concentration of species C_l is given by

$$\begin{aligned} \frac{\partial C_l(t)}{\partial t} &= \kappa_+(m_l - n_l)C_1^{n_1}(t)C_2^{n_2}(t)...C_N^{n_N}(t) \\ &+ \kappa_-(n_l - m_l)C_1^{m_1}(t)C_2^{m_2}(t)...C_N^{m_N}(t) \ . \end{aligned} \tag{6.6}$$

The stationary state is given by $\frac{\partial C_i(t)}{\partial t} = 0$, and the following relation holds:

$$\frac{\kappa_-}{\kappa_+} = \frac{C_1^{n_1}(t)C_2^{n_2}(t)...C_N^{n_N}(t)}{C_1^{m_1}(t)C_2^{m_2}(t)...C_N^{m_N}(t)} \,. \tag{6.7}$$

6.2 Reaction-Subdiffusion

Many phenomena in nonequilibrium systems can be described in terms of reaction–diffusion equations, if fluctuations can be neglected. One condition for this to hold is that the mean free paths of the reacting particles are much smaller than the characteristic scales of spatial inhomogeneities. Moreover, a three-dimensional mean-field description of reaction is considered throughout this exposition, since otherwise the assumption of a constant rate coefficient would not be correct. At lower dimensions fluctuations have to be taken into account so that a mean–field description must fail, not only in normal reaction–diffusion but also in reaction–subdiffusion. In the fluctuation dominated regime, other methods are necessary, and sometimes it is even possible to find exact solutions. Examples are immediate reactions on encounter under subdiffusion in one dimension and were given in [101, 102]. The authors adapted a method already known from the respective problems under normal diffusion and found exact solutions for the A + A coagulation and annihilation problems in terms of the distribution of empty intervals, which obeys a subdiffusion equation. Here, we assume that all equations explicitly depending only on one spatial variable x correspond to spatial homogeneity of the system within the planes perpendicular to x, so that the description via constant rate coefficients applies.

Under normal diffusion, transport of particles and reaction are independent of each other. Hence, the temporal change in particle concentration for the species C_l is obtained by adding the transport term known from the diffusion equation, and the reaction rate term,

$$\frac{\partial C_l(x,t)}{\partial t} = D_l \Delta C_l(x,t) + R_l(x,t) \,. \tag{6.8}$$

Although reaction-diffusion equations can be solved analytically only in the minority of the cases, they have been studied intensely. Applications range from physics as e.g. electron–hole recombination, to chemistry, and to ecology comprising e.g. predator-prey relationships or the spread of populations. Reaction–diffusion systems may exhibit a rich variety of dynamical behaviors, especially when the reaction rate term introduces nonlinearities. For example, travelling waves may occur or stationary or spatiotemporally oscillating patterns, e.g. Turing patterns, may arise [22]. Another phenomenon is pattern formation in the wake of a reaction front such as Liesegang bands [103].

In the following, a compilation of the hitherto existing reaction-subdiffusion equations shall be given. First attempts of setting up reaction-subdiffusion equations were based on mere conclusions by analogy. As in the case of normal reaction-diffusion, a classical reaction rate term was added to the transport term in order to obtain the change in particle concentration. Although

it is rather unlikely that this type of equations corresponds to a physical reaction-subdiffusion situation at all, it will briefly be presented here for the sake of completeness and it will be referred to as the phenomenological reaction-subdiffusion equations.
Later on, the focus will be on those reaction-subdiffusion equations that are more in use today to model reaction-subdiffusion phenomena. In reaction-subdiffusion, we may have two different situations. From the CTRW point of view, the first one pertains to the reaction taking place at a certain probability when a particle jumps (and, where applicable, encounters a reaction partner) and will be called "Subdiffusive Reaction Kinetics". The second variant is subsumed under the title "Classical Reaction Rate Kinetics", alluding to a normal, diffusion controlled reaction mechanism according to the classical Smoluchowski rate kinetics at a microscopic scale, whereas the subdiffusive motion takes place on a mesoscopic scale. Here, the reaction takes place during the waiting times and independently of the performed steps.

6.2.1 Phenomenological Reaction–Subdiffusion Equations

Analogously to normal reaction–diffusion, several authors [104, 105] have set up equations for reaction subdiffusion by adding the transport term known from time–fractional diffusion and a classical reaction rate term:

$$\frac{\partial C_l(x,t)}{\partial t} = {}_0\mathrm{D}_t^{1-\alpha} K_\alpha \Delta C_l(x,t) + R_l(x,t)\ . \tag{6.9}$$

${}_0\mathrm{D}_t^{1-\alpha}(\cdot) = \frac{1}{\Gamma(\alpha)}\frac{d}{dt}\int_0^t (t-t')^{\alpha-1}(\cdot)dt'$ is the Riemann–Liouville fractional derivative, α the subdiffusion parameter and K_α the generalized diffusion constant.

The reasoning to put up the reaction–subdiffusion equations in that way was the idea of treating the reaction term as a source term [104, 32]. In the case of a present source in subdiffusion, the amount of particles added or removed at a position x are explicitly given for all times t. Even though in reaction–subdiffusion particles are added or removed during their dispersal as well, this addition or removal is no longer explicitly time dependent, but depends on time only through the particle densities. The resultant problem in the case of reaction–subdiffusion consists in the fact that if the reaction takes place at a certain (classical) rate, there is a growing disparity between the time scales at which reactions and jump events take place. With the waiting time periods on all scales, it is obvious that especially the long waiting times are likely not to be completed because the particle vanishes due to reaction before the next step is taken. One may therefore expect qualitative effects of the reaction on the transport. These effects were not taken into account in Eq. (6.9). As we will see in section 6.2.3, taking into account the reaction probability for a particle during a waiting time in the CTRW picture indeed leads to equations where transport and reaction no longer decouple.

This problem does not appear in normal reaction diffusion where the time scales of reaction and jump events remain constant. In that situation, the average relative change in particle concentration due to reactions taking place during a waiting time is equivalent to adding or removing a proportion of particles at once, e.g. at the end or beginning of a waiting time period. In subdiffusion however, these situations have to be carefully distinguished. Hence, the specification of the dependence of reaction on time or on the amount of performed steps is crucial. These

considerations lead us directly to the next two sections.

6.2.2 Microscopic Model and Subdiffusive Reaction Kinetics

The microscopic models are based on the assumption that particles react on encounter with a certain probability, under the premise that the transport on small scales is governed by subdiffusion. Seki et al. put forth such a microscopic model of the reaction rates arising in geminate pair recombination under subdiffusion [106]. They adapted the basic idea of Smoluchowski and introduced a primary particle onto which the other particles diffuse. Instead of introducing a partially reflecting boundary at a radius r_S, a reaction zone $[r_S, r_S + \delta r]$ was defined in which reactions were supposed to occur at a certain intrinsic rate κ_{int}. Using a CTRW approach, the probability to escape the reaction zone is given by $\psi(t)e^{-\kappa_{int}t}$. With an appropriate waiting time pdf $\psi(t) \propto t^{-1-\alpha}$, the memory arising from the subdiffusive motion carries over to the reaction rate. The resultant reaction–subdiffusion equations exhibit a fractional derivative acting upon both the transport and the reaction term so that

$$\frac{\partial C_l(x,t)}{\partial t} = {}_0\mathrm{D}_t^{1-\alpha}\left[K_\alpha \Delta C_l(x,t) + R_l(x,t)\right] . \tag{6.10}$$

This type of equation was the object of study for several authors. In the case of linear reaction kinetics, a probabilistic derivation within the framework of CTRW with heavy–tailed waiting time densities where reactions take place at a certain rate at the beginning of each waiting time period led to similar reaction subdiffusion equations [31]. Ref. [29] investigated scaling properties of density and reaction profiles of the $\mathrm{A} + \mathrm{B} \to \mathrm{C}$ reaction. The respective reaction terms for the species A and B are then $R_{A,B} = -\kappa A(x,t)B(x,t)$. For the initial conditions of a sharp front with A-particles at one side and B-particles on the other, a broadening reaction zone where the product C is produced appears. The qualitative behavior of that system can be characterized by a number of exponents. Thus, the width of the depletion zone w_d where the concentrations are significantly smaller than their initial values is determined by $A(x,t) - B(x,t)$, which obeys a time–fractional diffusion equation, and was shown to scale as $w_d \propto t^{\alpha/2}$. Other quantities studied were the width $w_r \propto t^{\alpha/6}$ and height $h_r \propto t^{\alpha/3-1}$ of the reaction zone $\kappa A(x,t)B(x,t)$. The reactant concentrations go as $t^{-\alpha/3}$. We note here that the underlying quantities from which the exponents are deduced, namely $A(x,t) - B(x,t)$ and $\kappa A(x,t)B(x,t)$, are subordinated to the respective quantities under normal diffusion. It is therefore not surprising that the scaling behavior under subdiffusion can be obtained from the respective behavior under normal diffusion, as e.g. in [107, 108], and substituting t by t^α. A generalization to the reactions $n\mathrm{A} + m\mathrm{B} \to 0$ with different generalized diffusion coefficients for either species, $K_{\alpha,A}$, $K_{\alpha,B}$ was obtained by solving the reaction-subdiffusion equations under the quasi–static assumption [30].
Turing pattern formation in the context of equations of type (6.10) was investigated e.g by [32].

6.2.3 Mesoscopic Model and Classical Reaction Rate Kinetics

Another scenario to be considered is reaction in porous media such as e.g. sediments. Subdiffusion arises on a mesoscopic level due to trapping of particles in stagnant regions of the flow, and

is modelled by CTRW with heavy-tailed waiting time pdfs. On the microscopic scale, within the pores and cavities, the transport is normal and hence the classical reaction rate kinetics applies. The situation is sketched in Fig. 6.1. The particle jumps now take place between well mixed compartments at sites i, so that during the waiting times at a site the particles may react according to classical rate kinetics. This corresponds to the situation we will focus on in all following considerations.

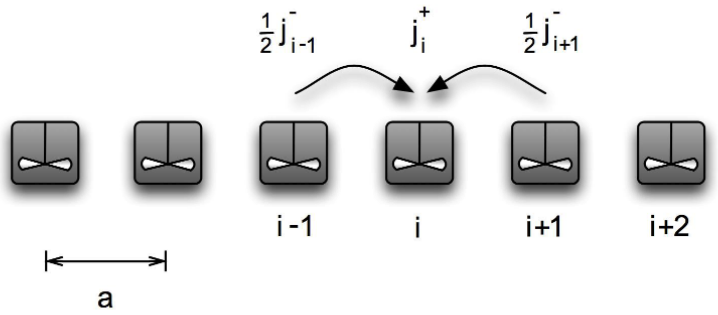

Figure 6.1: Compartment model for CTRW with on–site reaction according to classical rate kinetics. In the unbiased situation, the gain flux at a site i consists of $1/2$ the loss fluxes at the neighboring sites; the lattice constant is a.

In a setting like this, the particles can undergo reactions even when they are trapped. As a consequence, the transport term and the reaction term of the corresponding reaction–subdiffusion equations no longer decouple. Particularly when particles vanish, there is a concentration-dependent cutoff of the long ranged memory kernel in the transport term.
Moreover, it is important to define whether a reacting particle is re-labelled and keeps its waiting time, or whether it is assigned a new waiting time which. In the latter case, the effective mobility of the product particles can be considerably increased, which may result in qualitatively different dynamics and violations of local conservation laws. These implications yet lack a theoretical basis, and therefore we will only consider re-labelling in the following.

6.3 Linear Kinetics

Considering arbitrary linear reactions, the local kinetic rate equations generalize to

$$\frac{\partial \mathbf{C}(x,t)}{\partial t} = \mathcal{R}\mathbf{C}(x,t)\,, \tag{6.11}$$

where $\mathbf{C}$ is the vector of the concentrations of the reacting species C_l and $\mathcal{R}$ the constant reaction rate matrix. This reaction rate matrix represents the interdependencies between the different species that are due to reaction. Accordingly, the survival- and transformation probabilities during a waiting time from $t_0 = 0$ to t are given by the matrix exponential

$$\mathcal{P}(t) \quad = \quad e^{\mathcal{R}t} \; . \tag{6.12}$$

The corresponding reaction subdiffusion equations were derived by Langlands et al. [35] by means of a probabilistic approach akin to that put forward in [109, 34]. Here, an alternative derivation of the linear reaction subdiffusion equations is given. Again, the local fluxes at site i are considered, so that we have

$$\begin{aligned} \frac{\partial \mathbf{C}_i(t)}{\partial t} &= \mathbf{j}_i^+(t) - \mathbf{j}_i^-(t) + \mathcal{R}\mathbf{C}_i(t) \\ &= \frac{1}{2}\mathbf{j}_{i-1}^+(t) + \frac{1}{2}\mathbf{j}_{i+1}^+(t) - \mathbf{j}_i^-(t) + \mathcal{R}\mathbf{C}_i(t) \; . \end{aligned} \tag{6.13}$$

The entries of the flux vector $\mathbf{j}_i(t)$ are the fluxes of the different species at i. The fluxes of particles leaving site i are given by

$$\begin{aligned} \mathbf{j}_i^-(t) &= \psi(t) e^{\mathcal{R}t} \mathbf{C}_i(0) \\ &\quad + \int_0^t \psi(t-t') e^{\mathcal{R}(t-t')} \left[\frac{\partial}{\partial t'} \mathbf{C}_i(t') + \mathbf{j}_i^-(t') - \mathcal{R}\mathbf{C}_i(t') \right] dt' \; , \end{aligned} \tag{6.14}$$

i.e. the flux of particles leaving site i at t is firstly made up of those particles that were at i from the very beginning, did not vanish, though probably having experienced several transformations, and did not jump until t, or were created by transformations of particles that did not jump until t. This part is represented by the first summand on the rhs of (6.14). Secondly, the loss flux comprises as well those particles that came to i at a later time t', did not jump until t and either did not vanish or were created during that time by reaction. These particle fluxes are represented by the second summand on the rhs of (6.14). Of course, in the general case of the reaction matrix not being diagonal, the summands on the rhs of (6.14) may consist of several summands themselves when the equation is written down elementwise, i.e. for each species separately. Multiplication of (6.14) with $e^{-\mathcal{R}t}$ and passing to Laplace domain yields

$$\begin{aligned} \mathcal{L}\left\{ e^{-\mathcal{R}t} \mathbf{j}_i^-(t) \right\} &= \tilde{\psi}(u) \mathcal{L}\left\{ e^{-\mathcal{R}t} \left[\frac{\partial}{\partial t} \mathbf{C}_i(t) + \mathbf{j}_i^-(t) - \mathcal{R}\mathbf{C}_i(t) \right] \right\} \\ &= \tilde{\psi}(u) \left[u\mathcal{L}\left\{ e^{-\mathcal{R}t} \mathbf{C}_(t) \right\} + \mathcal{L}\left\{ e^{-\mathcal{R}t} \mathbf{j}_i^-(t) \right\} \right] , \end{aligned} \tag{6.15}$$

where we exploited the chain rule of differentiation, $\frac{\partial}{\partial t}\left[e^{-\mathcal{R}t}\mathbf{C}_i(t)\right] = e^{-\mathcal{R}t}\left[\frac{\partial}{\partial t}\mathbf{C}_i(t) - \mathcal{R}\mathbf{C}_i(t)\right]$. Furthermore,

$$\mathcal{L}\left\{e^{-\mathcal{R}t}\mathbf{j}_i^-(t)\right\} = \frac{u\tilde{\psi}(u)}{1-\tilde{\psi}(u)}\mathcal{L}\left\{e^{-\mathcal{R}t}\mathbf{C}_i(t)\right\} . \tag{6.16}$$

For algebraic waiting time pdfs $\tilde{\psi}(u) \simeq 1 - \tau^\alpha u^\alpha$, $0 < \alpha < 1$, we recognize the Laplace representation of the Riemann-Liouville fractional derivative so that back in time domain,

$$\mathbf{j}_i^-(t) = e^{\mathcal{R}t}\frac{1}{\tau^\alpha\Gamma(1-\alpha)}{}_0\mathrm{D}_t^{1-\alpha}e^{-\mathcal{R}t}\mathbf{C}_i(t) . \tag{6.17}$$

Inserting this expression into the balance equation (6.13) and passing to continuous coordinates results in the reaction-subdiffusion system

$$\frac{\partial\mathbf{C}(x,t)}{\partial t} = e^{\mathcal{R}t}K_{\alpha 0}\mathrm{D}_t^{1-\alpha}e^{-\mathcal{R}t}\Delta\mathbf{C}(x,t) + \mathcal{R}\mathbf{C}(x,t) \tag{6.18}$$

with $K_\alpha = \frac{a^2}{2\tau^\alpha\Gamma(1-\alpha)}$ and a being the lattice constant. Note that the exponential factor indicating the survival probability or per capita increase factor of particles enters the equation as a part of the memory kernel, since $e^{\mathcal{R}t}{}_0\mathrm{D}_t^{1-\alpha}e^{-\mathcal{R}t}f(t) = \frac{1}{\Gamma(\alpha)}\frac{\partial}{\partial t}\int_0^t M(t-t')e^{\mathcal{R}(t-t')}f(t')\,dt'$ with $\tilde{M}(u) = \frac{u\tilde{\psi}(u)}{1-\tilde{\psi}(u)}$. In the case of exponential waiting time pdfs $\psi(t) = \frac{1}{\tau}e^{-\frac{t}{\tau}}$, i.e. $\tilde{\psi}(u) = 1/(u\tau+1)$, we have $M(t) = \frac{1}{\tau}\delta(t)$, the additional exponential factor does not play any role and the normal reaction diffusion equation is reproduced.
The Green function of (6.18) is given by

$$\mathbf{C}(x,t) = \mathbf{C}_0 e^{\mathcal{R}t}G_{SD}(x,t) , \tag{6.19}$$

where $\mathbf{C}_0$ denotes the initial concentrations of the species and G_{SD} the Green function of the subdiffusion equation without reaction.
Note that it is often possible to diagonalize $\mathcal{R}$. In that case there exists a representation in terms of independent reaction subdiffusion equations for the respective eigenvectors. To underline this statement, two special cases shall serve as an example [35]. The first one is the irreversible $\mathrm{A} \rightarrow \mathrm{B}$ reaction. With κ being the reaction rate coefficient, the reaction matrix $\mathcal{R}$ takes on the form

$$\mathcal{R} = \begin{bmatrix} -\kappa & 0 \\ \kappa & 0 \end{bmatrix} . \tag{6.20}$$

The matrix exponentials are readily evaluated, so that for the concentration of both species

$$\begin{aligned} \frac{\partial A(x,t)}{\partial t} &= e^{-\kappa t} K_{\alpha 0} \mathrm{D}_0^{1-\alpha} \left[e^{\kappa t} \Delta A(x,t) \right] - \kappa A(x,t) && (6.21) \\ \frac{\partial B(x,t)}{\partial t} &= K_{\alpha 0} \mathrm{D}_0^{1-\alpha} \Delta \left[A(x,t) + B(x,t) \right] \\ &\quad - e^{-\kappa t} K_{\alpha 0} \mathrm{D}_0^{1-\alpha} \left[e^{\kappa t} \Delta A(x,t) \right] + \kappa A(x,t) . && (6.22) \end{aligned}$$

This reproduces the system of equations obtained in a previous work by Sokolov et al., [28]. Note that the eigenvectors for which the equations decouple are A and $A + B$, with the respective eigenvalues $-\kappa$ and 0. Hence, the respective decoupled system is

$$\begin{aligned} \frac{\partial A(x,t)}{\partial t} &= e^{-\kappa t} K_{\alpha 0} \mathrm{D}_0^{1-\alpha} \left[e^{\kappa t} \Delta A(x,t) \right] - \kappa A(x,t) && (6.23) \\ \frac{\partial \left[A(x,t) + B(x,t) \right]}{\partial t} &= K_{\alpha 0} \mathrm{D}_0^{1-\alpha} \Delta \left[A(x,t) + B(x,t) \right] , && (6.24) \end{aligned}$$

and the solution to the IVP with $A(x,0) = A_0 \delta(x)$ and $B(x,0) = B_0 \delta(x)$.
The second example is the reversible A $\rightleftharpoons$ B reaction. We have

$$\mathcal{R} = \begin{bmatrix} -\kappa_1 & \kappa_2 \\ \kappa_1 & -\kappa_2 \end{bmatrix} \tag{6.25}$$

with the forward reaction rate coefficient κ_1 and the backward rate coefficient κ_2. The resultant reaction-subdiffusion system is given by

$$\begin{aligned} \frac{\partial A(x,t)}{\partial t} &= \rho_2 K_{\alpha 0} \mathrm{D}_t^{1-\alpha} \Delta \left(A(x,t) + B(x,t) \right) - \kappa_1 A(x,t) + \kappa_2 B(x,t) \\ &\quad + e^{-\kappa^* t} K_{\alpha 0} \mathrm{D}_t^{1-\alpha} \left[e^{\kappa^* t} \Delta \left(\rho_1 A(x,t) - \rho_2 B(x,t) \right) \right] && (6.26) \\ \frac{\partial B(x,t)}{\partial t} &= \rho_1 K_{\alpha 0} \mathrm{D}_t^{1-\alpha} \Delta \left(A(x,t) + B(x,t) \right) + \kappa_1 A(x,t) - \kappa_2 B(x,t) \\ &\quad - e^{-\kappa^* t} K_{\alpha 0} \mathrm{D}_t^{1-\alpha} \left[e^{\kappa^* t} \Delta \left(\rho_1 A(x,t) - \rho_2 B(x,t) \right) \right] && (6.27) \end{aligned}$$

with

$$\begin{aligned} \kappa^* &= \kappa_1 + \kappa_2 \,, \\ \rho_1 &= \frac{\kappa_1}{\kappa*} \,, \qquad \rho_2 = \frac{\kappa_2}{\kappa^*} \,. \end{aligned} \tag{6.28}$$

The same reaction-subdiffusion system was derived by Sagues et al., [110]. Note that the system of equations (6.26), (6.27) can be written as the decoupled system [35]

$$\begin{aligned} \frac{\partial (A(x,t)+B(x,t))}{\partial t} &= K_{\alpha 0} \mathrm{D}_t^{1-\alpha} \Delta (A(x,t)+B(x,t)) \\ \frac{\partial (\rho_1 A(x,t) - \rho_2 B(x,t))}{\partial t} &= +e^{-\kappa^* t} K_{\alpha 0} \mathrm{D}_t^{1-\alpha} \left[e^{\kappa^* t} \Delta (\rho_1 A(x,t) - \rho_2 B(x,t)) \right] \\ &\quad -\kappa^* (\rho_1 A(x,t) - \rho_2 B(x,t)) \end{aligned} \tag{6.29}$$

for $A(x,t)+B(x,t)$ and $\rho_1 A(x,t) - \rho_2 B(x,t)$ with the eigenvalues of the reaction matrix 0 and $-\kappa^*$, respectively. The solutions for the initial conditions $A(x,0) = A_0\delta(x)$, $B(x,0) = B_0\delta(x)$ are then

$$\begin{aligned} A(x,t) &= A_0 \left(\rho_2 + \rho_1 e^{-\kappa^* t} \right) G_{SD}(x,t) + B_0 \rho_2 \left(1 - e^{-\kappa^* t} \right) G_{SD}(x,t) \\ B(x,t) &= A_0 \rho_1 \left(1 - e^{-\kappa^* t} \right) G_{SD}(x,t) + B_0 \left(\rho_1 + \rho_2 e^{-\kappa^* t} \right) G_{SD}(x,t) \,. \end{aligned} \tag{6.30}$$

Recall again that G_{SD} denotes the Green function of the mere subdiffusion equation without reaction.

6.4 Boundary Value Problems under Reaction-Subdiffusion

It may be of practical interest to consider boundary problems in reaction-subdiffusion since in laboratory experiments the reaction volume is finite. The reactant supply may be provided by a bath of particle solution maintaining the respective concentration at the boundaries of the reaction volume. It should however be noted that it is not yet clear how boundary conditions can be controlled in practice, since one can expect that a bath where particles move according to normal diffusion in contact with a subdiffusive medium will lead to an ever increasing accumulation of particles in the boundary layer of the medium. This increase may only be restricted due to a finite capacity of the medium. Since this issue is not in the scope of the present work, we take the boundary conditions for granted.

In the following, the very simple case of a Dirichlet Boundary value problem for degrading particles under subdiffusion will be studied [111]. The issue of degradation under subdiffusion was also studied by Hornung et al. [112] in order to describe morphogen degradation in cellular tissue. They used a CTRW model where the particles were only allowed to degrade by a certain rate when they had performed a jump before and found that stationary profiles do not exist. We

will see later that in contrast to that, in our model stationary profiles do exist.
For normal reaction-diffusion equations in general, it is impossible to express the solutions to BVPs analytically. However, there are some special cases which allow for a fully analytical representation of the solution to special BVPs. One of them is the Dirichlet BVP for degrading particles, i.e. the simple irreversible reaction $A \to 0$. For normal diffusion, it was shown that in order to obtain the solution to the Dirichlet BVP for degrading particles, one has to subject the solution to the same BVP without degradation to a transformation [113]. As will turn out, this holds true as well for the subdiffusion-reaction equations. Moreover, this transformation is the same as the one in the normal diffusive case.

6.4.1 Degradation–Subdiffusion Solution to the Dirichlet BVP

We use the equation for linear reactions under subdiffusion derived earlier, cp. Eq. (6.18), writing the time fractional operator in integral form:

$$\frac{\partial A(x,t)}{\partial t} = \frac{a^2}{2}\Delta \int_0^t M(t-t')\exp\left[-\kappa(t-t')\right]A(x,t')\,dt' - \kappa A(x,t)\,. \tag{6.31}$$

The Green function of this equation, i.e. the response to a δ-peak at $x = 0$ and $t = 0$, can be found by making use of the shift theorem of the Laplace transform:

$$\tilde{G}(x,u) = \frac{1}{\sqrt{K_\alpha}(u+\kappa)^{1-\alpha/2}}\exp\left[-\sqrt{\frac{(u+\kappa)^\alpha}{K_\alpha}}|x|\right] \tag{6.32}$$

which is exactly the Green function of the subdiffusion equation without reaction, with u changed to $u+\kappa$. We know that the solutions to the subdiffusive Dirichlet BVP with degradation will be, generally speaking, linear combinations of temporal convolutions of functions of the type (6.32). A constant boundary value requires a boundary condition proportional to $\frac{1}{u}$ in Laplace domain, and we are able to express the solution with degradation in terms of the solution without degradation, but for the same boundary conditions. Let for now A^* be the solution to the problem without degradation. The solution with degradation included is then in Laplace domain:

$$\tilde{A}(x,u) = \frac{\kappa+u}{u}\tilde{A}^*(x,\kappa+u) \tag{6.33}$$

and in original domain (again using the shift theorem):

$$A(x,t) = \kappa\int_0^t A^*(x,t')\exp\left[-\kappa t'\right]dt' + A^*(x,t)\exp\left[-\kappa t\right]\,, \tag{6.34}$$

a result already found for the construction of the solution for normal diffusion with degradation [113], corresponding to the formal substitution $\alpha \to 1$, $K_\alpha \to D$.
In the following, we examine a one-dimensional system with given boundary concentrations. We account for two cases: one fixed boundary value in a semi-infinite domain, and two fixed boundary values at a finite interval. In all these considerations we assume that initially, the interior of the region of interest is completely empty, $A(x, t = 0) = 0$, and its boundaries are

determined by the aforementioned Dirichlet boundary conditions.

6.4.2 Degradation–Subdiffusion on the Semi–infinite Domain

To find the solution to the Dirichlet BVP in degradation–subdiffusion, we have to take into account that the modified Green function (6.32) constitutes the basic structure of the solution. Fitting the boundary, we find for an initially empty domain $x > 0$

$$\tilde{A}(x,u) = \frac{A_0}{u} \exp\left[-\sqrt{\frac{(u+\kappa)^\alpha}{K_\alpha}} |x| \right] . \tag{6.35}$$

The large time limit corresponds to $u \to 0$ so that we deduce immediately the stationary profile:

$$A(x, t \to \infty) = A_0 \exp\left[-\sqrt{\frac{\kappa^\alpha}{K_\alpha}} |x| \right] , \tag{6.36}$$

an exponential just as in the normal diffusive case $\alpha = 1$, differing only by the exponent α in the rate coefficient which increases the profile's steepness (if $\kappa < 1$). Figure 6.2 shows the profiles under reaction-subdiffusion at different times. The profiles were again obtained by means of a series expansion and term-by-term inversion of the corresponding expressions in Laplace domain. The different times were chosen according to the corresponding profiles $C(x,t)$ for the same BVP without degradation that were derived in the previous chapter, Fig. 5.4, so that a direct comparison is possible. The profiles under subdiffusion with degradation for the times $t = 5$ and $t = 50$ coincide, i.e. the profile has reached stationarity. Fig. 6.3 is the counterpart to Fig. 5.3 including degradation. The difference in the profiles for $t = 2$ and $t = 8$ is very small, and the profile at $t = 8$ corresponds to the stationary one.

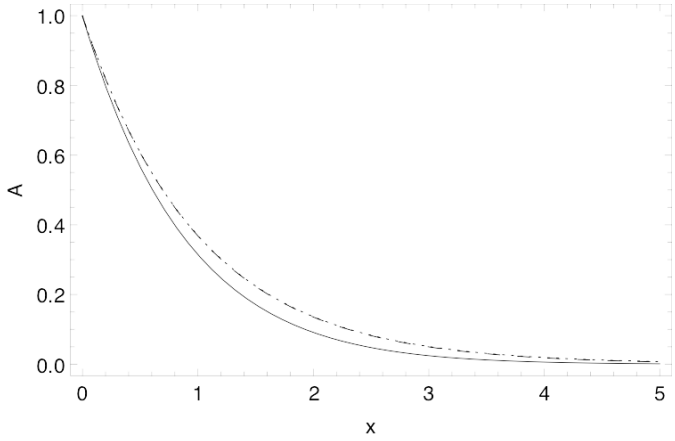

Figure 6.2: Particle profiles under reaction-subdiffusion, $\alpha = 0.5$ for $t = 0.5$ (solid line), $t = 5$ (dashed) and $t = 50$ (dotted); $K_\alpha = 1$, $\kappa = 1$. Prescribed boundary value $A(0,t) = 1$.

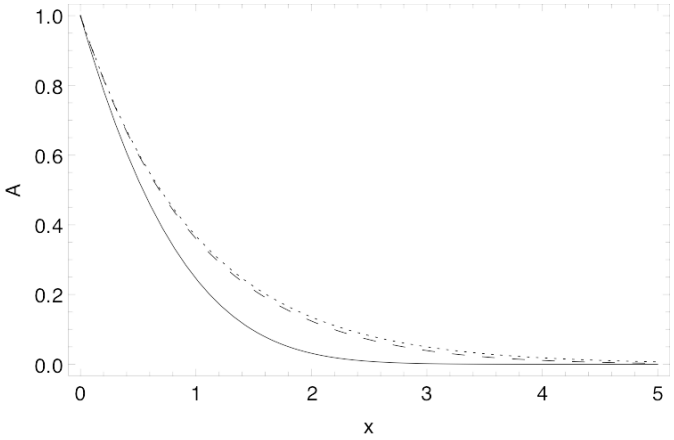

Figure 6.3: Particle profiles under reaction-diffusion for $t = 0.5$ (solid line), $t = 2$ (dashed) and $t = 8$ (dotted); $D = 1$, $\kappa = 1$. Prescribed boundary value $A(0,t) = 1$.

6.4.3 Degradation–Subdiffusion on the Finite Interval

For subdiffusion with degradation we again modify the ansatz (5.74) for the respective BVP on the interval $(0, L)$ under mere subdiffusion according to (6.32) and finally find the solution in Laplace domain:

$$\tilde{A}(x,u) = \frac{A_0}{u} \frac{\exp\left[-\sqrt{\frac{(u+\kappa)^\alpha}{K_\alpha}}x\right] - \exp\left[-\sqrt{\frac{(u+\kappa)^\alpha}{K_\alpha}}(2L-x)\right]}{1-\exp\left[-\sqrt{\frac{(u+\kappa)^\alpha}{K_\alpha}}2L\right]} \,. \tag{6.37}$$

The stationary profile is obtained in the limit $u \to 0$,

$$A(x, t\to\infty) = A_0 \frac{\exp\left[-\sqrt{\frac{\kappa^\alpha}{K_\alpha}}x\right] - \exp\left[-\sqrt{\frac{\kappa^\alpha}{K_\alpha}}(2L-x)\right]}{1-\exp\left[-\sqrt{\frac{\kappa^\alpha}{K_\alpha}}2L\right]} \,,$$

shown in Fig. 6.4. The relaxation behaviour is governed by the exponential survival probability. At large times the rate coefficient κ governs the time scale of relaxation as seen from Eq.(6.34).

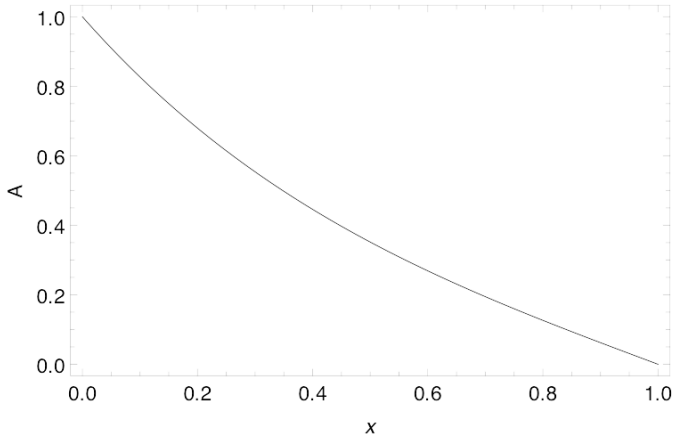

Figure 6.4: Stationary particle profile for a Dirichlet BVP under reaction–subdiffusion, $\alpha = 0.5$, $K_\alpha = 1$, $\kappa = 10$, $L = 1$, $A_0 = 1$, $A_L = 0$.

Let us now turn to the case where both boundaries have non–zero constant values, $A(0,t) = A_0$, $A(L,t) = A_L$. Proceeding as above we find the solution for the reaction–subdiffusion equation

$$\begin{aligned}
&\tilde{A}(x,u) \\
&= \frac{1}{u}\left[A_0\left(1 - \frac{A_L}{A_0}\frac{\exp\left[-\sqrt{\frac{(u+\kappa)^\alpha}{K_\alpha}}L\right] - \frac{A_0}{A_L}\exp\left[-\sqrt{\frac{(u+\kappa)^\alpha}{K_\alpha}}2L\right]}{1-\exp\left[-\sqrt{\frac{(u+\kappa)^\alpha}{K_\alpha}}2L\right]}\right)\right. \\
&\times\exp\left[-\sqrt{\frac{(u+\kappa)^\alpha}{K_\alpha}}x\right] \\
&\left.+A_L\left(\frac{1-\frac{A_0}{A_L}\exp\left[-\sqrt{\frac{(u+\kappa)^\alpha}{K_\alpha}}L\right]}{1-\exp\left[-\sqrt{\frac{(u+\kappa)^\alpha}{K_\alpha}}2L\right]}\right)\exp\left[-\sqrt{\frac{(u+\kappa)^\alpha}{K_\alpha}}(L-x)\right]\right]
\end{aligned} \tag{6.38}$$

and the stationary solution for degrading particles shown in Fig.6.5:

$$\begin{aligned}
A(x,t\to\infty) \quad = \quad & A_0\left(1 - \frac{A_L}{A_0}\frac{\exp\left[-\sqrt{\frac{\kappa^\alpha}{K_\alpha}}L\right] - \frac{A_0}{A_L}\exp\left[-\sqrt{\frac{\kappa^\alpha}{K_\alpha}}2L\right]}{1-\exp\left[-\sqrt{\frac{\kappa^\alpha}{K_\alpha}}2L\right]}\right)\exp\left[-\sqrt{\frac{\kappa^\alpha}{K_\alpha}}x\right] \\
& +A_L\left(\frac{1-\frac{A_0}{A_L}\exp\left[-\sqrt{\frac{\kappa^\alpha}{K_\alpha}}L\right]}{1-\exp\left[-\sqrt{\frac{\kappa^\alpha}{K_\alpha}}2L\right]}\right)\exp\left[-\sqrt{\frac{\kappa^\alpha}{K_\alpha}}(L-x)\right].
\end{aligned}$$

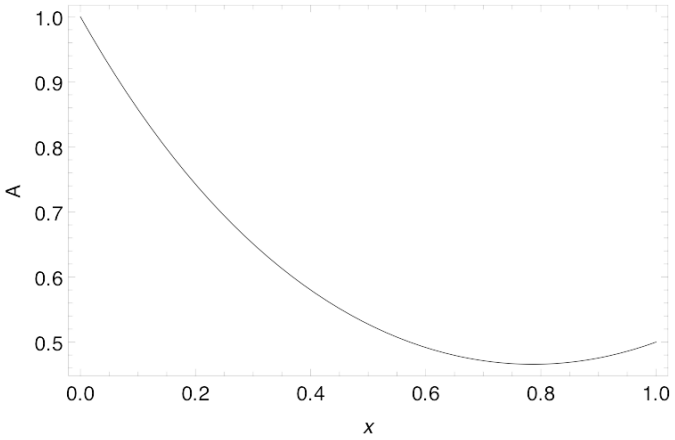

Figure 6.5: Stationary particle profile for a Dirichlet BVP under reaction–subdiffusion, $\alpha = 0.5$, $K_\alpha = 1$, $\kappa = 10$, $L = 1$, $A_0 = 1$, $A_L = 0.5$.

Resumé We examined the solutions to the equations that describe degradation of subdiffusing particles, $A \to 0$, under Dirichlet boundary conditions. The type of reaction–subdiffusion equations we use here is based on a CTRW approach and takes into account the fact that particles that react during their waiting times do not contribute to transport anymore, which leads to an exponential (reaction-dependent) cutoff of the long-ranged kernel in the transport term. For such kind of equations we have shown that the problem of the Dirichlet BVP with degradation in subdiffusion can be reduceded to the Dirichlet BVP without degradation, just as in normal diffusion. The resultant stationary profiles do not differ qualitatively from the ones obtained in normal diffusion, the only difference is that the rate coefficient κ enters the respective expression for the stationary profile with a different power. We note again that for this treatment of the reaction-subdiffusion equation with degradation the exponential cutoff of the transport kernel due to reaction is essential.

6.5 Nonlinear Kinetics

In a first attempt to set up the corresponding nonlinear reaction subdiffusion equations, [34] used a probabilistic approach put forward by [109] in another context and arrived at the equations

$$\begin{aligned}\frac{\partial C_l(x,t)}{\partial t} &= R_l^+(x,t) + R_l^-(x,t) \\ &\quad + \frac{a^2}{2}\Delta \int_0^t M(t-t') \exp\left[\int_{t'}^t \frac{R_l^-(x,t'')}{C_l(x,t'')}\,dt''\right] C_l(x,t')\,dt' \end{aligned} \tag{6.39}$$

where the reaction term R_l was divided into a part $R_l^+ > 0$ accounting for creation and a part $R_l^- < 0$ accounting for annihilation of particles, and a is the lattice constant. The memory kernel

consist of one part corresponding to the kernel of the mere subdiffusion equation related to the waiting time pdf $\psi(t)$ in Laplace domain via $\tilde{M}(u) = \frac{u\tilde{\psi}(u)}{1-\tilde{\psi}(u)}$, and another part representing the survival probability of the particles. This survival probability depends on the densities of the reacting species entering the negative part of the reaction term R_l^- and imposes a cutoff upon the long-ranged memory kernel M. These equations however do not account for interdependencies of the particle densities arising from conversions between the species. In the special case of linear kinetics $R_l(x,t) \propto C_l(x,t)$ this would correspond to decoupled equations for the different species. The full survival- and transformation-probabilities for the particles are determined by the respective system of classical rate equations (6.6) which in general, due to its nonlinearity, has no analytic solution. It is therefore often impossible to set up the reaction-subdiffusion equations.
If the reaction is irreversible, it is possible to write the equation for the change in concentration of the species depending only on the actual concentrations themselves, but not on the actual creation or annihilation of other species. In some cases, conservation laws prove useful in finding the correct reaction-subdiffusion equations. The remainder of the work focuses on some selected problems in nonlinear reaction-subdiffusion.

6.6 The $\mathrm{A}+\mathrm{B} \to 0$ Reaction under Subdiffusion

For the reaction $\mathrm{A}+\mathrm{B} \to 0$, both equations can be written down in a form similar to (6.39). We derive the reaction-subdiffusion equation for B by considering again the flux balance at site i:

$$\begin{aligned} \frac{\partial B_i(t)}{\partial t} &= j^+_{B,i}(t) - j^-_{B,i}(t) - \kappa A_i(t) B_i(t) \\ &= \frac{1}{2} j^-_{B,i-1}(t) + \frac{1}{2} j^-_{B,i+1}(t) - j^-_{B,i}(t) - \kappa A_i(t) B_i(t) \end{aligned} \tag{6.40}$$

so that with the probability not to react within t being $P_{B,i}(t|0) = \exp\left[-\int_0^t \kappa A_i(t')\,dt'\right]$ the loss flux at i is

$$\begin{aligned} j^-_{B,i}(t) &= \psi(t) P_{B,i}(t|0) B_i(0) \\ &\quad + \int_0^t \psi(t-t') P_{B,i}(t|t') \left[\frac{\partial B_i(t')}{\partial t'} + \kappa A_i(t') B_i(t') + j^-_{B,i}(t') \right] dt' \,, \end{aligned} \tag{6.41}$$

which, neglecting the initial condition, can be rewritten as

$$
\begin{aligned}
&\bar{j}_{B,i}(t)\exp\left[\int_0^t \kappa A_i(t'')dt''\right] = \\
&\int_0^t \psi(t-t')\exp\left[\int_0^{t'} \kappa A_i(t'')dt''\right]\left[\frac{\partial B_i(t')}{\partial t'} + \kappa A_i(t')B_i(t') + \bar{j}_{B,i}(t')\right]dt' \ .
\end{aligned}
\tag{6.42}
$$

Using

$$
\begin{aligned}
&\frac{\partial}{\partial t}\left(B_i(t)\exp\left[\int_0^t \kappa A_i(t'')dt''\right]\right) = \\
&\exp\left[\int_0^t \kappa A_i(t'')dt''\right]\frac{\partial}{\partial t}B_i(t) + B_i(t)\kappa A_i(t)\exp\left[\int_0^t \kappa A_i(t'')dt''\right]
\end{aligned}
$$

and applying Laplace transformation results in

$$
\mathcal{L}\left\{\bar{j}_{B,i}(t)\exp\left[\int_0^t \kappa A_i(t'')dt''\right]\right\} = \frac{u\tilde{\psi}(u)}{1-\tilde{\psi}(u)}\mathcal{L}\left\{B_i(t)\exp\left[\int_0^t \kappa A_i(t'')dt''\right]\right\} \ . \tag{6.43}
$$

Together with the balance equation (6.40) and multiplying $\exp\left[-\int_0^t \kappa A_i(t'')dt''\right]$ we finally arrive at

$$
\begin{aligned}
\frac{\partial B(x,t)}{\partial t} &= \frac{a^2}{2}\Delta\int_0^t M(t-t')\exp\left[-\int_{t'}^t \kappa A(x,t'')\,dt''\right]B(x,t')\,dt' \\
&\quad -\kappa A(x,t)B(x,t) \ .
\end{aligned}
\tag{6.44}
$$

in continuous coordinates $x = ai$, provided the relative change in concentration is small compared to the lattice spacing. Note that the transition from occupation numbers $B_i(t)$ to concentrations $B(x,t) = B_i(t)/a^3$ requires absorption of the corresponding dimensional constant into the new reaction rate coefficient, $\kappa_{cont} = a^3\kappa_{discrete}$. The respective equations for A are obtained by interchanging A and B in (6.44). This system of equations does not allow for a scaling ansatz for profiles and reaction zones as its subdiffusive kinetics analogue. The survival probabilities affect the transport terms in that they impose a cutoff upon the subdiffusion kernel that depends on the concentrations of the respective reaction partners at all previous times. Stationary solutions to that system of equations on a bounded domain were considered in a previous work [114]. In order to derive the stationary solutions, it was argued that if stationary states exists, all relevant quantities can only be functions of their time differences. The survival probabilities for example take on the form $P_{B,i}(t|t') = P_{B,i}(t-t') = \exp[-\kappa A(x)(t-t')]$, due to the stationarity of A and B.

By virtue of the shift theorem of the Laplace transformation, Eq. (6.44) becomes in Laplace domain

$$u\tilde{B}(x,u) - B(x,t_0|t_0) = \frac{a^2}{2}\Delta\frac{[u+\kappa A(x)]\tilde{\psi}(u+\kappa A(x))}{1-\tilde{\psi}(u+\kappa A(x))}\tilde{B}(x,u) - \kappa\tilde{B}(x,u)A(x)\ . \tag{6.45}$$

Hence, inserting the asymptotics of a heavy-tailed waiting time pdf $\tilde{\psi}(u) \simeq 1-(\tau u)^\alpha\Gamma(1-\alpha)$, which requires in this particular case that $\kappa B(x)\tau \ll 1$, and taking the limit $u \to 0$ results in

$$K_\alpha\Delta A(x)^{1-\alpha}B(x) - \kappa^\alpha A(x)B(x) = 0\ , \tag{6.46}$$

where $K_\alpha = a^2/2\tau^\alpha\Gamma(1-\alpha)$. The same equation with A and B interchanged holds for $A(x)$. The stationary state is hence described by a system of stationary reaction-diffusion equations with a nonlinear diffusion term.
Consider a system on an interval $(0,1)$ with given concentrations of reactants on the boundaries, e.g. a subdiffusive gel reactor in contact with two well mixed reservoirs on both sides. For the sake of simplicity we address here a symmetric situation with $A(0) = B(1) = 1$ and $A(1) = B(0)$, so that consequently $B(x) = A(1-x)$.

Figs. 6.6 and 6.7 show the numerical results for the steady-state Eqs. (6.46) in the normal case and the subdiffusive case for different values of α. The results were obtained by a semi-implicit relaxation algorithm, details see [115].

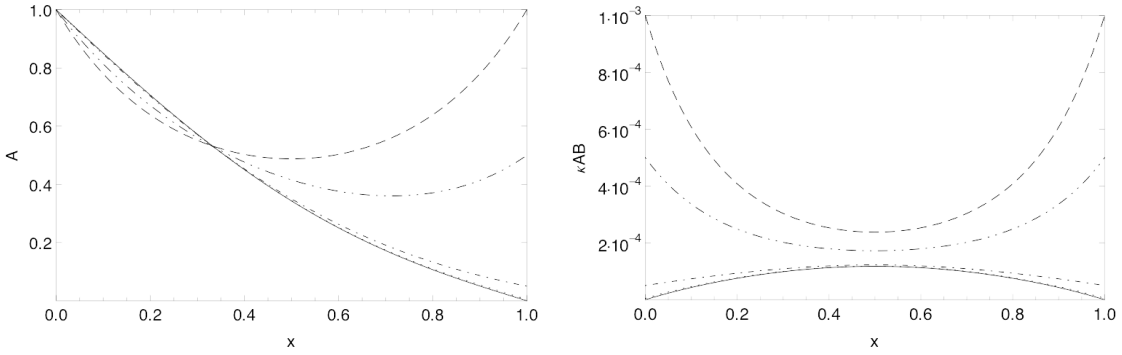

(a) (b)

Figure 6.6: (a) Stationary particle concentration $A(x)$ and (b) stationary reaction intensity $R(x) = \kappa A(x)B(x)$ under normal diffusion; different boundary values: $A(1) = 1$ (dashed), 0.5 (dash-dot-dot), $5\cdot10^{-2}$ (dash-dot), $5\cdot10^{-3}$ (dotted), and $1\cdot10^{-4}$ (solid line); $\kappa = 0.001$, $D = 1/2$.

For symmetric boundary conditions, the concentration profile in the in reaction-diffusion and in reaction-subdiffusion situations is very similar. Maximal concentrations are achieved close to the boundaries. For asymmetric conditions the profiles in the two cases differ strongly. The most marked difference corresponds to accumulation of A particles in the interior of the subdiffusive

medium close to the boundary with the larger value. Its counterpart is a depletion zone on the other side of the system which corresponds to the symmetric accumulation zone for B.

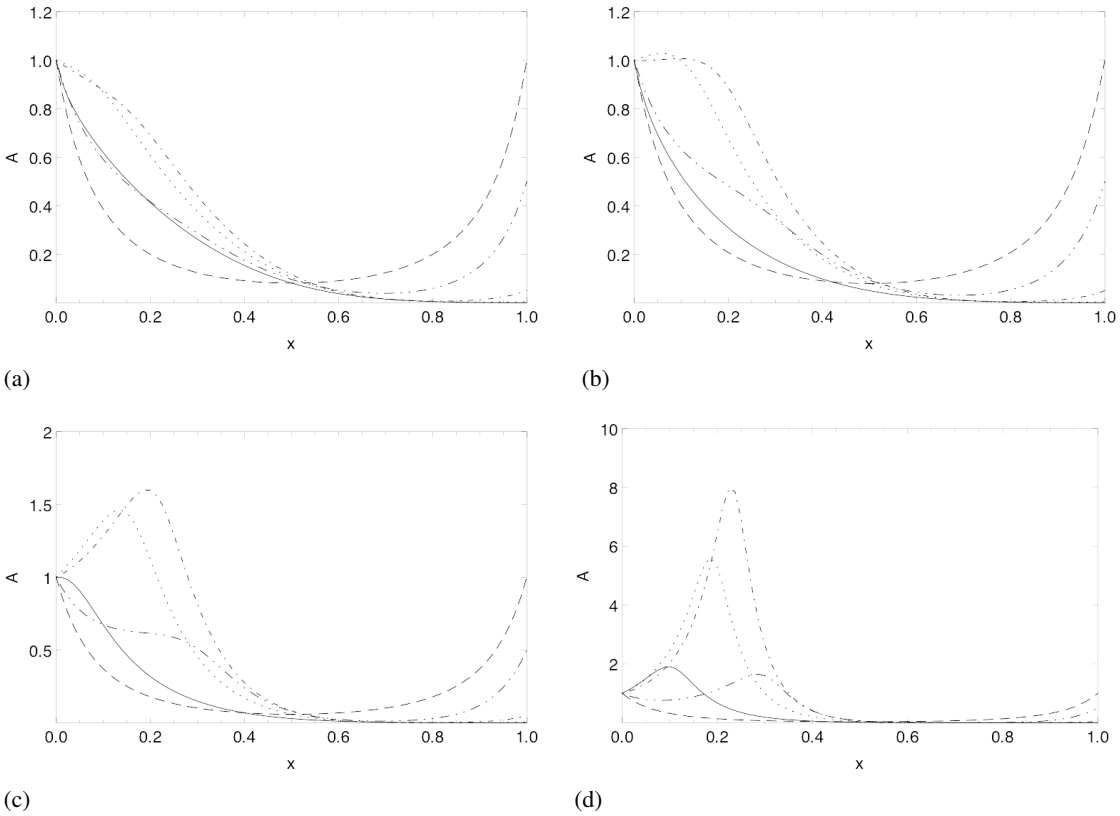

Figure 6.7: Stationary particle concentrations $A(x)$ for (a) $\alpha = 0.9$, (b) $\alpha = 0.8$, (c) $\alpha = 0.7$, (d) $\alpha = 0.6$; $A(1) = 1$ (dashed), 0.5 (dash-dot-dot), $5 \cdot 10^{-2}$ (dash-dot), $5 \cdot 10^{-3}$ (dotted), and $1 \cdot 10^{-4}$ (solid line); $\kappa = 0.001$, $K_\alpha = 1/(2\Gamma(1-\alpha))$. The smaller the α, the more pronounced get the peak and the depletion zone.

The dependence of the height of the accumulation peak on the strength of sources is non-monotonic. Lowering the prescribed concentration at the right boundary $A(1) = B(0)$ leads first to growth of the peak, and then to its motion closer to the boundary accompanied by decay. Whereas in reaction-diffusion $A(x)$ reaches a limiting form for $A(1) \to 0$, no stationary concentration profile exists in the subdiffusive case. For equal boundary values at both sides of the domain, A-particles react in vicinity of the boundary before they could travel a considerable distance. For smaller $A(1) = B(0)$ some of A-particles can travel without reaction, due to lack of reaction partners. They accumulate inside the system and form the peak, since the effective mobility of the particles decays in the course of time, i.e. the number of performed steps goes as $t^{\alpha-1}$. Moreover, the smaller the α, the more pronounced get the peak and the depletion zone, [114, 115].

The nonmonotonic behavior with respect to the boundary values is mirrored in a corresponding nonmonotonicity in the reaction zones $\kappa A(x)B(x)$, Fig. 6.8. Smaller α result in smaller reaction intensities. A peak in the reaction profile at the center of the domain tends to evolve already at larger $A(1)$ for smaller α.

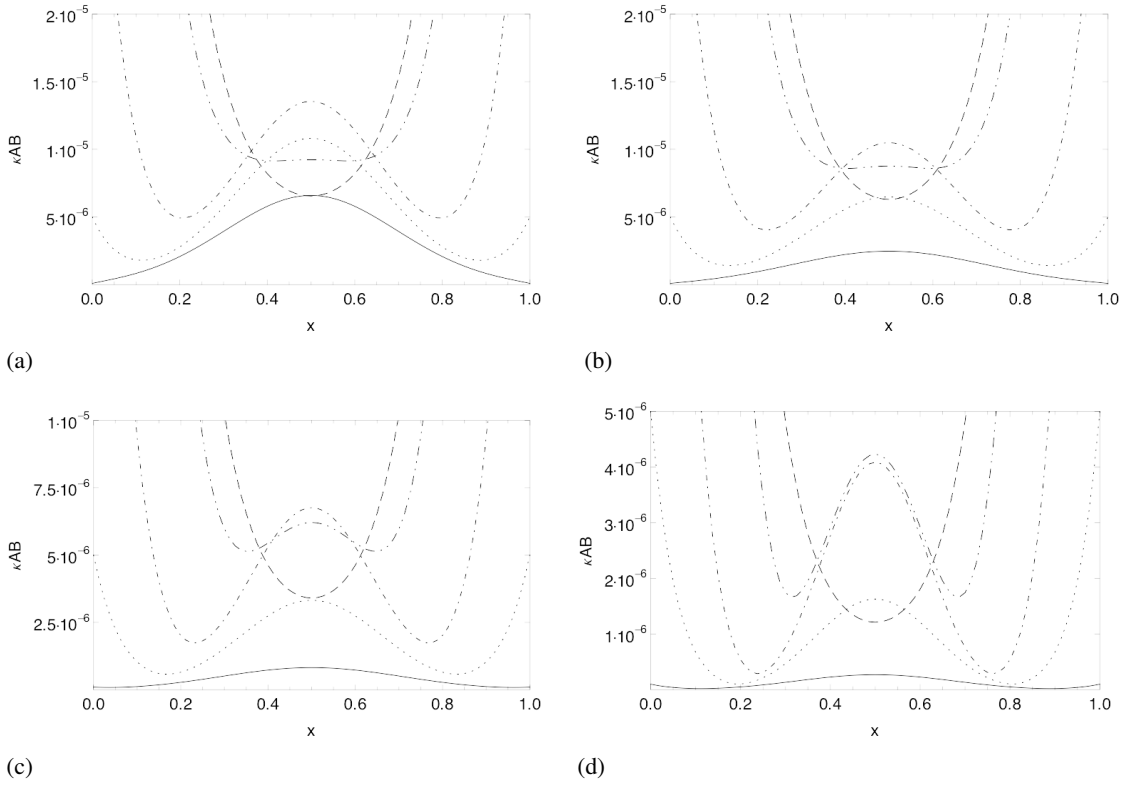

Figure 6.8: Stationary reaction intensity $\kappa A(x)B(x)$ for (a) $\alpha = 0.9$, (b) $\alpha = 0.8$, (c) $\alpha = 0.7$, (d) $\alpha = 0.6$; $A(1) = 1$ (dashed), 0.5 (dash-dot-dot), $5 \cdot 10^{-2}$ (dash-dot), $5 \cdot 10^{-3}$ (dotted), and $1 \cdot 10^{-4}$ (solid line); $\kappa = 0{,}001$, $D_\alpha = 1/2\Gamma(1-\alpha)$. The smaller the α, the smaller becomes the reaction intensity. A peak at the center of the domain tends to evolve at larger $A(1)$ for smaller α (note the curve for $A(1) = 0.5$, dash-dot-dot).

7 Front Propagation in the $A + B \rightarrow 2A$ Reaction

The $A + B \rightarrow 2A$ reaction is especially interesting since its solutions represent propagating fronts of A into the unstable B-domain for appropriate initial conditions. Several recent works were dedicated to the theoretical description of fronts under subdiffusion [116, 117] for different reaction schemes and different conditions. Ref.[116] examined the front behavior in a system that in the case of the normal diffusion would be described by the Fisher-Kolmogorov-Petrovskii-Piskounov (FKPP) equation. Under the description adopted, the authors have shown that there exists a (minimal) stable propagation velocity of such front, just as in the normal diffusive case. The behavior of the fronts under subdiffusion must not necessarily resemble the front behavior under normal diffusion, though. Depending on the details of the reaction and the special assumptions on the characteristics of the waiting times after the elementary act of reaction, the behavior of the propagating front under subdiffusion may strongly differ from its corresponding normal diffusive counterpart. There has been a variety of literature on different (sub-) diffusion reaction systems modelled on the basis of CTRW, all of them including the diffusive FKPP equation as a special case, [118, 119, 120, 116]. Virtually all of these systems exhibited travelling front solutions with stable front shapes and constant propagation velocities. Fedotov and Mendez [118] developed an elegant method to determine the front velocities which was based on a hyperbolic scaling ansatz and a Hamilton Jacobi equation. This method is equivalent to the leading edge linearization in a comoving frame with constant velocity. In a later contribution, Yadav et al. [116] adapted this method to reaction- transport equations of the type put forward in [34] for a reversible branching-coalescence scheme. Based on the different assumptions about the detailed reaction kinetics and/ or the handling of the waiting times at the instance of an elementary reaction, these models led to different equations.

This section discusses a specific setting leading to front dynamics that is genuinely due to subdiffusion. We consider the fully irreversible subdiffusive analogue of the $A + B \rightarrow 2A$ reaction diffusion equation with the overall particle concentration being locally conserved. In a first attempt to find the asymptotic front velocity we adopted the method of linearizing about the leading edge of the front. We draw upon the assumption that also in the subdiffusive case the front will be a pulled one. Under the premise of a stable front shape, we show that a minimal constant propagation velocity is zero, which hints at the fact that the propagation of a stable front at constant velocity is impossible. Later on, results of Monte-Carlo simulations are presented that suggest two different regimes of front propagation, both exhibiting a decay in propagation velocity. The first one corresponds to the continuous reaction-subdiffusion scheme with an asymptotic front velocity going as $v \propto t^{(\alpha-1)/2}$, and the latter corresponding to the fluctuation dominated situation where the front velocity goes asymptotically as $v \propto t^{\alpha-1}$. However, the ansatz of an asymptotic front with invariant shape and a velocity $v \propto t^{(\alpha-1)/2}$ does not conform to the respective

linearized reaction-subdiffusion equations describing the the leading edge of the front in the continuous regime. A crossover argument will be given in favor of an ansatz for a front that exhibits not only a decaying velocity, but also a decaying width. It will be shown that an ansatz fulfilling these properties is in accordance with the linearized reaction-subdiffusion equations describing the leading edge of the front. In longer simulations, Campos and Mendez [117] observed that the continuous regime is only valid for intermediate times, whereas for longer times the power exponent in the time dependence of the front velocity sets in to decay. In the light of the knowledge about the decreasing front width in the continuous regime, these findings can be interpreted as the transition to the fluctuation dominated regime which inevitably sets in when at large times the width of the front reaches the magnitude of the lattice constant. This fluctuation dominated regime is not amenable to a continuous reaction-subdiffusion description and will be discussed in detail as well.

7.1 The FKPP Equation

Before we go into the details of the A + B → 2A reaction under subdiffusion, a brief overview of the corresponding situation under normal diffusion shall be given.

The Fisher-Kolmogorov-Petrovskii-Piscounov (FKPP) equation was first proposed by R. A. Fisher in 1937 [21] as a model for propagation of a favorable gene in a population. Kolmogorov, Petrovskii and Piscounov studied the equation in more detail, focusing on certain preconditions under which travelling wavefront solutions evolve [25]. Under the assumption of the local conservation of the overall particle density $A(x,t) + B(x,t) = c_0$, this equation corresponds to the mathematical description of the (irreversible or reversible) reaction with the bimolecular autocatalytic conversion A + B → 2A representing the main stage. Initially the whole system is homogeneously filled with particles. A reasonable initial condition is that the A-individuals occupy some bounded spacial domain, which can be described by an initial condition sharply concentrated in vicinity of the coordinate origin, whereas the B-species fills almost the whole space homogeneously (except in the vicinity of the coordinate origin). Initial conditions of that type lead to the propagation of a front of A into the B-domain, which corresponds physically to a front propagating into the unstable state. Under normal diffusion, the process is described by a system of partial differential equations

$$\begin{aligned} \frac{\partial A(x,t)}{\partial t} &= D\Delta A(x,t) + \kappa A(x,t)B(x,t) \\ \frac{\partial B(x,t)}{\partial t} &= D\Delta B(x,t) - \kappa A(x,t)B(x,t) \end{aligned} \tag{7.1}$$

for an irreversible reaction. Under the given initial conditions, the overall concentration is locally conserved, since the local stoichiometry of the reaction does not change the number of particles.

Making use the conservation law $A(x,t) + B(x,t) = c_0$, the system of reaction-diffusion equations can be rewritten as

$$\frac{\partial A(x,t)}{\partial t} = D\Delta A(x,t) + \kappa A(x,t)c_0 - \kappa A^2(x,t) \; . \tag{7.2}$$

The equation for the reversible reaction differs only by the coefficients in front of the two last terms in the right hand side [121]. It is immediately clear that in the spatially homogeneous situation, $A(x,t) = c_0$ and $A(x,t) = 0$ are steady states, the first being stable and the latter unstable. The FKPP equation represents the simplest model of front propagation into an unstable state and serves as a prototype for systems exhibiting travelling fronts.

Let us now consider the non-dimensionalized version of Eq. (7.2) by making the substitutions $t \to \kappa c_0 t$, $x \to x\sqrt{\kappa c_0/D}$. Moreover, if a travelling wave front solution exists, we can change into the comoving frame $z = x - vt$. The velocity is now measured in $v = \left[\sqrt{D\kappa c_0}\right]$, and the concentration of A-particles $A(z)$ in c_0, and we have

$$\frac{\partial^2 A(z)}{\partial z^2} + v\frac{\partial A(z)}{\partial z} + A(z)\,(1 - A(z)) = 0 \; . \tag{7.3}$$

The solution should obey the boundary conditions $A(z \to -\infty) = 1$ and $A(z \to \infty) = 0$ (for positive v), since we only expect a travelling wave if the solution is in one steady state at one end and in another steady state at the other.
The singular points in the phase plane $(A(z), \frac{\partial}{\partial z}A(z))$ are given by $(0,0)$ and $(0,1)$. A linear stability analysis yields the respective eigenvalues $\frac{1}{2}\left[-v \pm \sqrt{v^2 - 4 + 8A(z)}\right]$ for the singular points, so that by exclusion of oscillatory behavior, which is in this case equivalent to forbidding negative concentrations, the only stable solution left requires $v^2 \leq 4$ [22]. Again in dimensional quantities, the range of allowed front velocities satisfies the relation

$$v \geq v_{min} = 2\sqrt{\kappa c_0 D} \; . \tag{7.4}$$

An exact analytic travelling wave solution to the FKPP equation can only be given for $v = \frac{5}{\sqrt{6}}$ [22]. In general, it is necessary to resort to approximations.
Concerning the steepness of the front, one may approximate the front shape by regarding the inflection point where the second derivative with respect to z vanishes [22, 122],

$$\begin{aligned} 0 &= v\frac{\partial A}{\partial z} + A(1-A) \\ A(z) &\approx \frac{1}{1 + \exp\left[z/v\right]} \end{aligned} \tag{7.5}$$

which provides an appropriate means to relate the steepness of the front to its velocity, as shown in Fig. 7.1. Steeper fronts correspond to smaller propagation velocities.

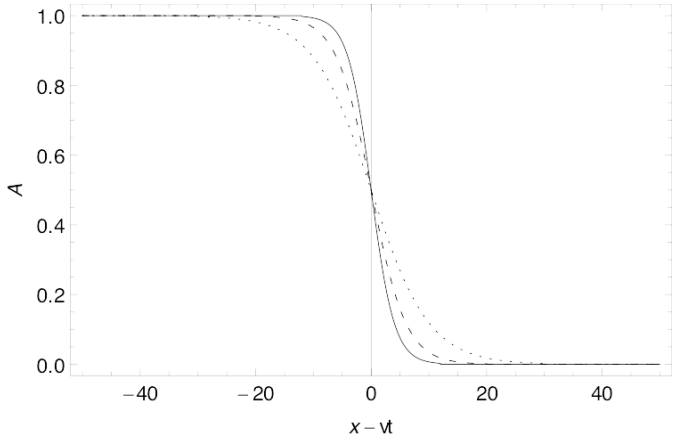

Figure 7.1: Approximated front shapes according to (7.5) for $v = 2$ (full line), $v = 3$ (dashed) and $v = 5$ (dotted).

Far away from the inflection point, at the far edge of the front $z \to \infty$, $A(x,t)$ is small (and $B \to c_0$) so that the FKPP-equation (7.2) can be linearized,

$$\frac{\partial A}{\partial t} = \Delta A + A \; . \tag{7.6}$$

At the leading edge $z \gg 1$ we may look for solutions of the form

$$A(z) \propto \exp[-\lambda(v)z] \; . \tag{7.7}$$

Inserting this front form at the leading edge into the linearized equation (7.6) yields a dispersion relation between the parameter describing the steepness of the front at the leading edge, and the propagation velocity

$$v(\lambda) = \lambda + \frac{1}{\lambda} \; . \tag{7.8}$$

The minimum is given by $v_{min} = 2$ and $\lambda_{v_{min}} = 1$, in accordance with (7.4).
The development of a travelling front depends on the choice of the initial conditions. Kolmogorov et. al have shown that if the initial condition $A(x,0)$ has a compact support, the solution of the FKPP equation is the travelling front with the minimal propagation velocity, $v = 2$ [25]. For exponential initial conditions at the far edge $A(x,0) \propto e^{-\lambda x}$ for $x \to \infty$ steeper than $e^{-\lambda_{v_{min}} x}$, i.e. $\lambda > 1$, further stability analysis of the leading edge profile yields a convergence of the front velocity to $v_{min} = 2$ [27, 123]. We may conclude that a travelling front with the minimal velocity

$v_{min} = 2$ evolves from initial conditions that are sufficiently steep in that sense, i.e. sufficiently localized. This fact is sometimes referred to as the marginal stability principle. Conversely, if initially the leading edge is given by $e^{-\lambda x}$ with $\lambda < 1$, the selected front velocity will be given by (7.8). In all the following considerations, we will concentrate only on sufficiently localized initial conditions so that the asymptotic front velocity under normal diffusion is given by the linear marginal stability velocity $v_{min} = 2$.
The front in the FKPP system represents an example of the so-called pulled fronts, as its behavior is determined by the small perturbation around the unstable state far ahead of the front, and the rest of it gets pulled along by the leading edge. The propagation velocity is independent of the bulk of the front where the particle conversion mainly takes place, in contrast to the so-called pushed fronts where the nonlinear growth in the bulk governs the behavior of the fronts, pushing the front velocities to higher values [26].

7.2 Modelling the Autocatalytic $A + B \rightarrow 2A$ Reaction under Subdiffusion

In the following, the derivation of a subdiffusive analogue to the classical FKPP equation shall be given. Obviously, the equation for B is the same as in the reaction $A + B \rightarrow 0$, since the survival probabilities are determined by the same kinetic rate term, cp. Eq. (6.44) in section 6.6. For A we have

$$\frac{\partial A_i(t)}{\partial t} = \frac{1}{2} j^-_{A,i-1}(t) + \frac{1}{2} j^-_{A,i+1}(t) - j^-_{A,i}(t) + \kappa A_i(t) B_i(t) \tag{7.9}$$

with the loss flux for the A-particles, cp. [124]

$$\begin{aligned} j^-_{A,i}(t) &= \psi(t) P_A(t|0) B_i(0) + \psi(t) A_i(0) \\ &\quad + \int_0^t \psi(t-t') \left[\frac{\partial A_i(t')}{\partial t'} + j^-_{A,i}(t') - k A_i(t') B_i(t') \right] dt' \\ &\quad + \int_0^t \psi(t-t') P_A(t|t') \left[\frac{\partial B_i(t')}{\partial t'} + j^-_{B,i}(t') + k A_i(t') B_i(t') \right] dt' \qquad (7.10) \\ P_B(t|t') &= \exp\left[- \int_0^t \kappa A(x,t')\, dt' \right] \qquad (7.11) \\ P_A(t|t') &= 1 - P_B(t|t') \,. \qquad (7.12) \end{aligned}$$

The first term on the right hand side of Eq. (7.10) corresponds to the particles that were at i from the beginning and converted from B to A until t. The second term represents the A-particles that were at i from the very beginning. The third and fourth term describe the particles that arrived

at i at a time t' as A-particles, or arrived as B-particles and reacted until t. The probability P_A to gain new A-particles arises from the conservation of the total number of particles and the probability P_B that the B-particles react. The A-concentration depends on the B-concentrations at all previous times.

Observe that the quantity $A + B = C_{A+B}$ obeys a subdiffusion equation and is even locally conserved for initial conditions $A + B = \text{const}$. The respective loss and gain fluxes add up to $j^-_{A,i} + j^-_{B,i} = j^-_{A+B,i}$ and $j^+_{A,i} + j^+_{B,i} = j^+_{A+B,i}$, so that adding the balance equations for both particle types yields the balance equation for the overall occupation number at site i,

$$\frac{\partial C_{A+B,i}(t)}{\partial t} = j^+_{A+B,i}(t) - j^-_{A+B,i}(t) = \frac{1}{2} j^-_{A+B,i-1}(t) + \frac{1}{2} j^-_{A+B,i+1}(t) - j^-_{A+B,i}(t) \,. \tag{7.13}$$

The overall loss flux at site i is given by (7.12) and (6.41), where the expressions for the survival probabilities cancel, so that

$$\begin{aligned} j^-_{A+B,i}(t) &= \psi(t)[B_i(0) + A_i(0)] + \int_0^t \psi(t-t') \\ &\quad \times \left[\frac{\partial}{\partial t'} B_i(t') + \frac{\partial}{\partial t'} A_i(t') + j^-_{A,i}(t') + j^-_{B,i}(t') \right] dt' \\ &= \psi(t) C_{A+B,i}(0) + \int_0^t \psi(t-t') \left[\frac{\partial}{\partial t'} C_{A+B,i}(t') + j^-_{A+B,i}(t') \right] dt' \,. \end{aligned} \tag{7.14}$$

This equation can be solved by means of Laplace transformation,

$$\tilde{j}^-_{A+B,i}(u) = \frac{u\tilde{\psi}(u)}{1-\tilde{\psi}(u)} \tilde{C}_{A+B,i}(u) \,. \tag{7.15}$$

Specifying the waiting time pdf that enters the kernel $\tilde{M} = \frac{u\tilde{\psi}(u)}{1-\tilde{\psi}(u)}$ yields either a diffusion equation for $C_{A+B,i}(t)$ in the Markovian case $\psi(t) = \frac{1}{\tau} \exp\left[-\frac{t}{\tau}\right]$, or a time-fractional subdiffusion equation in the non-Markovian case $\psi(t) \propto t^{-1-\alpha}$. Hence, the behavior of the total particle concentration is diffusive or subdiffusive, respectively. Moreover, if the initial condition is chosen such that $C_{A+B,i}(t) = c_0$, the total number of particles is also locally conserved for all times, $C_i(t) = C_i(0) = c_0$. The assumption of a locally conserved overall particle concentration allows for a description of the situation in terms of a single reaction-subdiffusion equation. It is convenient to use the concise equation for the B-particles (6.44) as a basis. Passing to continuous variables, we have either

$$\begin{aligned} \frac{\partial B(x,t)}{\partial t} &= \frac{a^2}{2} \Delta \int_0^t M(t-t') \exp\left[\int_{t'}^t -\kappa(c_0 - B(x,t''))\, dt'' \right] B(x,t')\, dt' \\ &\quad -\kappa(c_0 - B(x,t))\, B(x,t) \end{aligned} \tag{7.16}$$

or equivalently

$$
\begin{aligned}
-\frac{\partial A(x,t)}{\partial t} &= \frac{a^2}{2}\Delta\int_0^t M(t-t')\exp\left[\int_{t'}^t -\kappa A(x,t'')\,dt''\right](c_0-A(x,t'))\,dt' \\
&\quad -\kappa A(x,t)(c_0-A(x,t))\ . \qquad (7.17)
\end{aligned}
$$

It is important to note that under subdiffusion the assumption of the reaction as a relabelling of the particles is crucial. At reaction, the particles do not start a new waiting time period, for otherwise the effective mobility of particles within the reaction region may be increased so that the local conservation of the overall particle concentration is no longer given. As a consequence, the system for the $A+B\to 2A$ reaction under subdiffusion could not be reduced to one single equation, although this is the case for its normal diffusive counterpart. Since the classical FKPP equation is a (nonlinear) single species equation, (7.17) or its analogue (7.16) will be referred to as the subdiffusive FKPP equation in the following. With the subdiffusive analogue of the classical FKPP equation at hand, the resultant front behavior is amenable to detailed study.

7.3 Asymptotic Front Velocity: A First Approach

In a first attempt of finding the asymptotic front velocity, the subdiffusive FKPP equation (7.17) is linearized about the leading edge. We conjecture here that the front will be a pulled one, as in the normal case. A rigorous proof for this assumption can only be given by a thorough stability analysis of the full nonlinear equations, for which the theory is still lacking. In general, it is not quite clear under which conditions the nonlinearities in reaction-subdiffusion systems, especially those in the memory kernel introduced by reaction, are crucial to the qualitative behavior of the system.
Anyhow, for our FKPP system we expect pulled fronts from our intuitive understanding. Pushed fronts require nonlinearities in the bulk phase of the front to enhance the growth, which is not the case here. Moreover, since all reacting particles keep their waiting times and exhibit the same decrease in effective mobility we do not expect that particles from the bulk are able to outpace those in the leading edge, which means that also the transport term in the reaction-subdiffusion equation (7.17) cannot account for a pushed front behavior. Therefore the leading edge of the front, i.e. the region of small concentrations of the stable reactant, determines the dynamics and linearization is justified. In the leading edge $A(x,t)$ becomes small, so that

$$
\begin{aligned}
-\frac{\partial A}{\partial t} &= \frac{a^2}{2}\int_0^t \Delta\left\{M(t-t')(c_0-A(x,t'))\exp\left[-\kappa\int_{t'}^t A(x,t'')\,dt''\right]\right\}dt' \\
&\quad -\kappa(c_0-A(x,t))A(x,t), \qquad (7.18)
\end{aligned}
$$

where the sequence of differentiation over x and temporal integration was interchanged. The exponential term in the integrand $\exp\left[-\kappa\int_{t'}^t (A(x,t''))\,dt''\right]$ tends to unity at the leading edge so

that the integrand can be rewritten as

$$M(t-t')\Big[\Delta A(x,t') - 2\nabla A(x,t')\int_{t'}^{t}\kappa\nabla A(x,t'')\,dt'' \\ +(c_0 - A(x,t'))\int_{t'}^{t}\kappa\Delta A(x,t'')\,dt'' - (c_0 - A(x,t'))\Big(\int_{t'}^{t}\kappa\nabla A(x,t'')\,dt''\Big)^2\Big]$$

so that finally the subdiffusive FKPP equation reads:

$$\begin{aligned}\frac{\partial A}{\partial t} &= \frac{a^2}{2}\int_0^t M(t-t')\Big[\Delta A(x,t') - 2\nabla A(x,t')\int_{t'}^{t}\kappa\nabla A(x,t'')\,dt'' \\ &\quad +(c_0 - A(x,t'))\int_{t'}^{t}\kappa\Delta A(x,t'')\,dt'' - (c_0 - A(x,t'))\Big(\int_{t'}^{t}\kappa\nabla A(x,t'')\,dt''\Big)^2\Big]dt' \\ &\quad +\kappa(c_0 - A(x,t))A(x,t)\,. \end{aligned} \tag{7.19}$$

We know that the stationary solutions to linear reaction-subdiffusion equations are given by exponentials, cp. section 6.3. Under the assumption of a stable front at a constant velocity v, the front should therefore take on a form $A(x,t) = A_0\exp[-\lambda(x-vt)]$ at the leading edge. Insertion into equation (7.19) and retaining only leading orders in particle concentration yields

$$\begin{aligned}\frac{\partial}{\partial t}(A_0\exp[-\lambda(x-vt)]) &= \kappa c_0 A_0\exp[-\lambda(x-vt)] \\ &\quad -\frac{a^2}{2}\int_0^t M(t-t')\Big[-\lambda^2 A_0\exp[-\lambda(x-vt')] \\ &\quad +\frac{\kappa c_0\lambda}{v}A_0\exp[-\lambda(x-vt')] - \frac{\kappa c_0\lambda}{v}A_0\exp[-\lambda(x-vt)]\Big]dt' \\ &= \kappa c_0 A_0\exp[-\lambda(x-vt)] \\ &\quad -\frac{a^2}{2}A_0\Big[-\lambda^2 + \frac{\kappa c_0\lambda}{v}\Big]\int_0^t M(t-t')\exp[-\lambda(x-vt')]\,dt' \\ &\quad +\frac{a^2}{2}\frac{\kappa c_0\lambda}{v}A_0\exp[-\lambda(x-vt)]\int_0^t M(t-t')\,dt'\,, \end{aligned} \tag{7.20}$$

with the familiar kernel for which

$$\tilde{M}(u) = \frac{u\tilde{\psi}(u)}{1-\tilde{\psi}(u)}$$

in Laplace domain.

Markovian case

Let us first reproduce the standard expression for the minimal velocity of the stable propagation in the Markovian case of exponential waiting time distributions. Taking $\psi(t) = \frac{1}{\tau}\exp\left[-\frac{t}{\tau}\right]$, one obtains $M(t-t') = \frac{1}{\tau}\delta(t-t')$ and

$$\begin{aligned} 0 &= \frac{\partial}{\partial t}(A_0 \exp[-\lambda(x-vt)]) - \kappa c_0 A_0 \exp[-\lambda(x-vt)] \\ &+ \frac{a^2}{2\tau} A_0 \exp[-\lambda(x-vt)]\left[-\lambda^2 + \frac{\kappa c_0 \lambda}{v} - \frac{\kappa c_0 \lambda}{v}\right] \\ &= \lambda v \exp[-\lambda(x-vt)] - \kappa c_0 A_0 \exp[-\lambda(x-vt)] - \frac{a^2}{2\tau}\lambda^2 A_0 \exp[-\lambda(x-vt)] \ , \end{aligned} \tag{7.21}$$

which for $z = x - vt$, $z \to \infty$ leads us to the standard dispersion relation for the front:

$$\frac{a^2}{2\tau}\lambda^2 - v\lambda + \kappa c_0 = 0 \ .$$

Nonnegative particle concentrations require real values of λ and are only possible for $v \geq v_{min} = 2\sqrt{a^2 \kappa c_0 / 2\tau} \equiv 2\sqrt{D\kappa c_0}$ with $D = a^2/2\tau$ being the diffusion coefficient. Observe that the corresponding result emerges due to the fact that the kernel M reduces to a Delta-function and the two terms of different nature in Eq. (7.21) cancel each other. As we proceed to show, this cancellation does not take place in the non-Markovian case.

Non-Markovian case

With a power law waiting time pdf $\psi(t) \propto t^{-1-\alpha}$, $0 < \alpha < 1$ for large t or $\tilde{\psi}(u) \simeq 1 - \tau^\alpha u^\alpha$ for small u, the integral operator with the kernel M becomes the Riemann-Liouville fractional derivative. Using the substitution $t^* = t - t'$, we get

$$\begin{aligned} \int_0^t M(t-t')\exp[\lambda v t']\, dt' &= \exp[\lambda v t] \int_0^t M(t^*)\exp[-\lambda v t^*]\, dt^* \\ &= \exp[\lambda v t]\, \tilde{M}(\lambda v) \ . \end{aligned}$$

Moreover,

$$\int_0^t M(t-t')\exp[\lambda v t]\, dt' = \frac{\text{const}}{\tau^\alpha} t^{\alpha-1} \ ,$$

so that the contribution of last term in (7.20) vanishes in the large t asymptotics,

$$\begin{aligned}\frac{\partial}{\partial t}(A_0\exp[-\lambda(x-vt)]) &= \kappa c_0 A_0\exp[-\lambda(x-vt)] \\ &\quad -\frac{a^2}{2}A_0\exp[-\lambda(x-vt)]\Big(-\lambda^2+\frac{\kappa c_0\lambda}{v}\Big)\tilde{M}(\lambda v)\,.\end{aligned}$$

We obtain the sought dispersion relation,

$$\begin{aligned}\lambda v A_0\exp[-\lambda z] &= \kappa c_0 A_0\exp[-\lambda z] \\ &\quad -\frac{a^2}{2}A_0\exp[-\lambda z]\Big(-\lambda^2+\frac{\kappa c_0\lambda}{v}\Big)\tilde{M}(\lambda v)\,, \\ 0 &= -v\lambda+\kappa c_0+\frac{a^2}{2}(\lambda^2-\frac{\kappa c_0\lambda}{v})\tilde{M}(\lambda v)\,, \qquad (7.22)\end{aligned}$$

with $z = x - vt$. For power-law asymptotics $\psi(t) \propto t^{-1-\alpha}$ we have $\tilde{\psi}(u) \simeq 1-(u\tau)^\alpha$ and $\tilde{M}(u) = \tau^{-\alpha}u^{1-\alpha}$, so that

$$0 = -v\lambda+\kappa c_0+\frac{a^2}{2\tau^\alpha}\Big(\lambda^2-\frac{\kappa c_0\lambda}{v}\Big)(\lambda v)^{1-\alpha}\,.$$

This equation is equivalent to

$$(v\lambda-\kappa)c_0\Big(\frac{a^2}{2\tau^\alpha}\lambda^{2-\alpha}v^{-\alpha}-1\Big) = 0\,. \qquad (7.23)$$

Since this equation possesses two nonnegative roots for any $v \geq 0$, the minimal propagation velocity is zero so that the front velocity tends to zero in the course of time.
Note that these results are reproduced when the above model (7.18) is subjected to an analysis put forward in [116], for a detailed calculation see Appendix D. These authors used a Hamilton–Jacobi approach and found a minimal propagation velocity in the case of subdiffusion. The Hamilton–Jacobi approach and the method of leading–edge linearization are basically equivalent. Hence, the reason for their seemingly contradictory result lies in the fact that a different reaction-subdiffusion model was used that also comprises the classical FKPP dynamics as a limiting case.

7.4 Simulational Results

Having shown the absence of the stable front propagating at a constant velocity, we now turn to the numerical simulation of the irreversible $A + B \to 2A$ reaction on a one-dimensional lattice [1]. The simulations are carried out on a lattice of length L and a lattice spacing $a = 1$ where the initial condition is implemented such that the B particles are distributed homogeneously on the sites with the average occupation number ac_0. In order to initiate the reaction, a single A-particle is introduced at the left end of the lattice. All particles perform unbiased CTRWs with waiting times corresponding to the pdf

$$\psi(t) = \frac{\alpha}{(1+t)^{1+\alpha}} , \tag{7.24}$$

where $0 < \alpha < 1$. A particle arriving at lattice site i at some instant of time stays there for a sojourn time t drawn from the pdf (7.24) and subsequently makes a jump either to the left or right neighboring site with equal probabilities. It has to be emphasized again that CRTWs with waiting time pdfs lacking the first moment are nonstationary and nonergodic, see e.g. [18]. As a consequence, effective simulational algorithms of the Gillespie type that rely on the Markovian property of normal diffusion do not apply here. To account for the non-Markovian nature of the involved transport process, it is necessary to assign an individual sequence of jumping times to each particle . To do so, the particles are labelled irrespective of their A- or B-nature. The jumping time sequence for each of them is generated by adding up the waiting times following from (7.24). Then, all jumping times are sorted and stored. Particles of the same type do not interact, they do not possess any excluded volume. Particles of different types may react according to the $A + B \to 2A$ reaction scheme when encountered at the same site.

Before specifying the implementation of the reaction process, we address the issue of different regimes of front propagation encountered under normal diffusion. Essentially these regimes correspond to the limit of very high and very low concentrations. Considering the effectively one-dimensional system, the concentration c_0 of reactants has the dimension $[\mathsf{c_0}] = [\mathsf{L}^{-1}]$, and the reaction rate coefficient $[\kappa] = [\mathsf{L}/\mathsf{T}]$. According to the classical FKPP theory, the $A + B \to 2A$ reaction results in the propagation of a stationary front of width $w \propto \sqrt{D/\kappa c_0}$ moving at a constant velocity $v = 2\sqrt{D\kappa c_0}$. At sufficiently low particle concentrations, fluctuation effects come into play and the mean-field FKPP picture does no longer apply. This is the case if the typical interparticle distance $l = c_0^{-1}$ becomes larger than the front's width predicted by the continuous FKPP theory. Hence, for the classical theory to apply, $w \gg l$ or $c_0 \gg \kappa/D$ must hold. Thus, the continuous regime is encountered at large concentrations or/and small reaction rates $c_0 \to \infty, \kappa \to 0$ [122]. Conversely, in the fluctuation-dominated regime the asymptotic propagation velocity is considerably smaller than in the continuous regime, i.e. for large enough κ or small enough c_0 the velocity of the front approaches $v \simeq cD$ [126]. The effect of fluctuations on front propagation were studied in detail e.g. by Brunet and Derrida [127] or Riordan et al. [121]. A review was given by Panja [27].

In order to account for fluctuation effects due to small particle concentrations or large reaction

[1] All simulations concerning the $A + B \to 2A$ reaction under subdiffusion were performed by Hauke Schmidt-Martens, for the most part in conjunction with his Diploma thesis [125].

rates in the case of subdiffusion, two different situations with respect to the reaction probabilities are considered:
In the first case the reactions are implemented such that when an A particle encounters B particles at a site i, the reaction takes place immediately, which allows for an event-driven algorithm: The particle that is to jump next is selected and performs the jump to the new site i. All the B particles present at site i are converted to A instantaneously by renaming them. This setting corresponds to the limit of large reaction rates and was simulated in Ref. [126] for normal diffusion. We will refer to this situation as the Reaction-on-contact model in the following.
The second case corresponds to the reaction with a finite rate. Attempts to react occur at constant time intervals $\Delta t_r = 1$, and the transformation of B into A at a site i takes place with probability $p_r N_A(i) N_B(i)$ per attempt. $N_A(i)$ and $N_B(i)$ are the number of A and B particles at site i respectively. If a reaction takes place, a B-particle at the site is chosen at random and renamed into A. Here, each individual site has to be checked for reactions taking place at time intervals $\Delta t_r = 1$. This model corresponds to the situation discussed in section 7.2, see also [128]. On the lattice sites the classical rate kinetics applies, so that the classical reaction rate can be expressed in terms of $\kappa = p_r/\Delta t_r$, i.e. in the units used here, κ equals p_r.

In order to obtain the velocity of the propagating front in both cases, we make use of the total amount of A-particles $N_A(t)$ as a measure of the front position $x(t) = N_A(t)/c_0$. That definition has the advantage that it does not require an averaging procedure over several realizations, but can be defined for a single realization as well. On the other hand, the obtained front position is preaveraged in the sense that it contains information of the integrated amount A-particles in the whole system. In contrast to e.g. taking the rightmost A-particle as the position of the front, in this definition the contribution of the fluctuations in interparticle distance to the fluctuations in the front position is suppressed and allows for the extraction of good data from relatively few simulation runs. Various definitions of the front position and their implications are discussed in [122] for the normal diffusive FKPP system. Most of these considerations can be transferred to the case of anomalous diffusion as well.

7.4.1 Reaction on Contact

The reaction-on-contact model corresponds to the simplest situation and can be simulated relatively fast, due to the possibility to use the event-driven algorithm. In the simulations of the reaction-on-contact model, a chain of length $L = 10000$ sites and with a particle concentration $c_0 = 0.3$ is set up.

The total amount of particles in dependence of time, $N_A(t)$, is shown in Fig. 7.2 for different values of the subdiffusion parameter α in the pdf Eq. (7.24). The double-logarithmic plot of $N_A(t)$ reveals a power law dependence

$$N_A(t) \propto t^{\beta} \,. \tag{7.25}$$

As seen from the slopes of the graphs in the double-logarithmic plot, the values of β are clearly all smaller than one. The front position $N_A(t)$ does not grow at a constant, but at a decreasing

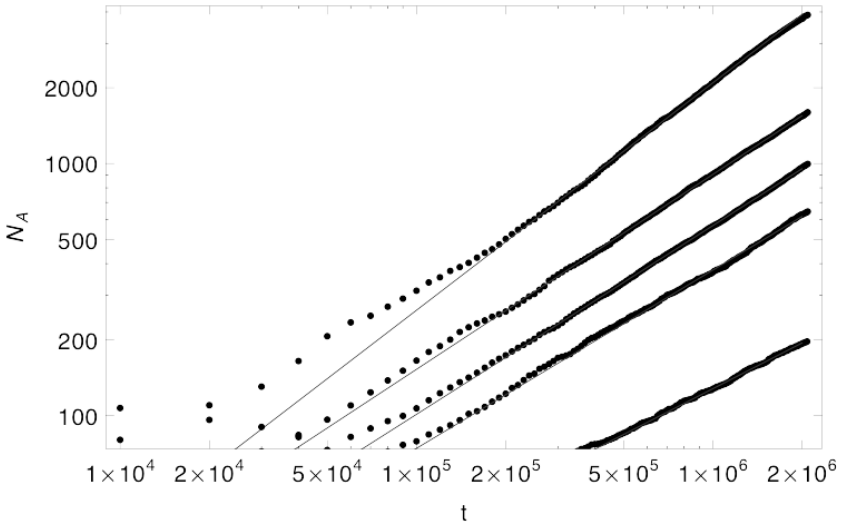

Figure 7.2: Total amount of A particles as a function of time in the the reaction-on-contact model, subdiffusion parameter (upper to lower graphs) $\alpha = 0.9,\ 0.8,\ 0.75,\ 0.7,\ 0.6$; $c_0 = 0.3$ The full lines correspond to the power–law fits, Eq. (7.25).

rate. The fitted exponents β are shown in Table 7.1.

α	0.6	0.7	0.75	0.8	0.9
β	0.604 ± 0.004	0.708 ± 0.004	0.750 ± 0.001	0.775 ± 0.003	0.890 ± 0.003

Table 7.1: Exponents for the fit $N_A \propto t^\beta$ for different α, reaction–on–contact.

The behavior of $N_A(t)$ is consistent with the assumption $N_A(t) \propto t^\alpha$. Hence, the velocity of the front is decaying with time as

$$v \propto t^{\alpha-1} \ . \tag{7.26}$$

In the Markovian case, $\psi(t) = \frac{1}{\tau} e^{-t/\tau}$, $N_A(t)$ grows linearly in t, which corresponds to a constant front velocity. This situation served as a test of the algorithm and reproduced the findings of Ref. [126] such as the linear dependence on concentration and on $1/\tau$ of the front velocity, for details see [125, 128].

7.4.2 Reaction with Finite Probability

In the situation where the reaction takes place with a probability $p_r < 1$ per unit time, the position of the front shows again a power-law dependence on time t.

The results for $L = 10000$, $c = 0.3$ and reaction probability $p_r = 0.1$ are given in Fig. 7.3. Again, a power-law of the form Eq. (7.25) adequately describes the data. The estimated values

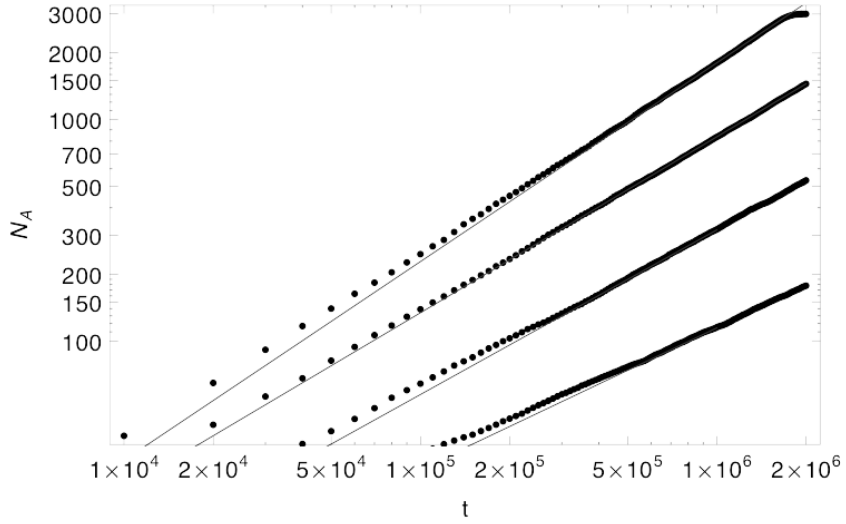

Figure 7.3: Total amount of A particles in dependence of time for the reaction with probability $p_r = 0.1$ per unit time and $c_0 = 0.3$; subdiffusion parameter from upper to lower graphs: $\alpha = 0.9, 0.8, 0.7, 0.6$. The lines represent the power-law fits, Eq. (7.25).

of the fit-parameter β for different values of α are given by Table 7.2.

α	0.6	0.7	0.8	0.9
β	0.636 ± 0.005	0.743 ± 0.006	0.795 ± 0.003	0.898 ± 0.003

Table 7.2: Exponents for the fit $N_A \propto t^\beta$ for different α in the fluctuation dominated regime.

These results show again that $\alpha \simeq \beta$ and hence the velocity of the front goes as $v \propto t^{\alpha-1}$. We note that the value of the concentration $c_0 = 0.3$ is comparatively small and the value of the reaction probability $p_r = 0.1$ is still relatively large so that, due to fluctuation effects and to low dimensionality of the system, deviations from the behavior in the continuous description corresponding to the classical FKPP behavior in the Markovian case are expected. A comparability of simulational results with the continuous theory put forward in section 7.2 requires large concentrations and very small reaction probabilities. Therefore the simulations are carried out for the parameter values $c_0 = 10$, $p_r = 0.006$, for which the behavior for the analoguous Markovian system is well-described by the classical FKPP results. The underlying lattice was of length $L = 1000$.

Figure 7.4 represents the total amount of A particles $N_A(t)$ obtained by the simulations. Due to the slow convergence to the asymptotic behavior of front propagation, only the last decade of the data is subjected to a least square fitting procedure. Also those data points indicating that the front has reached the end of the lattice were omitted. The resultant fits are shown by solid lines in the figure and given in Table 7.3.

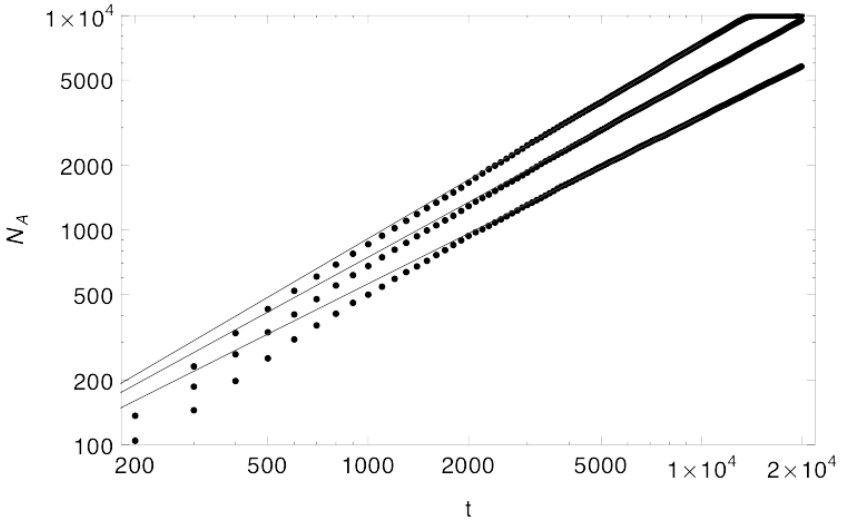

Figure 7.4: $N_A(t)$ in the continuous regime with $c = 10$, $p = 0.006$ for different $\alpha = 0.8,\ 0.7,\ 0.6$ (upper to lower graphs). The solid lines represent the fits.

α	0.6	0.7	0.8
β	0.779 ± 0.001	0.850 ± 0.001	0.910 ± 0.002

Table 7.3: Exponents for the fit $N_A \propto t^{\beta}$ for different α in the continuous regime.

The estimated values of the fit parameter β for the different $\alpha = 0.8,\ 0.7,\ 0.6$ are again all significantly smaller than one, indicating a slowing down of the reaction font. Thus, the velocity of its propagation tends to zero, in accordance with the analytical results derived earlier. A more detailed analysis of the exponents in this case reveals that $\beta = 1/2 + \alpha/2$. As a consequence, the propagation velocity decays approximately as $v(t) \propto t^{(\alpha-1)/2}$.

7.4.3 Discussion

The results of the simulations for the fluctuation-dominated regime as well as for the regime corresponding to the continuous subdiffusive FKPP system suggest an interpretation that describes the underlying complex transport process in terms of a time–dependent mean diffusion coefficient $D(t)$. This picture was put forward by Batchelor in context of turbulent diffusion [129]. For a CTRW with the waiting time distribution characterized by the exponent α, the mean squared displacement of a single particle goes as $\left\langle x^2(t) \right\rangle \propto t^{\alpha}$, a behavior that can be reproduced by a diffusive process with a diffusion coefficient $D(t) \propto t^{\alpha-1}$. The corresponding front velocities follow from the time-dependence of this diffusion coefficient, so that $v(t) \propto D(t) \propto t^{\alpha-1}$ in the fluctuation-dominated regime, where concentrations are small and reaction rates high, and $v(t) \propto \sqrt{D(t)} \propto t^{(\alpha-1)/2}$ in the classical limiting case. Mancinelli et al. [130] considered the clas-

sical FKPP equation with a time dependent diffusion constant $D(t) \propto t^{\alpha-1}$ and found the same front velocity $v(t) \propto t^{(\alpha-1)/2}$ by direct calculations of the partial differential equation. Moreover, they found a decrease of the front's width, although this decrease could not be quantified. The fact that the constant minimal propagation velocity does not exist corresponds essentially to a continuum approaching of $v_{min} \propto \sqrt{D}$ to zero for the case when $D \to 0$ as it is the case in subdiffusion.

Regarding front shapes, the simulations suggest the existence of a front with a constant form moving with velocity $v \propto t^{(\alpha-1)/2}$ in the continuous regime [128]. However, these findings do not comply with the detailed considerations in the following sections so that the constant front shape obtained in the simulations has to be regarded as a numerical artefact.
Note again that the equations under study (7.16), (7.17) correspond to the situation where converted particles are only re-labelled and keep their actual waiting time. Simulations of the autocatalytic A + B → 2A reaction by Campos and Mendez [117] have shown that in the case of re-labelling particles the resultant dynamics is dominated by the tail of the waiting time pdf of the particle jumps, and a decelerating front evolves. On the contrary, when reacting particles are assigned a new waiting time, the front dynamics is governed by the bulk of the waiting time pdf and its velocity remains constant.
In the same contribution, Campos and Mendez repeated our simulations for the case of very small reaction probabilities $p_r = 0.006$, and increased the simulation time considerably. The front behavior in the range covered by our simulations was reproduced, but for very large times, a decrease in the exponent of the front velocity set in. The alleged exponent conjectured from the continuous picture is not the final one and is associated with an intermediate regime that ranges over less than two orders of magnitude in time. However, the simulation times were still not large enough to determine the final asymptotics. The next sections shall give an explanation to these facts.

7.5 Crossover Argument

Assuming a front of constant shape with decreasing velocity $v \propto t^{(\alpha-1)/2}$, one may deduce an asymptotic solution to the linearized equation (7.19) of the form

$$A(x,t) = A_0 \exp\left[-\lambda\left(x - v_0 t^{\frac{\alpha+1}{2}}\right)\right] , \tag{7.27}$$

where the comoving variable was obtained by $z = x - \int_0^t v(t')dt' = x - v_0 t^{\frac{\alpha+1}{2}}$, and v_0 is a constant of dimension $\mathsf{L}/\mathsf{T}^{(\alpha+1)/2}$. However, inserting (7.27) into (7.19) shows that this ansatz is not an appropriate solution describing the leading edge of the front. Hence, the front solution in the subdiffusive analogue of the FKPP equation cannot be of constant shape and a velocity going as $v \propto t^{(\alpha-1)/2}$.

This fact, together with the findings that the front velocity found for the case of small reaction probability may not correspond to the the final behavior of the front [117], puts into question whether the asymptotic propagation velocity $v \propto t^{(\alpha-1)/2}$ holds in the continuous regime. In order to gain intuition about the front behavior in this regime, we make use of a crossover argument based on the following idea:

For any waiting time pdf $\psi(t)$ with finite mean $\langle t\rangle$, the behavior at very long times $t \gg \langle t\rangle$ corresponds to normal diffusion, so that the behavior pertinent to reaction-diffusion schemes is recovered if only the time t is large enough. On the other hand, if the pdf is constructed such that its initial domain is given by a power-law $\psi(t) \propto t^{-1-\alpha}$ up to a truncation time T, subdiffusive behavior should be recovered for short times. We therefore consider a truncated power-law waiting time pdf with truncation parameter T,

$$\psi_T(t) = \frac{(t_0+T)^\alpha}{(t_0+T)^\alpha - t_0^\alpha}\frac{\alpha t_0^\alpha}{(t_0+t)^{1+\alpha}}\theta(T-t)\,, \tag{7.28}$$

which has the mean value

$$\langle t\rangle = \frac{\alpha T t_0^\alpha + t_0\left(t_0^\alpha - (T+t_0)^\alpha\right)}{(\alpha-1)\left(t_0^\alpha - (T+t_0)^\alpha\right)}\,. \tag{7.29}$$

If $T \gg t_0$, the mean waiting time can be approximated by the more convenient expression $\langle t\rangle \approx \frac{\alpha}{1-\alpha}t_0^\alpha T^{1-\alpha}$. At small times $t_0 < t \ll T$, the jumping particles do not yet feel the cutoff, and the behavior of the front velocity will be similar to that in subdiffusion. At large times the behavior is expected to be the classical one with a constant velocity given by the marginal propagation velocity from FKPP theory. Between the two regimes, there must be a crossover taking place at a time t_{cr}. We conjecture a time-dependent front velocity $v \sim \text{const}\times t^\beta$ in the anomalous domain, followed by a crossover to normal behavior. Recall that the normal behavior is characterized by the marginal front velocity $v = \text{const} \sim \sqrt{c_0\kappa D}$, with $D = a^2/2\langle t\rangle$ and a being the step length of the corresponding random walk process. The temporal behavior of the velocity in the anomalous regime is given by the equation

$$\text{const}\times t_{cr}^\beta \simeq \left[c_0\kappa\frac{a^2}{2\langle t(t_{cr})\rangle}\right]^{1/2}\,. \tag{7.30}$$

In order to determine the crossover time we make use of the number of performed steps. This basic quantity represents a measure of mobility and is well suited for the characterization of transport. We have

$$n_D(t) = \frac{t}{\langle t\rangle} \tag{7.31}$$

in the normal regime $t \gg t_{cr}$, and

$$n_{SD}(t) = \frac{t^\alpha}{\Gamma(1+\alpha)t_0^\alpha} \tag{7.32}$$

in the subdiffusive regime $t \ll t_{cr}$, cp. section 4.3.1.

A continuous transition from one regime to the other requires that all quantities characterizing the behavior of the system, such as the number of performed steps, the front velocities etc., match for the two regimes at the time t_{cr} the crossover takes place. This fact can be used to determine the crossover time. Enforcing $n_{SD}(t_{cr}) = n_D(t_{cr})$, we find

$$\frac{1-\alpha}{\alpha}\frac{t_{cr}}{t_0^\alpha T^{1-\alpha}} = \frac{t_{cr}^\alpha}{\Gamma(1+\alpha)t_0^\alpha} \; ; \tag{7.33}$$

and hence $t_{cr}^{1-\alpha} = \frac{\alpha}{\Gamma(1+\alpha)(1-\alpha)} T^{1-\alpha}$, i.e. $t_{cr} \propto T$. Obviously, the larger the cutoff-parameter T, the larger becomes the crossover time.

The proportionality between the crossover time and the cutoff parameter allows for tuning the T in order to obtain the respective values of all quantities of interest at the crossover time t_{cr}, for example the mean waiting time $\langle t \rangle \propto t_{cr}^{1-\alpha}$ for the normal case in terms of t_{cr}. Eq. (7.30) then yields

$$v(t < t_{cr}) \propto t^{\frac{\alpha-1}{2}} \tag{7.34}$$

in the subdiffusive regime. Fig. 7.5 illustrates the situation for $\alpha = 0.5$. The log-log plot of the crossover times and their corresponding classical front velocities reveals the inverse power law behavior of the asymptotic front velocity (7.34) in the anomalous case.

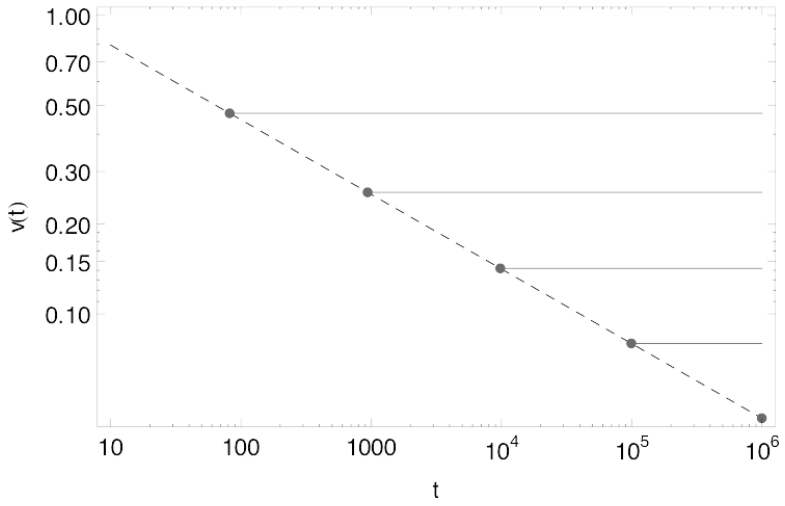

Figure 7.5: Asymptotic front velocity (dashed line) obtained by the crossover argument. The full lines denote the classical front velocities, the grey dots indicate the respective crossover times according to Eq. (7.33) for cutoff parameters $T = 10^2, 10^3, 10^4, 10^5, 10^6$; $t_0 = 1$, $\alpha = 0.5$.

All other time-dependent characteristics in the anomalous regime can be defined in the same

fashion, so that the effective mean waiting time is $\langle t \rangle_{eff} \propto t^{1-\alpha}$, where parameter t_{cr} is now changed to t. The resultant effective time dependent diffusion coefficient is given by $D_{eff} \propto 1/t^{1-\alpha}$. Eq. (7.34) can be obtained by inserting this effective diffusion coefficient into the classical formula $v = 2\sqrt{c_0 \kappa D_{eff}}$. The front velocity (7.34) is well in accordance with the behavior of the anomalous front velocity found in the simulations the regime of small reaction rates. Moreover, the width of the front in the normal FKPP regime is of the order $w \propto D/v = \sqrt{D/\kappa c_0}$, as can easily be seen by dimensional analysis. Hence, applying the same crossover argument we expect the width of the front to go as $w \propto \sqrt{D_{eff}/\kappa c_0}$ in the anomalous case, i.e. the width of the front decreases with time as

$$w(t) \propto t^{(\alpha-1)/2} \,. \tag{7.35}$$

Going to the particle picture, in addition to the front width, the interparticle distance $l_{ip} = c_0^{-1}$ comes into play as a characteristic length scale. The continuous description is only valid if $w \gg l$, i.e. $\sqrt{D/c_0\kappa} \gg c_0^{-1}$ and hence holds for large concentrations and diffusion coefficients, and for small reaction rates. In this case there are enough particles within the front region for the continuous description to hold. In the case of subdiffusion, the effective diffusion coefficient decreases permanently, so that the continuous description must fail after some time, no matter how large the concentration or small the reaction rates are. The fully developed final regime will thus be the fluctuation dominated one, with the width of the front being characterized by the interparticle distance, so that the front gets atomically sharp, $w \simeq l = c_0^{-1}$. With $w \propto D/v$ for the normal diffusive fluctuation dominated case we have again $v \propto Dc_0$ [126]. Employing the same crossover argument to the velocity in the fluctuation dominated case, we arrive at

$$v(t) \propto t^{\alpha-1} \tag{7.36}$$

for the front velocity under subdiffusion. The transition from the continuous to the fluctuation dominated regime is presumably accountable for the observation made in the simulations by [117] that after an intermediate regime where (7.34) holds, the front velocity sets in to decay faster at very large times.

To close the considerations on crossover arguments, it has to be noted that the transition from anomalous to normal behavior does of course not take place immediately. Particularly the use of truncated long-tailed probability distributions results in very long transients [131]. In what follows we briefly discuss an alternative approach in defining a time at which the passage to normal behavior takes place. A measure of the convergence to normal behavior is given by the Theorem of Berry and Esséen, see section 3.3 [52, 132]. Making use of this theorem, we find with $\left\langle t^3 \right\rangle \propto T^{3-\alpha}$ and $\left\langle t^2 \right\rangle^{3/2} \propto T^{3-3\alpha/2}$ that the scaling law for the amount of steps needed to obtain normal behavior is $n_{norm} \propto T^{\alpha}$. Consequently, the corresponding time obeys $t_{norm} \propto n_{norm} \langle t \rangle \propto T$, a relation similar to that between the cutoff parameter T and the crossover time t_{cr} established above. Thus, taking into account the additional information of the shape of the waiting time

pdf does not lead to a qualitatively different relation between the cutoff parameter and the time after which normal behavior is attained. The rest of the calculations does not differ from those presented above. Consequently, also the behavior of the deduced quantities such as effective diffusion coefficient and front velocities will be the same as above.

7.6 Asymptotic Front Velocity in the Continuous Reaction-Subdiffusion Regime

In what follows we first show that the "classical" asymptotics, Eq. (7.34), indeed appears as a possible solution of the reaction subdiffusion equation. With the strong evidence at hand that the front in the continuous reaction-subdiffusion regime features a decay in velocity and width, we start a second attempt to put up an ansatz to solve the linearized subdiffusive FKPP equation. With the width going as $\lambda_0^{-1} t^{\frac{\alpha-1}{2}}$ and the front position being $x(t) \propto v_0 t^{\frac{1+\alpha}{2}}$, we assume the front to be given by an exponential at its leading edge,

$$A(x,t) = A_0 \exp\left[-\lambda_0 t^{\frac{1-\alpha}{2}} \left(x - v_0 t^{\frac{1+\alpha}{2}}\right)\right] = A_0 \exp\left[-\lambda_0 t^{\frac{1-\alpha}{2}} z\right] , \tag{7.37}$$

where $z = x - v_0 t^{\frac{1+\alpha}{2}}$ is the comoving variable and λ_0 is a constant. The exponential Ansatz is due to the fact that we will linearize the equations at the front's far edge later, and we know that the (stationary) solutions of linear reaction-subdiffusion equations are exponentials, see section 6.3 and Ref. [133]. Recall again that the equation for the A-particles is

$$\begin{aligned} \frac{\partial A(x,t)}{\partial t} &= \frac{a^2}{2}\Delta \int_0^t M(t-t')(A(x,t') - c_0) \exp\left[-\int_{t'}^t \kappa A(x,t'')dt''\right] dt' \\ &\quad + \kappa(c_0 - A(x,t))A(x,t) , \end{aligned} \tag{7.38}$$

so that with $A(x,t)$ being small at the leading edge $x \to \infty$, and $\exp\left[-\int_{t'}^t \kappa A(x,t'')dt''\right] \approx 1$,

$$\begin{aligned} \frac{\partial A(x,t)}{\partial t} &= \frac{a^2}{2} \int_0^t \Delta \left\{ M(t-t')(A(x,t') - c_0) \exp\left[-\kappa \int_{t'}^t A(x,t'')\, dt''\right]\right\} dt' \\ &\quad + \kappa(c_0 - A(x,t))A(x,t) \end{aligned} \tag{7.39}$$

$$\begin{aligned} &\approx \frac{a^2}{2} \int_0^t M(t-t') \Big[\Delta A(x,t') - 2\nabla A(x,t') \int_{t'}^t \kappa \nabla A(x,t'')\, dt'' \\ &\quad + (c_0 - A(x,t')) \int_{t'}^t \kappa \Delta A(x,t'')\, dt'' - (c_0 - A(x,t'))\Big(\int_{t'}^t \kappa \nabla A(x,t'')\, dt''\Big)^2 \Big] dt' \\ &\quad + \kappa(c_0 - A(x,t))A(x,t) . \end{aligned} \tag{7.40}$$

With ansatz (7.37) and taking into account that the term $t^{-\frac{1+\alpha}{2}}$ is negligible for large t, we calcu-

late

$$\begin{aligned}
\frac{\partial A(x,t)}{\partial t} &= A_0 \exp\left[-\lambda_0 t^{\frac{1-\alpha}{2}}\left(x - v_0 t^{\frac{1+\alpha}{2}}\right)\right]\times \\
&\quad \left[v_0\lambda_0 t^{\frac{1-\alpha}{2}} t^{\frac{\alpha-1}{2}} \frac{\alpha+1}{2} - \lambda_0 t^{-\frac{1+\alpha}{2}} \frac{1-\alpha}{2}\left(x - v_0 t^{\frac{1+\alpha}{2}}\right)\right] \\
&= A_0 \exp\left[-\lambda_0 t^{\frac{1-\alpha}{2}}\left(x - v_0 t^{\frac{1+\alpha}{2}}\right)\right]\times \\
&\quad \left[v_0\lambda_0 - \frac{1-\alpha}{2}\lambda_0 x t^{-\frac{1+\alpha}{2}}\right] \\
&\approx A_0 \exp\left[-\lambda_0 t^{\frac{1-\alpha}{2}}(x - v_0 t^{\frac{\alpha+1}{2}})\right] v_0\lambda_0 \qquad (7.41) \\
\nabla A(x,t) &= -A_0\lambda_0 t^{\frac{1-\alpha}{2}} \exp\left[-\lambda_0 t^{\frac{1-\alpha}{2}}\left(x - v_0 t^{\frac{1+\alpha}{2}}\right)\right] \\
\Delta A(x,t) &= A_0\lambda_0^2 t^{1-\alpha} \exp\left[-\lambda_0 t^{\frac{1-\alpha}{2}}\left(x - v_0 t^{\frac{1+\alpha}{2}}\right)\right] .
\end{aligned}$$

Retaining only first order terms in concentration for the A-particles simplifies the equation governing the particle concentration at the leading edge,

$$\begin{aligned}
\frac{\partial A(x,t)}{\partial t} &\approx \frac{a^2}{2}\int_0^t M(t-t')\Delta A_0 \exp\left[-\lambda_0 t'^{\frac{1-\alpha}{2}}\left(x - v_0 t'^{\frac{\alpha+1}{2}}\right)\right] dt' \\
&\quad + \frac{a^2}{2}\int_0^t M(t-t') c_0\kappa \int_{t'}^t \Delta A_0 \exp\left[-\lambda_0 t''^{\frac{1-\alpha}{2}}\left(x - v_0 t''^{\frac{1+\alpha}{2}}\right)\right] dt'' dt' \\
&\quad + c_0\kappa A(x,t) , \qquad (7.42)
\end{aligned}$$

and hence, inserting the ansatz (7.37),

$$\begin{aligned}
&A_0 \exp\left[-\lambda_0 t^{\frac{1-\alpha}{2}}\left(x - v_0 t^{\frac{\alpha+1}{2}}\right)\right] v_0\lambda_0 \\
\approx\ & \frac{a^2}{2}\int_0^t M(t-t') A_0\lambda_0^2 t'^{1-\alpha} \exp\left[-\lambda_0 t'^{\frac{1-\alpha}{2}}\left(x - v_0 t'^{\frac{\alpha+1}{2}}\right)\right] dt' \\
&+ \frac{a^2}{2}\int_0^t M(t-t') c_0\kappa A_0\lambda_0^2 \int_{t'}^t t''^{1-\alpha} \exp\left[-\lambda_0 t''^{\frac{1-\alpha}{2}}\left(x - v_0 t''^{\frac{1+\alpha}{2}}\right)\right] dt'' dt' \\
&+ c_0\kappa A_0 \exp\left[-\lambda_0 t^{\frac{1-\alpha}{2}}\left(x - v_0 t^{\frac{\alpha+1}{2}}\right)\right] , \qquad (7.43)
\end{aligned}$$

with the kernel $\tilde{M}(u) = \frac{u\tilde{\psi}(u)}{1-\tilde{\psi}(u)}$ in Laplace domain. In the following we assume $\psi(t) \propto \tau^\alpha t^{-1-\alpha}$. For $z = x - v_0 t^{\frac{1+\alpha}{2}}$ and t large we finally get

$$\lambda_0 v_0 \exp\left[-\lambda_0 t^{\frac{1-\alpha}{2}} z\right] =$$
$$\exp\left[-\lambda_0 t^{\frac{1-\alpha}{2}} z\right]\left[\frac{a^2}{2\Gamma(\alpha)\Gamma(1-\alpha)\tau^\alpha}\left[B_{int}\lambda_0^2 + \frac{c_0\kappa\lambda_0}{v_0}[1-B_{int}]\right] + c_0\kappa\right] . \tag{7.44}$$

B_{int} is a constant that originates from the estimation of the involved integrals, see Appendix D, for which the Beta-function $B(\nu,\mu)$ represents an upper bound, $B(\alpha,2-\alpha) \geq B_{int} \geq 0$. This yields the dispersion relation for λ_0 and v_0:

$$0 = \lambda_0^2 + \frac{\frac{c_0\kappa K_\alpha^*}{v_0}[1-B_{int}] - v_0}{K_\alpha^* B_{int}}\lambda_0 + \frac{c_0\kappa}{K_\alpha^* B_{int}} \tag{7.45}$$

with $\frac{a^2}{2\Gamma(\alpha)\Gamma(1-\alpha)\tau^\alpha} = K_\alpha^* = \frac{K_\alpha}{\Gamma(\alpha)}$, where K_α is the generalized diffusion constant. From the possible solutions

$$\lambda_{0_{1,2}} = -\frac{\frac{c_0\kappa K_\alpha^*}{v_0}[1-B_{int}] - v_0}{2K_\alpha^* B_{int}} \pm \sqrt{\frac{\left(\frac{c_0\kappa K_\alpha^*}{v_0}[1-B_{int}] - v_0\right)^2}{4K_\alpha^{*2}B_{int}^2} - \frac{c_0\kappa}{K_\alpha^* B_{int}}} \tag{7.46}$$

and by requiring non-oscillatory behavior of the concentration we find the restriction

$$\left(\frac{c_0\kappa K_\alpha^*}{v_0}[1-B_{int}] - v_0\right)^2 \geq 4c_0\kappa K_\alpha^* B_{int} , \tag{7.47}$$

a quartic equation in v_0 which results in

$$v_0^2 = K_\alpha^* c_0\kappa\left[1 + B_{int} \pm 2\sqrt{B_{int}}\right] . \tag{7.48}$$

Note that in the normal case where $M(t) = \delta(t)/\tau$ we have $B_{int} = 1$, so that the well known marginal front velocity $v_{min} = \pm 2\sqrt{c_0 D\kappa}$ is reproduced; the other solution is a double one at $v = 0$ for which there is no front. Recall again that $B(\alpha,2-\alpha) \geq B_{int} \geq 0$, and $B(\alpha,2-\alpha) > 1$ for all $\alpha < 1$. Therefore Eq. (7.47) always has real roots. In particular, any B_{int} other than $B_{int} = 1$ there exists a bounded domain of real roots around zero, $|v_0| < v_1$, and another domain of real roots $|v_0| > v_2$ where $v_1 < v_2$, see Appendix D. Concluding by analogy to the classical FKPP case, the upper boundary v_2 of the gap for the velocity coefficient v_0 can be interpreted in favor of the existence of the propagating front. Of course, this analysis is by far not complete and still requires a proper stability analysis.

Although the integrals appearing in the calculations can only be estimated approximately, this analysis shows that there exists a set of (nonzero) parameters λ_0 and v_0 for which Ansatz (7.37) yields a solution to the linearized reaction subdiffusion equation (7.42). Therefore it is plausible that the asymptotic front behavior in the continuous regime features decreasing velocity and decreasing width, both going as $t^{(\alpha-1)/2}$. We note again that neither an ansatz taking a front

velocity going as $v(t) \propto t^{\alpha-1}$ nor an ansatz with $v(t) \propto t^{\frac{\alpha-1}{2}}$ and a constant front width yield an asymptotic solution of the linearized subdiffusive FKPP equation, and therefore one may draw the conclusion that such types of behavior are impossible within the continuous scheme.

7.7 Breakdown of the Continuous Description at Large Times

In the course of time the subdiffusive front is slowing down and especially becoming steeper, so that a transition to another regime takes place. This far asymptotic regime is fluctuation dominated, and hence lies out of scope of the continuous description. At the leading edge of the front the reaction-induced cutoff in the kernel of the full transport term does not play any role, due to the small concentration of A-particles. The far edge region of the front is therefore governed by reaction-subdiffusion equations with the integral kernel $M(t)$, which determines the mean density of steps per time. The mean density of steps of the particles becomes so small in the course of time that all B-particles present at the same site as an A particle will react before the next jump from the site takes place. The reaction rate dependence disappears, and the behavior of the front becomes the same as in the reaction on contact scenario. The front gets atomically sharp so that at large times the front propagation is governed by the first A-particle stepping out of the front.

Under these conditions the propagation velocity of the front is determined by the rate at which an A-particle leaves the front. In what follows we use an argument by [134, 135] which we adapt to our sequential updating scheme. The front position is considered as fixed by the rightmost A-particle(s). If there is only one A-particle at the front position, the next jump takes place either backwards or forwards by an amount a, both with probability $1/2$. The net displacement of the front is zero on average, so that the configurations with one A-particle at the front do not contribute to the average velocity. Otherwise, if there is more than one particle at the front position, a step forward will lead the front to move a distance a to the right, and a step of the front particle backwards will make the front stay where it was and the remaining particles define the front position. The probability for the front to make a step forward is on average $1/2$ for configurations with more than one particle at the front position. Such configurations have the probability ac_0, provided the concentration c_0 is thought of as a particle number per unit length. Altogether, the front moves on average by a distance $a^2c_0/2$. Since the rate at which the particles perform jumps is defined by the time-integral of the memory kernel M, the propagation velocity of the front is given by

$$v \approx \frac{a^2 c_0}{2} \int_0^t M(t-t')dt' \ . \tag{7.49}$$

Consider the generic waiting time pdfs with the asymptotic behavior $\psi(t) \propto \tau^\alpha t^{-1-\alpha}$. In Laplace domain we have $\tilde{\psi}(u) \simeq 1 - \Gamma(1-\alpha)\tau^\alpha u^\alpha$. The rate for a particle to jump is $\int_0^t M(t-t')dt'$ or in Laplace domain

$$\frac{\tilde{M}(u)}{u} = \frac{\tilde{\psi}(u)}{1-\tilde{\psi}(u)} \simeq \frac{1}{\tau^\alpha \Gamma(1-\alpha)} u^{-\alpha} \tag{7.50}$$

for $u \to 0$. The velocity in the Laplace domain yields

$$\mathcal{L}\{v(t)\} = \frac{c_0 a^2}{2} \frac{1}{\tau^\alpha \Gamma(1-\alpha)} u^{-\alpha} , \tag{7.51}$$

or in time domain

$$v(t) = \frac{a^2}{2\Gamma(1-\alpha)\tau^\alpha} \frac{c_0}{\Gamma(\alpha)} t^{\alpha-1} = K_\alpha \frac{c_0}{\Gamma(\alpha)} t^{\alpha-1} = c_0 K_\alpha^* t^{\alpha-1} . \tag{7.52}$$

With $\frac{1}{\Gamma(\alpha)\Gamma(1-\alpha)} = \frac{\sin(\alpha\pi)}{\pi}$ the front velocity can be expressed as

$$v(t) = \frac{a^2}{\tau^\alpha} \frac{c_0}{2} \frac{\sin(\alpha\pi)}{\pi} t^{\alpha-1} . \tag{7.53}$$

The position of the front is then

$$x(t) = \frac{N_A}{c_0} = \int_0^t v(t)dt = \frac{a^2}{2\tau^\alpha} \frac{\sin(\alpha\pi)}{\alpha\pi} c_0 t^\alpha , \tag{7.54}$$

and N_A is again the total amount of A-particles.
For the normal case with converging mean $\tilde{\psi}(u) \simeq 1 - \langle t \rangle u$, the front velocity $v_{fluct} = c_0 D$ of the normal fluctuation dominated regime is recovered, with D being the diffusion constant [126].

The values of the prefactor found from the simulations of the reaction–on–contact scenario under subdiffusion turned out to be however larger than the predicted ones in (7.54) by around $30 - 40\%$. In order to find out about the origin of this difference, simultaneous simulations of subdiffusion and of subdiffusion with randomized particles were performed. The latter version is pertinent to the situation when the particles lost their individual memory and were chosen at random to jump when a jumping time was reached. This variant of the reaction closely mimics the behavior of the front propagation described by Eq.(7.49). The derivation of (7.49) rests on the assumption that the rate at which steps of the rightmost A particle occur is equal to the mean jump rate of each of the particles at time t. Thereby we fully disregard the fact that the rightmost A is changing its identity, i.e. the particles takes turn to be the rightmost A.

Fig. 7.6 shows the time dependence of the overall amount of A-particles for $\alpha = 0.75$. The theoretical curve (7.54) lies much closer to the simulation results of subdiffusion with randomized particles than to the simulated data from subdiffusion without randomization. The remaining difference between the simulation of the randomized particles and the theoretical result is presumably due to the fact that convergence to the asymptotic behavior in subdiffusion is very slow. Apparently, the full subdiffusive picture implies an additional fluctuation effect. In order to exclude a fluctuation effect due to small concentrations that was detected by Warren et al. [134] under normal diffusion, we also simulated the normal case. The inset of the figure shows the situation for an exponential waiting time pdf with mean 1, where the simulated front behavior converges to the predicted behavior indicated by the black line, $N_A = D c_0^2 t$. Due to the sequential update in our simulations, this effect does not come into play here and our theoretical approach

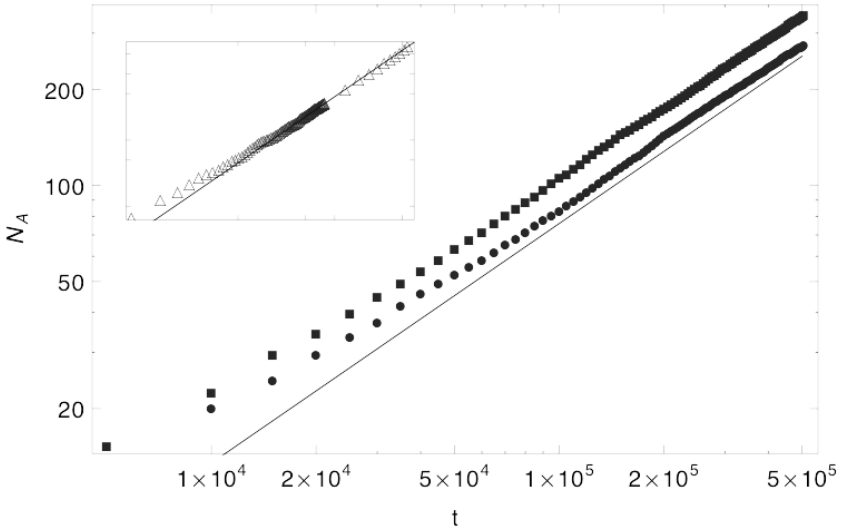

Figure 7.6: Time dependence of the total amount of A-particles N_A for the full subdiffusive case (squares) and subdiffusion with randomized particles (circles), $\alpha = 0.75$. The black line denotes the theoretical curve according to (7.54). The inset shows the situation for an exponential waiting time pdf (with mean 1), t goes from 10 to 5×10^4, N_A goes from 6 to 2000. The black line denotes again the theory, $N_A = Dc_0^2 t$; $c = 0.3$.

is sufficient to explain the front behavior in the normal case.

Fig. 7.7 shows the dependence of the total amount of A-particles on the total amount of steps performed for $\alpha = 0.75$. Comparing the two subdiffusive prescriptions (original and randomized) and normal diffusion reveals that the randomized version of subdiffusive front behavior is more akin to the normal diffusive front behavior than the full subdiffusive version. If the number of steps n is interpreted as the internal, operational time of the process, the randomized subdiffusive setting and the normal diffusive one have the same asymptotics, while the full original subdiffusive front position differs by a certain factor. Fig. 7.8 shows the quotient of the original subdiffusive front position and the randomized one for different values of α, which can be used to quantify this effect that turns out to be around at least $20-30\%$.

Obviously, the additional fluctuation effect of the front behavior is genuinely due to subdiffusion and cannot be explained within the mean-field description of the front behavior. Instead, it comes into play through the interaction of the particles at the front. The rate at which a particle at the front performs a jump is higher than the average jump rate of a single particle in the system. If the particle at the edge of the front is subject to a very long waiting time (which happens not often, but occasionally), other particles will outpace that particle and take the lead. The impact of the very long waiting times in the single particle dynamics on the front motion is hence considerably reduced.

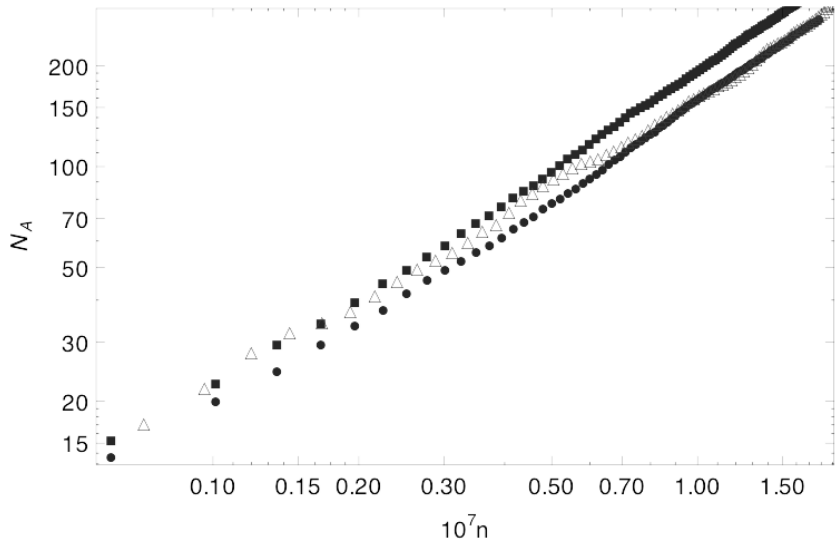

Figure 7.7: Total amount of A-particles N_A for the normal case (triangles), the subdiffusive case (squares) and subdiffusion with randomized jumps (circles), both $\alpha = 0.75$, depending on the total amount of performed steps; $c_0 = 0.3$.

7.8 Resumé

We discussed the propagation of the front in the irreversible autocatalytic reaction $A + B \to 2A$ under subdiffusion. The respective reaction–subdiffusion equations are based on a CTRWs picture where the reaction was assumed to be governed by the mass action law on a microscopic scale. The continuous description turned out to be valid at intermediate times, where the front velocity goes as $v \propto t^{\frac{\alpha-1}{2}}$. The decrease of the front velocity goes along with a decay of the width of the front. As a consequence, the front gets atomically sharp at large times and the continuous picture breaks down. Compared to the time scale at which the reaction takes place, the typical time scale of transport becomes very large in the course of time. Hence, at large times the front behavior is governed by fluctuations just as in the reaction on contact scenario. This regime is characterized by the front velocity $v \propto t^{\alpha-1}$ decaying faster than in the continuous regime, and additional fluctuation effects that are genuinely due to subdiffusion.

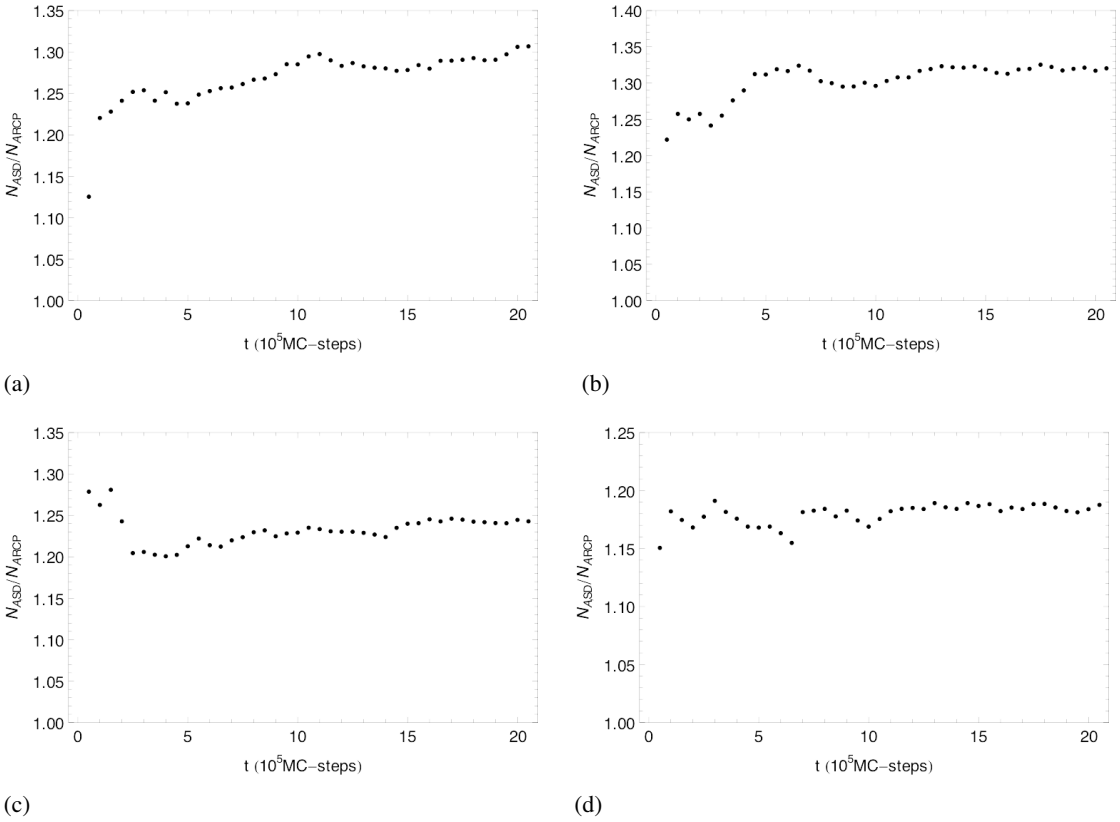

Figure 7.8: Quotient of the original subdiffusive front position and the randomized one $N_{A,SD}/N_{A,RCP}$ for a) $\alpha = 0.6$, (b) $\alpha = 0.7$, (c) $\alpha = 0.8$, (d) $\alpha = 0.9$; $c_0 = 0.3$.

8 The Stefan Problem under Subdiffusion

8.1 Motivation: Anomalously Slow Diffusion in Polyelectrolyte Multilayers

Polyelectrolytes are polymers that contain an electrolyte group in their repeating units. These electrolyte groups will be dissociated in aqueous solution so that the polymer is left with a charge which leads it to uncoil [136]. Polyelectrolyte multilayers are highly porous thin films that consist of oppositely charged molecular layers of polymers which can be assembled by consecutive adsorption, making use of the electrostatic attraction of the constituents [137, 138, 136].
A possible application are polyelectrolyte multilayer capsules in drug delivery, where it was shown that the release time of a drug can be prolonged considerably [139].
Recently, a closer investigation of the transport properties of polyelectrolyte multilayers was promoted by Donath et. al. [37]. The basic idea of their experiment is to assemble a multilayer with a fluorescent probe at a known location, as sketched in Fig. 8.1. The probe will be quenched irreversibly by a chemical reaction with the diffusing species. The resulting fluorescence decay was measured in a setup with a homogeneously distributed label.

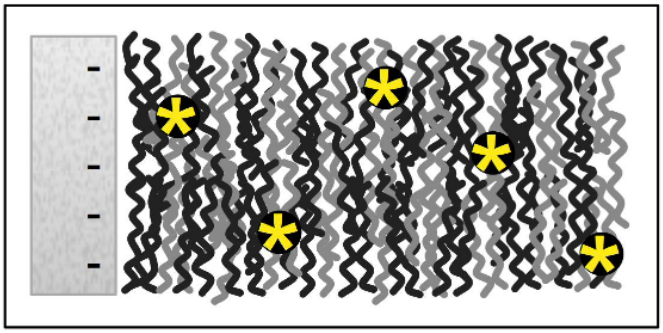

Figure 8.1: Sketch of a section of a polyelectrolyte multilayer with fluorescent marker. The block on the left denotes the negatively charged adsorbing surface, curly lines symbolize the polyelectrolytes; dark the positively charged ones and light grey the negatively charged ones. Stars depict the fluorescent label.

This experimental setup provides an elegant method to trace the transport of the reducing

agent and to measure the transport properties of the multilayer. The results have shown that a normal reaction- diffusion model did not even qualitatively comply with the experimental data. The preliminary experiments revealed a very slow decay of fluorescence. These results could not be described by means of a single (normal) diffusion process, but by a multitude of diffusion processes of different time scales. These facts raise the suspicion that the transport is anomalous. It is therefore desirable to develop a theoretical model for the specific experimental setup in order to be able to quantify the transport in as few parameters as possible. In the following we will propose a description of the retraction of the fluorescent label in terms of time-fractional diffusion, the subdiffusion parameter α being the only relevant parameter. The reducing agent and the fluorescent marker will be referred to as A and B, respectively.

Assume a volume (e.g. the positive half space) filled with a subdiffusive medium containing a homogeneous concentration $B(x, t = 0) = B_0$ of immobile species B. At the origin, referred to as the fixed boundary $x = 0$, another species A is introduced into the system. The concentration is kept constant at the boundary layer of the medium $A(x = 0, t) = A_0$, where A_0 is about as large as the initial homogeneous B-concentration, $A_0 \approx B_0$. The particles react according to the nonlinear reaction scheme $\mathrm{A} + \mathrm{B} \rightarrow (inert)$. In general, such subdiffusion equations involving nonlinear reactions cannot be solved analytically. In order to keep our model tractable, we need to make approximations. We know from the previous section that at large times reaction-subdiffusion approaches a behavior that can be described sufficiently by assuming $\kappa \rightarrow \infty$, provided that no particles are newly introduced in the vicinity of the reaction zone. Indeed, the experimental observations [37] also suggest that the reaction rate coefficient can be assumed to be very large compared to the time scales at which the transport takes place.

The assumption of reaction on contact still results in a nonlinear problem, but circumvents the appearance of concentration dependent transport terms in the equations since A and B are separated in space. As the A-particles (sub-) diffuse into the system and hit a B-particle, they react instantaneously. In this event-dominated regime, the progression of the domain that contains the A-particles, as well as the regression of the B-domain, is determined by the flux of A-particles at the free boundary that separates both domains. We fix the value of A-concentration at the free boundary so that $A(x = R(t)) = 0$.

This setting is similar to the problem of heat distribution in a 1d system that is initially filled e.g. with ice, and in which the free boundary, i.e. the surface of the ice is kept constantly at melting temperature. At the fixed boundary, there is a heat supply, maintaining a constant temperature larger than melting temperature. The melting of the ice leads to the propagation of the boundary between the liquid/solid domains. Such problems with moving boundaries between domains have been referred to as Stefan-Problems and were studied extensively for the normal diffusive case [38, 39].

8.2 The Stefan Problem: Normal Case

Let us first consider the Stefan problem under normal diffusion. Thereby we draw mostly upon the work by Meirmanov [39], which demonstrates a mathematically more rigorous analysis of the problem than presented here.

In the normal case, the above problem satisfies the diffusion equation in the domain $x \in [0, R(t)]$:

$$\frac{\partial A(x,t)}{\partial t} = D\frac{\partial^2 A(x,t)}{\partial x^2} \tag{8.1}$$

with

$$A(x=0,t) = A_0 \tag{8.2}$$

at the fixed boundary and

$$A(R(t),t) = 0 \tag{8.3}$$
$$\frac{\partial R(t)}{\partial t} = -D\frac{\partial A(R(t),t)}{\partial x} \tag{8.4}$$

at the free boundary. The latter condition emerges from mass conservation and reflects the fact that an infinitesimal movement ∂R of the free boundary is determined by the amount of particles crossing that boundary, $Jdt = dA$ at $x = R$, where J is the particle flux. Furthermore we have $R(0) = 0$.

The above problem can be solved by mapping it onto an initial-BVP with fixed boundaries. Therefore we introduce new variables:

$$\begin{aligned} \xi &= \frac{x}{R(t)} \\ \tau &= t\,, \end{aligned} \tag{8.5}$$

so that the function $A^*(\xi,\tau) = A(\xi R(\tau),\tau)$ is a solution of the following initial-BVP

$$\frac{\partial A^*(\xi,\tau)}{\partial \tau} - \frac{D}{R^2(\tau)}\frac{\partial^2 A^*(\xi,\tau)}{\partial \xi^2} = f \tag{8.6}$$
$$A^*(0,\tau) = A_0 \tag{8.7}$$
$$A^*(1,\tau) = 0 \tag{8.8}$$
$$A^*(\xi,0) = A(\xi R(\tau=0),\tau=0)\,, \tag{8.9}$$

with $R(\tau = 0) = x_0$ where $x_0 = 0$ is the initial position of the free boundary, and

$$f = -\frac{D\xi}{R^2(\tau)} \frac{\partial A^*(1,\tau)}{\partial \xi} \frac{\partial A^*(\xi,\tau)}{\partial \xi} .$$

This equation with the respective initial and boundary conditions constitutes a nonlinear initial-BVP. Hence, special solutions cannot be constructed by superposition, but must be determined directly.

Clearly, we find from expressing the flux-condition at the free boundary (8.4) in new variables and subsequent integration:

$$R(t) = \left(R(t=0)^2 - 2D \int_0^t \frac{\partial A^*(1,\tau)}{\partial \xi} d\tau \right)^{1/2} . \tag{8.10}$$

This expression and the equation together with initial- and boundary-conditions (8.6–8.9) for $A^*(x/R(t),t) = A(x,t)$, are amenable to determine the temporal behavior of the position of the free boundary as well as the profile of the A-particles numerically.

8.3 Asymptotic Behavior in the Normal Case

The Stefan problem does in general not allow for an analytic solution. However, it is possible to obtain analytic expressions for the asymptotics, indicated by subscript ∞ in the following. In this section we study the asymptotic behavior of the solution to the problem (8.1–8.4), following [39]. Knowing the scaling of the solutions of (8.1), we assume a new variable $\xi = \frac{x}{t^{1/2}}$. Then, we have

$$R_\infty(t) = C_\infty(A_0) t^{1/2} , \tag{8.11}$$
$$A_\infty(x,t) = A^*_\infty(xt^{-1/2}, A_0) , \tag{8.12}$$

where the constant $C_\infty(A_0)$ depends continuously on the concentration at the fixed boundary A_0, and $\lim_{A_0 \to 0} C_\infty(A_0) = 0$.
The diffusion equation (8.1) and the boundary conditions yield:

$$D \frac{\partial^2 A^*_\infty(\xi, A_0)}{\partial \xi^2} + \frac{\xi}{2} \frac{\partial A^*_\infty(\xi, A_0)}{\partial \xi} = 0 , \tag{8.13}$$
$$A^*_\infty(0, A_0) = A_0 , \tag{8.14}$$
$$A^*_\infty(C_\infty, A_0) = 0 , \tag{8.15}$$
$$D \frac{\partial A^*_\infty(C_\infty, A_0)}{\partial \xi} = -\frac{1}{2} C_\infty . \tag{8.16}$$

with $\xi \in (0, C_\infty)$. Clearly, for all the boundary conditions to be fulfilled at the same time, C_∞ must be chosen appropriately. For example, we have for (8.13-8.15)

$$A^*_\infty(\xi, A_0) = A_0 \left(1 - \frac{\mathrm{erf}\left[\frac{\xi}{2\sqrt{D}}\right]}{\mathrm{erf}\left[\frac{C_\infty}{2\sqrt{D}}\right]} \right), \tag{8.17}$$

and for (8.13), (8.14), (8.16)

$$A^*_\infty(\xi, A_0) = A_0 - \frac{1}{2} C_\infty \sqrt{\pi D} \exp\left[\frac{C_\infty^2}{4D}\right] \mathrm{erf}\left[\frac{\xi}{2\sqrt{D}}\right], \tag{8.18}$$

which are equal for

$$\frac{C_\infty}{2} \sqrt{\pi D} \exp\left[\frac{C_\infty^2}{4D}\right] \mathrm{erf}\left[\frac{C_\infty}{2\sqrt{D}}\right] - A_0 = 0, \tag{8.19}$$

determining C_∞.

8.4 The Subdiffusive Stefan Problem: An Estimation

Let us first reformulate the problem for the anomalous case. In the domain $x \in [0, R(t)]$, the equation

$$\frac{\partial A(x,t)}{\partial t} = K_{\alpha 0} \mathrm{D}_t^{1-\alpha} \frac{\partial^2 A(x,t)}{\partial x^2} \tag{8.20}$$

must hold.K_α is a generalized diffusion constant. For the flux and concentration at $x = R(t)$ and the concentration at $x = 0$ we have

$$K_{\alpha 0} \mathrm{D}_t^{1-\alpha} \frac{\partial A(R(t),t)}{\partial x} = -\frac{\partial R(t)}{\partial t} \tag{8.21}$$

$$A(R(t),t) = 0 \tag{8.22}$$

$$A(0,t) = A_0 \,. \tag{8.23}$$

Here, neither the anomalous Stefan-condition (8.21) nor the Subdiffusion Equation (8.20) can be cast into a concise form equivalent to (8.10) or (8.9), respectively, since the chain rule for the fractional Riemann-Liouville differ-integration implies an infinite series of integer order differentiations, cf. section 2.2. Nevertheless we can estimate the asymptotic velocity of the moving boundary, on the basis of the approach discussed in the preceding section. If we do so, the mapping of the problem onto a BVP with fixed boundaries should result in a time independent

expression. Let us thus introduce a new variable, $\xi = \frac{x}{t^{\alpha/2}}$, and reformulate our problem with respect to this variable $A(x,t) \to A^*(\xi, A_0)$. The choice of this variable is reasonable because we already know the scaling of the solutions of the subdiffusion equation, and the asymptotic solution we are looking for should only depend on t through ξ.

First, we rewrite the Stefan-condition at the free boundary R, assuming A^*_∞ to be analytic in ξ at least at the left hand side of the free boundary R.

$$\begin{aligned} -\frac{\partial R(t)}{\partial t} &= K_{\alpha 0}\mathrm{D}_t^{1-\alpha}\left[\frac{\partial \xi}{\partial x}\frac{\partial A^*_\infty(\xi, A_0)}{\partial \xi}\right]_R \\ &= K_{\alpha 0}\mathrm{D}_t^{1-\alpha}\left[\frac{\partial \xi}{\partial x}\sum_{i=1}^{\infty}\frac{1}{(i-1)!}\frac{\partial^{(i)} A^*_\infty(\xi_R, A_0)}{\partial \xi^i}(\xi-\xi_R)^{i-1}\right]_R \\ &= K_{\alpha 0}\mathrm{D}_t^{1-\alpha}\left[t^{-\frac{\alpha}{2}}\sum_{i=1}^{\infty}\frac{1}{(i-1)!}\frac{\partial^{(i)} A^*_\infty(\xi_R, A_0)}{\partial \xi^i}\left(\frac{x-R(t)}{t^{\alpha/2}}\right)^{i-1}\right], \end{aligned} \tag{8.24}$$

which for $t \to \infty$ results in

$$\frac{\partial R(t)}{\partial t} = K_\alpha \left.\frac{\partial A^*_\infty(\xi, A_0)}{\partial \xi}\right|_R \frac{\Gamma(1-\alpha/2)}{\Gamma(\alpha/2)} t^{-1+\alpha/2}, \tag{8.25}$$

or, if $R(0) = x_0 = 0$,

$$R(t) = K_\alpha \left.\frac{\partial A^*_\infty(\xi)}{\partial \xi}\right|_R \frac{\Gamma(1-\alpha/2)}{\Gamma(1+\alpha/2)} t^{\alpha/2}. \tag{8.26}$$

All the other elements of the series yield negative powers of the time t in $R(t)$ and hence vanish as $t \to \infty$. Here we made use of the Tauberian Theorems and performed the fractional differentiation in Laplace domain, see Appendix E for details. Note that, for $\alpha = 1$ and with $A^*_\infty(\xi_R) = A^*_\infty(C_\infty, A_0)$, the resultant relation for the moving boundary in the normal case, (8.16), is reproduced. We know that $\left.\frac{\partial A^*_\infty(\xi_R)}{\partial \xi}\right|_R < 0$, since $A^*_\infty(\xi_R) = 0$ and $A^*_\infty(\xi) \geq 0$.
So far we have seen that the Stefan condition in the subdiffusive case (8.24) is met if the boundary moves as $R(t) \propto t^{\frac{\alpha}{2}}$ for t large. For tackling the subdiffusion equation (8.20), we first calculate

$$\frac{\partial^2 A(x,t)}{\partial x^2} = \frac{1}{t^\alpha}\frac{\partial^2 A^*_\infty(\xi, A_0)}{\partial \xi^2},$$

$$\begin{aligned}\frac{\partial A(x,t)}{\partial t} &= -\frac{\alpha}{2}\frac{1}{t^{\alpha/2+1}}x\frac{\partial A^*_\infty(\xi,A_0)}{\partial \xi} \\ &= -\frac{\alpha}{2t}\xi\frac{\partial A^*_\infty(\xi,A_0)}{\partial \xi}\ .\end{aligned}$$

Again we assume $A^*_\infty(\xi)$ to be analytic and let the Riemann-Liouville fractional derivative act upon the corresponding series expression for the second spatial derivative:

$$\begin{aligned}& {}_0\mathrm{D}_t^{1-\alpha}\left[\frac{1}{t^\alpha}\frac{\partial^2 A^*_\infty(\xi_0,A_0)}{\partial \xi^2}\right] \\ =\ & {}_0\mathrm{D}_t^{1-\alpha}\left[\frac{1}{t^\alpha}\sum_{i=2}^{\infty}\frac{1}{(i-2)!}\frac{\partial^{(i)} A^*_\infty(\xi_0,A_0)}{\partial \xi^{(i)}}(\xi-\xi_0)^{i-2}\right] && (8.27)\\ =\ & {}_0\mathrm{D}_t^{1-\alpha}\left[\sum_{i=2}^{\infty}\frac{1}{(i-2)!}\frac{\partial^{(i)} A^*_\infty(\xi_0,A_0)}{\partial \xi^{(i)}}(x-x_0)^{i-2}t^{-(i-2)\alpha/2-\alpha}\right] && (8.28)\\ =\ & \sum_{i=2}^{\infty}\frac{1}{(i-2)!}\frac{\partial^{(i)} A^*_\infty(\xi_0,A_0)}{\partial \xi^{(i)}}\frac{\Gamma(1-(i-2)\alpha/2-\alpha)}{\Gamma(-(i-2)\alpha/2)}t^{-1}(\xi-\xi_0)^{i-2} && (8.29)\\ & && (8.30)\end{aligned}$$

so that, after multiplying t, (8.20) takes on a form

$$0 = \hat{O}\left[\frac{\partial A^{*2}_\infty(\xi,A_0)}{\partial \xi^2}\right]+\frac{\alpha}{2}\xi\frac{\partial A^*_\infty(\xi,A_0)}{\partial \xi}\ , \tag{8.31}$$

where the linear operator $\hat{O}$ acts upon the series expansion of a function in the following way (details see Appendix E):

$$\begin{aligned}K_\alpha\hat{O}\sum_{i=0}^{\infty}c_i(\xi-\xi_0)^i &= \sum_{i=0}^{\infty}c_i^*(\xi-\xi_0)^i \\ c_i^* &= \frac{\Gamma(1-i\alpha/2-\alpha)}{\Gamma(-i\alpha/2)}c_i \qquad (8.32)\end{aligned}$$

We note that for the limiting case $\alpha = 1$, the operator $\hat{O}$ becomes the identity operator, so that (8.31) becomes the corresponding expression for the normal case, cp. (8.13). The expressions (8.31), (8.32) depend on t only through ξ and, together with (8.26) and the boundary conditions $A^*_\infty(0,A_0) = A_0$, $A^*_\infty(\xi_R,A_0) = 0$, provide all information needed to solve the anomalous moving boundary problem numerically for the asymptotic profile of $A^*_\infty(\frac{x}{t^{\alpha/2}},A_0)$ and the behavior of the

free boundary $R(t)$.

We have shown that the mapping of the problem onto a finite interval is possible and leads to an asymptotically time independent solution in the new variables.
However, the argumentation presented lacks mathematical rigor, in particular concerning proofs of existence and uniqueness of solutions to the system (8.31, 8.26) and boundary conditions. At this point, we conjecture existence and uniqueness. Moreover, the next section will show by simple reasoning that the solution to the anomalous Stefan problem must exist and be unique, since it emerges from subordination of the (existing and unique) solution to the normal Stefan problem.

8.5 Asymptotic Behavior in the Anomalous Case

The asymptotic solution of the anomalous Stefan problem (8.20–8.23) was proven to scale as $\frac{x}{t^{\alpha/2}}$ in the preceding section, where we established an approach analogous to that used in normal diffusion by mapping the interval $(0, R(t))$ onto a fixed domain. The system (8.20-8.23) is subordinated to the normal analogue (8.1-8.4). Recall that subordination $\mathcal{T}_\alpha$ takes on an especially simple form in Laplace domain,

$$\mathcal{T}_\alpha\left\{\tilde{F}(u)\right\} = \frac{1}{u^{1-\alpha}}\tilde{F}(u^\alpha)\,. \tag{8.33}$$

A different way to obtain an asymptotic solution is hence to solve the normal analogue to the anomalous Stefan problem and perform the corresponding integral transform, i.e. subordination, afterwards. Let us first Laplace–transform the expressions for the solution, (8.17), (8.18)

$$\tilde{A}^*_\infty(x,u) = \frac{A_0}{u\mathrm{erf}\left[\frac{C_\infty}{2\sqrt{D}}\right]}\left[\mathrm{erf}\left[\frac{C_\infty}{2\sqrt{D}}\right] - \left(1-\exp\left[-\sqrt{\frac{u}{D}}|x|\right]\right)\right]\,, \tag{8.34}$$

and for (8.13), (8.14), (8.16)

$$\tilde{A}^*_\infty(x,u) = \frac{A_0}{u} - \frac{1}{2u}C_\infty\sqrt{\pi D}\exp\left[\frac{C_\infty^2}{4D}\right]\left(1-\exp\left[-\sqrt{\frac{u}{D}}|x|\right]\right)\,. \tag{8.35}$$

Performing Subordination, we obtain the solution to the anomalous Stefan problem in Laplace domain where the constant C_∞ is the same as in the normal case:

$$\tilde{A}^*_\infty(x,u) = \frac{A_0}{u\mathrm{erf}\left[\frac{C_\infty}{2\sqrt{D}}\right]}\left[\mathrm{erf}\left[\frac{C_\infty}{2\sqrt{D}}\right] - \left(1-\exp\left[-\sqrt{\frac{u^\alpha}{D}}|x|\right]\right)\right]\,, \tag{8.36}$$

$$\tilde{A}^*_\infty(x,u) = \frac{A_0}{u} - \frac{1}{2u} C_\infty \sqrt{\pi D} \exp\left[\frac{C_\infty^2}{4D}\right]\left(1 - \exp\left[-\sqrt{\frac{u^\alpha}{D}}|x|\right]\right) . \tag{8.37}$$

For the sake of completeness, we transform the expression for the free boundary in the normal case,

$$u\tilde{R}(u) = \frac{C_\infty}{2}\frac{\Gamma(1/2)}{u^{1/2}} , \tag{8.38}$$

apply the transform for subordination,

$$\frac{u^\alpha \tilde{R}(u^\alpha)}{u^{1-\alpha}} = C_\infty \frac{\Gamma(3/2)}{u^{1-\alpha/2}} \tag{8.39}$$

$$\frac{\tilde{R}(u^\alpha)}{u^{1-\alpha}} = C_\infty \frac{\Gamma(3/2)}{u^{1+\alpha/2}} , \tag{8.40}$$

so that for the anomalous free boundary the asymptotic behavior at large times is found to be

$$\frac{dR(t)}{dt} = C_\infty \frac{\Gamma(3/2)}{\Gamma(\alpha/2)} t^{\alpha/2-1} \tag{8.41}$$

$$R(t) = C_\infty \frac{\Gamma(3/2)}{\Gamma(1+\alpha/2)} t^{\alpha/2} . \tag{8.42}$$

We find the same expression by transforming the expression (8.11) for $R(t)$ in the normal case directly.
Note that the general solution to the anomalous Stefan problem is of course subordinated to its normal analogue (8.6–8.10) as well, but due to the non-linear character of the problem it is not possible to find a general analytic expression for the solution or its Laplace Transform. Hence, the subordination must be performed in original domain once the solution to the normal Problem is found numerically. There, we cannot establish relationships between the constants in the normal and anomalous case.

8.6 Simulations

In order to check the above findings, simulations on the subdiffusive Stefan problem were made. All simulations pertaining this section were carried out by Michael Borinsky. The basic method was similar to that already used in the section on the subdiffusive FKPP problem, with the difference that this time particles were permanently introduced into the system: A one dimensional lattice with lattice constant $a = 1$ and a constant concentration c_0 of immobile particles was prepared. At the leftmost site $A(0)$, mobile A-particles were introduced into the system such that

in average their constant concentration $A(0,t) = c_0$ was maintained. Whenever a particle was introduced, the respective jumping times were calculated according to the waiting time pdf (7.24) and sorted with the jumping times of the other particles, always keeping the information of the particle's identity. When an A–particle hit a site where B– particles were present, the respective A–particle and a B–particle were removed from that site. All data were averaged over 100 runs.

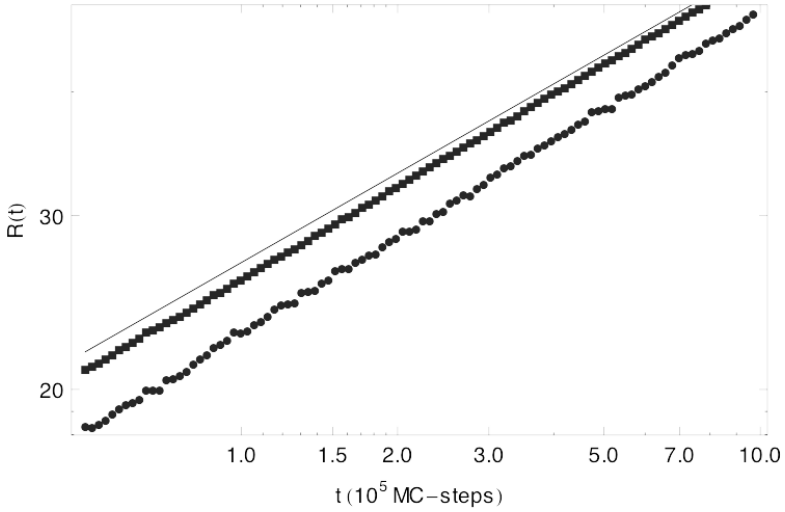

Figure 8.2: Simulational results for the position of the moving boundary with $\alpha = 0.6$; $K_\alpha = 1/(2\Gamma(1-\alpha))$, $c_0 = 10$. Circles denote the position of the rightmost A–particle, squares the leftmost B–particle, and the full line a guide for the eye, indicating the slope for the theoretical exponent $\alpha/2$.

Figs. 8.2, 8.3 and 8.4 show the position of the rightmost A and the leftmost B particles for different values of α. The position of the leftmost B particle is less prone to fluctuations and therefore better suited as a measure for the position of the moving boundary $R(t) \propto t^\beta$. Note that the convergence of the asymptotic exponent β of the position of the leftmost B and the rightmost A with respect to the theoretically predicted one obtained from (8.42) differs with α. For larger α, the simulations tend to converge to the theoretical power exponent $\alpha/2$ of the position of the moving boundary from below, the slope in the double–logarithmic plot slightly increases. On the contrary, for smaller α the data approach the theoretical asymptotic exponent from above, indicated by a slightly decreasing slope in the double–logarithmic data plots.

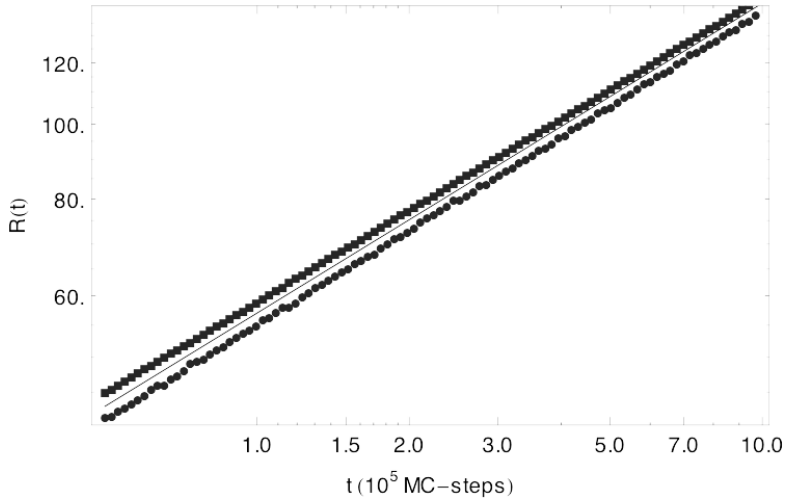

Figure 8.3: Simulated position of the moving boundary for $\alpha = 0.8$. $K_\alpha = 1/(2\Gamma(1-\alpha))$, $c_0 = 10$. Circles denote the position of the rightmost A–particle, squares the leftmost B–particle. Again, the full line indicates the slope for the theoretical exponent $\alpha/2$.

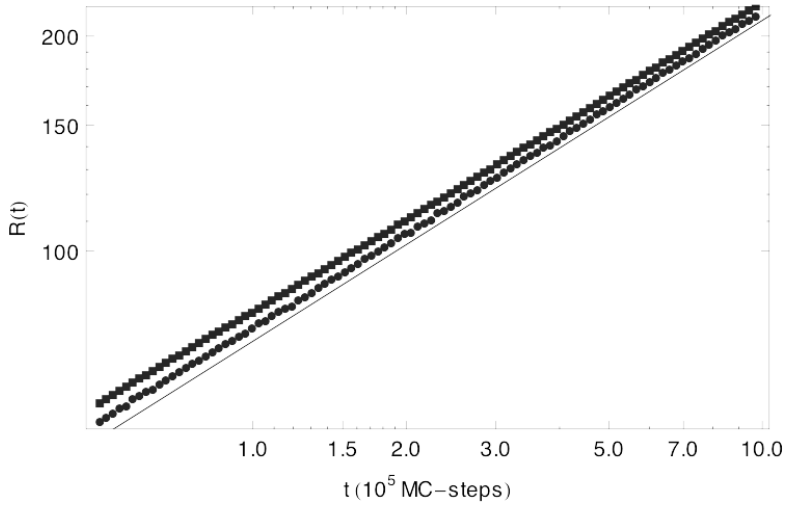

Figure 8.4: Simulational results for the moving boundary position, $\alpha = 0.9$. $K_\alpha = 1/(2\Gamma(1-\alpha))$, $c_0 = 10$; the circles denote the position of the rightmost A–particle, squares the position of the leftmost B–particle. The full line represents the slope for the theoretical exponent $\alpha/2$.

Fig. 8.5 depicts the fitted power exponents β of the moving boundary position obtained from the positions of the leftmost B particle for many different α. Data for small times that had not yet converged sufficiently to a power law were discarded and not used in fitting procedure. The respective fits for the exponents are given in Table 8.1.

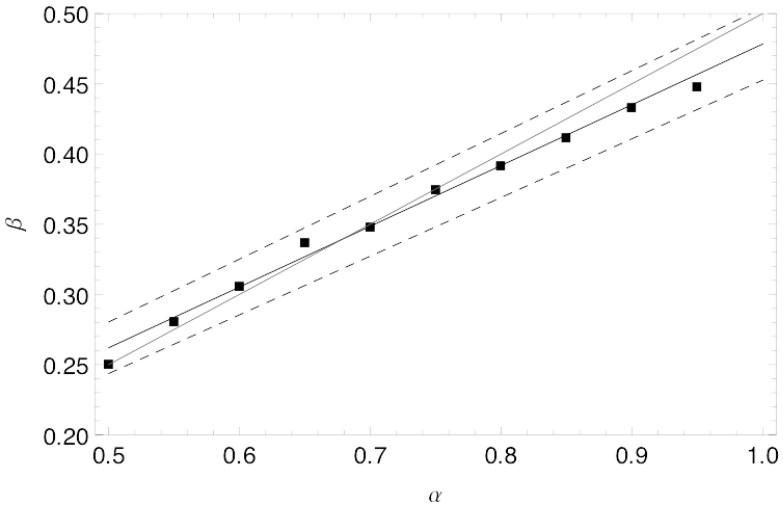

Figure 8.5: Fitted power exponent β of the moving boundary position. The data were obtained by regarding the leftmost B particle as the position of the boundary. The black solid line shows the fit, the dashed lines the error bounds of the fit. The grey solid line denotes the theoretically predicted behavior $\beta \propto \alpha/2$.

α	0.5	0.55	0.6	0.65	0.7
β	0.25 ± 0.01	0.28 ± 0.01	0.31 ± 0.01	0.34 ± 0.01	0.35 ± 0.01
α	0.75	0.8	0.85	0.9	0.95
β	0.38 ± 0.01	0.39 ± 0.01	0.41 ± 0.01	0.43 ± 0.01	0.45 ± 0.01

Table 8.1: Exponents for the fit $R(t) \propto t^{\beta}$ for different α.

The theoretical predictions of an exponent $\alpha/2$ lie well within the error bounds of the fitted linear model, $\beta = (0.05 \pm 0.02) + (0.44 \pm 0.04)\alpha$. The linear fit of the exponents obtained from the simulations β against the subdiffusion parameter α is systematically slightly tilted with respect to the theoretical line given by $\beta = \alpha/2$. This is due to the fact that the convergence is very slow. As already stated above, the asymptotic value of the power exponent appears to be reached from below for larger α and from above for smaller α. Therefore one would expect that the deviations from the theoretical predictions reduce for much larger simulation times.

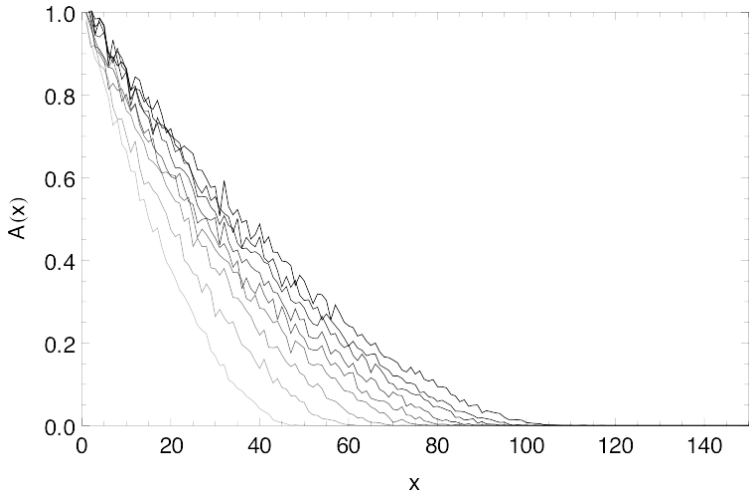

Figure 8.6: A–particle profiles, $\alpha = 0.7725$, $K_\alpha = 1/(2\Gamma(1-\alpha))$, $c_0 = 10$; $t = 1.03 \cdot 10^5$, $2.04 \cdot 10^5$, $3.02 \cdot 10^5$, $4.07 \cdot 10^5$, $5.02 \cdot 10^5$, $6.01 \cdot 10^5$, $7.19 \cdot 10^5$, $8.11 \cdot 10^5$, $9.70 \cdot 10^5$ (from light grey to black).

The simulational results for the A–particle profiles for $\alpha = 0.725$ at different times are presented in Fig. 8.6. Note that the fixed boundary value of A is still $c_0 = 10$, so that a unit of A corresponds to 10 particles.
Fig. 8.7 depicts the same data as Fig. 8.6, but this time mapped onto the interval $[0,1]$. Each of the curves was rescaled such that the rightmost A–particle lies on the right boundary $\xi = 1$. In this frame, the profiles for the different times coincide roughly. The fluctuations between the different profiles are about as large as those within each individual profile. One may therefore assume that the asymptotics, where the profiles in the transformed frame ξ are constant in time, is reached for the times under study. From these profiles, the curve for $t = 9.70 \cdot 10^5$ is taken as an exemplary one and compared to theory in Fig. 8.8.
The exemplary profile is shown together with the theoretical curve for the asymptotic shape and the asymptotic shape of the corresponding normal diffusive Stefan problem with the adapted diffusion constant $D = K_\alpha$. The theoretical curve was obtained by a series expansion of Eq. (8.37), term–by–term Laplace inversion and subsequent substitution $x/t^{\alpha/2} = C_\infty \Gamma(3/2)/\Gamma(1+\alpha/2)\xi$. The theoretical asymptotic profile for the for the subdiffusive case is almost congruent to the respective profile for normal diffusion. Deviations of the normal curve may be due to the fact that the underlying series expansion around $\xi = 0$ for the subdiffusive case converges only slowly, observe that at $\xi = 1$ the concentration has not yet reached the prescribed value $A(R) = 0$. The simulations show qualitativley the same behavior as the theoretical predictions. However, the profiles $A(\xi)$ appear to be lower than predicted. The position of the moving boundary is systematically overestimated when the rightmost A–particle is taken as its definition.

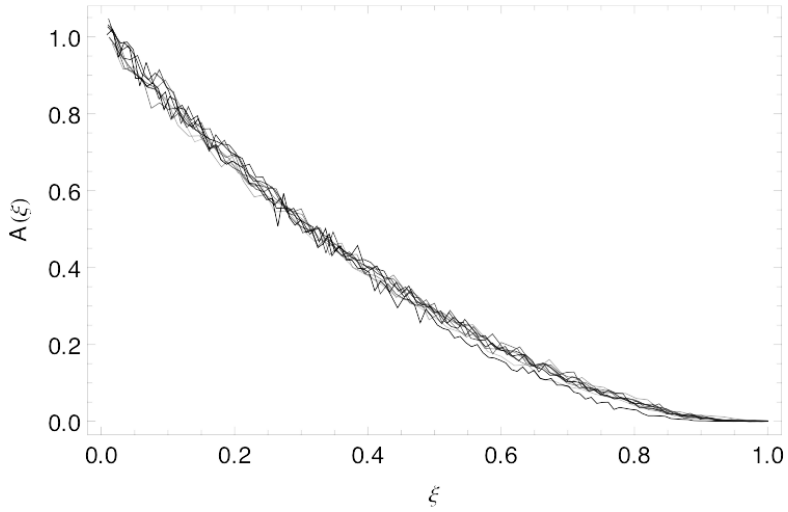

Figure 8.7: A–particle profile under reaction-subdiffusion in the transformed frame ξ, same parameters and times as in Fig. 8.6.

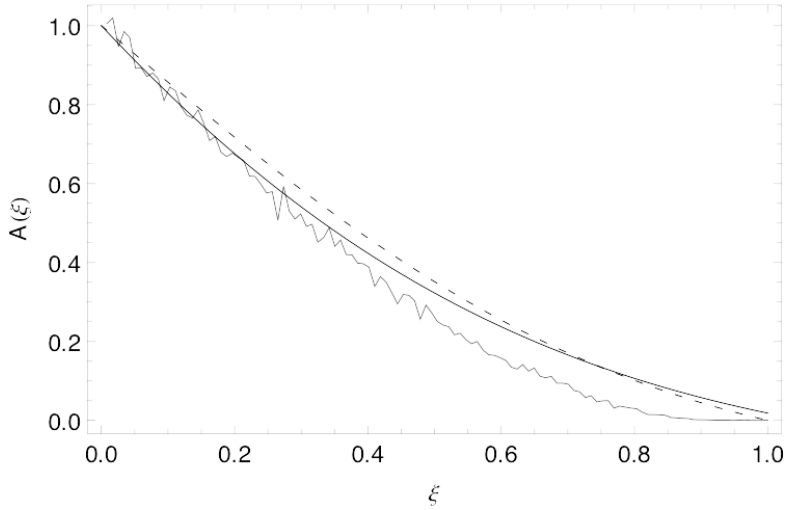

Figure 8.8: A–particle profile under reaction-subdiffusion in the transformed frame, theoretical prediction for subdiffusion (full black line) with $\alpha = 0.725$, simulational result at $t = 9.70 \cdot 10^5$ (full grey line), theoretical profile for normal diffusion (dashed line); $K_\alpha = 1/(2\Gamma(1-\alpha))$, $c = 10$.

8.7 Resumé

We suggested the Stefan problem under anomalous diffusion as a model for the diffusion of a mobile reactant A into a polyelectrolyte multilayer containing a constant concentration of immobile reactants B. In particular we assumed that the reaction takes place instantaneously when an A encounters a B particle. Moreover, the A–concentration in the boundary layer of the medium was assumed to be constant in time, a condition that must not necessarily hold in experimental setups. The model itself is consistent, the theoretical predictions of the moving boundary position were corroborated by the numerical simulations. The propagation of the moving boundary between the A– and B–domain was found to go as $R(t) \propto t^{\alpha/2}$. Since in the specific setting under consideration the B particles do not play a role in the mathematical description, we were able to predict the asymptotic profiles of A–particles by using subordination of the asymptotic solutions to the normal diffusive analogue of the system.

A comparison with experiments is still lacking. Only extensive experimental studies can disclose whether the subdiffusive Stefan problem considered above provides a good model for the specific setup of a quencher diffusing into a polyelectrolyte multilayer.

9 Conclusion

In this work, subdiffusion of particles in conjunction with chemical reaction has been studied. The subdiffusive motion was modelled by means of continuous–time random walks on a mesoscopic scale with a heavy–tailed waiting time pdf lacking the first moment. The reaction itself was assumed to take place on a microscopic scale, obeying the classical mass action law. This situation corresponds to that in a porous medium where the particles are trapped within the catchments and pores, but are still able to react during their waiting times. In the preparatory work involving partial time–fractional differential equations, the introduction of source terms was discussed, which entails the interpretation of the lower terminal of the Riemann–Liouville fractional derivative as the time of the preparation of the system. Laplace– and image methods of solution were found to lead to equivalent results, although both methods presume different "ages" of the involved particles. This fact can be explained on the stochastic level by the independence of subsequent jumps of the particles. Though having a long ranged memory, the process is only semi–Markovian. The obtained solutions especially to the Dirichlet BVP could be made further use of in the case of degrading particles.

In reaction–subdiffusion, the transport is generally affected by reaction, so that the resultant integro–differential equations are no fractional equations anymore.
For linear reaction–subdiffusion, an alternative derivation of the already known equations was given. In the case of linear reaction kinetics, the kernel of the transport term is dependent on the rate coefficents, but independent of the particle concentration which results in a system of linear integro-differential equations describing the situation. For the simplest linear reaction, the degradation $A \to 0$, a general expression for the solution to arbitrary Dirichlet Boundary Value Problems was derived. It turned out that, just as is the case under normal diffusion, the solution can be expressed in terms of the solution to the corresponding Dirichlet Problem under mere subdiffusion, i.e. without degradation. For this treatment of the reaction-subdiffusion equation with degradation the exponential cutoff of the transport kernel due to reaction is crucial. The resultant stationary profiles obtain a specifically simple form that does not differ qualitatively from the stationary profiles in normal reaction diffusion. These results differ from those obtained by Hornung et al. [112] who developed a different CTRW model for degradation under subdiffusion that allowed for degradation of a particle only after a jump was performed and exhibited no stationary profiles. The existence of stationary profiles in reaction–subdiffusion is distinct to models where the reactions take place per unit time rather than per amount of performed steps. Stationary profiles for reaction–subdiffusion with locally classical rates were also found in an earlier work [114], for the nonlinear reaction $A + B \to 0$ on a bounded domain.

In contrast to linear reaction kinetics, there is no unified representation for general nonlinear reaction–subdiffusion under classical rate kinetics. The respective survival– and transformation probabilities that account for an additional factor in the memory kernel are determined by a nonlinear system of reaction rate equations. Closed equations that were put up earlier [34,

109] and were claimed to represent reaction–subiffusion with arbitrary nonlinear classical rate kinetics do not imply the mutual conditionality of appearance/ vanishing of the different species. Thus, there is often no other choice than to put up equations via the CTRW approach adapted to the specific problem under study, making use of the conservation laws that account for the interdependencies between the different species concentrations. Special care has to be taken with respect to the treatment of the waiting times of the generated particles. Under conversion, a particle can either keep its waiting time so that only a re–labelling takes place, or it can be assigned a new waiting time that begins at the moment the particle is generated, which may have crucial effects on the qualitative dynamics.

As an example for a nonlinear reaction–subdiffusion system, the CTRW approach was applied to the irreversible autocatalytic reaction $\mathrm{A}+\mathrm{B} \rightarrow 2\mathrm{A}$ under subdiffusion. This reaction represents the simplest one that, under certain conditions, may develop moving fronts between domains occupied by the different species. Under the assumptions of a spatially and temporally constant overall particle concentration $A(x,t)+B(x,t) = \text{const}$ and re–labelling of the converted particles, a subdiffusive analogue of the classical FKPP equation was derived. The normal diffusive FKPP equation is known to exhibit travelling wave solutions for sufficiently steep initial conditions. There exists a minimal constant velocity that will be attained asymptotically at large times. The challenge of this part of the work was therefore to find the asymptotic front behavior in the subdiffusive case. For that purpose, the method of leading edge linearization was adopted, an approach that works well for the class of the so–called pulled fronts. This method has the advantage that a linearization about the instable state $A(z) = 0$ in a comoving frame z makes us get rid of the reaction dependence in the transport term. However, the specification of the comoving frame requires a presupposition on the asymptotic front behavior. Therefore, in a first attempt to find the asymptotic front behavior, a front with a constant shape and (yet unknown) constant velocity was assumed, in analogy to the situation under normal diffusion. It turned out that under these conditions, a minimal front velocity does not exist, which was interpreted as propagation arrest.

In order to gain insight on how exactly this arrest takes place, Monte–Carlo simulations of the underlying CTRW were performed. Indeed, the resultant fronts exhibited a decay in velocity. Moreover, two different regimes were detected, one corresponding to large particle concentrations and small reaction rates, and a fluctuation dominated one corresponding either to reaction on first contact or to small particle concentrations and large reaction rates. The first regime was characterized by a front velocity decaying as $v \propto t^{\frac{\alpha-1}{2}}$, the latter by $v \propto t^{\alpha-1}$, α being the subdiffusion parameter. These results together with the knowledge of the respective asymptotic front behavior in both regimes led us to consult a crossover argument, which conformed with the simulational findings on the front velocities. In addition, a decay in the width of the front was predicted for the continuous regime. This decay in width was not found in the simulations, which was probably due to numerical artefacts.

This knowledge enabled us to study both regimes in more detail. In order to investigate the continuous regime, the leading edge linearization procedure was carried out anew, this time with a comoving frame that conformed with the findings from the simulations and the predictions of the crossover argument, i.e. a decelerating and contracting frame. These assumptions led to a reasonable analogue of the dispersion relation in the normal case, establishing a relationship between the constant prefactors of the time dependent width and velocity of the front. This

fact was interpreted such that the previously derived linearized subdiffusive FKPP equation is a suitable candidate for the description of the continuous regime where the velocity and the width decay as $t^{\frac{\alpha-1}{2}}$. However, a mathematically rigorous stability analysis is still lacking, so that our findings may provide starting points for mathematicians to investigate the field of front propagation under subdiffusion more thoroughly. A first step in this direction was taken by Nec et al. [36]. It has to be noted that the assumption of decaying velocity, but constant width of the front did not lead to consistent results.

The decay of the width of the front has implications on the large time behavior of the front: With longer times the front gets atomically sharp since the typical time scale of transport becomes very large compared to the typical time scale of reaction. This situation corresponds effectively to the reaction on contact scenario. Hence, at very large times a transition from the continuous to the fluctuation dominated regime takes place. Indeed, Campos et al. [117] reproduced our simulations, running them for a longer time and detected that, after a stage where $v \propto t^{\frac{\alpha-1}{2}}$ holds, the velocity sets in to decay faster at very large times. This result can be interpreted in favor of the onset of a transition from the continuous to the fluctuation dominated regime. Additional simulations pertaining the reaction on contact scenario, i.e. the fluctuation dominated regime, revealed additional fluctuation effects that are genuinely due to subdiffusion.

These findings reveal a general problem pertinent to arbitrary reactions under subdiffusion with local classical reaction rate kinetics. In the course of time, the mobility of the particles decreases, whereas the governing time scales of the reaction remain constant. This leads to the situation where waiting times become so large that any currently possible reaction happens within a waiting time. This imposes limits onto the applicability of the continuous reaction subdiffusion equations. Particularly in the long time limit, a transition to the fluctuation dominated regime corresponding to the reaction on the first contact ($\kappa \to \infty$) is expected.

Such an effect can be suppressed if all diffusing species are exchanged regularly, e.g. by appropriate particle supplies at the boundaries and vanishing of the particles inside the system, which ensures that no particle remains in the system for too long times [1], as was the case in e.g. [114]. Another example of a nonlinear reaction–subdiffusion system was the subdiffusion of a mobile reactant A into a medium initially containing a constant concentration of immobile reactants B, the A–concentration was kept constant at the boundary layer of the medium. Both species react according to the scheme $A + B \to (inert)$. These considerations were motivated by experiments [37] that suggest anomalously slow diffusion within polyelectrolyte multilayers. A constant concentration of an immobile fluorescent marker B was included into the material during assembly, so that a quencher A introduced at the boundary leads to the retraction of the front of fluorescent B. The aim was therefore to predict the large time behavior of the moving front of the fluorescent B inside a subdiffusive medium, which would allow to quantify the relevant parameters.

In order to keep the model tractable, we made use of the fact that at large times the reaction on first contact scenario provides a good description in reaction–subdiffusion with classical rate kinetics. This leads to a sharp boundary between domains of A– and B–particles, where the concentration of both particle concentrations is zero. The velocity of this boundary is fully de-

[1] The notion of "too long times" is closely connected to the reaction rate, whose inverse should not be very much smaller than the observed waiting times.

termined by the flux of A–particles at the boundary. The system could therefore be described in terms of the A–concentrations only. Such a setting with prescribed values at a fixed and at a moving boundary are known as Stefan problems from the theory of heat conduction. The Stefan problem under anomalous diffusion with a constant A–concentration in the fixed boundary layer of the medium provided analytical expressions for the asymptotic behavior of the moving boundary as well as for the profile of the concentration by using subordination of the asymptotic solutions to the normal diffusive analogue of the system. The theoretical predictions concerning the moving boundary were corroborated by the numerical simulations. The main result was that the propagation of the moving boundary between the A– and B–domain goes as $R(t) \propto t^{\alpha/2}$. What remains to be done is to compare the above results with experiments. In particular it has to be clarified whether the assumption of a constant concentration at the fixed boundary conforms with experiments, or whether the concentration in the boundary layer of the medium is amenable to experimental control at all.

Appendix A

The Gamma Function

The Gamma function is defined as [43]

$$\Gamma(x) = \int_0^\infty e^{-t} t^{x-1}\, dt, \tag{1}$$

and the following relations hold:

$$\begin{aligned} \Gamma(n+1) &= n! \\ \Gamma(x+1) &= x\Gamma(x)\ , \end{aligned}$$

where $n \in \mathbb{N}$, $x \in \mathbb{R}$.

Multiplication Formula for the Gamma function

$$\Gamma(x)\Gamma\left(x+\frac{1}{n}\right)\ldots\Gamma\left(x+\frac{n-1}{n}\right) = \frac{(2\pi)^{(n-1)/2}}{n^{nx-1/2}}\Gamma(nx),$$

A special case of this is the duplication formula:

$$\Gamma(x)\Gamma(x+\frac{1}{2}) = \frac{\sqrt{\pi}}{2^{2x-1}}\Gamma(2x)\ .$$

Beta-function The Gamma function is connected to the Beta function as follows:

$$B(x,y) = \frac{\Gamma(x)\Gamma(y)}{\Gamma(x+y)}\ . \tag{2}$$

Appendix B

An Alternative Representation of Stable Distributions

It is sometimes more convenient to use a representation of stable laws that goes back to Zolotarev [140, 141, 53],

$$\log \hat{p}^{c^*,\gamma^*}_{\alpha^*,\beta^*}(k) = \mathrm{i}\gamma^* k - c^*|k|^{\alpha^*} \exp\left[-\mathrm{i}\frac{\pi}{2}\beta^* \mathrm{sign}(k)\right] \tag{3}$$

for $\alpha^* \neq 1$ and

$$\log \hat{p}(k)^{c^*,\gamma^*}_{1,\beta^*} = \mathrm{i}\gamma^* k - c^*|k|\left(1 - \mathrm{i}\frac{2}{\pi}\beta^* \mathrm{sign}(k)\log|k|\right) \tag{4}$$

for $\alpha^* = 1$. The new constants are related to those appearing in the original Lévy- and Khintchine (LK) representation Eq. (3.24) in the following way:

$$\begin{aligned} \alpha_{LK} &= \alpha^* \\ \beta_{LK} &= \cot\left(\frac{\pi\alpha^*}{2}\right)\tan\left(\frac{\pi\beta^*}{2}\right) \\ \gamma_{LK} &= \gamma^* \\ c_{LK} &= c^* \cos\left(\frac{\pi\beta^*}{2}\right). \end{aligned} \tag{5}$$

Hence, the new constant β^* can take the values

$$|\beta^*| \leq \begin{cases} \alpha^* & \text{if} \quad 0 < \alpha^* < 1 \\ 2 - \alpha^* & \text{if} \quad 1 < \alpha^* < 2\,. \end{cases} \tag{6}$$

The corresponding Lévy densities with new parameters are given by the Fourier transform of $\tilde{p}^{c^*,\gamma^*}_{\alpha^*,\beta^*}(k)$,

$$
\begin{aligned}
p^{c^*,\gamma^*}_{\alpha^*\neq 1,\beta^*}(x) &= \frac{1}{2\pi}\int_{-\infty}^{\infty}\exp\left[-\mathrm{i}kx+\mathrm{i}\gamma^*k-c^*|k|^{\alpha^*}e^{-\mathrm{i}\frac{\pi}{2}\beta^*\mathrm{sign}(k)}\right]dk \\
p^{c^*,\gamma^*}_{\alpha^*=1,\beta^*}(x) &= \frac{1}{2\pi}\int_{-\infty}^{\infty}\exp\Big[-\mathrm{i}kx+\mathrm{i}\gamma^*k \\
&\quad -c^*|k|\left(1-\mathrm{i}\frac{2}{\pi}\beta^*\mathrm{sign}(k)\log|k|\right)\Big]dk\,. \qquad (7)
\end{aligned}
$$

In new parameters we have again

$$
\begin{aligned}
p^{c^*,\gamma^*}_{\alpha^*\neq 1,\beta^*}(x) &= c^{*-1/\alpha^*}p^{1,0}_{\alpha^*\neq 1,\beta^*}\left(c^{*-1/\alpha^*}(x-\gamma^*)\right) \\
p^{c,\gamma^*}_{\alpha^*=1,\beta^*}(x) &= c^{*-1}p^{1,0}_{\alpha^*=1,\beta^*}\left(c^{*-1}(x-\gamma^*)-2\beta^*\pi^{-1}\log c^*\right)\,. \qquad (8)
\end{aligned}
$$

Therefore we restrict ourselves to $c^*=1$, $\gamma^*=0$, so that

$$
p_{\alpha^*,\beta^*}(-x)=p_{\alpha^*,-\beta^*}(x)\,. \qquad (9)
$$

Hence only positive x have to be taken into account, and

$$
\begin{aligned}
p_{\alpha^*\neq 1,\beta^*}(x) &= \frac{1}{\pi}\mathrm{Re}\int_0^{\infty}\exp\left[-\mathrm{i}kx-k^{\alpha^*}e^{-\mathrm{i}\frac{\pi}{2}\beta^*}\right]dk\,, \qquad (10)\\
p_{\alpha^*=1,\beta^*}(x) &= \frac{1}{\pi}\mathrm{Re}\int_0^{\infty}\exp\left[-\mathrm{i}kx-|k|\left(1-\mathrm{i}\frac{2}{\pi}\beta^*k\log k\right)\right]dk\,. \qquad (11)
\end{aligned}
$$

In the following only densities with $\alpha\neq 1$, (10) are considered. This representation of the characteristic function of stable laws allows for inversion by making a detour via the Mellin-transform, so that finally

$$
\mathcal{M}\left\{p_{\alpha^*\neq 1,\beta^*}(x),s\right\}=\epsilon_1\frac{\Gamma(s)\Gamma(\epsilon_1-\epsilon_1 s)}{\Gamma(\epsilon_2-\epsilon_2 s)\Gamma(1-\epsilon_2+\epsilon_2 s)} \qquad (12)
$$

for $0<\mathrm{Re}(s)<1$ where $\epsilon_1=1/\alpha^*$ and $\epsilon_2=(\alpha^*+\beta^*)/(2\alpha^*)$. Details of the derivation may be found e.g. in [142]. Using the definition of the H-function and choosing an appropriate substitution for the Mellin- parameter, it is easy to read off the analytic representation 2.3.2

$$
p_{\alpha^*,\beta^*}(x) = \epsilon_1 H^{1,1}_{2,2}\left[x\,\middle|\,\begin{matrix}(1-\epsilon_1,\epsilon_1) & (1-\epsilon_2,\epsilon_2)\\ (0,1) & (1-\epsilon_2,\epsilon_2)\end{matrix}\right] \qquad (13)
$$

for $\alpha^* > 1$, and in the case of $\alpha^* < 1$

$$p_{\alpha^*,\beta^*}(x^{-1}) = \epsilon_1 x^2 H^{1,1}_{2,2}\left[x \left| \begin{array}{ll} (-1,1) & (-\epsilon_2,\epsilon_2) \\ (-\epsilon_1,\epsilon_1) & (-\epsilon_2,\epsilon_2) \end{array} \right.\right] . \tag{14}$$

Laplace–Asymptotics of Power–Law Distributions

All waiting time pdfs with the asymptotic behavior

$$\psi(t) \propto \tau^\alpha t^{-1-\alpha} .$$

for t large have a corresponding (cumulative) probability to make a step until t

$$\Psi(t) \simeq 1 - \tau^\alpha t^{-\alpha} .$$

Using the Tauberian theorem, Laplace transformation yields

$$\tilde{\Psi}(u) \simeq \frac{1}{u} - \Gamma(1-\alpha)\tau^\alpha u^{-1+\alpha} , \tag{15}$$

so that the Laplace asymptotics of the pdf can finally be obtained by using the differentiation theorem of Laplace transformation

$$\tilde{\psi}(u) \simeq 1 - \Gamma(1-\alpha)\tau^\alpha u^\alpha . \tag{16}$$

Appendix C

Iterative Solution of a Time–fractional Differential Equation

The direct path to the solution (5.22) to the equation with initial conditions (5.21) via the iterative method goes as follows:
First, we set up the corresponding integral equation,

$$\begin{aligned} y(t) = y_0(t) \quad &+ \quad \frac{1}{\Gamma(\nu)} \int_0^t (t-t')^{\nu-1} \lambda y(t')\, dt' \\ &+ \quad \frac{1}{\Gamma(n)} \int_0^t (t-t')^{n-1} h(t')\, dt' \end{aligned}$$

with the initial condition

$$y_0(t) \quad = \quad \sum_{i=1}^{n} b_i \frac{t^{n-i}}{\Gamma(n-i+1)} \, . \tag{17}$$

By successive approximation,

$$\begin{aligned} y_l(t) = y_0(t) \quad &+ \quad \frac{1}{\Gamma(\nu)} \int_0^t (t-t')^{\nu-1} \lambda y_{l-1}(t')\, dt' \\ &+ \quad \frac{1}{\Gamma(n)} \int_0^t (t-t')^{n-1} h(t')\, dt' \end{aligned}$$

we finally find, provided all integrals converge,

$$
\begin{aligned}
y_1(t) &= y_0(t) + \lambda \sum_{i=1}^{n} b_i \frac{t^{\nu+n-i}}{\Gamma(n-i+1)} + \frac{1}{\Gamma(n)} \int_0^t (t-t')^{n-1} h(t')\, dt' \ , \\
y_2(t) &= y_1 + \lambda^2 \sum_{i=1}^{n} b_i \frac{t^{\nu+n-i}}{\Gamma(n-i+1)} + \lambda \frac{1}{\Gamma(\nu+n)} \int_0^t (t-t')^{\nu+n-1} h(t')\, dt' \ , \\
&\vdots \\
y_l(t) &= \sum_{i=1}^{n} b_i \sum_{j=1}^{l+1} \lambda^{j-1} \frac{t^{(j-1)\nu+n-i}}{\Gamma((j-1)\nu+n-i+1)} \ , \\
&\quad + \sum_{j=1}^{l} \lambda^{j-1} \frac{1}{\Gamma((j-1)\nu+n)} \int_0^t (t-t')^{(j-1)\nu+n-1} h(t')\, dt' \ , \\
&= \sum_{i=1}^{n} b_i \sum_{j=1}^{l+1} t^{n-i} \frac{(\lambda t^\nu)^{j-1}}{\Gamma((j-1)\nu+n-i+1)} \ , \\
&\quad + \int_0^t (t-t')^{n-1} \sum_{j=1}^{l} \frac{(\lambda (t-t')^\nu)^{j-1}}{\Gamma((j-1)\nu+n)} h(t')\, dt' \ ,
\end{aligned}
$$

which, after taking the limit $l \to \infty$, results in (5.22),

$$
y(t) = \sum_{i=1}^{n} b_i t^{n-i} \mathrm{E}_{\nu,1+n-i}(\lambda t^\nu) + \int_0^t (t-t')^{n-1} \mathrm{E}_{\nu,n}\left(\lambda (t-t')^\nu\right) h(t')\, dt' \ .
$$

Calculation of the Mode Decay in a Dirichlet Problem

Eq. 5.85 yields in the long time limit, $u \to 0$:

$$
\begin{aligned}
\tilde{C}(x,u) &= \left[C_0 \frac{2K_\alpha}{L} u^{-\alpha} \right] \times \\
&\quad \left[\frac{u^{\alpha-1}}{L} \sum_{n=0}^{\infty} e^{\pi \mathrm{i}(2n+1)x/(2L)} \frac{1}{u^\alpha + K_\alpha (2n+1)^2 \pi^2 / 4L^2} \right]
\end{aligned}
$$

which corresponds in time domain to a fractional integration of order α of (5.80):

$$C(x,t) = C_0 \frac{2K_\alpha}{L^2} \sum_{n=0}^{\infty} e^{\pi \mathrm{i}(2n+1)x/(2L)} {}_0\mathrm{D}_t^{-\alpha} \left\{ E_\alpha \left[-K_\alpha \frac{(2n+1)^2\pi^2}{4L^2} t^\alpha \right] \right\} .$$

Let us denote $K_\alpha \frac{(2n+1)^2\pi^2}{4L^2} := \lambda$. From Eq. (2.43) and shifting the summation index in the definition of the Mittag–Leffler–function (2.36), we find

$$\begin{aligned} {}_0\mathrm{D}_t^{-\alpha} \left[E_\alpha \left[-\lambda t^\alpha \right] \right] &= t^\alpha \mathrm{E}_{\alpha,1+\alpha} \left[-\lambda t^\alpha \right] \\ &= t^\alpha \sum_{n=0}^{\infty} \frac{(-\lambda t^\alpha)^n}{\Gamma(\alpha n + 1 + \alpha)} \\ &= (-\lambda t^\alpha)^{-1} t^\alpha \sum_{n=1}^{\infty} \frac{(-\lambda t^\alpha)^n}{\Gamma(\alpha n + 1)} \\ &= -\frac{1}{\lambda} \left[E_\alpha \left[-\lambda t^\alpha \right] - 1 \right] , \end{aligned}$$

so that in the end

$$C(x,t) = 8C_0 \sum_{n=0}^{\infty} \frac{e^{\pi \mathrm{i}(2n+1)x/(2L)}}{\pi^2(2n+1)^2} \left[1 - E_\alpha \left[-K_\alpha \frac{\pi^2(2n+1)^2}{4L^2} t^\alpha \right] \right] .$$

The Poisson Summation Formula

The periodic summation of a function can be expressed in terms of the original function's Fourier transform,

$$\sum_{n=-\infty}^{\infty} f(x+nT) = \frac{1}{T} \sum_{k=-\infty}^{\infty} \hat{f}\left(\frac{k}{T}\right) \exp\left[2\pi \mathrm{i} \frac{k}{T} x \right]$$

where T is the period of the function [143].

H-Function Representation of the Solution to the Dirichlet BVP on the Semi-infinite Domain

We seek to find an analytic expression for Eq. (5.66),

$$\tilde{C}(x,u) = \frac{C_0}{u}\exp\left[-\sqrt{\frac{u^\alpha}{K_\alpha}}|x|\right] \tag{18}$$

in original domain.
First, express the exponent as an H-function

$$\tilde{C}(x,u) = C_0 a^{2/\alpha} H_{0,1}^{1,0}\left[(a^{2/\alpha}u)^{\alpha/2}\,\middle|\,(-2/\alpha,1)\right] \tag{19}$$

with $a = \frac{|x|}{\sqrt{K_\alpha}}$. Scaling the argument,

$$\tilde{C}(x,u) = C_0 a^{2/\alpha}\frac{2}{\alpha} H_{0,1}^{1,0}\left[a^{2/\alpha}u\,\middle|\,(-2/\alpha,2/\alpha)\right] \tag{20}$$

and Laplace inverting this expression, we get

$$\begin{aligned} C(x,t) &= C_0 a^{2/\alpha}\frac{2}{\alpha}\frac{1}{t} H_{1,1}^{1,0}\left[\frac{a^{2/\alpha}}{t}\,\middle|\,\begin{matrix}(0,1)\\(-2/\alpha,2/\alpha)\end{matrix}\right] \\ &= C_0\frac{2}{\alpha} H_{1,1}^{1,0}\left[\frac{a^{2/\alpha}}{t}\,\middle|\,\begin{matrix}(1,1)\\(0,2/\alpha)\end{matrix}\right] \\ &= C_0 H_{1,1}^{1,0}\left[\frac{a}{t^{\alpha/2}}\,\middle|\,\begin{matrix}(1,\alpha/2)\\(0,1)\end{matrix}\right]. \end{aligned}$$

Appendix D

Hamilton-Jacobi Method and Front Propagation

In the following, a functional integration method is introduced that has proven especially useful in deriving the asymptotic front velocity in FKPP systems under normal diffusion [144]. Its most remarkable advantage consists in the fact that it allows for a calculation of the asymptotic front velocity without requiring special assumptions on the front shape.
Yadav and Fedotov et al. adopted this method to systems under anomalous transport [116, 145, 118]. Under the precondition of a constant asymptotic front velocity, the concentration of A-particles can be expressed in terms of variables that were subjected to the hyperbolic scaling, $x \to x/\varepsilon$, $t \to t\varepsilon$:

$$A^{\varepsilon}(x,t) = A\left(\frac{x}{\varepsilon},\frac{t}{\varepsilon}\right) \approx A^{*}\left(\frac{x-vt}{\varepsilon}\right) ,$$

for large t. For positive small ε, the asymptotic A-concentration $A^{*}(\frac{x-vt}{\varepsilon})$ is close to 1 for $x < vt$ and close to 0 otherwise. We will make use of the fact that for $\varepsilon \to 0$ the rescaled front shape trends to a step function,

$$A^{\varepsilon}(x,t) \approx A^{*}\left(\frac{x-vt}{\varepsilon}\right) \to \theta(-x+vt) ,$$

θ is the Heaviside step function. With

$$\begin{aligned} \frac{\partial}{\partial t}A(x,t) &= \varepsilon\frac{\partial}{\partial t}A^{\varepsilon}(x,t) , \\ \Delta A(x,t) &= \varepsilon^{2}\Delta A^{\varepsilon}(x,t) , \end{aligned}$$

$c_0 = 1$ and the substitution $(t - t' \to t')$ we rewrite Eq. (7.18) for A^{ε} as

$$
\begin{aligned}
\varepsilon\frac{\partial}{\partial t}A^{\varepsilon}(x,t) &= \varepsilon^2\frac{a^2}{2}\int_0^t M(t') \\
&\quad \Delta\left[A^{\varepsilon}(x,t-t')-1\right]\exp\left[-\kappa\int_0^{t'}A^{\varepsilon}(x,t-t'')\,dt''\right]dt' \\
&\quad +\kappa A^{\varepsilon}(x,t)\left(1-A^{\varepsilon}(x,t)\right) \\
&= \varepsilon^2\frac{a^2}{2}\int_0^t M(t') \\
&\quad \left[\Delta A^{\varepsilon}(x,t-t')-2\kappa\nabla A^{\varepsilon}(x,t-t')\int_0^{t'}\nabla A^{\varepsilon}(x,t-t'')\,dt''\right. \\
&\quad -\kappa(A^{\varepsilon}(x,t-t')-1)\int_0^{t'}\Delta A^{\varepsilon}(x,t-t'') \\
&\quad \left.+\kappa^2(A^{\varepsilon}(x,t-t')-1)\left(\int_0^{t'}\nabla A^{\varepsilon}(x,t-t'')\,dt''\right)^2 dt''\right] \\
&\quad \times\exp\left[-\kappa\int_0^{t'}A^{\varepsilon}(x,t-t'')\,dt''\right]dt'+\kappa A^{\varepsilon}(x,t)\left(1-A^{\varepsilon}(x,t)\right)\ . \qquad (21)
\end{aligned}
$$

We now define an action functional G [2] describing the logarithmic asymptotic form of the A-concentration profile

$$
A^{\varepsilon}(x,t)=A_0\exp\left[-\frac{G^{\varepsilon}(x,t)}{\varepsilon}\right], \qquad (22)
$$

where $\lim_{\varepsilon\to 0}G^{\varepsilon}(x,t)=G(x,t)$ and $G^{\varepsilon}(x,t)\geq 0$. For positive $G(x,t)$ we have $A^{\varepsilon}(x,t)\to 0$ for $\varepsilon\to 0$. Therefore, the front position $x(t)$ can be determined by the condition $G(x(t),t)=0$. Calculating

$$
\begin{aligned}
\frac{\partial}{\partial t}A^{\varepsilon}(x,t) &= -\frac{A_0}{\varepsilon}\left[\frac{\partial}{\partial t}G^{\varepsilon}(x,t)\right]\exp\left[-\frac{G^{\varepsilon}(x,t)}{\varepsilon}\right] \\
\Delta A^{\varepsilon}(x,t) &= \left[\frac{A_0}{\varepsilon^2}\left(\nabla G^{\varepsilon}(x,t)\right)^2-\frac{A_0}{\varepsilon}\Delta G^{\varepsilon}(x,t)\right]\exp\left[-\frac{G^{\varepsilon}(x,t)}{\varepsilon}\right]
\end{aligned}
$$

and retaining leading order in A^{ε} or $\exp\left[-\frac{G^{\varepsilon}}{\varepsilon}\right]$, we obtain for (21)

[2] Throughout this section, G is the action functional and must not be confused with the Green functions of the previous sections.

$$\begin{aligned}\frac{\partial G^\varepsilon(x,t)}{\partial t} &= \frac{a^2}{2}\int_0^{t/\varepsilon} M(t')\Big\{\exp\left[\frac{G^\varepsilon(x,t)-G^\varepsilon(x,t-\varepsilon t')}{\varepsilon}\right]\\ &\times\left[\varepsilon\Delta G^\varepsilon(x,t-\varepsilon t')-(\nabla G^\varepsilon(x,t-\varepsilon t'))^2\right]\\ &+\kappa\int_0^{t'}\exp\left[\frac{G^\varepsilon(x,t)-G^\varepsilon(x,t-\varepsilon t'')}{\varepsilon}\right]\\ &\left[\varepsilon\Delta G^\varepsilon(x,t-\varepsilon t'')-(\nabla G^\varepsilon(x,t-\varepsilon t''))^2\right]dt''\Big\}dt'-\kappa\,. \end{aligned} \tag{23}$$

Performing the transition $\varepsilon\to 0$, we have $\lim_{\varepsilon\to 0} G^\varepsilon(x,t)=G(x,t)$ and hence $\frac{1}{\varepsilon}(G^\varepsilon(x,t)-G^\varepsilon(x,t-\varepsilon t'))=\frac{\partial}{\partial t}G(x,t)t'$. Insertion into Eq. (23) yields the Hamilton-Jacobi-Equation

$$\begin{aligned}\frac{\partial}{\partial t}G(x,t) &= \frac{a^2}{2}(\nabla G(x,t))^2\left\{\int_0^\infty M(t')\exp\left[\frac{\partial}{\partial t}G(x,t)t'\right]dt'\right.\\ &\left.+\kappa\int_0^\infty M(t')\int_0^{t'}\exp\left[\frac{\partial}{\partial t}G(x,t)t''\right]dt''\,dt'\right\}-\kappa\,. \end{aligned} \tag{24}$$

Since G is the action functional, we are able to define a Hamilton-function $H=-\frac{\partial G}{\partial t}$ and momentum $p=\frac{\partial G}{\partial x}$ so that

$$\begin{aligned}H &= \frac{a^2}{2}p^2\left\{\int_0^\infty M(t')\exp[-Ht']\,dt'\right.\\ &\left.+\kappa\int_0^\infty M(t')\int_0^{t'}\exp[-Ht'']\,dt''\,dt'\right\}+\kappa\,. \end{aligned}$$

Using the definition of the Laplace transformation we finally arrive at

$$H = \frac{a^2}{2}p^2\tilde{M}(H)+\frac{a^2}{2}p^2\frac{\kappa}{H}\left[-\tilde{M}(H)+\int_0^\infty M(t')\,dt'\right]+\kappa\,, \tag{25}$$

with H being the Laplace variable conjugate to time. Rewriting the action in terms of the Lagrangian, $G(x,t)=\int_0^t[p(s)\dot{x}(t')-H(p(t',x(t')))]\,dt'=0$, and minimizing the action results in

$$\begin{aligned}v=\dot{x} &= \frac{\partial H}{\partial p}\,,\\ \frac{H}{p} &= \frac{\partial H}{\partial p}\,. \end{aligned}$$

Markovian case Exponential waiting time pdfs, $\psi(t) = \frac{1}{\tau}\exp\left[-\frac{t}{\tau}\right]$, i.e. $\tilde{\psi}(H) = \frac{1}{1+H\tau}$, result in $\tilde{M}(H) = \frac{1}{\tau}$ and $\int_0^\infty M(t')\,dt' = \frac{1}{\tau}$ so that the Hamilton function (25) obeys the equation

$$H = \frac{a^2}{2\tau}p^2 + \frac{a^2}{2}p^2\frac{\kappa}{H}\left[-\frac{1}{\tau}+\frac{1}{\tau}\right]+\kappa\,,$$

and the momentum yields

$$p^2 = \frac{2\tau}{a^2}(H-\kappa)\ .$$

With $\frac{H}{p} = 2Dp$, $D = \frac{a^2}{2\tau}$, $H = 2\kappa$, the asymptotic front velocity of the classical FKPP system is reproduced,

$$v = 2\sqrt{\kappa D}\,.$$

Non-Markovian case Let $\psi(t) \propto t^{-1-\alpha}$, $\tilde{\psi}(H) \simeq 1-(H\tau)^\alpha\Gamma(1-\alpha)$. Then, $\tilde{M}(H) = \frac{H^{1-\alpha}}{\tau^\alpha}$ and the integral $\int_0^\infty M(t')\,dt'$ does not converge. The Hamilton function is determined by

$$H \quad = \quad K_\alpha p^2 H^{-\alpha}\left[H-\kappa+H^{\alpha-1}\kappa\tau^\alpha\int_0^\infty M(t')\,dt'\right]+\kappa$$

with $K_\alpha = \frac{a^2}{2\tau^\alpha}$ being the generalized diffusion coefficient. The momentum is given by

$$p^2 = \frac{H-\kappa}{K_\alpha H^{-\alpha}\left[H-\kappa+H^{\alpha-1}\kappa\tau^\alpha\int_0^\infty M(t')\,dt'\right]}\,.$$

By virtue of $\frac{H}{p} = \frac{\partial H}{\partial p}$ we obtain the rather involved equation

$$K_\alpha p H^{-\alpha}\left[H-\kappa+H^{\alpha-1}\kappa\tau^\alpha\Gamma(-1+\alpha)\int_0^\infty M(t')\,dt'\right]+\frac{\kappa}{p} = \frac{2K_\alpha p H^{-\alpha}\left[H-\kappa+H^{\alpha-1}\kappa\tau^\alpha\int_0^\infty M(t')\,dt'\right]}{1-K_\alpha p^2\left[(1-\alpha)H^{-\alpha}+\alpha\kappa H^{-1-\alpha}+(\alpha-1)H^{\alpha-2}\kappa\tau^\alpha\int_0^\infty M(t')\,dt'\right]}$$

which can, if at all, only hold true for $H = 0$. Consequently, a constant asymptotic propagation velocity of the front does not exist, $v = 0$. This reproduces the result obtained in section 7.3, and

does not provide any information about how the asymptotics is reached.
The Hamilton-Jacobi method is basically equivalent to the leading edge linearization under the assumption of a constant asymptotic front velocity. The hyperbolic scaling procedure only makes sense if the x and t coordinates of the front position have a constant ratio, which accounts for the shortcoming of this method in cases where the asymptotic front velocity is not a constant. From the physical point of view, the hyperbolic scaling in the case of non-constant front velocities does not properly define the front position since the reference points taken at the front at different times are different and not comparable. Only constant front velocities ensure that the reference point defining the front is always the same (although this reference point is not specified).

Supplements to the Calculations of the Asymptotic Subdiffusive Front Velocity

Calculation of the Integrals

We investigate the integrals in expression (7.43) term by term, from left to right. For the sake of brevity, the constant A_0 is omitted.

$$\begin{aligned} I_1 = & \int_0^t M(t-t')\lambda_0^2 t'^{1-\alpha} \exp\left[-\lambda_0 t'^{\frac{1-\alpha}{2}}(x - v_0 t'^{\frac{\alpha+1}{2}})\right] dt' \\ = & \frac{\lambda_0^2}{\Gamma(1-\alpha)\tau^\alpha} \exp\left[-\lambda_0 t^{\frac{1-\alpha}{2}}\left(x - v_0 t^{\frac{1+\alpha}{2}}\right)\right] \times \\ & \frac{1}{\Gamma(\alpha)}\frac{d}{dt}\int_0^t \frac{1}{(t-t')^{1-\alpha}} t'^{1-\alpha} \exp\left[-\lambda_0 t'^{\frac{1-\alpha}{2}}\left(x - v_0 t'^{\frac{1+\alpha}{2}}\right) + \lambda_0 t^{\frac{1-\alpha}{2}}\left(x - v_0 t^{\frac{1+\alpha}{2}}\right)\right] dt' \ . \end{aligned} \tag{26}$$

This expression is estimated from above using $t' \leq t$:

$$\begin{aligned} I_1 \leq & \frac{\lambda_0^2}{\Gamma(1-\alpha)\tau^\alpha} \exp\left[-\lambda_0 t^{\frac{1-\alpha}{2}}\left(x - v_0 t^{\frac{1+\alpha}{2}}\right)\right] \frac{1}{\Gamma(\alpha)}\frac{d}{dt}\int_0^t \frac{1}{(t-t')^{1-\alpha}} t'^{1-\alpha} dt' \\ = & \frac{\lambda_0^2}{\Gamma(1-\alpha)\tau^\alpha} \exp\left[-\lambda_0 t^{\frac{1-\alpha}{2}}\left(x - v_0 t^{\frac{1+\alpha}{2}}\right)\right] \frac{1}{\Gamma(\alpha)}\frac{d}{dt} t \int_0^1 \frac{1}{(1-t')^{1-\alpha}} t'^{1-\alpha} dt' \\ = & \frac{\lambda_0^2}{\Gamma(1-\alpha)\tau^\alpha} \exp\left[-\lambda_0 t^{\frac{1-\alpha}{2}}\left(x - v_0 t^{\frac{1+\alpha}{2}}\right)\right] \frac{1}{\Gamma(\alpha)} B(\alpha, 2-\alpha) \ . \end{aligned} \tag{27}$$

The integral in (26) is monotonic, i.e. it must tend to a constant value $B_{int} \leq B(\alpha, 2-\alpha)$ for large times ($B_{int} = 1$ for the normal diffusive case, in particular).
We used here the definition of the Beta-function $B(\mu,\nu) = \frac{\Gamma(\mu)\Gamma(\nu)}{\Gamma(\mu+\nu)}$. The other integral to be evaluated is

$$I_2 = \int_0^t M(t-t')c_0\kappa\lambda_0^2 \int_{t'}^t t''^{1-\alpha} \exp\left[-\lambda_0 t''^{\frac{1-\alpha}{2}}\left(x - v_0 t''^{\frac{1+\alpha}{2}}\right)\right] dt'' \, dt' \, . \tag{28}$$

At the far edge of the front, the comoving variable $z = x - v_0 t^{\frac{1+\alpha}{2}}$ is very large. The transition to large z can be achieved by introducing a large parameter ϱ, so that the integral appearing in the integrand of (28) obtains the form of a Laplace integral which allows for an asymptotic estimation for $\varrho \to \infty$:

$$\begin{aligned} & \lim_{\varrho\to\infty} \frac{\lambda_0^2}{\Gamma(1-\alpha)\tau^\alpha} \int_0^t t''^{1-\alpha} \exp\left[-\lambda_0 t''^{\frac{1-\alpha}{2}} \varrho\left(x - v_0 t''^{\frac{1+\alpha}{2}}\right)\right] dt'' \\ = \; & \frac{\lambda_0}{v_0\Gamma(1-\alpha)\tau^\alpha} t^{1-\alpha} \exp\left[-\lambda_0 t^{\frac{1-\alpha}{2}}\left(x - v_0 t^{\frac{1+\alpha}{2}}\right)\right] , \end{aligned} \tag{29}$$

that means that for large ϱ the value of the above integral is asymptotically determined by the points where the exponent in the integrand attains its maximum, see e.g. [146].
Hence, (28) becomes

$$\begin{aligned} & \frac{\lambda_0 c_0\kappa}{v_0} \exp\left[-\lambda_0 t^{\frac{1-\alpha}{2}}\left(x - v_0 t^{\frac{1+\alpha}{2}}\right)\right] \times \\ & \left[t^{1-\alpha} \int_0^t M(t-t')\, dt' - \right. \\ & \left. \int_0^t M(t-t') t'^{1-\alpha} \exp\left[-\lambda_0 t'^{\frac{1-\alpha}{2}}\left(x - v_0 t'^{\frac{1+\alpha}{2}}\right) + \lambda_0 t^{\frac{1-\alpha}{2}}\left(x - v_0 t^{\frac{1+\alpha}{2}}\right)\right] dt'\right] \\ = \; & \frac{\lambda_0 c_0\kappa}{v_0\Gamma(1-\alpha)\tau^\alpha} \exp\left[-\lambda_0 t^{\frac{1-\alpha}{2}}\left(x - v_0 t^{\frac{1+\alpha}{2}}\right)\right] \times \\ & \left[t^{1-\alpha} \frac{1}{\Gamma(\alpha)} \frac{d}{dt} \int_0^t \frac{1}{(t-t')^{1-\alpha}}\, dt' - \right. \\ & \left. \frac{1}{\Gamma(\alpha)} \frac{d}{dt} \int_0^t \frac{1}{(t-t')^{1-\alpha}} t'^{1-\alpha}\, dt' \exp\left[-\lambda_0 t'^{\frac{1-\alpha}{2}}\left(x - v_0 t'^{\frac{1+\alpha}{2}}\right) + \lambda_0 t^{\frac{1-\alpha}{2}}\left(x - v_0 t^{\frac{1+\alpha}{2}}\right)\right]\right] \\ = \; & \frac{\lambda_0 c_0\kappa}{v_0\Gamma(1-\alpha)\tau^\alpha} \exp\left[-\lambda_0 t^{\frac{1-\alpha}{2}}\left(x - v_0 t^{\frac{1+\alpha}{2}}\right)\right] \times \frac{1}{\Gamma(\alpha)} \left[1 - B_{int}\right] , \end{aligned} \tag{30}$$

with $B_{int} \leq B(\alpha, 2-\alpha)$, cf. (27).

Annotations on the Dispersion Relation

Recall that the emerging dispersion relation (7.45) requires

$$\left(\frac{c_0\kappa K_\alpha^*}{v_0}\left[1-B_{int}\right]-v_0\right)^2 \geq 4c_0\kappa K_\alpha^* B_{int} \tag{31}$$

for λ_0 to be real and nonnegative. In the normal case, $B_{int} = 1$, so that the marginal front velocity $v_{min} = \pm 2\sqrt{c_0 D\kappa}$ is reproduced. Another double solution exists in that case at $v = 0$, for which there is no front. Eq. (31) has real roots for any possible B_{int}. Except for $B_{int} = 1$ there exists a bounded domain of real roots around zero, $|v_0| < v_1$, and another domain of real roots $|v_0| > v_2$ where $v_1 < v_2$. The relation (31) is plotted in Fig. 1, the grey color indicates the regions where the relation is fulfilled.

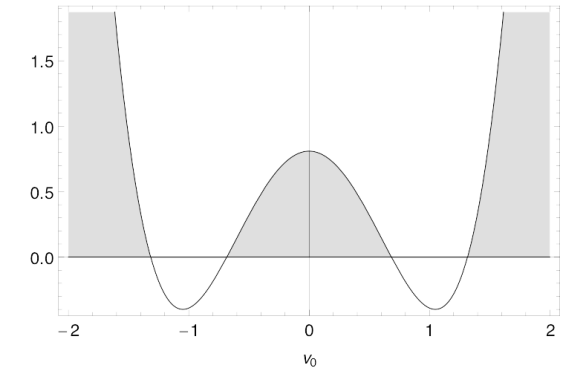

(a)

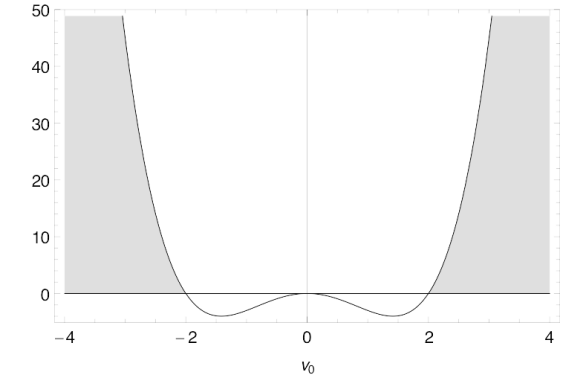

(b)

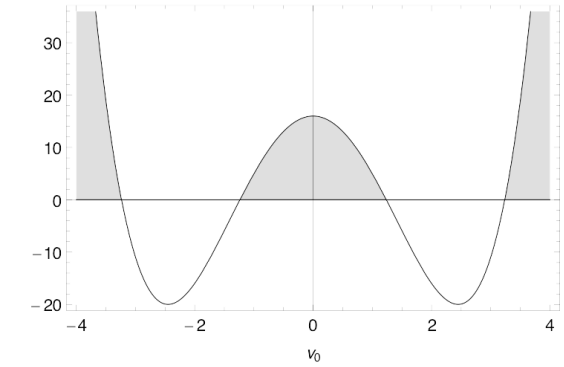

(c)

Figure 1: Plot of relation (31) for $B_{int} = 0.1,\ 1,\ 5$ (upper to lower panel).

Appendix E

Supplementary Calculations for the Variable Change in the Subdiffusive Stefan–Problem

The Laplace transformation of Eq. (8.24) yields:

$$
\begin{aligned}
& K_{\alpha\,0}\mathrm{D}_t^{1-\alpha}\left[t^{-\frac{\alpha}{2}}\sum_{i=1}^{\infty}\frac{1}{(i-1)!}\frac{\partial^{(i)}A^*_\infty(\xi_R)}{\partial\xi^i}\left(\frac{x-R(t)}{t^\alpha/2}\right)^{i-1}\right] \\
= \;& K_{\alpha\,0}\mathrm{D}_t^{1-\alpha}\left[\sum_{i=1}^{\infty}\frac{1}{(i-1)!}\left.\frac{\partial^{(i)}A^*_\infty}{\partial\xi^i}\right|_R (x-R(t))^{i-1}\,t^{-i\alpha/2}\right] \\
\doteq \;& K_\alpha u^{1-\alpha}\sum_{i=1}^{\infty}\frac{1}{(i-1)!}\left.\frac{\partial^{(i)}A^*_\infty}{\partial\xi^i}\right|_R (x-R(t))^{i-1}\,\frac{\Gamma(1-i\alpha/2)}{u^{\alpha-i\alpha/2}} \\
\doteq \;& K_\alpha\sum_{i=1}^{\infty}\frac{1}{(i-1)!}\left.\frac{\partial^{(i)}A^*_\infty}{\partial\xi^i}\right|_R (x-R(t))^{i-1}\,\frac{\Gamma(1-i\alpha/2)}{\Gamma(-i\alpha/2+\alpha)}t^{-1-i\alpha/2+\alpha}\,.
\end{aligned}
$$

For the transformation of the Riemann-Liouville fractional derivative acting upon the spatial Laplacian in the subdiffusion equation we find:

$$
\begin{aligned}
& {}_0\mathrm{D}_t^{1-\alpha}\left[\sum_{i=2}^{\infty}\frac{1}{(i-2)!}\frac{\partial^{(i)}A^*_\infty(\xi_0,A_0)}{\partial\xi^{(i)}}(x-x_0)^{i-2}t^{-(i-2)\alpha/2-\alpha}\right] && (32)\\
\doteq \;& u^{1-\alpha}\sum_{i=2}^{\infty}\frac{1}{(i-2)!}\frac{\partial^{(i)}A^*_\infty(\xi_0,A_0)}{\partial\xi^{(i)}}(x-x_0)^{i-2}\Gamma(1-(i-2)\alpha/2-\alpha)u^{-1+(i-2)\alpha/2+\alpha} && (33)\\
= \;& \sum_{i=2}^{\infty}\frac{1}{(i-2)!}\frac{\partial^{(i)}A^*_\infty(\xi_0,A_0)}{\partial\xi^{(i)}}(x-x_0)^{i-2}\Gamma(1-(i-2)\alpha/2-\alpha)u^{+(i-2)\alpha/2} && (34)\\
\doteq \;& \sum_{i=2}^{\infty}\frac{1}{(i-2)!}\frac{\partial^{(i)}A^*_\infty(\xi_0,A_0)}{\partial\xi^{(i)}}(x-x_0)^{i-2}\frac{\Gamma(1-(i-2)\alpha/2-\alpha)}{\Gamma(-(i-2)\alpha/2)}t^{-(i-2)\alpha/2-1} && (35)\\
= \;& \sum_{i=2}^{\infty}\frac{1}{(i-2)!}\frac{\partial^{(i)}A^*_\infty(\xi_0,A_0)}{\partial\xi^{(i)}}\frac{\Gamma(1-(i-2)\alpha/2-\alpha)}{\Gamma(-(i-2)\alpha/2)}t^{-1}(\xi-\xi_0)^{i-2}\,. && (36)
\end{aligned}
$$

Glossary

Abbreviations

BVP	Boundary Value Problem
CLT	Central Limit Theorem
CTRW	Continuous Time Random Walk
FKPP	Fisher–Kolmogorov–Petrovskii–Piscounov
GME	Generalized Master Equation
iid	independently identically distributed
IVP	Initial Value Problem
lhs	left hand side
MC step	Monte–Carlo step
ODE	Ordinary Differential Equation
PDE	Partial Differential Equation
pdf	probability density function
rhs	right hand side
RW	Random Walk

Symbols

a	lattice constant
α	subdiffusion parameter
A, B, C	particle species
$A(x,t)$, $B(x,t)$, $C(x,t)$	particle concentrations of species A, B, C
$A_i(t)$, $B_i(t)$, $C_i(t)$	occupation numbers of species A, B, C at a lattice site i
D	diffusion constant
${}_{t_0}\mathrm{D}_t^{\gamma}$	Riemann–Liouville fractional derivative
Δ	spatial Laplace operator, $\frac{\partial^2}{\partial x^2}$
∇	Nabla operator, $\frac{\partial}{\partial x}$
$\mathrm{E}_{\alpha,\beta}(z)$	generalized Mittag–Leffler function
$\mathrm{erf}(z)$	Error function
$\mathrm{erfc}(z)$	Error function complement
$\mathcal{F}$, $\mathcal{F}^{-1}$	Fourier Transform, inverse Fourier Transform
$\Gamma(z)$	Gamma function
$H_{p,q}^{m,n}(z)$	Fox's H–Function
i	imaginary unit, $\sqrt{-1}$
j^+, j^-	gain flux, loss flux
k	Fourier variable, conjugate to x
k_B	Boltzmann constant
K_α	generalized diffusion constant
κ	reaction rate coefficient
$\mathcal{L}$, $\mathcal{L}^{-1}$	Laplace Transform, inverse Laplace Transform
$M(t)$	memory kernel
$\mathcal{M}$, $\mathcal{M}^{-1}$	Mellin Transform, inverse Mellin Transform
N_A	total amount of A–particles
p	probability density function
$p_{\alpha,1}$	one–sided Lévy stable density
P	(cumulative) probability
$\varphi(x)$	step length pdf
$\psi(t)$	waiting time pdf
$\Psi(x,t)$	jump pdf
s	Mellin variable, conjugate to t
t	time variable
$\mathcal{T}_\alpha$, $\mathcal{T}_\alpha^{-1}$	Subordination Transform with parameter α, inverse Subordination Transform
$\theta(z)$	Heaviside step function
τ	typical time scale
u	Laplace variable, conjugate to t
v	front velocity
x	space variable
$\doteqdot$	"the (Laplace-) image of"
$\doteqdot$	"the reverse (Laplace-) image of"

Software used and Simulations

- Mathematica 8.0
- Matlab 7.8.0
- TEX Live 2008
- All simulations pertaining Chapter 7 were programmed by Dipl. Phys. H. H. Schmidt–Martens, mostly in conjunction with his Diploma thesis. All simulations in Chapter 8 are due to M. Borinsky. The simulations were programmed in C/C++.

Bibliography

[1] A. Einstein. *Ann. Phys.*, **322**:549–560, 1905.

[2] I. M. Sokolov and J. Klafter. *Chaos*, **15**:026103, 2005.

[3] G. Nicolis and C. Nicolis. *Foundations of Complex Systems*. World Scientific, Singapore, 2007.

[4] R. Metzler and J. Klafter. *Phys. Rep.*, **339**:1–77, 2000.

[5] J. W. Haus and K. W. Kehr. *Phys. Rep.*, **150**(5 & 6):263–406, 1987.

[6] A. Blumen, J. Klafter, and G. Zumofen. Models for reaction dynamics in glasses. In I. Zschokke, editor, *Optical Spectroscopy of Glasses*, pages 199–265. D. Reidel Publishing, Dordrecht, 1986.

[7] D. ben Avraham and S. Havlin. *Diffusion and Reactions in Fractals and Disordered Systems*. Cambridge University Press, 2000.

[8] I. Golding and E. C. Cox. Physical nature of bacerial cytoplasm. *Phys. Rev. Lett.*, **96**: 098102, 2006.

[9] M. Weiss, M. Elsner, F. Kartberg, and T. Nilsson. *Biophys. J.*, **87**:3518, 2004.

[10] J. Szymanski and M. Weiss. *Phys. Rev. Lett.*, **103**:038102, 2009.

[11] I. Y. Wong, M. L. Gardel, D. R. Reichman, E. R. Weeks, M. T. Valentine, A. R. Bausch, and D. A. Weitz. *Phys. Rev. Lett.*, **92**:178101, 2004.

[12] H. Scher and E. W. Montroll. *Phys. Rev. B*, **12**:2455, 1975.

[13] B. Berkowitz and H. Scher. *Phys. Rev. Lett.*, **79**:4038, 1997.

[14] B. Berkowitz and H. Scher. *Phys. Rev. E*, **57**:5858, 1998.

[15] F. Mainardi, M. Roberto, R. Gorenflo, and E. Scalas. *Physica A*, **278**:468, 2000.

[16] R. Metzler and J. Klafter. *J. Phys. A*, **37**:R161–R208, 2004.

[17] G. Bel and E. Barkai. *Phys. Rev. E*, **73**:016125, 2006.

[18] A. Lubelski and I. M. Sokolov. *Phys. Rev. Lett.*, **100**:250602, 2008.

[19] Y. He, S. Burov, R. Metzler, and E. Barkai. *Phys. Rev. Lett.*, **101**:058101, 2008.

[20] W. Ebeling and I. M. Sokolov. *Statistical Thermodynamics and Stochastic Theory of Nonequilibrium Systems*. World Scientific, Singapore, 2005.

[21] R. A. Fisher. *Annals of Eugenics*, **7**:355, 1937.

[22] J. D. Murray. *Mathematical Biology*, volume 1. Springer, 2002.

[23] A. J. Lotka. *Elements of Mathematical Biology*. Dover Publications, New York, 1956.

[24] N. G. van Kampen. *Stochastic processes in physics and chemistry*. North-Holland, 1987.

[25] A. Kolmogoroff, I. Petrovskii, and N. Piscounoff. *Mosc. Univ. Math. Bull.*, **1**:1–25, 1937.

[26] W. van Saarloos. *Phys. Rep.*, **386**:29–222, 2003.

[27] D. Panja. *Phys. Rep.*, **393**:87–174, 2004.

[28] M. G. W. Schmidt, I. M. Sokolov, and F. Sagues. *Phys. Rev. E*, **73**:031102, 2006.

[29] S. B. Yuste, L. Acedo, and K. Lindenberg. *Phys. Rev. E*, **69**:036126, 2004.

[30] T. Kosztolowicz and K. D. Lewandowska. *Phys. Rev. E*, **78**:066103, 2008.

[31] B. I. Henry, T. A. M. Langlands, and S. L. Wearne. *Phys. Rev. E*, **74**:031116, 2006.

[32] T. A. M. Langlands, B.I. Henry, and S. L. Wearne. *J. Phys. Cond. Mat.*, **19**:065115, 2007.

[33] J. Crank. *The Mathematics of Diffusion*. Clarendon Press, Oxford, 1 edition, 1956.

[34] A. Yadav and W. Horsthemke. *Phys. Rev. E*, **74**:066118, 2006.

[35] T. A. M. Langlands, B.I. Henry, and S. L. Wearne. *Phys. Rev. E*, **77**:021111, 2008.

[36] Y. Nec, V. A. Volpert, and A. A. Nepomnyashchy. *DCDS*, **27**:827–846, 2010.

[37] E. Donath. private communication.

[38] H. S. Carslaw and J. C. Jaeger. *Conduction of Heat in Solids*. Clarendon Press, Oxford, 2 edition, 1959.

[39] A. M. Meirmanov. *The Stefan Problem*. De Gruyter, Berlin, 1992.

[40] V. A. Ditkin and A. P. Prudnikov. *Integral Transforms and Operational Calculus*. Pergamon Press, Oxford, 1965.

[41] A. M. Mathai and H. J. Haubold. *Special Functions for Applied Scientists*. Springer, New York, 2008.

[42] I. Podlubny. *Fractional Differential Equations*. Academic Press, San Diego, 1999.

[43] I. N. Bronstein and K. A. Semendjajew. *Taschenbuch der Mathematik*. B. G. Teubner, Leipzig, 24th edition, 1989.

[44] G. Doetsch. *Handbuch der Laplace-Transformation*, volume 1-3. Birkhäuser Verlag, Basel, 1971-73.

[45] S. G. Samko, A. A. Kilbas, and O. I. Marichev. *Fractional Integrals and Derivatives*. Gordon and Breach, Yverdon, 1993.

[46] K. Oldham and J. Spanier. *The fractional Calculus: Theory and Applications of Differentiation and Integration to Arbitrary Order*. Academic Press, New York, 1974.

[47] H. Bateman. *Tables of Integral Transforms*, volume 1 of *Bateman Manuscript Project*. McGraw-Hill, New York, 1954.

[48] C. Fox. *Trans. Amer. Math. Soc.*, **98**:395–429, 1961.

[49] H. M. Srivastava, K. C. Gupta, and S. P. Goyal. *The H-Functions of one and two Variables with Applications*. South Asian Publishers, New Delhi, 1982.

[50] A. M. Mathai and R. K. Saxena. *The H-Function with Applications in Statistics and other Disciplines*. Wiley Eastern, New Delhi, 1978.

[51] S. Wolfram. *Mathematica Documentation*. Wolfram Research Inc., March 2011. URL `http://reference.wolfram.com/mathematica/guide/Mathematica.html`.

[52] W. Feller. *An Introduction to Probability Theory and its Applications*, volume 1& 2. Wiley, New York, 1966.

[53] I. A. Ibragimov and Yu. V. Linnik. *Independent and Stationary Sequences of Random Variables*. Wolters–Nordhoff Publishing, Groningen, 1971.

[54] G. H. Weiss. *Aspects and Applications of the Random Walk*. North-Holland, Amsterdam, 1994.

[55] K. Sato. *Lévy Processes and Infinitely Divisible Distributions*. Cambridge University Press, Cambridge, 1999.

[56] P. Lévy. *Théorie de l'Addition des Variables Aléatoires*. Gauthier–Villars, Paris, 2 edition, 1954.

[57] A. Khinchine. *Bull. Univ. Mosc. Sér. Int. A*, **1**:4, 1937.

[58] J.-P. Bouchaud and A. Georges. *Phys. Rep.*, **195**:127–293, 1990.

[59] S. Chandrasekhar. *Rev. Mod. Phys.*, **15**:1–89, 1943.

[60] B. V. Gnedenko and A. N. Kolmogorov. *Limit distributions for sums of independent random variables*. Addison Wesley, Reading (MA), 1954.

[61] E. W. Montroll and G. H. Weiss. *J. Math. Phys.*, **6**:167, 1965.

[62] E. W. Montroll and B. West. On an enriched collection of stochastic processes. In E. W. Montroll and J. L. Lebowitz, editors, *Fluctuation Phenomena*, chapter 2, pages 61–175. North Holland, 1979.

[63] R. Pyke. *Ann. Math. Statist.*, **32**:1231–1243, 1962.

[64] G. Pfister and H. Scher. *Adv. in Phys.*, **27**:747–798, 1978.

[65] H. Scher and M. Lax. *Phys. Rev. B*, **7**:4491, 1973.

[66] J. Klafter and R. Silbey. *Phys. Rev Lett.*, **44**:55, 1980.

[67] G. Margolin and B. Berkowitz. *J. Phys. Chem. B*, **104**:3942–3947, 2000.

[68] M. Levy and B. Berkowitz. *J. Contam. Hydrol.*, **64**:203–226, 2002.

[69] Y. Li, G. Farrher, and R. Kimmich. *Phys. Rev. E*, **74**:066309, 2006.

[70] T. Kosztolowicz, K. Dworecki, and St. Mrowczynski. *Phys. Rev. Lett.*, **94**:170602, 2005.

[71] M. Dentz, A. Cortis, H. Scher, and B. Berkowitz. *Adv. Water Resour.*, **27**:155–173, 2003.

[72] B. Bijeljic and M. J.Blunt. *Water Resour. Res.*, **42**:W01202, 2006.

[73] B. Bijeljic and M. J.Blunt. *Water Resour. Res.*, **43**:W12S11, 2007.

[74] D. L. Koch and J. F. Brady. *J. Fluid Mech.*, **154**:399–427, 1985.

[75] G. H. Weiss and R. J. Rubin. *Adv. Chem. Phys.*, **32**:363–505, 1983.

[76] J. K. E. Tunaley. *Phys. Rev. Lett.*, **33**:781, 1974.

[77] C. Godreche and J. M. Luck. *J. Stat. Phys.*, **104**:489–524, 2001.

[78] M. F. Shlesinger, G. M. Zaslavsky, and J. Klafter. *Nature*, **363**:31–37, 1993.

[79] H. C. Fogedby. *Phys. Rev. E*, **50**:1657–1660, 1994.

[80] V. Kenkre, E. Montroll, and M. Shlesinger. *J. Stat. Phys.*, **9**:45, 1973.

[81] J. Klafter, A. Blumen, and M. F. Shlesinger. *Phys. Rev. A*, **35**:3081, 1987.

[82] D. Bedeaux, K. Lakatos-Lindenberg, and K. E. Shuler. *J. Math. Phys.*, **12**:2116, 1971.

[83] A. Compte. *Phys. Rev. E*, **53**:4191, 1996.

[84] S. Bochner. *PNAS*, **35**:368–370, 1949.

[85] R. Gorenflo, F. Mainardi, and A. Vivoli. *Chaos,Solitons and Fractals*, **34**:87–103, 2007.

[86] A. I. Saichev and G. M. Zaslavsky. *Chaos*, **7**:753, 1997.

[87] A. I. Burshtein, A. A. Zharikov, and S. I. Temkin. *Theor. Math. Phys.*, **66**:166, 1986.

[88] A. V. Chechkin, R. Gorenflo, and I. M. Sokolov. *J. Phys. A*, **38**:L697–L684, 2005.

[89] W. G. Glöckle and T. F. Nonnenmacher. *J. Stat. Phys.*, **71**:741–757, 1993.

[90] C. Friedrich. *Rheol. Acta*, **30**:151–158, 1991.

[91] C. Friedrich. *J. Non-Newtonian Fluid Mech.*, **46**:307–314, 1993.

[92] W. G. Glöckle and T. F. Nonnenmacher. *Macromolecules*, **24**:6426–6436, 1991.

[93] R. Metzler and J. Klafter. *Physica A*, **278**:107–125, 2000.

[94] W. Preuss, A. Bleyer, and H. Preuss. *Distributionen und Operatoren*. VEB Fachbuchverlag, 1985.

[95] J. Mikusinsky. *Operatorenrechnung*. Deutscher Verlag der Wissenschaften, 1957.

[96] R. G. Buschman. *Integral Transformations, Operational Calculus, and Generalized Functions*. Kluwer Academic Publishers, 1996.

[97] Yu. F. Luchko and H. M. Srivastava. *Comput. Math. Appl.*, **29**:73–85, 1995.

[98] T. Kosztolowicz. *J. Phys. A*, **37**:10779–10789, 2004.

[99] M. v. Smoluchowski. *Z. Phys. Chem.*, **92**:129, 1917.

[100] S. A. Rice. *Diffusion limited reactions*. Elsevier, 1985.

[101] S. B. Yuste and K. Lindenberg. *Phys. Rev. Lett.*, **87**:118301, 2001.

[102] S. B. Yuste and K. Lindenberg. *Chem. Phys.*, **284**:169–180, 2002.

[103] R. E. Liesegang. *Naturwiss. Wochenschr.*, **11**:353, 1896.

[104] B. I. Henry and S. L. Wearne. *Physica A*, **276**:448–455, 2000.

[105] J. Sung, E. Barkai, R. Silbey, and S. Lee. *J. Chem. Phys.*, **116**:2338, 2002.

[106] K. Seki, M. Wojcik, and M. Tachiya. *J. Chem. Phys.*, **119**:2165, 2003.

[107] L. Galfi and Z. Racz. *Phys. Rev. A*, **38**:3151, 1988.

[108] H. Larralde, M. Araujo, S. Havlin, and H. E. Stanley. *Phys. Rev. A*, **46**:R6121–R6123, 1992.

[109] M. O. Vlad and J. Ross. *Phys. Rev. E*, :061908, 2002.

[110] F. Sagues, V. P. Shkilev, and I. M. Sokolov. *Phys. Rev. E*, **77**:032102, 2008.

[111] D. Froemberg and I. M. Sokolov. *Acta Phys. Pol. B*, **41**:989, 2010.

[112] G. Hornung, B. Berkowitz, and N. Barkai. *Phys. Rev. E*, **72**:041916, 2005.

[113] P. V. Danckwerts. *Trans. Faraday Soc.*, **47**:1014–1023, 1951.

[114] D. Froemberg and I. M. Sokolov. *Phys. Rev. Lett.*, **100**:108304, 2008.

[115] D. Froemberg and I. M. Sokolov. *Acta Phys. Pol. B*, **39**:1199, 2008.

[116] A. Yadav, S. Fedotov, V. Mendez, and W. Horsthemke. *Phys. Lett. A*, **371**:371, 2007.

[117] D. Campos and V. Mendez. *Phys. Rev. E*, **80**:021133, 2009.

[118] S. Fedotov and V. Mendez. *Phys. Rev. E*, **66**:030102, 2002.

[119] V. Mendez, D. Campos, and S. Fedotov. *Phys. Rev. E*, **70**:066129, 2004.

[120] S. Fedotov and Y. Okuda. *Phys. Rev. E*, **66**:021113, 2002.

[121] J. Riordan, C. R. Doering, and D. ben Avraham. *Phys. Rev. Lett.*, **75**:565, 1995.

[122] J. Mai, I. M. Sokolov, and A. Blumen. *Phys. Rev. E*, **62**:141, 2000.

[123] W. van Saarloos. *Phys. Rev. A*, **39**:6367–6390, 1989.

[124] D. Froemberg, H. Schmidt-Martens, I. M. Sokolov, and F. Sagues. *Phys. Rev. E*, **78**: 011128, 2008.

[125] H. H. Schmidt-Martens. Diplomarbeit: Reaction fronts in systems with anomalous diffusion. 2008.

[126] J. Mai, I. M. Sokolov, and A. Blumen. *Phys. Rev. Lett.*, **77**:4462, 1996.

[127] E. Brunet and B. Derrida. *J. Stat. Phys.*, **103**:269–282, 2001.

[128] H. H. Schmidt-Martens, D. Froemberg, I. M. Sokolov, and F. Sagués. *Phys. Rev. E*, **79**: 041135, 2009.

[129] G. K. Batchelor. *Q. J. R. Meteorolog. Soc.*, **76**:133–146, 1950.

[130] R. Mancinelli, D. Vergni, and A. Vulpiani. *Physica D*, **185**:175–195, 2003.

[131] R. N. Mantegna and H. E. Stanley. *Phys. Rev. Lett.*, **73**:2946, 1994.

[132] M. F. Schlesinger. *Phys. Rev. Lett.*, **74**:4959, 1995.

[133] D. Froemberg and I. M. Sokolov. *Acta Phys. Pol,*, **41**:989, 2010.

[134] C. P. Warren, E. Somfai, and L.M. Sander. *Braz. J. Phys.*, **30**:157, 2000.

[135] C.P. Warren, G. Mikus, E. Somfai, and L.M. Sander. *Phys. Rev. E*, **63**:056103, 2001.

[136] G. Decher. *Science*, **277**:1232–1237, 1997.

[137] F. V. Chavez and M. Schönhof. *J. Chem. Phys.*, **126**:104705, 2007.

[138] G. Decher, J. D. Hong, and J. Schmitt. *Thin Solid Films*, **210**:831, 1992.

[139] X. P. Qiu, S. Leporatti, E. Donath, and H. Möhwald. *Langmuir*, **17**:5375, 2001.

[140] V. M. Zolotarev. *Vestnik Leningrad Univ.*, **1**:49–52, 1956.

[141] V. N. Kolokoltsov. *Semiclassical Analysis for Diffusions and Stochastic Processes*. Springer, Berlin, 2000.

[142] W. R. Schneider. *Stable Distributions: Fox Function Representation and Generalization*, volume 262 of *Lecture Notes in Physics*. Springer, Heidelberg, 1986.

[143] P. M. Morse and H. Feshbach. *Methods of Theoretical Physics*. McGraw-Hill, 1953.

[144] M. Freidlin. *Functional Integration and Partial Differential Equations*. Princeton Univerity Press, 1985.

[145] S. Fedotov. *Phys. Rev. Lett*, **86**:926, 2001.

[146] N. Bleistein and R. A. Handelsman. *Asymptotic Expansions of Integrals*. Holt, Rinehart and Winston, 1986.

[147] A. M. Mathai. *A Handbook of Generalized Special Functions for Statistical and Physical Sciences*. Clarendon Press, Oxford, 1993.

[148] M. Lax and H. Scher. *Phys. Rev. Lett.*, **39**:781, 1977.

[149] M. Pollak. *Phil. Mag.*, **36**:1157–1169, 1977.

[150] J. K. E. Tunaley. *J. Stat. Phys.*, **11**:397, 1974.

[151] G. Zumofen and J. Klafter. *Phys. Rev. E*, **51**:1818, 1995.

[152] G. M. Zaslavsky. *Phys. Rep.*, **371**:461, 2002.

[153] H. C. Fogedby, T. Bohr, and H. Jensen. *J. Stat. Phys.*, **66**:583–593, 1992.

[154] B. D. Hughes. *Random Walks and Random Environments*, volume 1. Oxford University Press, Oxford, 1995.

[155] D. Froemberg, H. H. Schmidt-Martens, I. M. Sokolov, and F. Sagués. *Phys. Rev. E*, **83**: 031101, 2011.

List of Figures

List of Tables

Acknowledgements

In the first place, I wish to thank Prof. I. M. Sokolov for introducing me into the fascinating field of anomalous transport and his support over the years, and for the opportunities to participate in interesting workshops and conferences. Thanks also to Prof. F. Sagués for fruitful discussions and collaboration. The stimulating E-mail correspondence with A. Iomin, Ph. D., is very much appreciated. The questions raised by him brought up new aspects and productive considerations. I also thank Prof. E. Donath for reporting on his recent experiments, which motivated further theoretical investigations. I am especially obliged to Dipl. Phys. H. H. Schmidt–Martens and M. Borinsky for sacrificing their free time and programming the simulations, which was an enormous help to me. Without their contribution, this work would certainly not have been possible in this way. Moreover I thank Prof. R. Metzler for useful hints and for showing me some mathematical tricks. I am grateful to Dr. PD B. Esser for generously leaving me a part of his collected references. Thanks go as well to Dr. S. Fugmann and Dipl. Phys. B. Kohlhoff for helpful remarks and proofreading the manuscript. I also thank all colleagues of the Statistical Physics/ Nonlinear Dynamics and Stochastic Processes groups at HU Berlin for the pleasant working atmosphere. Finally, I want to thank my friends and family for their support and encouragement during all the time.

List of Publications

1. D. Froemberg and I. M. Sokolov, *Stationary fronts in an $A + B \to 0$ reaction under subdiffusion*, Phys. Rev. Lett. **1**00, 108304 (2008)

2. D. Froemberg and I. M. Sokolov, *$A + B \to 0$ reaction under non-Markovian subdiffusive kinetics: Equations and stationary solutions* Acta Physica Polonica B **3**9, 1199 (2008)

3. D. Froemberg, H. Schmidt-Martens, I. M. Sokolov, F. Sagués, *Front propagation in an $A + B \to 2A$ reaction under subdiffusion*, Phys. Rev. E **7**8, 011128 (2008)

4. H. H. Schmidt-Martens, D. Froemberg, I. M. Sokolov, and F. Sagués, *Front propagation in a one-dimensional autocatalytic reaction-subdiffusion system*, Phys. Rev. E **7**9, 041135 (2009)

5. D. Froemberg and I. M. Sokolov, *Boundary value problems for subdiffusion under degradation*, Acta Physica Polonica **4**1, 989 (2010)

6. D. Froemberg, H. H. Schmidt-Martens, I. M. Sokolov, and F. Sagués, *Asymptotic front behavior in an $A + B \to 2A$ reaction under subdiffusion*, Phys. Rev. E **8**3, 031101 (2011)

Selbständigkeitserklärung

Ich erkläre, dass ich die vorliegende Arbeit selbständig und nur unter Verwendung der angegebenen Literatur und Hilfsmittel angefertigt habe.

Berlin, den 31.03.2011 Daniela Frömberg